University of BRISTOL

EPSRC Centre for Doctoral Training
in Advanced Composites
for Innovation and Science

accis
ADVANCED COMPOSITES COLLABORATION FOR INNOVATION & SCIENCE

A Closed-Loop Recycling Process for Discontinuous Carbon Fibre Composites

by

Rhys James Tapper

Bristol Composites Institute

Queen's Building

University of Bristol

Bristol BS8 1TR

This thesis is submitted for the degree of Doctor of Philosophy of The University of Bristol

2018

Abstract

The carbon fibre reinforced polymer industry is growing rapidly and is becoming a realistic consideration for mass-manufacturing markets. The superior specific properties of composites make them ideal lightweighting materials, but their high cost, high environmental impact and limited recyclability are substantial deterrents. The aim of this work was to develop a closed-loop recyclable material and an associated closed-loop recycling process for carbon fibre reinforced composites that could present solutions to these obstacles.

The current technological outlook was evaluated to determine the progress made in composites recycling and, more importantly, the areas of development required to meet industrial demands. It was discovered that the industry requires high-value, recyclable, carbon fibre reinforced composites in order to produce an economically sustainable production cycle. The only way to provide this was to develop a closed-loop recycling process, that can reclaim fibres and matrix without mechanical property reductions. To achieve this, it was clear that a shift from thermosetting to thermoplastic matrices was required.

A closed-loop recycling methodology was produced, which enabled the closed-loop recycling of discontinuous carbon fibre thermoplastic composites. Proof-of-concept evaluation showed that it was possible to maintain mechanical properties over two recycling loops. The closed-loop material produced was improved by including a higher-performance thermoplastic matrix. Experimental analysis showed that the mechanical performance was predominantly affected by the fibre quality and not by degradation of intrinsic constituent properties. Closed-loop recycled materials exhibited a 20 % and 39 % decrease in tensile stiffness and strength after the first loop and did not substantially degrade after the second loop. However, the final mechanical properties were suitable for use in semi-structural automotive applications and were therefore of a high-value.

The closed-loop recycling process was evaluated by a life cycle assessment and resulted in the lowest environmental impact out of a range of contemporary lightweighting alternatives and conventional materials.

This body of work proves that it is possible to produce a high-performance, high-value, recyclable composite material with a low environmental impact at a potentially low cost.

Table of Contents

List of Figures

List of Tables

Acknowledgements

I'd like to thank Dr Marco Luigi Longana for his dedicated supervision during my PhD. His unyielding support was incredibly valuable, for which I am truly grateful.

I wish to extend my gratitude to Professor Kevin D. Potter and Professor Ian Hamerton for their guidance and overall contribution to the progression of this thesis.

Thank you to the Engineering and Physical Sciences Research Council for their support of this thesis, but also for my entire four years of training as part of the Centre for Doctoral Training at the Bristol Composites Institute (EP/L016028/1). I would also like to take this opportunity to thank both the academic and administrative staff at the Bristol Composites Institute for their contribution to my doctoral training and any input they have had during my thesis.

I would also like to thank the Solvay Group, The National Composites Centre, and The School of Chemistry at the University of Bristol for their support of manufacturing materials, analytical services and helpful advice towards the experimental work herein.

Without the support of my family and close friends the challenge of my thesis would have been insurmountable. I am forever grateful for your kind words of encouragement and humbling hospitality, Thank you all.

Publications

Several Chapters from this thesis have been disseminated through a combination of peer reviewed journals and conference publication; these are presented below:

Journal Publication

R.J. Tapper, M.L. Longana, H. Yu, I. Hamerton, K.D. Potter. Development of a closed-loop recycling process for discontinuous carbon fibre polypropylene composites. Composites: Part B. 2018. Vol 146. 222-231.

R.J. Tapper, M.L. Longana, A. Norton, K.D. Potter, I. Hamerton. A review of life cycle assessment for carbon fibre reinforced polymers: A further demonstration of the benefits of recycling. Resources, Conservation & Recycling. - Under Review.

R.J. Tapper, M.L. Longana, H. Yu, I. Hamerton, K.D. Potter. Development of a closed-loop recycling process for discontinuous carbon fibre polyamide 6 composites. Composites: Part B. – Under Review

Conference Papers

R.J. Tapper, M.L. Longana, H. Yu, I. Hamerton, K.D. Potter. *A closed-loop recycling method for short carbon fibre thermoplastic composites*. 18th European Conference on Composite Materials. Athens. June 2018.

R.J. Tapper, M.L. Longana, H. Yu, I. Hamerton, K.D. Potter. *Development of a closed-loop recycling method for highly aligned, short carbon fibre composites*. 21st International Conference on Composite Materials. Xi'an, China. August 2017.

Conference Presentations

R.J. Tapper, M.L. Longana, H. Yu, I. Hamerton, K.D. Potter. *A closed-loop recycling method for short carbon fibre thermoplastic composites*. 18th European Conference on Composite Materials. Athens. June 2018.

R.J. Tapper, M.L. Longana, H. Yu, I. Hamerton, K.D. Potter. *A closed-loop recycling method for short carbon fibre thermoplastic composites*. ACCIS CDT Conference. Bristol. 7th April 2018

R.J. Tapper, M.L. Longana, H. Yu, I. Hamerton, K.D. Potter. *Development of a closed-loop recycling method for highly aligned, short carbon fibre composites*. 21st International Conference on Composite Materials. Xi'an, China. August 2017.

R.J. Tapper, M.L. Longana, H. Yu, I. Hamerton, K.D. Potter. *Development of a closed-loop recycling method for aligned short carbon fibre composites*. ACCIS CDT Conference. Bristol. 6th April 2017.

R.J. Tapper, M.L. Longana, H. Yu, I. Hamerton, K.D. Potter. *Development of a closed-loop recycling method for aligned short carbon fibre composites*. BPF Thermoplastic Composites 2016. London. October 2016.

R.J. Tapper, M.L. Longana, H. Yu, I. Hamerton, K.D. Potter. *A closed-loop recycling method for aligned short carbon fibre composites*. ACCIS CDT Conference. Bristol. 5th April 2016.

Abbreviations

ABS	Acrylonitrile-co-butadiene-co-styrene
ACS	American Chemical Society
AF	Aramid Fibre
AHSS	Advanced High Strength Steel
ASTM	American Society for Testing Materials
BA	Benzyl Alcohol
BMC	Bulk Moulding Compound
CAFE	Corporate Average Fuel Economy
CED	Cumulative Energy Demand
CF	Carbon Fibre
CFPA6	Carbon Fibre Reinforced Polyamide 6
CFPP	Carbon Fibre Reinforced Polypropylene
CFRP	Carbon Fibre Reinforced Polymer
CFRTP	Carbon fibre Reinforced Thermoplastic
CFRTS	Carbon fibre Reinforced Thermoset
CLRM	Closed-Loop Recyclable Material
CLRP	Closed-Loop Recycling Process
CSA	Canadian Standards Agency
DCF	Discontinuous Carbon Fibre
DSC	Differential Scanning Calorimetry
EOL	End of Life
EV	Electric Vehicle
FA	Formic Acid
FLD	Fibre Length Distribution
FRP	Fibre Reinforced Polymer
FTIR	Fourier Transform Infrared
GF	Glass Fibre
GFRP	Glass Fibre Reinforced Polymer
GHG	Green House Gases
GMT	Glass Mat Thermoplastic

GPC	Gel Permeation Chromatography
GWP	Global Warming Potential
HiPerDiF	High Performance Discontinuous Fibre
HPLC	High Performance Liquid Chromatography
IFSS	Interfacial Shear Strength
JCMA	Japanese Composite Manufacturers Association
LCA	Life Cycle Assessment
LCC	Life Cycle Costing
LCE	Life Cycle Engineering
LCI	Life Cycle Inventory
LCIA	Life Cycle Inventory Analysis
MJ	Mega Joule
MS	Mass Spectrometry
MWD	Molecular Weight Distribution
NF	Natural Fibre
NMR	Nuclear Magnetic Resonance
PA	Polyamide
PC	Polycarbonate
PDI	Polydispersity Index
PEEK	Poly(ether ether ketone)
PEI	Poly(ether imide)
PES	Poly(ether sulfone)
PMB	Production and Manufacturing Burden
PP	Polypropylene
PPS	Poly(phenyl sulphide)
PVC	Poly(vinyl chloride)
QI	Quasi Isotropic
r-	Recycled
R&D	Research and Development
RIM	Reaction Injection Moulded
RIMCF	Reaction Injection Moulded Carbon Fibre
SEC	Size Exclusion Chromatography
SEM	Scanning Electron Microscope

SMC	Sheet Moulding Compound
TGA	Thermogravimetric Analysis
TRL	Technology Readiness Level
UD	Unidirectional
US EPA	United States Environmental Protection Agency
v-	Virgin
WTW	Well-To-Wheel

Symbols

A_x	Cross-sectional area
C_i	Total mass-induced fuel savings of material i
δ_s	Symmetric bending vibration
$\delta -$	Partial negative charge
$\delta +$	Partial positive charge
d	Fibre diameter; plate spacing; displacement
ΔE_{Use_i}	Change in use phase energy of material i
ΔH_m	Change in enthalpy of fusion
ΔH_c	Change in enthalpy of crystallisation
ΔH_c	Change in enthalpy of fusion of a pure polymer crystal
E_T	Tensile stiffness
E_C	Modulus of a composite
E_S	Modulus of steel
E_{FP}	Energy required to produce 1 kg of petrol
ε	Tensile strain
ε_{ult}	Ultimate tensile strain
F_{CP}	Mass-induced fuel change potential
i	Reference material
λ	Structural index
l_C	Composite length
L_C	Critical fibre length
$LTDD_v$	Lifetime driving distance of a vehicle
m_F	Fibre mass
m_M	Matrix mass
m_C	Composite mass
m_i	Mass of reference material i
m_b	Mass of baseline material b
m/z	Mass to charge ratio
M^+	Molecular ion
M_n	Number average molecular weight

M_w	Weight average molecular weight
υ_s	Symmetric stretching vibration
ρ	Density
ρ_C	Composite density
ρ_F	Fibre density; petrol density
ρ_M	Matrix density
ρ_S	Density of steel
R_{mass}	Mass ratio
R_{WTW}	Well-to-wheel conversion factor for 1 kg of petrol
σ	Tensile stress
σ_{ult}	Ultimate tensile strength
σ_F^*	Fibre tensile strength
τ	Shear strength
τ_i	Interfacial shear strength
τ_M	Matrix shear strength
$\bar{t}$	Average thickness
T_c	Crystallisation temperature
T_m	Melt transition temperature
T_g	Glass transition temperature
V_C	Composite volume
Vf_M	Matrix volume fraction
Vf_F	Fibre volume fraction
Vf_V	Void volume fraction
X_T	Tensile strength
χ	Crystallinity
$\bar{\omega}$	Average width

1 Introduction

This Chapter will introduce the key concepts of the thesis to provide the reader with a thorough understanding of the context of the work; the practical fundamentals and the technological landscape in which it sits. Section 1.1 details the fundamentals of composite materials and offers an insight into the current industrial outlook with regards to carbon fibre reinforced polymer composites. Section 1.2 outlines the aims and objectives of the research, Section 1.3 establishes the novelty of the work and the impact the novel ideas can bring to the industry, and Section 1.4 summarises the layout of the thesis.

1.1 Background & Motivation

A composite material comprises two or more phases that achieve mechanical and material properties superior to those of the single constituents. There are countless possible constituent combinations, one of the most common is the fibre reinforced polymer (FRP). FRPs are composed of a fibre reinforcement phase, a polymeric matrix phase and a variety of additives, which provide the matrix with additional properties. Fibres primarily provide stiffness to the composite along their longitudinal direction leading to a composite with fundamentally anisotropic behaviour. To account for the anisotropy, FRP components are usually made from multiple laminae, each with varying fibre orientations, resulting in a laminate with typically planar, quasi-isotropic properties. A generic depiction of a composite laminate can be found in Fig. 1.1. The polymeric matrix serves two fundamental purposes: the binding of the reinforcement phase(s) in place, and the distribution of stresses throughout the material whilst deforming under an applied force [1]. Secondary to this, it provides an environmental barrier for the

fibres and protects the fibre surface from environmental and mechanical degradation (*i.e.* abrasion, corrosion *etc.*) [1].

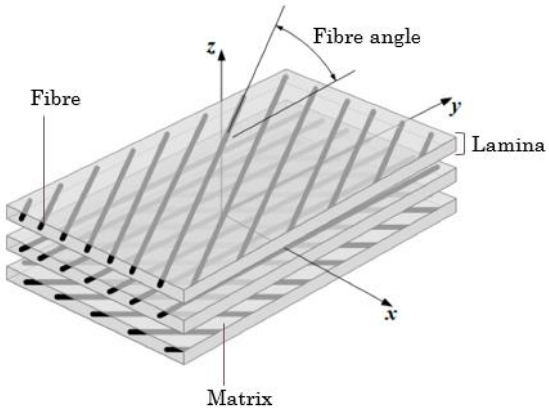

Fig. 1.1. Fundamental composition of a composite [1].

1.1.1 Fibres

Fibre type, fibre volume fraction, fibre orientation and fibre length have significant influence on the composite: tensile strength and modulus, compressive strength and modulus, fatigue strength, fatigue failure mechanisms, electrical and thermal conductivities, density and cost [2]. Common fibre types include carbon fibre (CF), glass fibre (GF), aramid fibre (AF, *e.g.* Kevlar) and natural fibre (NF *e.g.* flax, sisal, hemp, *etc.*) in a variety of lengths, *e.g.* from particles to continuous, each offering distinct processing or performance advantages:

- CFs have exceptionally high tensile strength-to-weight ratios, high fatigue strength and high thermal and electrical conductivity. When combined with an epoxy matrix, for example, carbon fibre reinforced polymers (CFRP) provide unrivalled specific tensile stiffness compared with other fibre types resulting in use in predominantly mechanically demanding applications in aerospace, defence, high-performance automotive and speciality sporting goods. Their high performance is reflected in their high cost [2].

- GFs are the most common reinforcement type for polymeric matrix composites, due primarily to: low cost, high tensile strength, excellent insulation properties, and high chemical resistance. Common GFRPs are made from woven fibre or chopped strand mat formats and impregnated with epoxy or polyester resins. Typical industrial applications include automotive body parts and wing structures for wind turbines, *i.e.* structurally less demanding than most CFRP, but at a reduced cost [2].

- AFs, *e.g.* Kevlar, are aromatic polyamide fibres with high crystallinity and can provide the highest specific tensile strength out of all fibre types. Common applications of AFs are in aerospace, marine and defence, where lightweight, high tensile strength, and resistance to impact are critical [2].

- NFs are biodegradable and, when compared to other fibre types, have a lower energy consumption associated with production. They can also provide increased acoustic damping, low density and are much cheaper than GF/CF. For these reasons, the most common applications for NF are as environmentally-friendly alternatives to GFs. The disadvantage of NFs is that they have reduced mechanical properties and high water absorption compared to synthetic fibre types [2].

1.1.2 Matrix

Matrices play a minor role in composite tensile load carrying capability however they do have a marked influence on the compression, interlaminar shear and in-plane shear behaviour. Polymer matrices are defined by two broad categories, thermosetting and thermoplastic, which generally refer to their formation and stability at high temperatures.

1.1.2.1 Thermosets

CFRP made using thermosetting polymers (CFRTS) are manufactured from a combination of resins, hardener and catalyst which, when mixed, start a chemical reaction, *i.e. curing*. Typical thermosetting matrices include; epoxy, polyester, phenolic and vinyl ester. Curing occurs around the fibres, embedding them within the macrostructure. The strength of the bonding interactions between the matrix and fibre surface, typically enhanced by a matrix-compatible polymer coating, or *sizing*, determines the degree of stress transfer between the two phases. The quality and strength of this interface underpins the composite mechanical performance [3]. The cure is complete when the initial resin components are bonded throughout the mixture, forming a covalently bonded matrix macrostructure *via cross-links*, see Fig. 1.2 [4]. Cross-links provide the polymer with enhanced stiffness and strength but, once cured, the strong covalent bonds cannot be reversed, making thermoset FRP reformatting impossible [5].

The superior tensile stiffness, in comparison with thermoplastic matrices, makes CFRTS ideal for structural applications where tensile performance is paramount. Typically, 76 % of CFRP have a thermosetting matrix, usually epoxy, with the remaining 24 % are made using thermoplastics [6].

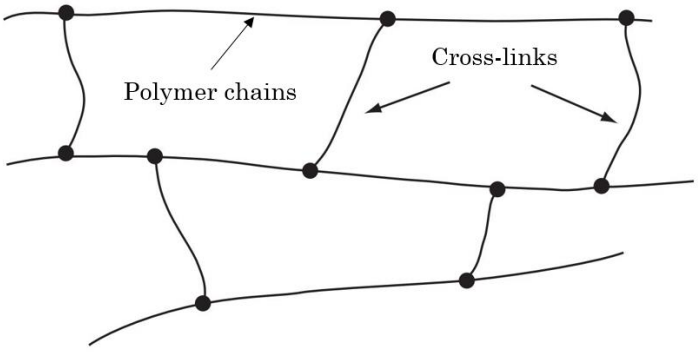

Fig. 1.2. Diagram showing the cross-linked nature of cured thermosets.

1.1.2.2 Thermoplastics

Thermoplastics, *e.g.* polypropylene (PP), polyamide (PA), polycarbonate (PC), poly (vinyl chloride) (PVC), poly(ether sulfone) (PES), poly(ether imide) (PEI), poly(phenyl sulphide) (PPS) or poly(ether ether ketone) (PEEK), have no cross-linking between polymer chains. They consist of a mixture of polymer chains varying from low to high molecular weight; the spread of chain lengths present in the bulk polymer is best represented by the molecular weight distribution (MWD) [4]. A detailed description of thermoplastic MWD can be found in Section 3.3.1.4.

Polymer chains are held together by temporary intermolecular interactions between functional groups on adjacent polymer chains, *i.e.* van der Waals' interactions or hydrogen bonding. van der Waals' are weak non-bonding interactions between the instantaneous dipoles formed by random electron distribution within neighbouring covalent bonds. Hydrogen bonds are strong non-bonding interactions between the partially negative ($\delta-$) oxygen or nitrogen atoms and partially positive ($\delta+$) hydrogen atoms.

Hydrogen bond and van der Waal's interactions are represented in Fig. 1.3, along with a table of average covalent and intermolecular bond strengths, Table 1.1. Thermoplastics are described as either amorphous or semi-crystalline. The latter denotes the presence of crystalline regions where polymer chains are highly aligned, enabling close packing and increased bonding potential, see Fig. 1.4.

Increasing the thermal energy of a thermoplastic only causes increased bond vibrations until the glass transition temperature (T_g) is reached. This is observed as a transition from a brittle 'glassy' state to a rubbery, visco-elastic state of the amorphous regions within the polymer [4]. For semi-crystalline polymers, this behaviour increases with temperature until the melting point (T_m), at this point the crystalline polymer regions have enough energy to break the intermolecular bonding interactions and begin to flow, albeit sluggishly in many cases. Most industrial thermoplastic composites are semi-crystalline and therefore experience both phase transitions however some are fully amorphous and only exhibit glass transition behaviour [7].

For CFRP made using thermoplastic matrices (CFRTP), the polymer melt is solidified around the fibres forming mechanical interlocking and temporary intermolecular bonding interactions between polymer chains and fibre sizing. The intermolecular bonding interactions of CFRTP have lower bond energies than covalent bonds, see Fig. 1.3 and Table 1.1, this is reflected in the generally inferior stiffness and strength of thermoplastics. However, the thermal phase transitions are entirely reversible which makes reprocessing possible, avoiding irreversible degradation of the polymeric macrostructure [8].

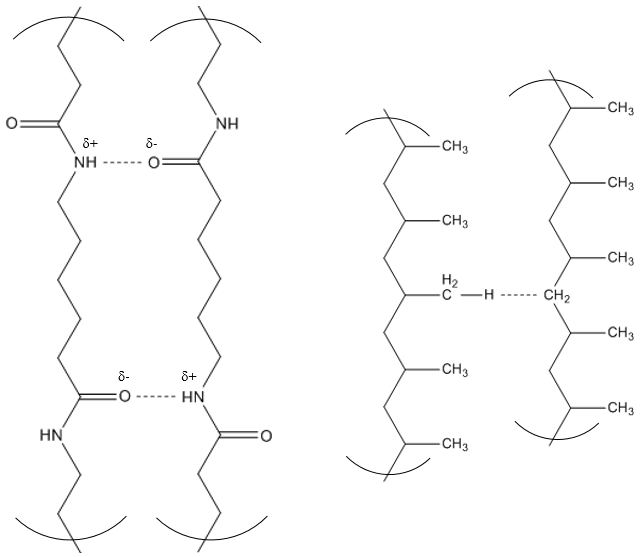

Hydrogen bonding **Van der Waals**

Fig. 1.3. Hydrogen bonding is shown for a section of nylon 6 and van der Waals' attractions are shown for a section of polypropylene. Brackets denote section is part of a repeated structure.

Table 1.1. Average bond strengths for typical polymeric inter- and intramolecular bonding interactions.

Bond type/interaction	Bond energy
	kcal/mol [9]
Covalent (C-C)	30-260
Hydrogen	1-12
Van der Waals	0.5-2

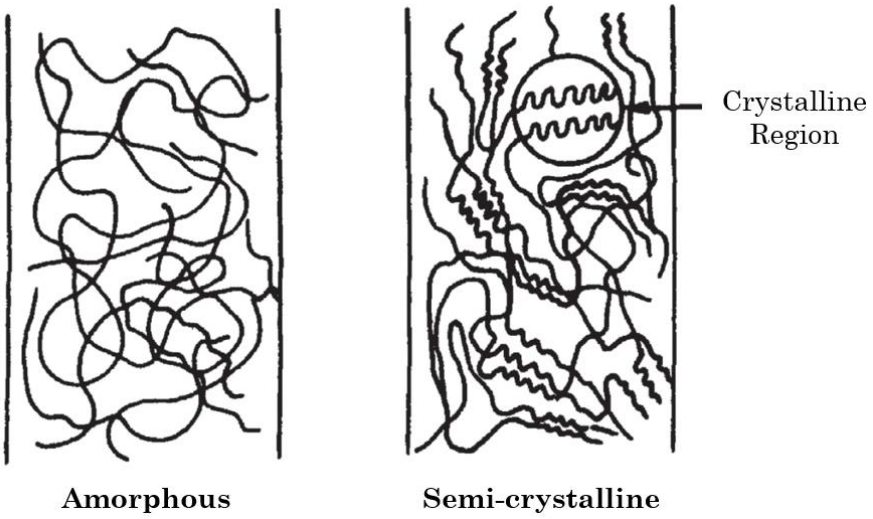

Fig. 1.4. Diagram showing the polymer chain orientations of typical amorphous and semi-crystalline thermoplastic polymers [2].

Discontinuous and long fibre CFRTP are used in applications where manufacturing lead times and high production volumes are a priority over mechanical performance; typically non-structural applications in the transport sector [10]. CFs are blended with polymer pellets in an extruder to form reinforced pellets which are used in injection moulding processes.

CFRTP can provide a range of application specific advantages over conventional CFRTS, these can be broadly categorized as provided in manufacturing or in use. The manufacturing benefits can be best exemplified in high volume manufacture:

- Compatibility with rapid thermoforming processes

- Lack of curing results in rapid production cycles, although increased pressures and temperatures are likely required. This is important for industries like the mass manufacture automotive as CFRTS are unable to make the < 1 min lead time required to maintain productivity rates of up to 100,000 units *p.a.* [10].

- There is a wider range of possible bonding and co-moulding techniques available, *e.g.* back-injection moulding, leading to a higher level of integration of composite parts, stronger bond strengths, reduced fixings/fasteners and substantially decreased assembly times.

- Storage costs are significantly reduced due to infinite shelf life and inexpensive storage requirements, *i.e.* no cold storage to supress catalysis [11].

The benefits that CFRTP can provide during the use phase are summarised below:

- Increased toughness and impact resistance over CFRTS are facilitated by molecular translation, *i.e.* increased strain, in response to stress. This is of benefit to applications that require increased energy absorption and crashworthiness [10].

- CFRTP can be repaired and reformed *in situ* enabling time and cost-effective maintenance of composite parts in service.

1.1.3 Industrial outlook

The superior specific mechanical performance of CFRPs, primarily afforded by the lightweight carbon fibre reinforcement, underpins their growing popularity across many industries. Constituent material combinations are continually diversifying, including novel fibres and matrices.

Global demand for CF in the year 2016 was around 63,500 tonnes with a consistently increasing growth rate of approximately 11.5 % since 2010, giving a projected demand of 77,000 tonnes for 2018 [12]. Most of the CFs produced are processed into composite materials, of which CFRPs hold 70 % of the share by volume. This corresponds to a global demand for CFRP of 101,000 tonnes in 2016, with annual growth rate of 12 % since 2010, mirroring that of CF [12].

This growth is necessitated by the adaptation of composites to new markets and driven by their design, cost and production volume requirements. CFRPs with thermosetting matrices, primarily epoxy, have been a leading material in this development due, in the most part, to their superior specific mechanical properties in comparison to other FRPs and conventional materials.

The aerospace industry, both commercial and defence, holds the largest share of CFRP usage by weight (30 %), followed closely by automotive (14 %), and wind energy (13 %), as of 2016. All of which are showing the same trends of increased CFRP usage [12].

Continual CFRP development has resulted in a slow, but observable, decrease in raw material costs and an increase in manufacturing technologies and capabilities. So much so that high-volume manufacturing markets, which had previously been priced out of CFRP use, are now considering it as a viable alternative to conventional materials [13].

The use of CFRP in these markets is still plagued by high costs and other complexities [14] but, the advent of their inclusion, however distant, is universally accepted by academia and industry to be within the next decade [15–17].

With the expected exponential growth of CFRP within high-volume manufacturing comes the substantial flow of composite waste, both from manufacturing, *i.e.* off-cuts and expired prepregs, and end of life (EOL). The classical waste treatment strategies have been landfilling and incineration, however, the last decade has seen the development of technologies attempting to recycle CFRP [18]. This is driven primarily by public opinion shifting towards sustainable production and the resulting legislation.

Growing publication interest around CFRP recycling reflects this, as represented by the citations plot in Fig. 1.5. A comprehensive evaluation of recycled (r-) CFRP markets and technologies can be found in Chapter 2.

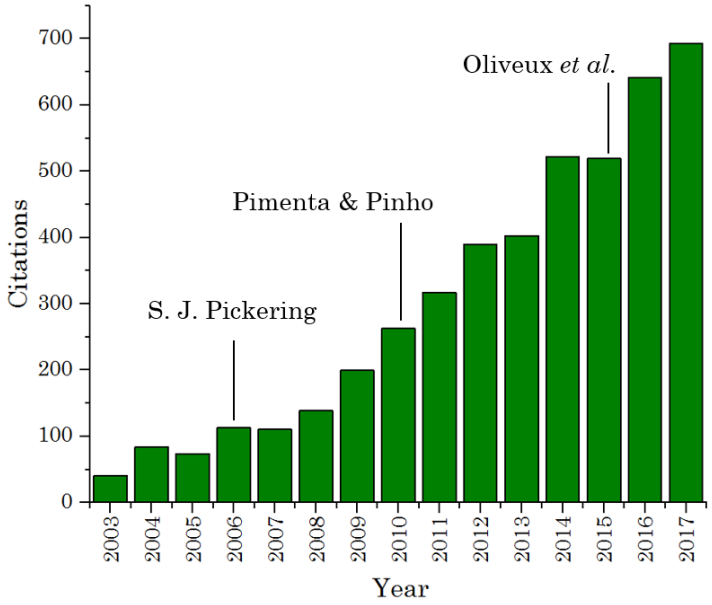

Fig. 1.5. Citation plot showing CFRP recycling research development over the past two decades. Plot is annotated with seminal review papers.

The UK Composites Strategy was developed back in 2009 to evaluate the British composites industry that, although somewhat behind in the technological infrastructure seen in the US and the rest of Europe, provided an accurate depiction of the state of composites recycling at the time. It reports that "further development of recycling process technologies and added value applications for recycled advanced composite materials are needed to satisfy growing end of life concerns" [19]. It states that the UK needs to "commercialise its offering in recycling advanced composite materials and continue work on the properties of sustainable composites" [19].

The UK Composites Strategy was updated in 2016 to determine the progress made since the last benchmark. It expresses a knowledge of: the lightweighting benefits of composites materials, the associated CO_2 reductions, and the acceleration of environmental impact reduction through increased market penetration [20]. It reinforces the importance of developing a capability in life cycle assessment and costing to show the benefits of composites materials [20]. Also, from the waste management perspective it strongly supports the Circular Economy paradigm for the production and recycling of novel composite materials; "there is

a strong need to incorporate circular economy principles alongside the rapid development of composites" [20].

The term circular economy refers to an economic model that aims to eliminate reliance on non-renewable resources and eradicate waste by intelligent product and process design [21]. This is contrary to the modern manufacturing model which follows the linear economy principles, of high-throughput of resources with minimal consideration of waste, where the focus is on producing large quantities of products at the lowest cost [22]. Flow diagrams showing the general CFRP linear economy production paradigm and a prospective closed-loop production cycle are shown in Fig. 1.6.

Adopting circular economy principles can be approached in two ways:

1. The closing of existing linear product systems by redirecting waste streams to become feedstock for the same or another system of value.

2. To design a new *closed-loop* system that, after the initial raw material input, requires no additional material to propagate, *i.e.* the waste material becomes feedstock for the next production cycle.

When reviewing the literature on the current technologies for the recycling of composite materials (see Chapter 2) two facts emerge: recycling is a two-step process (*i.e.* recycling = reclamation + remanufacture) and the matrix is lost or severely damaged during the reclamation step. Reclamation is defined as the collection of constituent material through a separation process. Remanufacturing is the process whereby either: separate, reclaimed constituents are combined to form a functional, recycled composite, *i.e.* what is typically observed with CFRTS; or, a waste composite is reformed into a functional composite without an intermediary reclamation step, *i.e.* the common CFRTP recycling procedure.

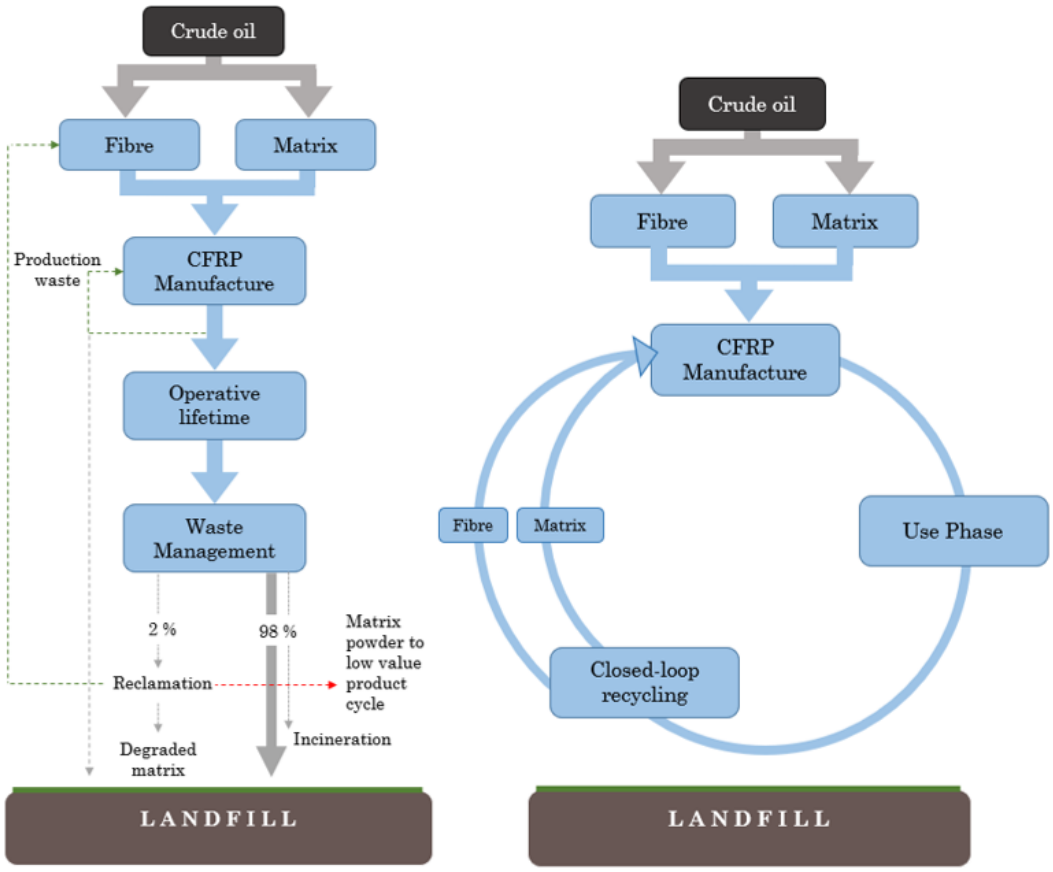

Fig. 1.6. *Left* - A flow diagram of the typical CFRP linear economy production paradigm. *Right* – A flow diagram of a prospective circular economy production paradigm for CFRP. Basic diagram shows complete value transferral from waste CFRP to recycled part.

Conventional thermosetting matrices must be fully degraded to enable fibre reclamation thus losing all the value of the matrix. Thermoplastics can be reprocessed, however, using conventional reclamation processes leads to both fibre and matrix property degradation, see Section 2.3. Using a thermoplastic matrix provides the ability to reclaim both the fibre and matrix. To the author's knowledge, there are no recycling processes that can separate constituents without degrading their quality and subsequently the quality of the remanufactured part.

The development of novel closed-loop recyclable composite materials requires the remanufacturing of high quality recyclate into a high value, recycled

composite. This necessitates the development of*: reclamation technologies which can reclaim both fibre and matrix*, and*, remanufacturing technologies that can combine constituents in a format which enables reuse, evading disposal over multiple cycles*. Closed-loop recyclable materials can therefore only be obtained in industry if thermoplastic matrices, and the relative processing/recycling methodologies, are adopted.

1.2 Aim & Objectives

This research aims to develop a closed-loop recyclable CFRP, and the relative closed-loop recycling process (CLRP), to enable the adoption of the circular economy paradigm in the composites industry. This requires addressing the following research challenges:

- To understand the limitations of state-of-the-art recycling processes and identify appropriate reinforcement and matrix phases. These findings will provide the basis of the closed-loop recyclable material and process to be developed.

- To design a closed-loop recyclable material (CLRM), and the relative closed-loop recycling process, that can reclaim and remanufacture constituents with the retention of material value, after each recycling loop, as a priority. Also, to develop an experimental framework for characterising material quality and monitoring degradation over two recycling loops.

- To experimentally evaluate the closed-loop recycling process and its ability to meet the aims. This initial evaluation will be a proof-of-concept to determine feasibility.

- To develop the process to incorporate high-performance constituents and produce composite material that provides

competitive properties for high-value applications after each recycling loop.

1.3 Novelty & Impact

The novelty of the presented work is characterised by the development of two outputs: a novel closed-loop recycling process, and, a closed-loop recyclable material. The novel contributions are presented below:

- The literature review is the most contemporary, comprehensive review of both CFRP reclamation and remanufacturing technologies available. The presentation of recycling using a value retention structure is particularly novel in that it provides valuable perspective for closed-loop development.

- The closed-loop recycling process developed in Chapter 3 is the first closed-loop recycling process for carbon fibre composites to be developed. It is the first to incorporate reclamation and remanufacturing principles to provide material over two recycling loops. It may be deemed closed-loop as both constituents and recycling materials are reclaimed above a realistic threshold (< 85 %).

- The closed-loop recyclable material developed in Chapter 4 is the first closed-loop recyclable CFRP to be produced. It is also the first recyclable composite to achieve mechanical performance retention after recycling, and to achieve a strength increase after recycling. The mechanical performance attained was greater than any discontinuous carbon fibre polypropylene composite in the literature.

- The closed-loop recyclable material developed in Chapter 5 attained the highest virgin (v-) mechanical performance of any

discontinuous carbon fibre thermoplastic in the literature. It also achieved the highest mechanical performance of any recycled discontinuous carbon fibre composite.

- Both closed-loop materials are the first low-cost, high-performance and environmentally friendly materials available to the automotive market, potentially providing industry with a material option that does not currently exist. It could potentially be the stepping stone that helps composites successfully break into the automotive market.

- The introductory review in Chapter 6 provides a novel perspective to composite life cycle assessment (LCA) in that it is tailored towards the adaptation of traditional LCA to closed-loop recycling of CFRP.

- The LCA evaluation in Chapter 6 is the first to assess the mechanical performance of a closed-loop recyclable material. It is also the first to evaluate the use phase performance of a composite over two lifetimes. The multiple use phase structure employed, specifically the tandem breakeven plot, is novel in its presentation of the benefits of composite materials and its application to closed-loop materials.

The research findings presented in this body of work are valuable to any work centred upon recycled CFRP, both in industry and academia. The impacts specific to each section are as follows:

- The comprehensive literature review in Chapter 2 has collated state-of-the-art progress of reclamation and recycling technologies. It also provides a thorough analysis of the requirements of emerging markets and the shortfalls of the composite industry towards meeting them. Any attempt to develop novel recyclable composites will find this invaluable.

- The experimental work in Chapters 4 and 5 provides useful insights into the reclamation, remanufacture and failure of closed-loop recyclable materials. It is also useful for the future evaluation of aligned discontinuous thermoplastic composites.

- The LCA review in Chapter 6 provides a comprehensive collation of all CFRP LCA evaluations and describes the advantages and disadvantages of current LCA methods. The data included are detailed, varied and contemporary which provides a useful source for future analysis. The multiple use phase structure employed, specifically the use of the tandem breakeven plot, creates valuable insight into the benefits of lightweighting materials. This information is of great value to the growing development of composites LCA.

Overall, this body of work proves that recycled composite materials of high-mechanical performance are achievable in a closed-loop production cycle, and that they can be a viable material option for emerging markets. This potentially provides a low-cost, high-performance and environmentally friendly material option that currently does not exist.

1.4 Thesis Structure

Chapter 2 reviews the available literature on the current state of CFRP recycling, from constituent reclamation to remanufacturing processes. It will evaluate the composites industry incentives for recycling, reinforcing the necessity for the closed-loop recycling method. The present market outlook for recycled CFRP will also be discussed in the final sections of the chapter.

Chapter 3 will detail the development of the closed-loop recycling process, through experimental model design, experimental analysis and discussion of the finalised experimental design that was used in the experimental chapters.

A proof-of-concept material will be used in Chapter 4 to evaluate the closed-loop recycling process through the experimental framework developed in Chapter 3. It will evaluate the process for its ability to reclaim quality recyclate and remanufacture quality composite material. The experimental analysis of the pure polymer matrices will quantify the mechanical performance of the polymer structure to aid in determining the degradative effects of the process.

Chapter 5 describes the incorporation of a high-performance matrix with the composite material and evaluates how the mechanical properties are retained after closed-loop recycling. It determines the effect different solvent systems can have on recycling performance and elucidates the key contributors to recycled composite performance.

Chapter 6 reviews the relevant literature on the use of Life Cycle Assessment for recycled CFRP. It will also include the LCA evaluation of the closed-loop recycling process in making the composites tested in Chapters 4 and 5, with a cross-comparison with conventional materials and contemporary recycling processes.

Chapter 7 will discuss the overall outcomes of the experimental chapters and how the thesis meets the targets set out in this Chapter. This will aid in determining the applicability of the process in modern high-volume markets and provide a strong metric for evaluating the potential benefits, both environmental and economical. The overall conclusions will be drawn and a consideration of future work for the development of the research will be made.

2 Recycling of carbon fibre reinforced polymers

This chapter evaluates the current state-of-the-art technologies available for CFRP recycling with an emphasis on the value retainable through both the reclamation and remanufacturing processes. Section 2.1 introduces key CFRP recycling concepts and the incentives for recycling from a market perspective. It also includes a thorough account of the emerging market opportunities for rCFRP, specifically for the automotive industry. Sections 2.2, 2.3, and 2.4 comprise a comprehensive analysis of the current reclamation and remanufacturing technologies for both CFRTS and CFRTP. Section 2.5 discusses the present industrial outlook that emerges from the previous section and compares them to the current opportunities and challenges facing the composites industry. The conclusions drawn in Section 2.6 will become the foundation of the method development detailed in Chapter 3.

2.1 Introduction

2.1.1 Industrial outlook

Despite the many advantages CFRP can provide, a significant consequence of its growth is the global increase in waste. CFRP waste comes from a variety of sources: testing materials from research and design (R&D); production waste, *e.g.*

dry fibre/pre-impregnated material (prepregs) off-cuts, tooling, and expired prepregs; and end of life (EOL) parts [23]. EOL components are either: damaged beyond repair and withdrawn from service, or, out of commission and have reached the end of their designed lifetime. EOL composites amount to approximately 60 % of all composites waste [24]. The remainder comes from production, *i.e.* off-cuts and expired material, which is predominantly due to the high scrap rate in prepreg based manufacture [24].

The current CFRP waste management route of choice is landfilling, due to the low cost and logistical ease compared to the recently developed alternatives [25]. In 2006, Halliwell reported that 98 % of composites waste is sent to landfill, whilst the remainder is sent to alternative routes, mainly mechanical recycling and incineration [26]. Updated values are not available however commercial recycling operations are small scale and have only recently been available, therefore landfilling and incineration still account for the vast majority.

Landfill is quickly becoming an unfavourable waste management method due to environmental, societal and economic drawbacks:

- For components with short operative lifetimes, *e.g.* sporting equipment, the waste volume has so far been manageable. However, the additional waste expected from market growth will undoubtedly exacerbate the issue.

- Growing social awareness of climate change, and an industrial recognition of the impending composite waste problem, led to the development of environmental legislature that regulates the recyclability of modern structures. For example, the most recent European Union EOL directive (ELV, 2000/53/EC) states that as of January 2015, 85 % of an automotive vehicle should be recyclable and that the responsibility of EOL composites disposal now lies with the component manufacturer [27]

- At £88.95 / metric tonne (as of April 2018, excluding gate fees) [28], landfill tax is becoming increasingly expensive as a disposal route; in some EU countries it has been completely outlawed [25].

Aside from the direct environmental impact and economic cost of landfilling there are benefits to avoiding the disposal of the economically valuable, and environmentally costly, constituent materials that comprise a CFRP:

- The production of CFRP material carries with it a considerable energy demand and environmental impact in terms of greenhouse gas emissions and reliance on non-renewable resources [29]. The major contribution is from CFs which have a high energy demand (up to 704 MJ/kg) [30] and greenhouse gas emissions (2.26 – 2.49 kg CO_{2eq}/kg) [31] associated with their production.

- CFs are expensive in comparison with conventional material; 16 £/kg for commercial grade PAN CF compared with aluminium and steel (AISI 1010) valued at approximately 2.5 and 0.6 £/kg, respectively.

- A reliable supply of rCF would also ease the production demand for vCF as rCF could be used as a replacement in applications where the properties allow. It also makes the UK composites industry more resilient as a steady production of rCF will provide a national supply, replacing a portion of the current international supply of vCF.

It is important to clarify at this stage that the term recycling is sometimes not explicitly defined in the literature leading to frequent misrepresentation. In this body of research, and in some seminal research [5,32], recycling is defined as comprising two key elements: *the reclamation of constituents from waste material, and, the remanufacture of these separate constituents into a useful composite.*

There are a variety of potential waste management methods which can be classified by the value retained from the process; from zero value retention to

direct reuse. This recycling hierarchy is split into four broad but distinct categories [33]:

1. Primary Recycling – This refers to methods that directly reuse the waste materials in a similar application thus retaining full material value with limited or no reprocessing costs. Examples of this include: the reuse of virgin prepreg off-cuts in a high value component, the reuse of a single-use plastic container, and the surface repair and reuse of a damaged vehicle component [34].

2. Secondary Recycling – This describes the reclamation of constituents from a waste material *via* a processing step. The recyclate can then be remanufactured into a material to be reused in an application where much of the virgin material value is retained. An example of this would be forming non-structural components from the extrudate of shredded CFRTP waste [35].

3. Tertiary Recycling – this entails a chemical or thermal decomposition of the material into fuel or other compounds, which can be reused in alternative applications. Examples of this are pyrolysis and solvolysis, where thermal degradation/solvent digestion of the polymer matrix is required to reclaim the fibre value.

4. Quaternary Recycling – There is no direct value obtained from the constituent materials; in some cases, there can be energy harvested from the calorific polymer matrix. Examples of this are landfilling and incineration [36].

The complex composition of CFRP materials, *i.e.* matrix, reinforcement fibre, and fillers makes waste components difficult to recycle. As most CFRP material functions within a greater structure there will undoubtedly be a mixed-material waste stream, *i.e.* adhesives, metal fixtures, core structures (honeycomb or foam) and coatings, which would require prior disassembly and separation. The majority of CFRP waste is therefore currently subjected to quaternary recycling

due mainly to the hitherto low cost and comparative logistical ease over alternative methods [27].

The development of recyclable composites, and processes with which to recycle them, has attracted increased research interest (see Fig. 1.5). In the last decade, CF recycling research has grown by 360 %, recently overtaking GF [37]. Over this period there have been three comprehensive reviews of the available technologies and future outlook: Pickering in 2006 [34], Pimenta & Pinho in 2011 [5] and Oliveux *et al.* in 2015 [32].

The value retention potential, *i.e.* the ability of a process to provide a product in a form and quality that enables re-use, of the current CFRP recycling hierarchy is displayed in the Fig. 2.1 flow diagram.

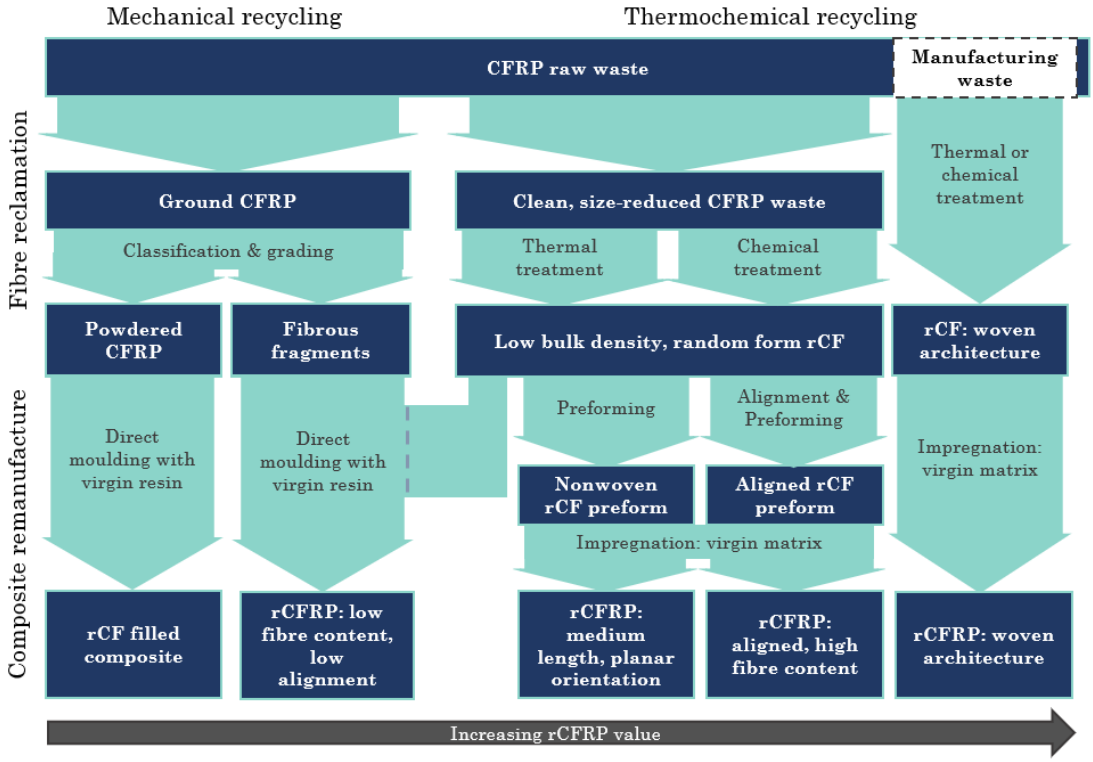

Fig. 2.1. A flow diagram showing the general value retention potential of current CFRP reclamation and remanufacturing processes. Diagram is modelled on that presented by Worrell (*c.*2014) [38].

2.1.2 Market opportunities for rCFRP

The automotive sector has used CFRP in motorsport and high-end vehicles for decades. FRP use in mass-manufactured vehicles has been limited to GF with either PP and PA thermoplastic matrices, for non-structural components [39], or unsaturated polyester and epoxy thermosetting matrices, for more demanding semi-structural components [5].

This is primarily driven by the high cost of CF, the cost sensitivity of mass-manufactured vehicle design, and the processing times of thermosetting matrices. Despite this, the automotive industry has predicted significant increases in CFRP growth rate as the mass-manufactured vehicle sector starts to adopt CFRP as a lightweighting strategy [19].

Vehicle fuel efficiency is heavily regulated, US Corporate Average Fuel Economy (CAFÉ) standards stipulate minimum fuel efficiency to 35 mpg by 2020 [40] and the European Commission set a target of 57.9 mpg by 2021 [41]. European carbon emissions regulations will also be reduced, from 130 g/km CO_2 in 2015 to 95 g/km CO_2 in 2021 with a level of 68-75 g/km CO_2 in 2025 [42]. The penalty for non-compliance with the regulation has also increased to approximately £4 / tenth of a mile per gallon, for each tenth under the target value, multiplied by the total amount of non-compliant vehicles for a given model year [40].

Decreasing vehicle fossil fuel emissions can be achieved by either adopting alternative fuel sources, increasing engine efficiency or by creating a lighter vehicle; the latter being the most cost effective and timely solution, in the author's opinion. There has been a wealth of development in alternative fuel drivetrains, *i.e.* battery and fuel cell powered electric vehicles (EVs), however these are currently much heavier than the internal combustion drivetrains they are replacing [43]. Weight limits the maximum range of EVs markedly, reducing the potential development of EVs. However, this provides an additional market for the lightweighting benefits of CFRP [43].

It is reported that a 6-8 % increase in fuel economy can be achieved by a 10 % drop in vehicle weight [44]. To meet these, and the inevitably conservative future

efficiency targets, automakers are looking at CFRP to save weight as a method of increasing fuel efficiency. CFRP is the primary material of choice due to the superior specific mechanical properties over conventional steels and alternative lightweighting materials, *i.e.* aluminium (Al), magnesium (Mg) and advanced high strength steel (AHSS). In general, CFRP can provide a 60 % and 40 % weight saving over steel and Al for the same component [45].

The automotive industry has many incentives for adopting CFRP material however there are equally as many obstacles hindering progress. The biggest challenges facing the adoption of vCFRP for the mass-manufactured automotive sector, and, the solutions provided by recycling (in italics) are summarised below:

- CFRP material is currently landfilled which poses a significant environmental problem for the automotive industry, considering government legislation, *i.e.* EU 2000/53/EC [27]. *Recycling provides alternative waste management for manufacturing and EOL waste. This helps meet legislative requirements, and, effectively increases the amount of CFRP that can be included in a vehicle.*

- As described previously, CFRP are expensive materials due to the high economic cost of raw material extraction and production. *Recycled (r-) carbon fibres can be a fraction of the cost of vCFs and therefore the subsequent remanufactured CFRP (rCFRP) will be at a reduced cost [46].*

- CFRP production has a substantial energy requirement, far greater than steel and Al [47]. *Recent LCA evaluations suggests that rCFRP has a substantially lower impact than vCFRP [48]. This is because the energy required to reclaim and remanufacture rCFRP is a fraction of the virgin manufacturing burden [49].*

- The wealth of existing expertise in metal component manufacturing. There is a significant disparity between the available technical expertise in CFRP and metal manufacture and

design. *This is a very difficult obstacle to overcome and can only really be remedied with time. The prevalence of a skilled CFRP workface is accelerated by the development of the market which will be substantially improved by the production of affordable, structural rCFRP.*

- The considerable capital costs required for implementing high-volume CFRP manufacturing infrastructure. Classical CFRP manufacture requires expensive equipment, tooling and consumables. It is therefore a substantial risk for automotive manufacturers to adopt composite structures in place of the pre-existing manufacturing equipment for metals. *Expensive infrastructure is an inevitable consequence of manufacturing a complex material format. The capital costs are difficult to reduce and therefore the investment needs to be incentivised by the benefits of the product. In this case, access to the markets made available by rCFRP may make the leap worthwhile.*

It was only in recent years that lightweighting incentives were enough for the consideration of CFRP in structural applications in the mass-manufactured vehicle. The large scale production of the BMW i-series, at around 100 i3 models per day, marks a huge step in the inclusion of CFRP material for structural components in mass-manufactured passenger vehicles [50]. This is considered a pioneering move and expected to be followed by many other car manufacturers, however the CFRP used was high performance non-crimp fabric CF epoxy, which is expensive and difficult to recycle. BMW developed an in-house recycling chain for the manufacturing waste, re-using off-cuts in other non-critical areas. However, this is only achievable due to the quality of the manufacturing waste, *i.e.* retention of the fibre architecture.

There are few vCFRP components in mass-manufactured vehicles for rCFRP to replace, however there are a variety of semi-structural components made from vGFRP that make likely candidates. Pimenta and Pinho provided an extensive summary of current structural GFRP components that could be

replaced by rCFRP and other foreseen markets; of which semi-structural automotive components were in majority [5]. Some of these semi-structural vehicle applications are provided in Table 2.1.

Table 2.1. Existing components made from vCFRP that are potential structural and semi-structural locations for rCFRP [5].

Component	Material	E_T	σ_{ult}
		GPa	MPa
Car door panel	GF+UP	14	36
Car roof shell	CF+EP	31	234
Wind turbine non-critical layers	GF+EP	22	367
Car body panels	CF+EP	53	450
Wind turbine critical layers	GF+EP	38	711

GF = glass fibre, CF = carbon fibre, UP = unsaturated polyester, EP = epoxy

2.2 CFRTS recycling

Recycling of CFRTS can be split into 3 main categories: pyrolysis (34 % including fluidised bed and microwave pyrolysis), solvolysis (24 %), and mechanical grinding (18 %); the remaining 24 % of the technologies are classified as 'other' [37]. The following section will outline the fundamentals of each process and their potential for producing recyclate of value.

2.2.1 Mechanical recycling

Mechanical recycling comprises the comminution of material, into a variety of reduced average particle sizes, either by crushing, grinding, cutting, shredding, milling, vibration or other analogous processes. The recyclate obtained is then graded based on composition; sieved fractions usually range from powdered, matrix-rich recyclate to fibre-dense chips containing fibres of varying lengths. Fibres can be loose, or still embedded in matrix however they are always discontinuous [18].

For CFRTS both shredding and impact reduction methods can be used due to the brittle failure of the matrix. Impact methods follow a hammer or ball mill process whereas shredding processes usually employ a guillotine or a cutting mill [51].

Ground recyclate can be used as either filler or reinforcement. Powdered, matrix-rich recyclate can be reused as filler in both thermoset [52] and thermoplastic [53] virgin matrices. Filler percentages are limited (< 10 wt%.) and the low cost of virgin fillers makes this economically unfavourable [32]. The limit is due to a sharp increase in virgin matrix/resin viscosity after inclusion which makes any scaled manufacturing effort complex [34,54].

Fibre-rich chips can be used as reinforcement in thermosetting and thermoplastic matrices with varying mechanical performance improvements. Palmer *et al.* incorporated ground epoxy CFRP into virgin GF sheet moulding compound (SMC) at 20 wt.% [55]. The recyclate had a CF content of approximately 70 wt.%. Flexural and impact strengths saw a knockdown of 14 % and 20 % respectively but a 7 % increase in flexural modulus was achieved.

Reduction in strength and toughness has been reported elsewhere, this is thought to be a consequence of poor bonding, between virgin matrix and recyclate matrix, and the large fibrous particles acting as stress raisers [34]. The mechanical properties of rCFRP from ground CFRTS are usually significantly impaired [56,57].

Ogi *et al.* employed shredding and ball milling to epoxy CFRP wastes creating graded recyclate used as a reinforcement in acrylonitrile-*co*-butadiene-*co*-styrene (ABS) to confer electrical shielding properties [58] and a boost in mechanical properties [57]. ABS reinforced with 50 wt.% recyclate, with an average fibre length of 200 μm, observed tensile strength and tensile modulus enhancements from 70 MPa to 170 MPa and 3 GPa to 20 GPa, respectively[57].

Mechanical recycling is considered a reclamation procedure however it is also employed as a size-reduction pre-treatment, *i.e.* comminution, for other processes [37]. Comminution is useful as it: reduces bulk volume for transport and storage, it produces a homogenous size distribution of feedstock, and it increases feedstock surface area; which is especially important for chemical reclamation [59].

2.2.2 Fibre reclamation

This section details the available fibre reclamation methods for CFRTS. Literature examples will invariably describe CFRTS, some explanations are derived from GFRTS examples, where the technique is transferrable, but this will be noted in the text. Some of these techniques are applicable for fibre reclamation from CFRTP which will be discussed in Section 2.3

2.2.2.1 Pyrolysis

Pyrolysis broadly refers to the thermal degradation of composite material at elevated temperatures, typically between 450 °C and 700 °C, depending on the matrix and atmospheric conditions used. Waste materials, mostly unused-prepregs, prepreg trim and cured laminates, are collected, washed and comminuted into coarse fragments before they are pyrolysed [34]. The application of thermal energy to a waste composite results in thermal degradation of the matrix after a threshold energy has been reached. This is directly related to bond strength, thus lower temperatures are used for polyester resins whilst epoxies and high performance thermoplastics require higher temperatures. [46].

Varying the process temperature and atmospheric conditions, *i.e.* temperature and atmospheric gas, results in a range of attainable fibre qualities, with respect to stiffness and strength. The literature suggests that pyrolysed rCFs typically exhibit a reduction in the tensile strength, with most reported cases in the range of – 5 % to – 80 % [32,60–62] from single fibre tests and composite analysis. Strength knockdowns are typically a result of surface char residue or intrinsic fibre defects from handling or fibre oxidation. Stiffness is generally unaffected by pyrolysis under controlled conditions [5,32].

The knockdown mechanism observed is a result of the pyrolysis conditions used. Char residue from virgin resin is observed at the lower end of the temperature scale [32,63]. Longana *et al.* reported a cumulative build up in residues left on the fibre surface after multiple pyrolysis cycles at 500 °C [63]. This was a contributing factor to the successive reductions in failure stress observed (- 16 % and 55 %) [63].

Elevated temperatures can be used to remove char residue (up to 1300 ℃), however it can significantly reduce fibre strength due to surface oxidation and surface defects [61].

Oxidants can be used to decrease the matrix degradation temperature through catalysed oxidative degradation mechanisms. This is used to remove char residue at lower temperatures, however, it results in additional process costs and can even reduce the mechanical properties [5].

Lopez *et al.* optimised a combined pyrolysis/gasification method for EOL CFRTS for the removal of char residue using oxidation. The waste CFRTS was pyrolysed at 600 ℃ in N_2 then introduced to air for 30 mins. rCFs exhibited no char residue with a tensile strength knockdown of 30 % [62].

The ReFiber optimised isothermal pyrolysis/oxidation process (550 ℃) by Meyer and Shulte achieved the lowest reported tensile strength knockdown; – 4% compared with virgin CF as obtained from single fibre tests [61].

There is a compromise between rCF mechanical properties and the removal of char residue. It is apparent that 500 – 550 ℃ is the upper limit in terms of fibre strength retention which, when combined with the appropriate oxidation process, can also provide clean surfaces.

Pyrolysis severely degrades the matrix leaving only thermally stable solids, *i.e.* fibres and other fillers, low molecular weights oils and gases. The value retained from the matrix is therefore minimal and is generally not pursued due to economic impracticality; filler resale is not economically viable and oils will usually require purification and reprocessing before resale which will decrease their value [64]. This represents a substantial loss of value in the case of aerospace CFRP as the matrix is usually of higher value than the fibre. Reclaimed oils can be burned as a fuel source, due to the high calorific content of the polymer, however this represents a fraction of the value of the virgin matrix material [5].

Pyrolysis is so far the most advanced reclamation process for CFRP, in terms of technology readiness level (TRL), as there are several commercial operators. The largest international operators are listed below:

ELG Carbon Fibre Ltd (previously Recycled Carbon Fibre Ltd.) [65]

ELG are the largest pyrolysis operation and can process 2,000 metric tonnes (*c.* 2017) of CFRP scrap per year. They provide a variety of rCF formats including; milled fibre, chopped tow, oversized chopped tow, and nonwovens. Their fibres have been used in a variety of demonstrator and R&D programmes with Tier 1 industrial suppliers in automotive and public transport sectors [66].

CFK Valley Recycling [67]

CFK is the largest commercial pyrolysis operation in mainland Europe, processing 1,000 metric tonnes per annum (*c.* 2017) of EOL CFRP automotive, aerospace and sports goods. The rCF are then sold in milled, chopped, wet-laid veils and air-laid nonwoven mats [68].

Japan Carbon Fibre Manufacturers Association (JCMA: Includes Toray Industries Inc. and Toho Tenax America Inc.) [69]

The JCMA formed a joint venture in 2008, opening a pyrolysis test plant for CFRP material. Output was reported up to 1,000 tonnes with rCF targeted at the automotive and consumer electronics industries [70]. Current recycling operation, production capabilities, target markets and commercial products are unreported.

Carbon Conversions (previously MIT-RCF) [71]

Carbon Conversions is America's largest commercial pyrolysis operation, processing 500 metric tonnes of EOL CFRP automotive, aerospace and sports goods [68]. They produce chopped fibres, sized (proprietary) or unsized, nonwoven mats and 3D nonwovens produced using the 3-DEP process [71,72]. rCF remanufacturing formats are explored in Section 2.4.

Karborek [73]

Karborek is an Italian pyrolysis operator that uses an oxygen rich pyrolytic method, patented in 2002, to produce chopped fibre, milled fibre and a nonwoven Karbo Felt mat from composite waste.

2.2.2.2 Microwave pyrolysis

Microwave irradiation breaks down matrix material from the core outwards in an inert atmosphere. This has the advantage of rapid and efficient heat transfer [74].

Lester *et al.* showed that microwaves can separate CF from the surrounding epoxy matrix leaving minimal residue on the fibre surface. This led to a reduction of 28 % and 10 % in tensile strength and tensile modulus respectively, as determined by single fibre tensile tests [75].

Condensation of volatilised polymer has the potential to permit the collection of a mixture of organic molecules derived from the matrix. A study by Akesson *et al.* reclaimed GF from a scrapped GFRP polyester wind energy blade that had previously been ground in a ball mill. A ground fibre fraction was collected but the quality unreported, however the matrix vapour was condensed into a complex mixture of oils [76].

Microwave pyrolysis offers similar fibre and matrix value retention potential to pyrolysis and has the added advantages of compatibility with GF and a reduced energy demand [75]. Despite this, microwave pyrolysis studies have never surpassed the lab scale. This makes direct comparison with commercial pyrolysis impractical [76].

2.2.2.3 Fluidised bed oxidation

This is a relatively similar thermal reclamation method to pyrolysis in that elevated temperatures (450 – 550 °C) are applied to degrade the polymeric matrix leaving the fibres intact. Composite waste is placed in a sand bed were combustion of the matrix is initiated by a high temperature, oxygen-rich flow causing thermo-oxidative degradation of the polymer [34]. Degradation products and fibres are blown higher up into the oxidation chamber by the rising air stream, separating the constituents from each other and any other heavy contaminants, *e.g.* metal fixings.

Matrix and fibre separation is completed in a cyclone where fibres are collected and the matrix is transferred to a higher temperature afterburner where it is fully oxidised [34]. The integrated separation process is an added benefit for CFRP waste treatment due to the likelihood of mixed material waste streams, giving it a high tolerance to contaminated waste.

Previous studies were able to reclaim fibres without char residue [77] but with a tensile strength reduction of anywhere between 18 % - 50 % [78,79], a significant disadvantage over alternative methods. Similarly to pyrolysis, there is no possibility of retaining much value from the matrix, other than a saving from energy harvesting [80].

There are currently no commercially available fluidised bed oxidation systems however a pilot plant scale process has been operational for the past 20 years:

Pickering *et al.* at the University of Nottingham [81]

The first fully operational pilot-scale fluidised bed pyrolysis plant was developed by Pickering *et al.* in 1998 [81], however, operations did not progress further than the pilot plant scale [79].

2.2.2.4 Chemical treatment

This describes any reactive, solution-based reclamation method used to break down the matrix material. Categories include: acid digestion, solvolysis, and supercritical fluid solvolysis. Reaction conditions are generally a compromise between temperature and the reaction rate. The latter is determined by the reactivity of the solvent, waste surface area and the bond strengths within the polymer structure. The reaction temperatures required are generally inversely proportional to the reactivity of the solvent.

2.2.2.4.1 Acid/Alkali digestion

The strong acidic and alkaline reactants used in acid/alkali digestion are concentrated and highly corrosive enabling favourable reactivity at low temperatures (< 150 °C). A variety of reactant systems exist within the literature,

the most common of which are: nitric acid [82,83], sulphuric acid [84], acetic acid [85,86], and some alkalis [87]. Reactants digest the matrix leaving clean fibres with potentially low surface damage, although it is reported that fibre surface alterations, *i.e.* residual resin or surface oxidation, may hinder future matrix adhesion [32].

Lee *et al.* reclaimed CF from a woven epoxy CFRP, using concentrated nitric acid, with the woven fibre architecture intact [83]. Single fibre tensile testing reported a tensile strength reduction of 2.9 % [83]. Strength reductions increased with acid concentration, this suggests that the acid is damaging the intrinsic fibre properties. Liu *et al.* reported a tensile strength reduction of just 1.1 % after solvolysis of epoxy CFRP in nitric acid (8M concentration) at 80 ℃ for 12 hours [82].

The corrosive nature of the reactants is key to low temperature reactivity however it makes them difficult and dangerous to handle, for both the user and the environment. This is a significant deterrent for industry, especially when considering scalability to commercial volumes [32].

2.2.2.4.2 Solvolysis

Solvolysis methods operate using less hazardous solvents than acids/alkalis, but require higher temperatures (200 – 300 ℃) to afford suitable reactivity. There are a variety of temperatures, pressures, solvents and catalysts that can be employed to suit a range of polymers or to improve the decomposition efficacy for a specific polymer [5].

The best mechanical performance retention achieved in the literature was by Pinero-Hernanz *et al.* The study evaluated the solvolytic efficiency of subcritical methanol, 1-propanol and acetone in temperatures and pressures between 200 - 450 ℃ and 4 – 16 MPa respectively. With the aid of alkali catalysts to speed up matrix degradation times (> 95 % of resin degraded in < 15 mins), clean CF were reclaimed with between 1 – 15 % tensile strength reductions [88].

2.2.2.4.3 Supercritical fluid solvolysis

Supercritical solvolysis methods employ higher temperatures (350 - 440 ℃) and pressures (20 – 30 MPa) to increase reaction rates, degradation efficiencies

and provide reactivity in non-hazardous solvents and without catalysts [88–90]. This is due to the low viscosities, high diffusivity, high mass transport coefficients and pressure based solvent power [91]. At supercritical conditions less aggressive solvents can be used, such as water, although a combination of water and a co-solvent is the most common system due to enhanced degradation rates [32].

Oliveux *et al.* used a water/acetone mixture (20:30 vol ratio) at supercritical conditions (320 ℃ and 18 MPa) to reclaim fibres from an aerospace grade epoxy CFRP panel [92]. Solvolysed rCFs were remanufactured into three panels using epoxy resin with different ply counts and solvolysed fibres of varying qualities. A tensile strength reduction of 25 – 30 %, compared with virgin fibres, was achieved from the two highest performing panels [92]. These were a result of lower fibre alignment, lower volume fractions (unnormalized) and 3 wt.% matrix residue on the fibre surface affecting interfacial shear strength [92].

Bai *et al.* reported no tensile strength reduction for CFs reclaimed from oxygen in supercritical water (440 ℃ at 30 MPa), however this was at the expense of degradation rate. At increased rates the excessive degradation caused a 38 % reduction in CF tensile strength [93].

A recent study by Okajima *et al.* used subcritical acetone (320 ℃ at 1 MPa) to reclaim CF from woven epoxy CFRP using a semi-flow type setup [94]. Whole CF woven plies were obtained with a strength knockdown of 9 % measured by single fibre tensile test. A previous study by the same group also reported the re-curing of thermoplastic epoxy residues collected after decomposition of a similar CFRP in supercritical methanol [95]. The mechanical properties of the re-cured matrix were not reported.

Solvolysis research is currently limited to laboratory scale practice however CF projects are slowly edging towards pilot scale production and demonstrators [37]. There has been a commercial attempt at catalysed, subcritical solvolysis in previous years:

Adherent Technologies Inc. (ATI) [96]

ATI developed a wet chemical solvolytic process which uses a proprietary liquid transfer fluid and catalyst mix under low temperature and pressure [97]. A

preliminary pyrolysis process is used to limit purity issues from mixed waste streams [98]. rCFs are reclaimed with marginal strength reductions (8.6 %) from the manufacturing and EOL waste, 1,000 metric tonnes per annum, of both aerospace and automotive industries [99,100].

2.2.3 Summary

A summary of the advantages and drawbacks of each recycling/reclamation method is collated in Table 2.2. Although some value can be retained by using CFRP mechanical recyclate, as a provider of niche functionality or performance enhancement, there is a significant disparity between the expected supply of waste CFRP and demand of low value rCFRP. The limited studies available for CFRP grinding are at the laboratory scale, to the author's knowledge there are no grinding processes for waste CFRP operating commercially [32]. This is a consequence of grinding difficulties and economic impracticality, as the value of CF recyclate through mechanical grinding is too low [37].

Excellent mechanical property retention has been observed for solvolysed CF when sub/supercritical conditions are optimised. Depending on the preliminary comminution process the virgin fibre architecture can potentially be retained, however the reaction rates will be significantly reduced compared with a high surface area shred [101]. The equipment required to sustain these conditions is both expensive and dangerous to set-up and maintain [89]. The degradation conditions can be controlled enough so that reclamation of matrix in the form of valuable monomers and organic molecules, *e.g.* phenols, is possible [89,102,103]. However, the value attainable is unreported and unclear, especially considering the complexity of the purification and separation of mixed organic species. For pyrolysis, the only value that can be retained is through the fibre, which show promising mechanical property retention over a number of commercial processes [32,49,60].

The most promising solvolysis research currently remains at the lab scale, at lower TRL than traditional pyrolysis and mechanical grinding, therefore the commercial scalability of the process is uncertain [37].

All fibre reclamation methods have reported excellent fibre property retention in single fibre tensile tests however the strength knockdowns increase when they are incorporated into virgin matrix. This is likely as the continuous, woven architecture is usually lost or not easily re-manufactured into an rCFRP. The mechanical properties of the fibres cannot be realised in composite performance without remanufacture into a similar architecture to virgin CFRP.

Table 2.2. Summary of advantages, disadvantages and value retention of current thermoset CFRP reclamation processes.

	Advantages	Disadvantages	Value retention
Mechanical	Lowest energy process [59]	Minimal control of constituent separation	Loss of fibre length and homogenous length distribution
	Simple and inexpensive to use and maintain	Substantial constituent mechanical property degradation	Matrix degradation and low purity
	Some separation of constituents [104]	Inconsistent fibre architecture	Low reincorporation percentages [34,54]
	Requires and produces no hazardous compounds [59]	Risk of ignition during shredding	Only suitable for low value applications
	Handles large waste volumes at high throughput		CFRP not economically viable [5,32,105]
Pyrolysis	High fibre quality [46,60,61,106]. Tensile strength knockdowns of – 5 % [61]. [(a)]	Fibre performance sensitivity to processing conditions [60]	Matrix value minimal - energy harvesting or polymeric oils [5,107]
	Energy harvesting from matrix - economic and energetic savings [108]	Hazardous by-products [108]	Fibre sizing removed
		Random fibre architecture	Potential for full fibre value retention
			Commercially available in different formats
Fluid. bed	Handles mixed density wastes [81]	Strength degradation (up to 50 %) [109]	No matrix reclamation possible
	A well-established process [81,109]	Substantial fibre length decrease [81,109]	Fibre reclamation but inferior quality to pyrolysis
		Low bulk density random fibre architecture	Inline sorting capability
Chemical	Excellent mechanical properties [90,94,95]. Tensile strength knockdowns of 1 – 3 %. [(b)]	Can require hazardous solvents [110]	Potential for full fibre value retention
	Potential for full fibre architecture reclamation [32,35]		
	Fibre length distribution unchanged [32]	Can require expensive equipment and maintenance	Low matrix value in monomeric oils
	Potential for moderate matrix value retention [89,111]	Architecture and reclamation rate compromise [5]	Solvent recapture [110]

[(a)] At 550 ℃ under oxidative conditions. [(b)] 8M nitric acid, 80 ℃ for 12 hours.

2.3 CFRTP recycling

In the context of recycling, CFRTP have a clear advantage over CFRTS in that the matrix can be reprocessed without significant degradation, owed to the lack of cross-links within the polymer macrostructure (see Section 1.1.2.2). When provided with the appropriate stimuli, either thermal energy or solvation, the intermolecular interactions between polymer chains can be temporarily broken giving the potential for fibre and matrix separation. However, current CFRTP recycling does not take advantage of this behaviour to separate constituents but reprocesses them as a combined recyclate. The usual reclamation and remanufacturing approach to recycling is therefore not applicable with CFRTP, in this case recycling refers simply to the conversion of waste into a new part. An example of this would be the pelletization of waste CFTRP and injection moulding of pellets into a component.

It is possible to reclaim fibres from CFRTP by the same thermal and chemical techniques used for CFRTS, with only a variation in processing conditions, *i.e.* solvent type, temperature and pressure. However, this approach completely degrades the matrix and therefore none of its original value is retained [32].

Tertiary and quaternary recycling of thermoplastics have been studied, however these are limited to commodity, low value materials such as poly(ethylene terephthalate) and low density polyethylene [107]. The premise of these studies was the search for alternatives to landfill for the significant volumes of waste from household products and single use items, and therefore value retention was not the primary research driver [112,113]. The low cost of virgin commodity polymers makes any secondary recycling processes economically impractical.

The incentive to recycle, and recover quality, increases with mechanical performance, and constituent value, therefore most research has so far been conducted with fibre reinforced PP, PA66, PC and PEEK.

2.3.1 Mechanical recycling

The plastic deformation behaviour of thermoplastics restricts the range of possible industrial comminution methods as impact, shear, and pressure will not result in brittle fracture. Cutting is the common comminution technique as it provides enough force over a sharp edge to fragment the polymer [51]. This limits the potential recyclate particle size distribution; shredding can only provide 40 % particles smaller than 0.5 mm, compared with the 90 % achievable for CFRTS through grinding [114].

Electrodynamic fragmentation has been used to create and propagate cracks within a CF-PEEK aircraft door hinge. This avoids shredder blade degradation and the production of harmful carbon dusts from the high CF content [115]. Reclaimed fragments were re-moulded into the original door hinge geometry. Tensile testing measured a 17 % strength knockdown compared with the virgin component.

There is limited economic viability in the use of CFRTP shred as a filler material for virgin thermoset matrices due to processing issues, *i.e.* blend viscosities and multiple temperature phases, and matrix bonding incompatibilities [116].

Mechanical recyclate is primarily produced as a precursor to compression moulding [117] and pelletization for injection moulding [118]. These remanufacturing processes will be explored subsequently in Section 2.3.2.

2.3.2 Melt processing

The ability of CFTRP to be thermally processed permits their primary and secondary recycling, *i.e.* repair and melt processing respectively. An example of primary recycling would be a dented CFRTP car part that can, in theory, be repaired *in situ* by heating beyond the T_g so that it can be remoulded back to the original dimensions. If the component is cracked, processing at melt may facilitate repair.

Secondary recycling for CFRTP refers to the shredding of a waste part to produce a variety of particle sizes, followed by the production of a homogenised recyclate. The recyclate is then remanufactured by processing above the matrix T_m and reforming into a new geometry [33].

Secondary recycling is the most commonly used in the literature. Primary recycling is rarely reported. This may be a consequence of a lack of repair performance data, *i.e.* the extent to which this may affect the fibre architecture, and thus the mechanical performance.

2.3.2.1 Injection moulding

Injection moulding is a closed moulding process used primarily for: long (> 3 mm) or short (1-3 mm) GF; or CF filled PP [119], PA6 [120], PA66 [121], and PEEK [122]. It is a common industrial technique for high-volume non-structural composite parts. This is due to the complex geometry and rapid processing capabilities.

The fibres and matrix are compounded, *i.e.* mixed at melt. The compound is extruded into a filament, which is then chopped into pellets. The compounding and chopping steps produce discontinuous fibres which, combined with a limited control of fibre orientation [123], restricts the mechanical performance of injection moulded parts [124]. This has so far limited the use of injection moulded CFRP to non-structural, low value applications.

High shear forces and temperatures are required during compounding for efficient mixing and homogenous fibre distribution. However, this has been shown to cause substantial fibre breakage and matrix degradation, Fig. 2.2 [33,116,125,126]. Fig. 2.2a shows how fibre length decreases as a function of extrusion/IM operations. The rheological frequency sweep in Fig. 2.2b indicates how complex viscosity decreases as a function of extrusion/injection operations. This is a major limitation of current CFRTP recycling as multiple extrusion/injection cycles can result in substantial property reduction.

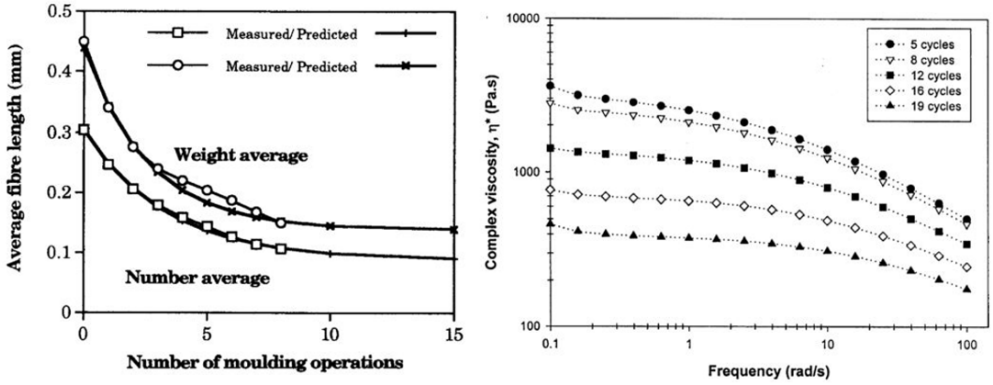

a) Average fibre length as a function of moulding operations

b) Complex viscosity as a function of rheological strain rate

Fig. 2.2. *a*) The degradation of fibre length as a function of extrusion/injection moulding cycle of CFRTP [126]. *b*) Complex viscosity as a function of strain rate and extrusion/injection moulding cycle [127].

Hausnerova *et al.* showed that multiple extrusion/injection cycles of CFPP caused a decrease in melt viscosity and die swell as a result of fibre breakage and degradation of the matrix. Severe fibre damage occurred at the first extrusion cycle, independent of extrusion speed or shear rate [124].

During processing the presence of fibres can also contribute to the amount of degradation through viscous heating [128]. Sarasua *et al.* recycled CF-PEEK, with both 10 % and 30 % Vf_F, over multiple extrusion/injection cycles. Over 10 cycles, the 30 % Vf_F specimens showed an additional 10 % and 12 % decrease in tensile stiffness and strength, respectively, compared the 10 % Vf_F specimens [129].

The non-structural applications of current injection moulded CFRTP make recycling economically unfeasible, considering the substantial performance reduction observed and the requirement of additional virgin material to enhance properties.

It is possible that, for this reason, there are no commercial CFRTP recycling operations. However, as CFRTP are emerging as a realistic alternative to CFRTS in some markets, there may be a greater incentive for CFRTP recycling technology R&D:

TenCate Advanced Composites [130]

TenCate has recently developed a new format of UD CF thermoplastic laminate that can incorporate a 'flow layer' comprised of long CF thermoplastic bulk moulding compound. The flow layer is used to provide value for reclaimed CFRTP as: a core material; a layer for tailoring thickness; or, a surface layer providing additional textures, *i.e.* overmoulding. The layer can be stamp formed to the outside of an existing CFRTP part to provide functionality, *i.e.* stiffeners, without expensive tooling equipment [131].

2.3.2.2 Compression moulding

Compression moulding of CFRTP involves the random scattering of CFTRP shred, prepreg off-cuts or EOL, into a press. The shred is heated to above the T_m and pressed to form the rCFRTP [132]. Li *et al.* mechanically recycled UD CF-PEEK material from aerospace waste, using a shredder as comminution. A range of particle sizes (19 – 4.9 mm) were collected and compression moulded into a panel. Results showed a drop in tensile strength of approximately 60 % for recycled parts [117].

Compression moulding direct from UD or woven CFRTP shred, either scrapped part or manufacturing waste, results in a composite with areas of high localised alignment but with a random global planar orientation, with respect to the loading direction. This produces a composite with variable mechanical properties throughout the structure and a significantly reduced mechanical performance compared with highly directional vCFRTP. Compression moulded chopped fibre CFRTP exhibit a complex failure with a combination of fibre tensile failure and interlaminar shear between the shred particles [132].

Compression moulding can produce rCFRTP with relatively high Vf_F and with long fibres as the shred is typically sourced from UD CFTRP scrap. However, the mechanical performance is significantly reduced compared with vCFRTP and thus the rCFRTP value will reflect this.

2.3.3 Thermoplastic Degradation

The character and magnitude of CFRTP performance reduction is based on how the thermoplastic polymer and fibre degrade under the specific processing conditions of the recycling method. Typically, fibre degradation during recycling occurs mainly under mechanical force however, if separate from the matrix, strong solvents and high temperatures can cause surface damage, see Section 2.2.2.4.

Thermoplastics are subject to a variety of degradative stimuli during manufacture, use and recycling. However, rapid degradation occurs primarily in processing, *i.e.* manufacture and recycling, due to excessive mechanical stresses and thermal stimuli. For example PP has shown temperature dependant degradation upon repeated cycles; multiple injection moulding extrusions at 240 °C showed acceptable degradation, as defined by the paper's authors, whereas in samples over 270 °C the degradation was extensive [127].

Degradation occurs through different mechanisms depending on stimuli and intensity [8]. For example, high-density polyethylene chain scission leads to chain branching and cross-linking under repeated mechanical and thermal stress, observed as an increase in viscosity. Whereas PP chain scission leads to a significant decrease in weight average molecular weight (M_w), and narrowing of the MWD, observed as a decrease in viscosity [116]. However, most semi-crystalline polymers exhibit chain scissions leading to a decrease in M_w [133].

Thermoplastics can degrade at elevated temperatures under thermal degradation pathways, *i.e.* thermal chain scissions, once the activation energy of the weakest bond has been reached. This does not require oxygen for propagation therefore is not observable by the appearance of oxygenated functionalities [8]. Thermo-oxidative degradation occurs at lower temperatures due to the catalytic effect of atmospheric oxygen on the associated chemical reactions. Hinsken *et al.* reported the successive reduction in M_w of unreinforced, unstabilized PP after multiple extrusions. A drop of 40 % was measured after the first extrusion then a 10 – 20 % decrease for every consecutive extrusion after that [134]. Thermooxidative degradation is easily observable using polymer characterisation techniques, *e.g.*

Fourier transform infrared spectroscopy, as the oxygen catalysed reactions form oxygenated functionalities along the polymer structure.

Either thermal or thermo-oxidative degradation will cause a reduction in mechanical performance. Semi-crystalline polymers are effectively composites of rigid polymer crystallites surrounded by amorphous polymer. Damage to the polymer chains causes variation in crystal structure, amorphous-crystal linkages and amorphous polymer lengths. Changes in polymer structure can affect crystal formation which may result in tensile stiffness reduction as this is strongly dependent on crystallinity [33]. Polymer chains in the amorphous regions uncoil and slide with respect to each other. This behaviour absorbs energy during loading therefore changes in polymer length will affect the tensile strength and toughness of a polymer [8].

It is possible to add virgin polymer to the recyclate blend to improve the mechanical properties. The effect of virgin and recycled blend ratios on the mechanical properties of thermoplastic homopolymer blends has been a topic of interest [135–137]. One of the major drawbacks to this is that even if the blended polymers are of the same type, *i.e.* virgin and recycled PA6, the mechanical properties of the blend materials are usually well below those expected [138]. This is due to the fact that the material properties do not obey additivity rules on the basis of a linear composition law, as a consequence of the variability in molecular weight distribution and molecular functionalities of virgin and degraded polymers [138]. This makes the rheological and mechanical performance of a homopolymer blend recycled CFRTP (rCFRTP) unpredictable and inevitably inferior in performance to vCFRP.

Much of the pure thermoplastic and thermoplastic composites recycling studies conducted over the past decades point to the degradative effect of the processing conditions as the primary source of component property reduction over repeated cycles [32,33,116]. The challenge for current recycling methods is therefore to develop a recycling process with limited thermal degradation and mechanical stresses.

2.3.4 Summary

Mechanical recycling for CFRTP produces a much coarser recyclate than for CFRTS therefore the degradation of CFs is less severe, however the collection of pure matrix recyclate is not possible. Shredding is used as precursory comminution, at different grades, for both injection and compression moulding recycling methods.

Electrodynamical fragmentation has reported promising results considering its early stages of development. However, the energy requirement of the process, and how this scales with industrial volumes, is unknown.

Injection moulding is the most common recycling process for CFRTP as the processes are analogous to virgin manufacture and are suitable for rapid manufacture. As most vCFRTP from injection moulding methods start with random orientation, the disadvantage of having no alignment process in remanufacture is less significant. Severe matrix degradation and fibre breakage results in low performance recyclate and thus low value rCFRTP. This makes recycling by extrusion/injection processes economically unviable for low value thermoplastic matrices.

Compression moulding of CFTRP recyclate can be used in rapid remanufacturing. Large shred sizes are applicable where UD CFRTP fibre architecture can be maintained, however the mechanical properties of the rCFRTP are poor due to crack propagation between distinct fibre regions.

These disadvantages are a consequence of the omittance of a fibre-matrix separation step; this would avoid extensive degradation observed in the reprocessing of reinforced recyclate.

2.4 Remanufacturing recyclate

Sections 2.2 and 2.3 have illustrated that fibre reclamation processes for thermosetting CFRP exist at the commercial and lab scale and can reclaim high yields of fibres with minimal reduction in mechanical properties. Maximum fibre

value retention is dependent on the quality of the rCF and the performance of the remanufacturing process.

Most commercial fibre reclamation processes result in a loss of fibre architecture, *i.e.* disorientation, and include preliminary comminution, which randomly cuts the composite, producing a discontinuous fibre architecture. The randomly oriented, low bulk density fibre 'fluff', Fig. 2.3, can be remanufactured, however, the final properties of the remanufactured material are highly dependent on the degree of fibre alignment [60,133]. Reclamation also strips fibres of their sizing therefore additional processing steps are required to produce rCFRP [32].

Fig. 2.3. Low bulk density (fluffy), randomly oriented dry fibre format of rCF from pyrolysis [139].

CFRP structural performance is largely dependent on the fibre fraction, fibre orientation, fibre-matrix adhesions and intrinsic fibre mechanical performance. The discontinuous nature of rCF necessitates fibre alignment to provide maximum performance and maximum value [140]. This is especially pertinent as the rCF obtained through contemporary reclamation techniques have almost equivalent properties to vCF. The subsequent processes are ordered in increasing ability for fibre alignment and thus increasing potential to produce high performance rCFRP.

2.4.1 Direct moulding

The most common methods for direct moulding of rCFs are injection moulding, bulk moulding compound (BMC) and SMC compression. All can be described as the compression moulding of a premixed material, or *charge,* consisting of virgin matrix impregnated with rCF. Injection moulding is more commonly used with thermoplastic matrices and is detailed in Section 2.3.2.1. The highest performance rCFRP from direct moulding are summarised in Table 2.3.

BMC and SMC have a similar composition however the latter can achieve a higher Vf_F. SMC is typically reinforced with longer fibres and is provided in sheet format, as opposed to the bulky BMC charge [141]. Any fibre length from micron-sized particles to long fibres can be used for BMC and SMC, although increased fibre length and fibre volume fraction afford improved properties. Typically, SMC is used in higher performance and therefore higher value applications [55].

SMC/BMC is a useful CFRP manufacturing technique mainly due to the manufacturing speed and simplicity afforded by sheet-form manufacture in comparison to traditional autoclave and hand lay-up methods. However, the maximum performance obtainable from SMC is limited if the fibre feedstock has a low level of alignment; a problem for the current rCF format. Although some SMC can be made from chopped continuous tows, the global material orientation is minimal. The low bulk-density rCF contributes to reduced mechanical performance by broadening fibre length distributions after chopping, as some fibres are too short for SMC manufacture [55]; and reducing fibre stacking, which translates to poor fibre distribution and increases potential for voids [142].

The literature indicates that the mechanical performance of SMC/BMC made using rCF is higher than those available for SMC made using vGF; which is this the most common SMC composition [32,143]. Comparable properties to vCF-SMC have been reported in the literature [32].

From a value perspective, SMC can be used to produce rCFRP material of comparable properties to vCF-SMC and therefore has the potential to retain fibre

value. However, if the rCF were reclaimed from structural, high performance CFRP there may be a significant disparity in market values. As the rCF feedstock is typically from thermal/chemical reclamation, the matrix value is completely lost, therefore additional virgin matrix is inevitably required for remanufacture.

Commercial sources of rCF provide milled, chopped and nonwoven fibre forms for out-of-house compounding and do not provide the BMC/SMC material directly. Turner *et al*. produced SMC and BMC using rCF from the University of Nottingham fluidised bed technique [144].

2.4.2 Compression moulding of nonwoven rCF preforms

Nonwoven fabrics are 2D or 3D discontinuous/long fibre preforms, of random orientation, which are prevented from losing their architecture by methods other than weaving, *i.e.* loose stitching, binding or entanglement. Common nonwoven formats include: 2D mats, 3D mats and veils. Examples of commercially available nonwovens can be found in Fig. 2.4. The highest performance compression moulded nonwoven rCFRP are summarised in Table 2.3.

The rCFs used for nonwovens can be short (< 10 mm) or long (40 – 90 mm), they are typically of random orientation, yet marginally superior to SMC due to alignment-inducing processing phenomena [65,145]. Nonwovens are dry fibre preforms, therefore they require additional processing to transform the loose, dry rCF into a dry fibre mat. These processes are typically analogous to wet paper making [146,147] and GF chopped strand mat production [148]. The mat is subsequently impregnated with virgin matrix, either in liquid [145] or resin film [63] formats, and subsequently compacted *via* compression moulding.

The University of Nottingham (Pickering, Wong and Turner *et al.*) compared the mechanical performance of a range of epoxy rCFRP materials made from different rCF (12 mm) formats and manufacturing processes [78,143,144]. It was determined that BMC products are limited to a Vf_F of 10 %, however if the fibres

can be made into an intermediate nonwoven they can reach a Vf_F of up to 44 % due to an alignment bias of the paper making technique used in preforming. However, high Vf_F was only achieved using high compaction pressures (14 MPa) which caused fibre damage and therefore capped the practical Vf_F at ~ 30 %. Nonwoven rCFRP showed good matrix-fibre adhesion and outperformed GFRP in terms of specific strength and could also be cost competitive with vGFRP if produced at industrial volumes.

Nakagawa *et al.* reported that rCF from solvolysis could be converted to a nonwoven and compression moulded with unsaturated polyester resin to form an rCFRP with enhanced σ_{ult} (+ 40 %) and similar E_T to mass production GFRP, *i.e.* chopped strand mat [149].

Shah *et al.* reviewed previous rCFRP manufactured through a liquid composite moulding process, covering nominally-random and partially-oriented nonwovens. Low areal density and poor compaction behaviour necessitated compression moulding (5 – 10 MPa) to achieve a practical Vf_F (~ 30 %). Results showed that although the partially aligned rCFRP performed better than the random rCFRP, the properties were less than predicted from rule of mixtures. This is likely due to a high void content (10 %) and fibre damage from high compaction pressures [145].

a) TFP rCF veil b) CFK rCF fleece c) ELG rCF mat

Fig. 2.4. A range of commercially available rCF nonwovens of varying areal weights [65,67,146].

Nonwoven rCF have also been impregnated with virgin thermoplastic matrices to form rCFRTP. Wei *et al.* produced rCF paper intermingled with PA6

fibres which were stacked and compacted into plates using compression moulding. A pressure range of 5 to 8 MPa was determined as the most ideal for ensuring good impregnation with minimal fibre fracture [150]. rCFRTP nonwovens are currently available at the commercial scale:

ELG, Carbon Fibre Recycling Ltd. [65]

ELG have used the papermaking technique to produce nonwoven mats using pyrolysed rCF from prepregs and cured laminate waste. These are commercially available, around 1000 metric tonnes per annum in a range of industrially applicable dimensions and areal weights. Commingled nonwovens are also available with PP, PA and PPS fibres [151].

TFP, Technical Fibre Products Ltd [146]

TFP produce nonwoven veils as surfacing or semi-structural layers, *i.e.* thermoset toughening. They have worked with Boeing, Ford, Toho Tenax, and the University of Nottingham in projects such as AFRECAR and HIRECAR to develop applications for rCFs [152]. They are currently world leaders in the dispersion and processing of single filament rCF for wet-laid nonwovens, however, commercial launch date and productivity is unreported [153].

Sigmatex [154]

Sigmatex have produced a commingled nonwoven mat made from rCF and PP or PA fibres. The are available as UD or multiaxial mats with a 180 g/m^2 areal weight and a 45 % Vf_F, 85 % of fibres are aligned which suggests the potential for use in high-performance applications however a 50 % and 30 % reduction in tensile and flexural moduli, respectively, have been reported [155].

2.4.3 Fibre alignment

Fibre alignment is of great importance when high performance is a design priority and when the fibre format is discontinuous and randomly oriented, *i.e.* rCFs. Intermediate nonwovens are bound by a maximum 30 % practical Vf_F thus techniques which can provide orientation to the fibres may aid in surpassing it. Fibre alignment also improves stacking which enables: improved matrix

impregnation, lower compaction pressures, and higher composite Vf_F [145]. The highest performance rCFRP from fibre alignment methods are summarised in Table 2.3.

There has been a wealth of research into increasing fibre alignment percentages, using: pneumatic, electric field, ultrasonic, and fluid based methods [140]. Of these, hydrodynamic alignment techniques have provided the highest degree of alignment. The following techniques can provide the highest alignment and thus the potential for the highest rCFRP performances:

Hydrodynamic centrifuge, the University of Nottingham (Pickering *et al.)* [156]

This method is a contemporary iteration of the original hydrodynamic centrifugal alignment process developed by the UK MoD in the mid-1970s, where a fibre dispersion in a water/glycerine mixture is sprayed *via* a convergent nozzle onto a rotating, perforated mesh drum [140]. Dispersion fluid is centrifugally separated from the mat through the drum perforations. Using short fibres (5 mm) enabled an alignment of 90 % within ± 10°, it was reported that alignment quality is dependent on fibre length and the fibre dispersion concentration [157]. The scalability of the process to industrial terms is a concern due to limited continuous production and long drying times that arise from using a glycerine carrier medium.

HiPerDiF alignment method, the University of Bristol (Yu, Longana *et al.*) [158]

The High Performance Discontinuous Fibre alignment method is a hydrodynamic fibre alignment technique that uses multiple directed streams of an aqueous fibre suspension to mechanically align the fibres by a momentum change upon impact with a near perpendicular collision surface. This method is described in detail in Section 3.1.2.1.

2.4.4 Summary

The highest performance examples of all remanufacturing methods outlined above are summarised in Table 2.3. Direct moulding techniques offer a rapid manufacturing solution for rCFRTS, however, the lack of fibre alignment is reflected in significantly reduced mechanical properties. They have been shown to outperform vGF-SMC yet, although this provides a viable market for rCF, it is a fraction of the market value of vCF and the vCFRP from which the fibres are reclaimed.

A higher degree of fibre alignment has been achieved using nonwoven preforms. When compression moulded into either rCFRTS or rCFRTP a higher Vf_F, and thus enhanced mechanical performance, can be achieved. Despite this improvement the properties only match the performance of vGF chopped strand matt and are substantially lower than vCFRP. Inferior mechanical properties are a consequence of a Vf_F plateau. This is limited by the fibre breakages caused from the high compaction pressures required due to fibre misalignment.

rCFRP produced from fibre alignment methods have reported the highest mechanical performances for vCFRP (from discontinuous fibres) and rCFRP. This is a consequence of improved stacking, improved matrix impregnation, lower compaction pressures and higher composite Vf_F. The high degree of alignment makes it possible to create high value rCFRP from reclaimed constituents therefore any novel recycling process must include alignment if the aim is to produce high performance rCFRP.

Table 2.3. Summary of the mechanical properties of rCFRP made from rCFs in order of increasing fibre alignment. The rCFs were recovered from mechanical, thermal and chemical reclamation methods.

Manufacturer	Recycled fibre format	Matrix	Manufacturing	Vf_F	E_T	σ_{ult}
				%	GPa	MPa
Ogi [57]	Mechanical recyclate (CFRTS)	ABS	Pelletization (IM)	24	12	102
Takahashi [159]	Mechanical recyclate (CFRTS)	PP	Pelletization (IM).	24	21	101
Szpieg [160]	Milled (200 micron)	MAPP	Film CM (13 MPa)	30	9	50
Turner *et al.* [144]	Fibres with resin and filler	Epoxy	BMC	10	20	71
Shah *et al.* [145]	nonwoven (10 mm)	Epoxy	Liquid CM. (2.5 MPa)	25-26	12-13	84-100
Nakagawa *et al.* [149]	long fibre nonwoven (25 mm)	UP		16	5.5	90
Feraboli *et al.* [84]	long fibre nonwoven (6-10 mm)	Epoxy	Liquid CM (Vacuum)	33	29	197
Wei *et al.* [150]	nonwoven paper (6 mm) [(a)]	PA6	Comingled CM (8 MPa)	23	18 [(b)]	460 [(b)]
ELG [151]	long fibre nonwoven (40-90 mm)	Epoxy	Liquid CM.	30	35 (weft)	430 (weft)
					23 (warp)	286 (warp)
				40	31.9 (weft)	312 (weft)
					18.1 (warp)	189 (warp)
Turner *et al.* [144]	Aligned fibre	Epoxy	SMC (5-10 MPa)	23	44	282
	Aligned nonwoven mat	Epoxy	Autoclave prepregs (0.7-1 MPa)	27	44	335
	Aligned nonwoven mat	Epoxy	Comp. mould prepregs (5-10 MPa)	44	80	422
	Aligned nonwoven mat	Epoxy	Liquid comp. mould. (5-10 MPa)	23	44	282
Shah *et al.* [145]	Aligned nonwoven mat (10 mm)	Epoxy	Liquid comp. mould. (2.5 MPa)	27-34	19-32	133-174
Pimenta and Pinho [60]	Aligned nonwoven mat (10 mm)	Epoxy	Resin film CM. (7 MPa)	30	25.4	358
Longana *et al.* [63]	Highly aligned preform [(c)]	Epoxy	Resin film CM (0.7 MPa)	28.3	52	614
	Highly aligned preform [(d)]	Epoxy	Resin film CM (0.7 MPa)	28.5	40.4	279
Pimenta and Pinho [161]	woven fabric (12 mm)	Epoxy	Resin film CM	55	66	271
	woven fabric (12 mm)	Epoxy	Resin film CM (0.7 MPa)	50	56	634

(a) Commingled fibre paper. (b) Flexural properties. (c) rCF after one recycling loop. (d) rCF after two recycling loops. CM = compression moulded. IM = injection moulded.

2.5 Discussion

2.5.1 Current technological outlook

Currently, there is a distinct disparity between rCFRP and vCFRP value. The value chains for the waste CFRP management processes explored previously are shown in Fig. 2.5 - Fig. 2.8.

Mechanical recycling can be employed for both CFRTS and CFRTP however the recyclate obtained from both is substantially limited in value. The value retention of mechanical recycling is illustrated in Fig. 2.5. Compared with thermal and chemical treatments the energy cost of recycling is favourable, however the low performance rCFRP produced renders this the lowest quality reclamation process for CFRP overall [59]. Mechanical comminution is a precursory step in most alternative reclamation technologies however the fragment size is significantly larger than that obtained from grinding. The shred obtained results in discontinuous fibres, but fibre breakage is less extensive.

Three fibre reclamation processes are available that provide value from the fibres; pyrolysis, fluidised bed pyrolysis, and solvolysis. Of these, pyrolysis is the only major reclamation process operating at a commercial scale, yet the cumulative throughput of these plants is a fraction of the prospective waste volumes [65,67,69,71]. The quality of the fibres produced makes pyrolysis economically feasible and has led to the development of remanufacturing processes. The value retention of commercially operational pyrolysis reclamation processes is depicted in Fig. 2.6.

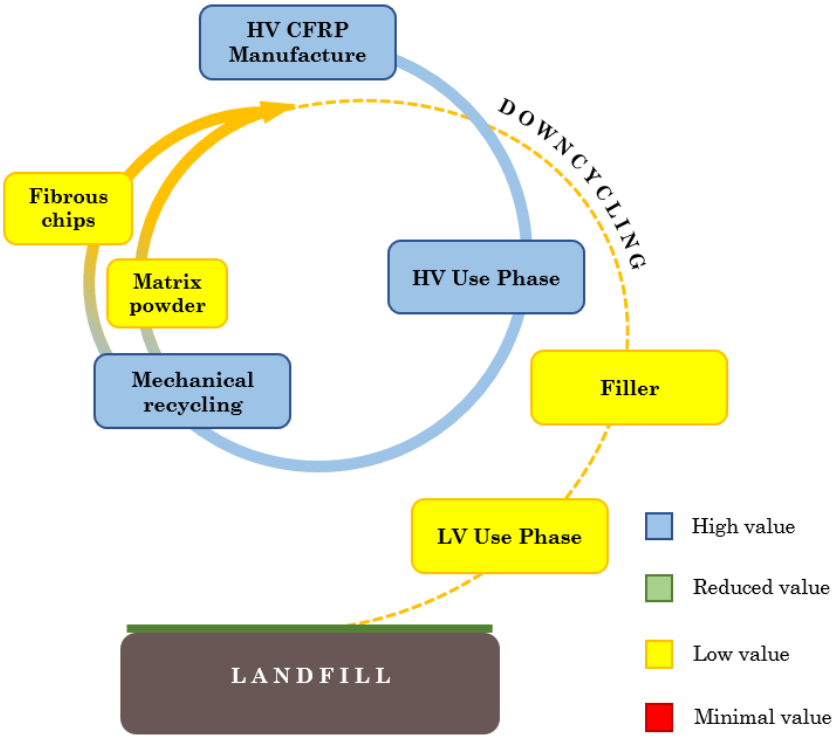

Fig. 2.5. The value cycle of mechanically recycled vCFRP. The value from high value (HV) CFRP is reduced to low value (LV) filler in virgin CFRP through downcycling. LV CFRP has one LV use phase before sent to landfill.

Fluidised bed pyrolysis has the added advantage that it incorporates a grading system for mixed waste streams. This is the most realistic CFRP waste stream format given the multi-material nature of its current application in industry, *i.e.* aerospace and automotive. However, the mechanical performance of the reclaimed fibres is inferior to pyrolytic and solvolytic methods, this may be a reason why it has not yet progressed beyond the pilot plant scale [109].

Solvolysis has the potential to provide high quality fibres and some value from the matrix in the form of polymeric oils or, in some cases, monomeric units [102,103]. Although, there is little proof of the commercial viability of the separation and purification processes required to provide industrially applicable matrix products and little evidence supporting the yields that can be obtained.

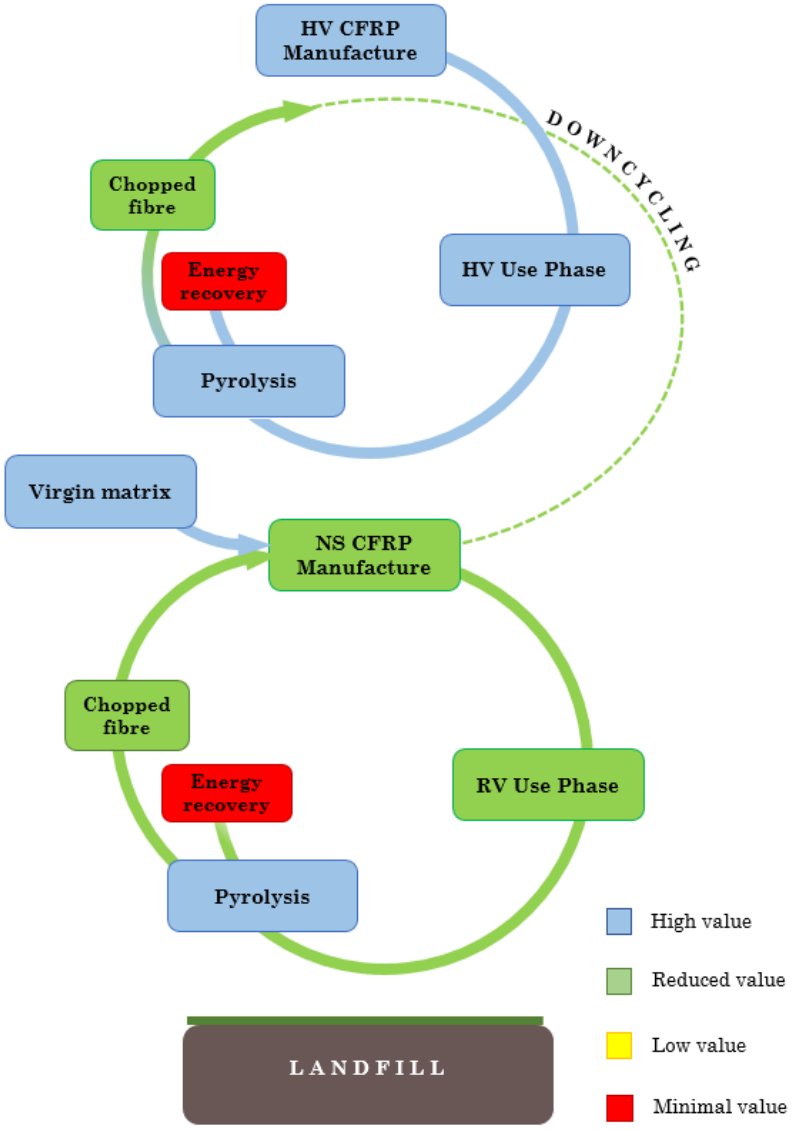

Fig. 2.6. The value cycles of vCFRP recycled using pyrolysis. Value from chopped reclaimed fibres is downcycled into a reduced value (RV) production cycle. Value is facilitated through remanufacture of non-structural (NS) CFRP *via* impregnation of nonwovens with virgin matrix. Value from matrix is severely reduced.

The studies reporting the highest quality fibres are all conducted at the laboratory scale and with industrially unfavourable solvents and reaction conditions. The value retention potential of the highest performance solvolysis reclamation processes, in terms of quality recyclate, is portrayed in Fig. 2.7. The non-structural CFRP (NS CFRP) manufacturing step describes the current

highest performance commercial remanufacture for CFRP, *i.e.* discontinuous CF nonwoven impregnation with epoxy. Supercritical fluid solvolysis can be conducted with lower hazard solvents however the apparatus required to create the reactive environment are dangerous to run, expensive to maintain and difficult to scale for industrial volumes.

Fibres reclaimed from pyrolysis/solvolysis require remanufacturing before their properties can be realised. It is evident that fibre orientation with the primary loading direction is paramount to obtaining their maximum performance. BMC/SMC offer a solution for rapid manufacture but at the cost of orientation, which is random and difficult to control. The re-impregnation of nonwoven mats is currently the most commercially viable technology and is already available, albeit in limited volumes compared with industrial demand.

Nonwoven reinforcement combined with compression moulding enables rapid manufacture however the rCFRP value is limited by fibre misalignment. Fibre alignment processes have shown the most promise in terms of performance, however, both highest performing processes currently operate at lab scale therefore their potential for scalability and thus their commercial viability is unknown. It is clear that a high level of alignment offers high fibre volume fractions which results in high mechanical performance.

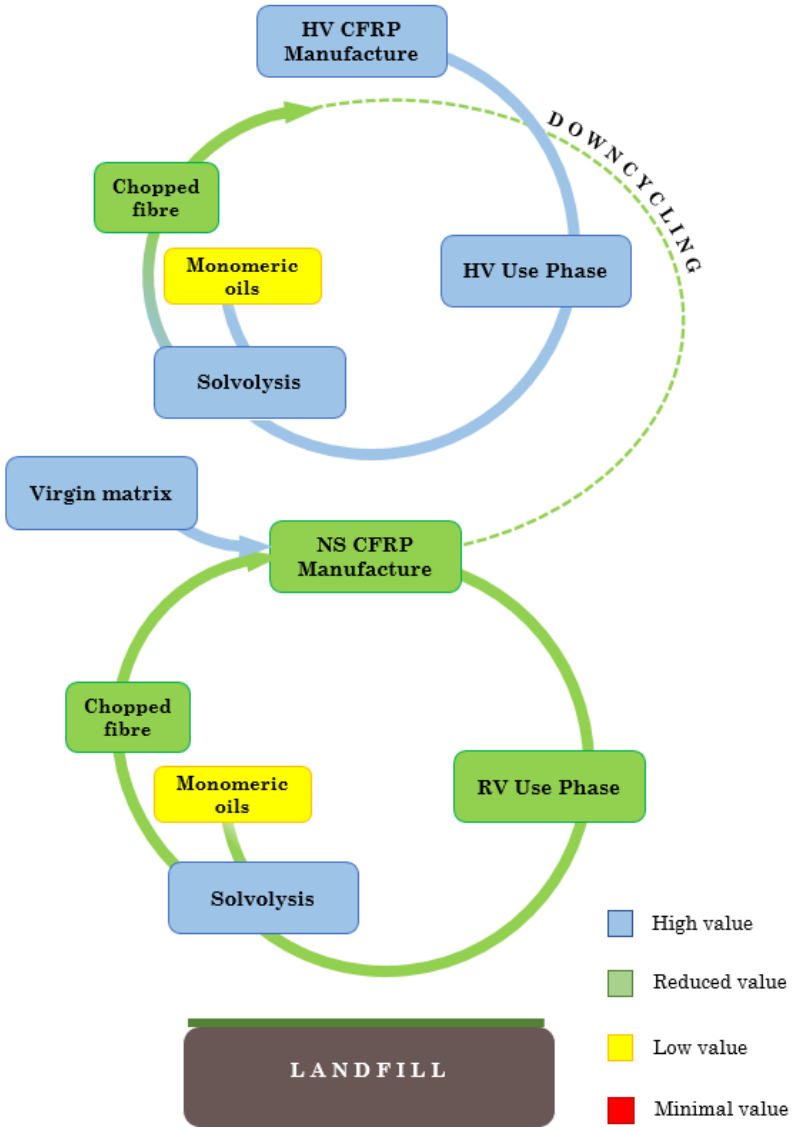

Fig. 2.7. The value cycles of vCFRP recycled using solvolysis. Value from chopped reclaimed fibres is downcycled into a reduced value (RV) production cycle. Value is facilitated through remanufacture of non-structural (NS) CFRP *via* impregnation of nonwovens with virgin matrix. Value from matrix is severely reduced but has some resale value.

CFRTP recycling has the potential to reclaim value from the matrix in addition to the fibres however current technologies result in mechanical performance knockdowns. This is a consequence of poor fibre alignment, fibre breakage, random fibre length distribution and matrix degradation or, typically, a combination of the four [33,125,126]. It is possible to enhance the properties of the

degraded rCFRTP by adding vCFRTP to the blend, but the low cost of virgin commodity polymers makes any secondary recycling processes for CFRTP economically impractical. The value retention potential of a CFRTP recycled following the extrusion/injection approach is illustrated in Fig. 2.8.

CFRTP manufacturing waste, *i.e.* prepreg offcuts, can be fed back into manufacturing lines or as shred for compression moulding; the former being the highest value application. TenCate have commercialised the ability of using discontinuous fibre rCFRTP, as interleaves (in compression moulding processes) or functionalising surfaces (as an over moulded layer). As the waste is providing additional functionality to the vCFRTP, *i.e.* as a performance enhancer (increased toughness) or enabling a reduction in manufacturing complexity (over moulding stiffeners) it can be considered a high value, primary recycling route [131]. This is an effective method for minimising manufacturing waste, but it is not a complete solution for the EOL CFRP.

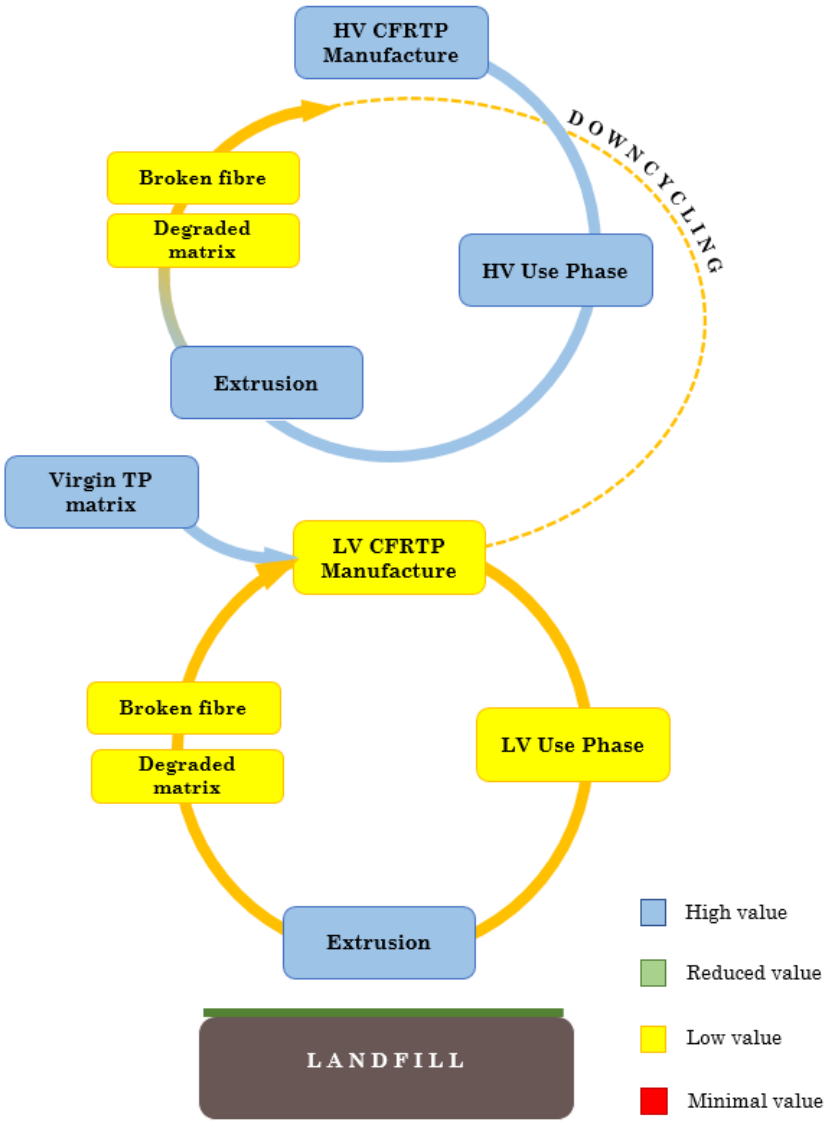

Fig. 2.8. The value cycle for CFRTP. high value (HV) CFRTP is extruded, forming a usable recyclate but causing substantial damage. Constituents are effectively downcycled to a low value (LV) CFRTP and LV application due to property reductions. Additional virgin matrix can be used to boost properties, but HV is never retained.

Reclamation processes can provide high quality fibres, and these have already been remanufactured into preforms used to create rCFRP of reasonable quality, thus avoiding landfill and, to some degree, closing the loop. The drawback to these processes is that for a truly closed-loop recycling process to be economically sustainable at high production volumes, it must produce a rCFRP

with properties equivalent to the vCFRP. The large volumes of high-quality waste will be downcycled to applications with reduced property requirements, *i.e.* non-structural applications, which will undoubtedly have a comparatively reduced industrial value and demand. This significant disparity between vCFRP waste supply and rCFRP demand will result in a partially redundant, low-value excess that may ultimately end up in landfill anyway.

For the industry to provide economically sustainable closed-loop production of CFRP, as stipulated by the Circular Economy paradigm supported by Composites UK for future composite manufacture, there needs to be a range of applications, from high-performance structural to non-structural, for the rCFRP it creates. Therefore, there needs to be reclamation and remanufacturing technologies that can provide it. It is not the ability of the rCFRP to match any vCFRP component performance, as there are many variants with correspondingly varied mechanical performance, but the ability to match the mechanical performance required for high-value applications. This increases the potential markets for rCFRP and reduces the downcycling of recyclate by closing the production loop.

To achieve high-value rCFRP the applied reclamation technology must provide high-quality recyclate, with limited degradation to either fibre or matrix properties. This can only be achieved by fibre-matrix separation and the use of thermoplastic matrices. The remanufacturing process must include a fibre alignment process to maximise the fibre value.

2.5.2 Market challenges for rCFRP

Despite the industry wide acceptance of the importance and necessity of CFRP recycling there are still numerous obstacles to the development of rCFRP. This section aims to cover the critical issues hindering the progression of CFRP recycling and rCFRP market inclusion. Over the past decade this topic has seen much debate [5,20,89,162,163], the frequently reported issues are as follows:

Industrial recycling infrastructure

The first major challenge facing CFRP recycling is the lack of a stable and robust CFRP recycling chain, starting with the logistically efficient collection, identification and sorting of mixed waste, and ending with reliable commercialisation of the finished rCFRP [5,18].

Intra-industry cooperation

There is a lack of organisation and communication between researchers, suppliers, manufacturers and end-users which is essential for understanding the current technological landscape and marrying the demands and outputs of industry, academia and the customer [164]. A coherent network of communication will help streamline development of CFRP recycling technologies and rCFRP products. Effective communication and trust through the supply chain, *i.e.* between suppliers, manufacturers and recyclers, is imperative to ensuring adequate certification of waste material provenance, continued and reliable waste volumes and the elimination of any reverse engineering of proprietary materials or components [165].

A global conversation will also aid in generating suitable legislation regarding: government penalties and credits for recycling compliance, regulations covering process and waste material re-certification, waste management licensing for health and safety and waste recycling responsibility, *i.e.* the determination of who is legally responsible for the recycling of CFRP manufacturing and EOL waste is not explicitly clear [26].

Identification, sorting and cleaning

For a reclamation process to operate efficiently it is important that the appropriate waste feedstock is used, or, that the appropriate reclamation process is used for the waste feedstock. In either case this relies on waste identification, sorting and purification. The mixed material applications of CFRP therefore pose a concern for CFRP reclamation process that use EOL waste streams [18]. Currently, most CFRP waste sorting is completed by hand which is time consuming, expensive, and unsuitable for managing predicted future waste volumes [166].

This will require a combination of material tracing and identification methods from the material supplier, *i.e.* serial codes or molecular tagging, chemical classification techniques used by the recycler prior to reclamation, *i.e.* Fourier Transform Infrared Spectroscopy, and selective sorting techniques for multi-materials, *e.g.* magnetic separators, floatation tanks for density separation; or selective dissolution [167].

Waste CFRP supply and rCFRP market demand

Most of the CFRP material currently operational were designed for a long service life [168]. The industry must provide and maintain a consistent supply of waste considering the disparity between component life span, and thus EOL waste frequency, from aerospace, wind and automotive components [18]. In combination with a stable waste supply there must also be an equally reliant recycling infrastructure in place to turn over rCFRP at a rate that can meet the demand of the market.

Although there are reclamation technologies operating commercially (see Section 2.2.2) they are not yet functioning at the volumes required to meet predicted waste volumes; ELGs productivity (*c.* 2014) is approximately 34 % of the predicted UK CFRP waste volume [169]. This is likely a direct consequence of the lack of market pull-through from limited applications of rCF, but also in some part due to the relatively contemporary emergence of pyrolysis and its continual development.

Limited rCFRP markets

The chopped, low bulk-density, random rCF obtained from all commercial reclamation processes is suitable for a limited range of products, applications and processes (see Section 2.4). One of the major challenges facing the industry is the development of remanufacturing technologies for rCF and applications and markets for the rCFRP produced, although remanufacturing technologies are showing academic and industrial investment of late (see Section 2.4). There has been substantial development in non-structural applications for rCF due mainly to the remanufacturing difficulties and the low mechanical performance requirements [5,109,162].

The inclusion of rCF in non-structural applications has been a catalyst in the development of remanufacturing techniques and an understanding of the performance characteristics and limitations of rCFRP. However, the major issue with non-structural applications is that the maximum performance, and thus maximum value, of the fibres is not exploited which is undesirable for the industry as it is not conducive to an acceleration in CFRP recycling and rCFRP adoption; the current trend in CFRP recycling is to seek higher value from recyclate [170].

Mechanical performance and environmental impact data

One of the major drawbacks for CFRP component designers is the lack of mechanical performance data for structural rCFRP, especially long-term stability data, *i.e.* fatigue and environmental stability. This is a direct consequence of the lack of structural rCFRP composite demonstrators available in industry and in the literature [5,32].

It is generally accepted that CF reclamation processes require a fraction of the energy of vCF production and therefore a rCFRP part is considered as having a lower environmental impact than conventional materials [5,49,89]. However, it is important to quantify the economic and environmental impacts of an emerging material and technology and to compare with alternative methods to greater understand the true benefits.

Life cycle analysis (LCA) is a cradle-to-grave evaluation tool, which can be used to summate the environmental and economic impacts of a recycling process, or recycled material, or the entire life-cycle. LCA is slowly gaining popularity in the composites industry however it is still in its infancy and is not an industry wide evaluation tool. Therefore, a lack of accurate data sources exists which has resulted in a difficulty in process cross-comparison and an inaccuracy in evaluation outputs, see Chapter 6.

2.6 Conclusions

This chapter presented an overview of the incentives for recycling, a critique of contemporary technologies used to reclaim and remanufacture CFRP, and an extensive evaluation of the market opportunities and challenges for rCFRP.

Reviewing the incentives for CFRP usage, and its effective recycling, it is apparent that there is a drive from end-users, governments and the composites industry to not only provide adequate waste management, for current and predicted waste volumes, but to develop a sustainable production cycle that fits into the Circular Economy paradigm. It is therefore equally important to recycle with the intent of finding a valuable application for the recyclate. The development of a recycling process able to produce a high value, structural rCFRP will successfully close the loop for CFRP manufacture and meet the requirements for the circular economy paradigm, as supported by The UK Composite strategy.

The critique of the state-of-the-art for recycling determined that the industry is currently able to reclaim CF on a commercial scale with a good retention of mechanical properties. Despite this, there is still a substantial disparity between commercial productivity and predicted waste volumes from market growth.

To achieve high-value rCFRP, the applied reclamation technology must provide high-quality recyclate, with no degradation to either fibre or matrix properties. This can only be achieved by fibre-matrix separation and thus the use of thermoplastic matrices. The remanufacturing process must include a fibre alignment process to maximise the composite value.

Establishing the market opportunities and challenges showed that for the continual development of CFRP recycling there must be a strong recycling supply chain. Without structural applications for rCFRP there will not be a broad enough market for rCF. This is an additional deterrent for industry, and for recyclers, who do not wish to be stuck with a growing stock of unusable rCF. Without a high-performance, high-value application for rCFRP the closed-loop production paradigm, and thus the stable recycling infrastructure, cannot be realised.

3 A closed-loop recycling process: experimental design

This section draws from the conclusions of the literature evaluation (see Chapter 2) to establish of what an idealised, economically sustainable closed-loop production cycle for CFRP might consist. It then compares the fundamental steps of the proposed production cycle with available technologies to establish the key areas for development.

A novel combination of processes is devised to fulfil the technological requirements of the closed-loop recycling process. The subsequent experimental investigations will quantify the efficacy of the process (see Chapters 4 and 5). The methodological details of which are thoroughly detailed in the subsequent sections; Section 3.2, Section 3.3, and Section 3.4.

3.1 CLRP: Concept development

The literature evaluation in Chapter 2 produced the following conclusions:

- A sustainable CFRP production cycle, *i.e.* closed-loop, is essential for compliance with societal, governmental and industrial demands for a CFRP waste solution.

- rCFRP must retain high mechanical performance for a closed-loop CFRP production cycle to be economically sustainable.

- Current reclamation technologies can produce rCF with marginally reduced mechanical properties however all continuous fibre architecture is lost. Reclamation methods also fail to retain any value from the matrix, this requires additional virgin matrix for remanufacture. *A novel reclamation method must be developed that limits fibre degradation and can retain value from the matrix.*

- Thermosetting matrices cannot currently be reclaimed without total degradation. Thermoplastics have the potential for reclamation without property reduction and the complete separation of fibre and matrix required for fibre alignment. Retention of fibre and matrix properties can be achieved if melt phase separation is avoided.

- Continuous fibre architecture is completely lost during reclamation. Discontinuous fibres are less prone to breakage during processing than continuous.

- Current commercial remanufacturing methods cannot provide the degree of fibre alignment required to produce rCFRP of similar performance to vCFRP. *A Novel remanufacturing method with an alignment stage is required to provide a high-value rCFRP.*

The closed-loop production cycle presented in Fig. 3.1 was developed to provide solutions to these issues. The cycle starts with a high-value CFRTP, *i.e.* of mechanical performance suitable for use in a high-value application; in this case, a vehicle semi-structural application. The lifetime of the vehicle being the high-value use phase (HV Use Phase).

The high-value CFRTP is made from discontinuous CFs and a thermoplastic matrix. An alignment process is included as part of the closed-loop

remanufacturing process to ensure high mechanical performance from the discontinuous fibres. The change in colour from blue-green-blue for discontinuous CFs represents how they lose value after reclamation due to the low bulk-density form but regain their value again through alignment.

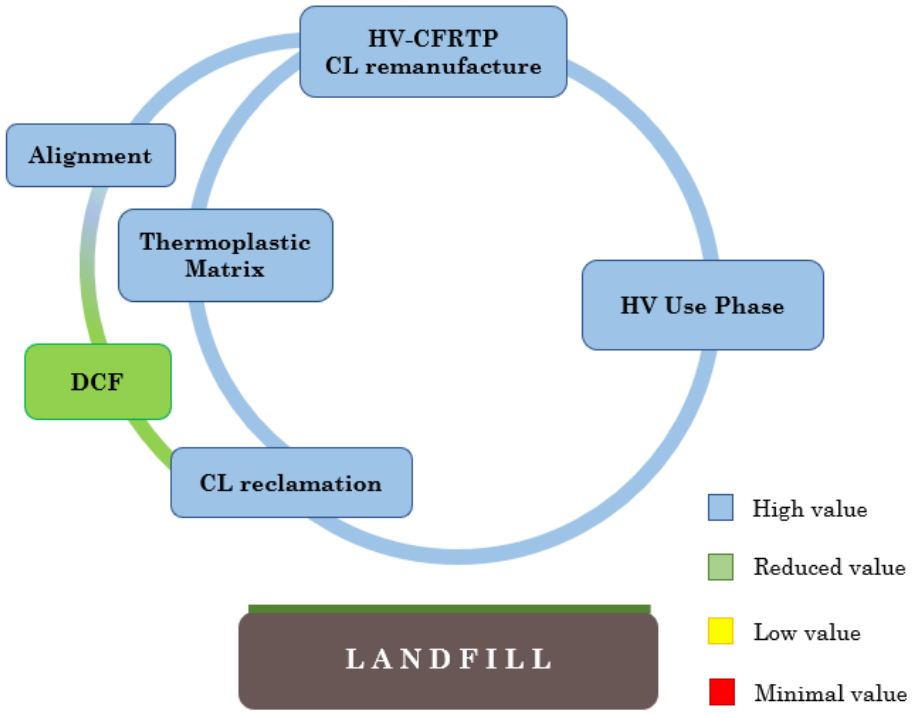

Fig. 3.1. The value cycle of a proposed closed-loop recycling process for high-value carbon fibre reinforced thermoplastic polymers (HV-CFRTP) based on the conclusions drawn from the literature. DCF = discontinuous carbon fibre. CL = closed-loop.

The closed-loop reclamation process must be non-thermal to provide full separation of fibres and matrix and to maintain the performance of the thermoplastic matrix. The high-value CFRTP manufacture must accommodate the use of discontinuous fibres and a thermoplastic matrix to produce a high-value CFRP material.

3.1.1 Closed-loop reclamation

Currently, thermoplastics are the only matrix material that can be reclaimed without complete matrix destruction, but melt processing consistently results in fibre breakage and matrix degradation. The van der Waals' attractions and hydrogen bonds within thermoplastic polymers can be dissociated by both thermal stimuli and through solvation. As melt processing is impractical, see Section 2.3.2, solvation was explored.

Solvent processing of pure thermoplastics has been examined previously but in the context of selective sorting of municipal wastes [171–173]. The dissolution/precipitation technique involves the dissolution of polymer waste in a solvent at a given temperature. Natural variation in solubility provides the selectivity. Once in solution, the polymer is forced out of solution, or *precipitated*, by the addition of a destabilising solvent, or *non-solvent* [174,175]. It is also possible to force precipitation upon cooling if the polymer is only soluble at high temperatures.

Papaspyrides *et al.* used the dissolution/precipitation technique in the 1990s to recycle pure PP wastes [176]. The study showed that solvent processing had minimal effect on the tensile stiffness and strength of compression moulded PP recyclate after two cycles [176]. Gouli *et al.* implemented a similar dissolution/precipitation technique when recycling poly(methyl methacrylate) decorative sheets. Similarly, the tensile stiffness and strength of compression moulded recyclate showed negligible variation after two cycles [175].

The dissolution/precipitation technique has also been applied to polystyrene [171], low density polyethylene [107,177], high density polyethylene [107,177], PA6 [174] and PA66 [174]. One of the additional benefits to a solvent based system is that the solvents also have the potential to be recycled through fractional distillation. Reported solvent reclamation yields vary, though are typically < 95 %, this is dependent on the physical properties of the solvent and non-solvent used, *i.e.* boiling points and miscibility [173,174,177].

The dissolution/precipitation technique has been used previously to recycle pure thermoplastic household wastes and consistently shown property retention over multiple loops, if the appropriate remanufacturing conditions are used. However, to the authors knowledge it has never been applied to CFRTP recycling, therefore its feasibility as a CFRP waste management method requires further exploration.

3.1.2 Closed-loop remanufacture

This section explores the two main phases of the closed-loop remanufacturing process; fibre alignment and compression moulding. Section 3.1.2.1 details a novel fibre alignment process for discontinuous carbon fibre, and Section 3.1.2.2 explores how compression moulding is the most beneficial route for remanufacturing aligned preforms with thermoplastic matrices.

3.1.2.1 Fibre alignment

Fibre alignment can be achieved in several ways; the methods which produce the highest degree of alignment are discussed in Section 2.4.3. The HiPerDiF alignment method has been used to create discontinuous CF epoxy composites with comparable mechanical properties to UD CF epoxy [158].

The HiPerDiF method is a continuous hydrodynamic alignment process, which uses jets of water, dispersed with discontinuous fibres, directed on to parallel orientation plates.

Fig. 3.2 shows the full HiPerDiF machine set up. The fibres are aligned transversely to the direction of the water jet by the sudden momentum change of the liquid as it contacts a perpendicular plate, steps 1-2 in Fig. 3.3, and then in the direction of the moving conveyor belt, steps 3-4 in Fig. 3.3. Vacuum suction draws the liquid, and the aligned fibres, down to the base of the orientation plates and through a perforated mesh conveyor belt, depositing the aligned fibres on the surface of the belt, see Fig. 3.4.

The alignment head is made up of a modular array of parallel plates, the deposited fibres from each plate converge at the end of the head to form a wet preform with a high degree of alignment, this passes through a heated section leaving a dried preform ready for impregnation.

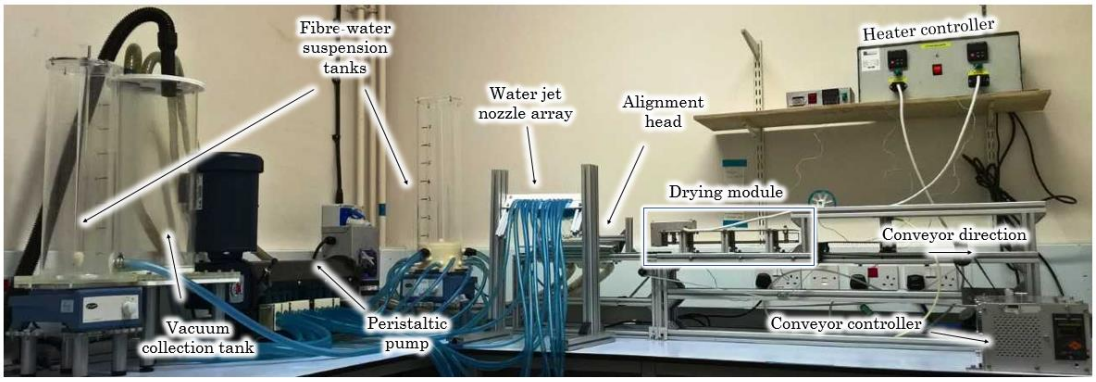

Fig. 3.2. A full view of the HiPerDiF alignment machine annotated with key components.

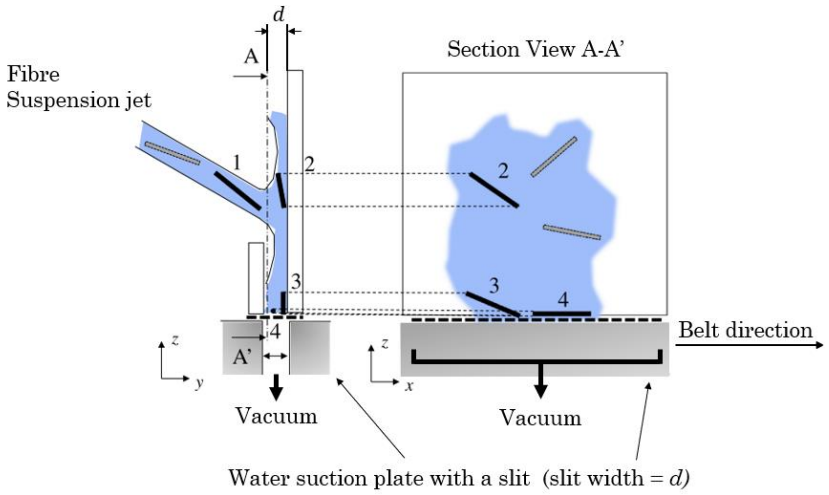

Fig. 3.3. Schematic drawing of the HiPerDiF orientation mechanism and multiple-nozzle array [178]. Fibres align with plate in steps 1-2 and along the direction of the moving belt in steps 3-4. Figure used with permission from author.

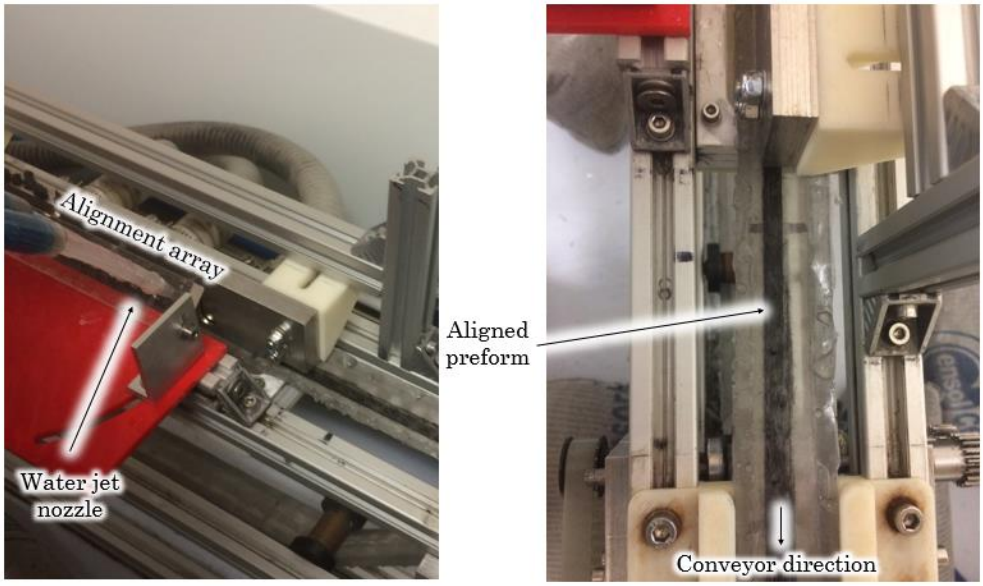

Fig. 3.4. *Left* – shows the closest water jet nozzle and alignment plate entry. *Right* – the alignment array producing a wet CF preform.

It can process a range of fibre lengths (3 – 12 mm) and fibre types (GF, CF, and NF) with the potential for continuous production of a tape-type dry preform, with a tailorable width and areal weight [179,180]. Yu *et al.* impregnated CF (3 mm) preforms by compression moulding with epoxy films producing composites with a Vf_F of 55 % and a tensile modulus and strength of 115 GPa and 1509 MPa, respectively, significantly higher than alternative short carbon fibre composites made using conventional methods [158].

The HiPerDiF method has previously been implemented within a recycling process, however using pyrolysis as the fibre reclamation technique. Longana *et al.* proved that alignment can be useful in forming high performance composites over multiple loops [63]. As epoxy matrix was used it could not be salvaged. Pyrolysis also led to fibre breakage and overall strength reduction [63]. This study presents the feasibility of fibre alignment within a closed-loop recycling process. It also supports the idea that separation of constituents is required for alignment and that thermosetting matrices cannot be reclaimed.

3.1.2.2 Compression moulding

Compression moulding was selected as the remanufacturing consolidation method to ensure sufficient fibre wet-out and minimise voidage in the CFRTP. Compression moulding has been used extensively in the literature for the remanufacture of rCF with thermoplastic and thermosetting resins. The low bulk-density of rCF required high compaction pressures to achieve complete fibre wet out and consolidation. This is especially true for thermoplastic matrices due to the increased melt viscosity in comparison with thermosets.

3.2 CLRP: Experimental method

This section explores the closed-loop recycling process in further experimental detail. An experimental model was developed by applying the dissolution/precipitation and fibre alignment technologies. A schematic of the model is shown in Fig. 3.5 below.

This model is novel in that it was designed, built and optimised by the author and it is the only solvent-based recycling method that provides matrix value. It is also the only study which takes the solvent-based recycling concept for CFRP through the methodological development of manufacture and characterisation. The dissolution/precipitation method was adapted from the literature to incorporate CF. The precipitation technique was optimised to enable separation of fibres without loss of matrix and required the design of a bespoke filtration device enabling efficient CF filtration at elevated temperatures. The remanufacturing methodology was developed over a period of trial and error to determine the conditions, which minimised potential matrix degradation.

The subsequent sections detail the final reclamation and remanufacturing method selected after many iterations of optimisation.

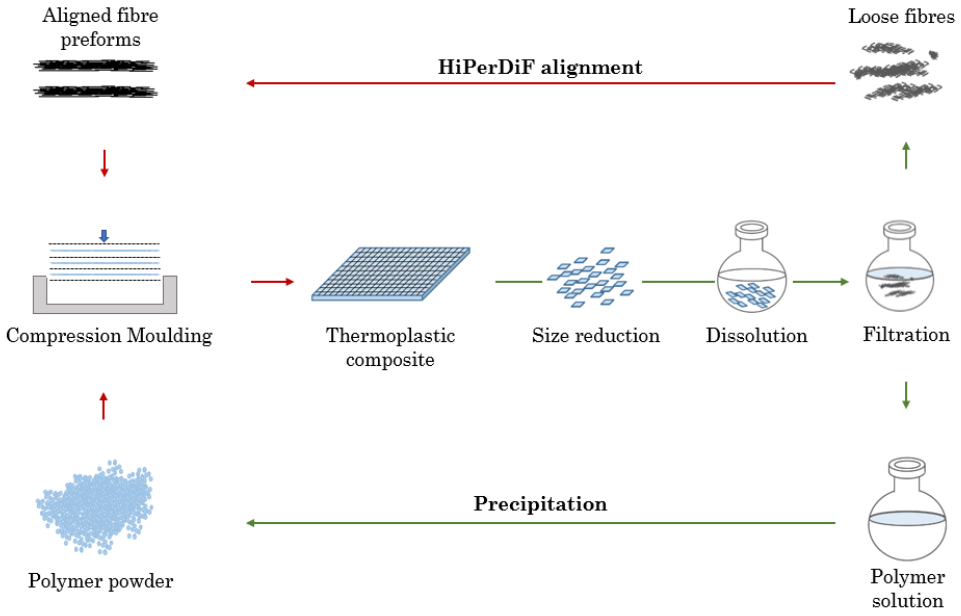

Fig. 3.5. The experimental CLRP model formed by combining the key technologies of fibre alignment and thermoplastic solvent reclamation. The reclamation and remanufacturing steps are denoted by green arrows and red arrows, respectively.

3.2.1 Reclamation

The process can be started arbitrarily with a waste thermoplastic composite which undergoes a solvent-based reclamation procedure, based upon the dissolution/precipitation technique. The reclamation method is described below, however any thermoplastic specific parameters will be detailed in the relevant experimental chapter.

Reclamation included an initial size reduction step as most composite waste undergoes size reduction to aid transportation and sorting of bulky, mixed material composite scrap. In addition to this, an increase in surface area significantly increases dissolution rates. Shredding was deemed the most appropriate size reduction method due to the extensive plastic deformation of thermoplastics. A shred size of 10 mm x 5 mm was selected as this was greater

than the fibre length and therefore minimised the shred contribution to fibre breakage and flattening of the fibre length distribution.

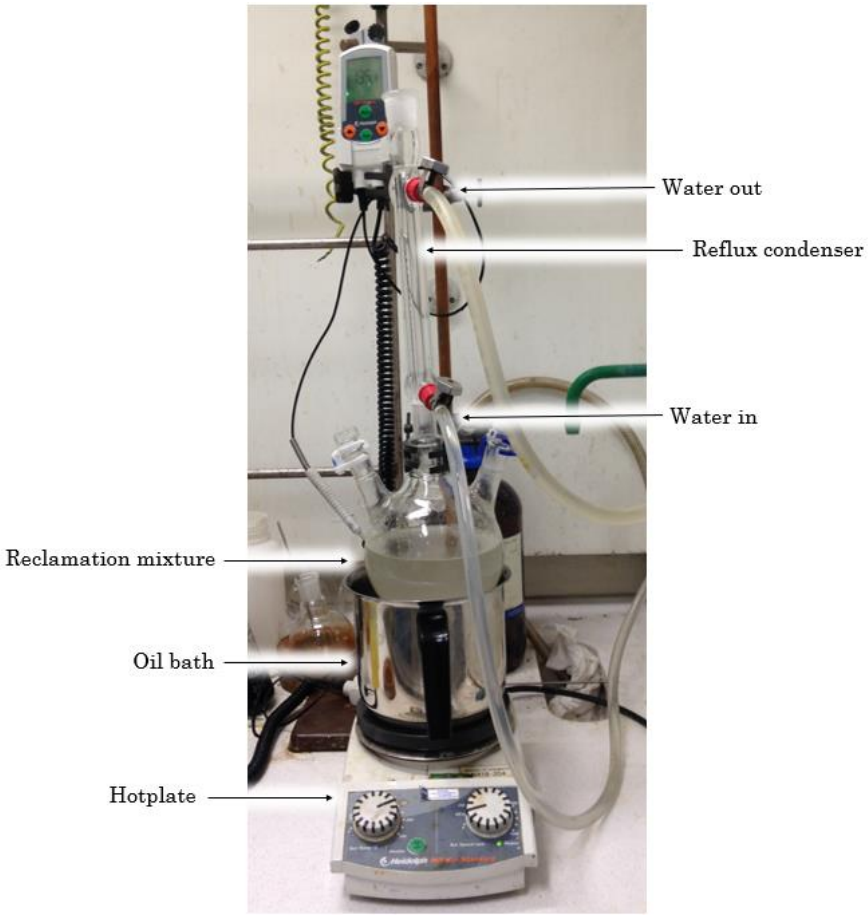

Fig. 3.6. The polymer reclamation set-up showing key components: reflux condenser, oil bath, and hotplate.

The comminuted material was washed, dried and then dissolved using an appropriate solvent system and under appropriate experimental conditions. For high temperature dissolution a reflux condenser was required to stop solution concentration increases from solvent evaporation during heating. An example of the high temperature dissolution set-up can be found in Fig. 3.6. Condensation was provided by a flow of cold water in and out of the reflux condenser. A hotplate, oil bath and digital thermometer were used to provide and regulate solution temperature.

The dissolution method was designed with versatility in mind so that it was applicable for a range of matrix materials, solvent systems, and dissolution temperatures. The temperature could be regulated to incorporate a range of potential operative temperatures depending on the solvent system and the solubility of the thermoplastic used. The method was also designed for scalability so that it can be used for lab scale and commercial volumes.

Full polymer dissolution produced a fibre suspension in a polymer solution, with the latter having an increased viscosity dependent on the concentration of solution, Fig. 3.7. Fibres were filtered from the solution, washed, and dried. The polymer was precipitated and filtered from the solution, washed with non-solvent, and dried. To initiate precipitation, the polymer solution was either mixed with an appropriate amount of non-solvent, cooled to room temperature or both, depending on the dissolution conditions used.

a) CFRTP after adding solvent

b) CFRTP after 1 hour in solvent

c) CFRTP after 3 hours in solvent

Fig. 3.7. *a - c)* showing images of the gradual dissolution of CFRTP in solvent. The discontinuous fibres become increasingly dispersed in the polymer solution.

Precipitate grain size varied significantly at this stage for different polymers, so an industrial blender was used as a size reduction step to homogenise grain size and increase surface area, see Fig. 3.8. This method can handle different types of thermoplastic across many initial grain sizes and is scalable to commercial volumes.

Liquid nitrogen-cooled solvent traps were used to reclaim the solvent removed during drying. Solvent from supernatants and solvent trap collections were separated into pure solvents/non-solvents using vacuum assisted fractional distillation.

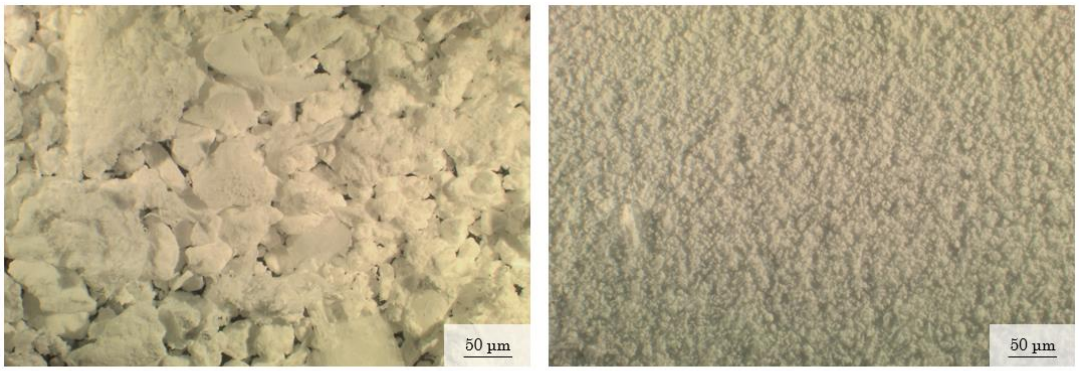

a) Precipitated polypropylene b) Size reduced polypropylene

Fig. 3.8. Grain size examples: a) Large variation in precipitated polypropylene grain size. b) Homogenous grain size distribution of precipitated polypropylene after size reduction.

3.2.2 Remanufacture

The dried rCFs collected from reclamation were in a highly agglomerated, low bulk-density form, which required separation before alignment. Agglomerated rCF clumps can be separated into loose fibres using two methods: dry fibre carding, and wet fibre sonication. An example of the dry rCF clumps and the result of separation via wet sonication are presented in Fig. 3.9.

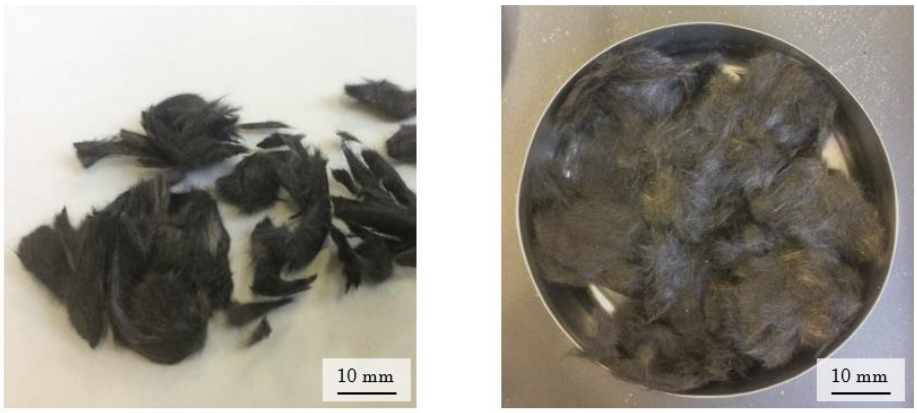

a) rCF filtered from polymer solution

b) rCF after wet separation using sonication

Fig. 3.9. A) recycled carbon fibre (rCF) filtered from polymer solution after polymer has fully dissolved. b) the filtered rCF collected after wet separation using sonication.

Dry fibre carding involves the brushing of fibre clumps into loose fibres using comb-like tools with fine teeth. This is the quickest method but has the lowest yield of the two processes as some fibre is lost on the work surface. Wet fibre sonication includes the separation of fibres through manual agitation and ultrasonic vibration of suspensions of fibre clumps in water.

Alignment produced highly aligned, dry, rCF preforms with dimensions 100 mm x 5 mm. The rCF preforms, and polymer precipitate, were combined in an alternating ABA stacking sequence so that each composite stack was made up of four preform layers and three matrix layers. Stacks were compression moulded in a steel tool under vacuum conditions. Vacuum conditions were required to provide an inert atmosphere, minimising atmospheric oxygen and its catalytic effects in thermo-oxidative polymer degradation.

3.3 CLRP: Experimental analysis

This section details the analytical techniques used to quantify the effects of the process on the composite properties. For a comprehensive evaluation of

properties, it was important to assess the behaviour of the matrix and the behaviour of the fibres. Fibre and matrix properties were then contrasted with the composite performance. Fluctuations in properties throughout recycling could be an indication of degradation and therefore cause a reduction in the potential value of the composite after each recycling loop.

3.3.1 Polymer characterisation

There are a variety of polymer characterisation techniques that investigate the behaviour of a polymer under controlled conditions. The following methods were selected for the most comprehensive analysis of polymer property variation as a function of recycling iteration.

3.3.1.1 Differential scanning calorimetry

Differential scanning calorimetry (DSC) is a thermoanalytical technique used to evaluate the thermal behaviour of a material by measuring the heat flow to and from the material as a function of temperature. Any physical transformations, such as the phase transitions T_g and T_m, have a marked effect on the heat flow through the sample and are therefore measurable.

Transitions where entropy increases, such as melting, are endothermic as energy is absorbed during the process; conversely, crystallization is exothermic [181]. The magnitude of the heat flow variation for a phase transition, as a function of temperature, is dependent on the amount of material contributing to the behaviour. For the melt transition, the magnitude of the integral of heat flow variation as a function of temperature, *i.e.* enthalpy of fusion for melting (ΔH_m), is dependent on the crystalline regions within the polymer, *i.e.* the percentage crystallinity ($\% X$). The percentage crystallinity of a polymer can be determined using equation 3.1 [181].

$$\% X = \frac{(\Delta H_m - \Delta H_c)}{{\Delta H_m}^0} . 100 \qquad 3.1$$

where ΔH_c is the enthalpy of fusion for the crystallization transition, $\Delta {H_m}^0$ is an enthalpy of fusion reference value for a pure crystal of the polymer *i.e.* if the polymer was 100 % crystalline. The crystallization enthalpy contribution is only accounted for when a re-crystallisation event, *i.e.* annealing, occurs. For PP and PA6, $\Delta {H_m}^0$ values of 207 J g^{-1} [182] and 230 J g^{-1} [183] were used, as found in the literature.

3.3.1.2 Thermogravimetric analysis

Thermogravimetric analysis (TGA) is a technique which accurately measures the mass variation of a material as a function of temperature; this is advantageous for quantifying loss of water, loss of solvent, loss of additives, pyrolysis, oxidation and degradation [184].

Isothermal experiments determine the thermal stability of a material, at a given temperature, as a function of time. Controlled air and N_2 atmospheres provide environments which demonstrate the catalytic effect of O_2 in the thermo-oxidative degradation of polymers.

TGA was used to establish the degradation onset temperature, isothermal stability and mass loss required to determine appropriate conditions for non-degradative remanufacture of the thermoplastics.

3.3.1.3 Fourier transform infrared spectroscopy

Fourier transform infrared spectroscopy (FTIR) measures the absorption of IR radiation by a material over a wide spectral range. IR irradiation excites bonds within a molecule causing them to vibrate at distinct vibrational frequencies, *i.e.* wavenumbers [185]. An FTIR spectrum plots the signal absorption as a function of wavenumber producing a spectrum with unique patterns, depending on the chemical environment of the bonds. The wavenumbers can then be used to qualitatively identify an unknown material by cross-referencing with the known wavenumbers of bond vibrations [185].

FTIR was used to qualitatively monitor polymer degradation as the chemical environment of a vibrating bond may be different after degradation,

causing a subtle shift in the wavenumber, and possibly, a variation in the absorption. This is especially so for functional groups which change during oxidation.

3.3.1.4 Gel permeation chromatography / Size exclusion chromatography (GPC/SEC)

GPC/SEC is a liquid state separation technique that can be used to separate polymeric mixtures. The columns used are packed with small, round, porous particles of varying pore size. The dissolved polymer chains become coiled when in solution and have a specific hydrodynamic volume. Longer chains have larger hydrodynamic volumes and pass through the column at a different rate to the smaller chains [186]. Small coils can access a greater number of pores and therefore take more time to pass through the column. Conversely, the largest coils can access far fewer pores and are eluted first [186].

From cross-referencing with a calibration plot, the chromatogram displays the range of coil sizes as a function of time, resulting in a quantified distribution of polymer chain sizes, or molecular weights, for a given polymer, *i.e.* molecular weight distribution.

The MWD of a polymer plots the distribution of chain lengths within the mixture, *i.e.* their prevalence as a function of molar mass. An example of a polydisperse, mono-modal MWD is shown in Fig. 3.10. The number average molecular weight (M_n) and the weight average molecular weight (M_w) represent the simple average and weighted average of molecular weights within a polymer. The latter being the most accurate representative as it accounts for the fact that the largest polymer chains contain a greater portion of the mass [186]. The polydispersity index (PDI) is the ratio of M_w/M_n and describes the broadness of the MWD [186].

The random chain scissions caused by degradation result in fluctuations of polymer chain length therefore a comparison of MWD after every recycling loop can be used to indicate degradation.

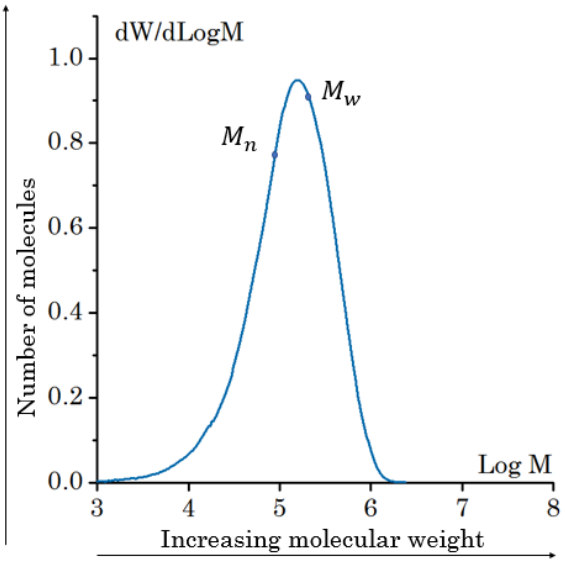

Fig. 3.10. Representative MWD for a polydisperse polymer showing the number average (M_n) and weight average (M_w) molecular weight positions on the curve.

3.3.1.5 High-performance liquid chromatography-mass spectrometry (HPLC-MS)

HPLC-MS is a hyphenated analytical system that combines molecular separation by HPLC and quantitative/qualitative analysis of the separated species by mass spectrometry. HPLC is an effective method for separating complex mixtures of organic compounds [187]. Compounds are separated through a column by their affinity to the mobile phase, therefore a mobile phase of a distinct polarity will pull each compound along the column, *i.e.* the stationary phase, at different rates [187].

After separation, the compounds are nebulized and sprayed into the mass spectrometer which ionizes them and sorts the ions based on their mass-to-charge (m/z) ratio [187]. The detected m/z are plotted against their relative abundance producing a mass spectrum of the organic mixture. Ionization occurs randomly, creating positively charged ions of varying masses. Ions can be either whole molecules or molecular fragments, broken by the energy of ionization. The largest ion, called the molecular ion (M^+), is formed by the loss of just one electron,

therefore the m/z charge can be used to determine the mass of an unknown molecule(s) [187]. The m/z of fragment peaks can be compared with masses of known chemical structures, *i.e.* benzene rings, to determine the possible molecular structures, of which they were originally comprised.

HPLC-MS was used to determine the presence of unknown molecules in the reclamation supernatant. If present, the structures were compared with known polymer additive structures to determine what may have been extracted.

3.3.2 Mechanical characterisation

3.3.2.1 Mechanical testing of pure thermoplastic

Mechanical testing was required to quantify the mechanical performance of the rCFRP after every recycling loop, to validate the value retention. Initially, the pure thermoplastic was evaluated to determine the effects on mechanical performance without the added contributions from the fibres *i.e.* fibre alignment, fibre matrix adhesion and fibre length distribution. The experimental method used for pure thermoplastic evaluation is presented in Fig. 3.11.

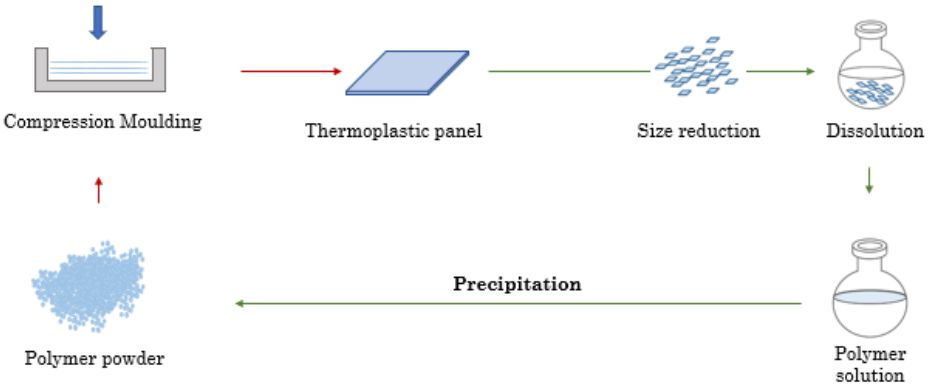

Fig. 3.11. Schematic of the CLRP adapted for pure thermoplastic recycling. The reclamation and remanufacturing steps are denoted by green arrows and red arrows, respectively.

In accordance with the American Society for Testing and Materials (ASTM) standard ASTM D38 a Type IV dumbbell specimen was used. The dimensions of a Type IV dumbbell specimen are shown in Fig. 3.12 and the exact dimensions used are displayed in Table 3.1.

Table 3.1. Type IV specimen dimensions for a thickness ≤ 4 mm.

	W	L	WO	LO	G	D	R	RO	T
	mm	mm	mm	mm	mm	mm	mm	mm	mm
PP	6	33	19	115	25	65	14	25	1

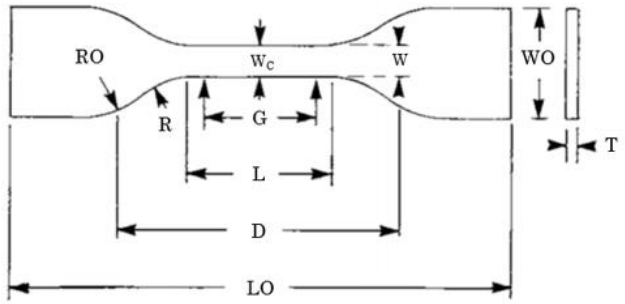

Fig. 3.12. Type IV dumbbell specimen dimensions according to ASTM D638 [188].

Shear testing was used to determine the ultimate shear strength of the pure thermoplastic material. Any variation in these properties was compared with the polymer characterisation data to determine the cause.

Referring to ASTM D732, the shear strength tests were performed using a shear punch tool. 50 mm diameter discs, with a thickness of 1 mm, were punched from panels; these were given a centre-punch of 10 mm diameter to be used as a datum for fixing to the tool. A diagram of the shear punch tool and the shear disc dimensions can be seen in Fig. 3.13.

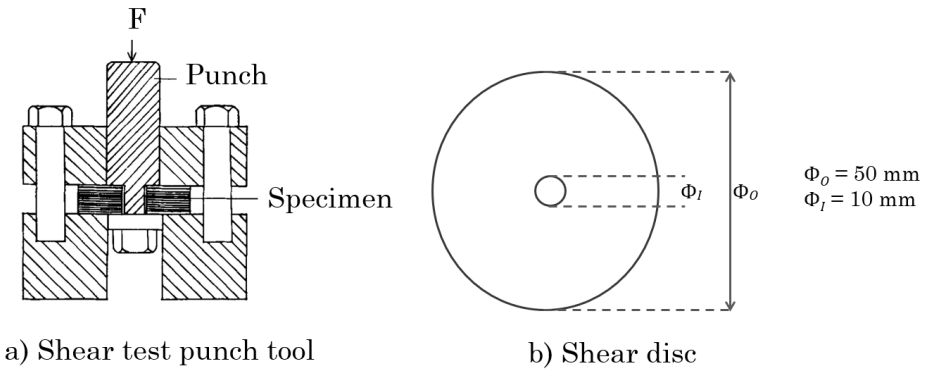

Fig. 3.13. ASTM D732 shear test: *a*) shear test punch tool assembly. *b*) Punched shear disc [189].

3.3.2.2 Mechanical testing of composite materials

Mechanical performance is the most influential determinant of composite value therefore it is important to evaluate this after each recycling loop. The in-plane tensile properties of the composite materials were measured in accordance with the ASTM D3039/D3039M standard. Tensile testing was used to determine the composite tensile stiffness, ultimate tensile strength and failure strain.

Tensile testing was selected as the only mechanical performance test as the thicker specimens required for shear and compression testing were impractical to produce given the HiPerDiF limited, batch production capabilities, the preform dimensions, and the research timeframe.

Specimens were tested for their tensile properties in accordance with ASTM D3039. The gauge length of the specimens was consistently 50 mm. Tensile specimen geometry and dimensions are displayed in Fig. 3.14 and reported in Table 3.2.

Table 3.2. Tensile test specimen dimensions.

	W	L	LO	G	T
	mm	mm	mm	mm	mm
CFRP	5	25	100	50	0.25-0.40

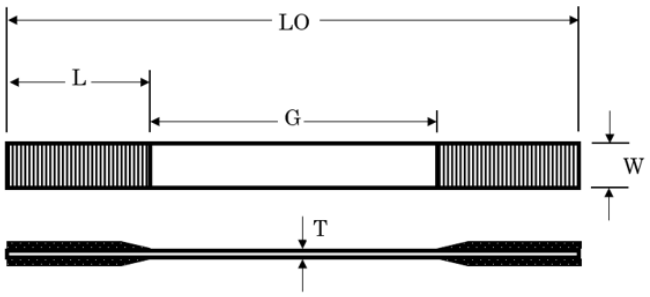

Fig. 3.14. Schematic of the tensile test specimen geometry annotated with dimensions.

All specimens were tested with the required GFRP end tabs bonded with cyanoacrylate adhesive. Three strain measurements were taken along the length of each specimen using an Imetrum video-gauge system. These were averaged to produce the presented strain measurement.

3.3.3 Composite composition analysis

The average thickness ($\bar{t}$), and width ($\bar{w}$), of the composite specimens was measured using a micrometer. Three measurements were taken at three different locations along the length and an average was taken. Volume fractions of the composite (V_C), fibres (V_{fF}), matrix (V_{fM}) and voids (V_{fV}), were calculated using the measured cross-sectional area (A_x), measured composite length (l_C), measured mass of fibre preforms (m_F), measured composite mass (m_C), calculated matrix mass (m_M), nominal fibre density (ρ_F) and matrix density (ρ_M), according to the expressions in equation 3.2:

$$A_x = \bar{t} \times \bar{w}, \quad V_C = l_C \times A_x, \quad m_M = m_C - m_F \tag{3.2}$$

$$V_{fF} = \frac{m_F}{\rho_F} \cdot \frac{100}{V_C}, \quad V_{fM} = \frac{m_M}{\rho_M} \cdot \frac{100}{V_C}, \quad V_{fV} = 1 - (\, V_{fF} + \, V_{fM})$$

Changes in V_{fF} were monitored as function of recycling loop. Tensile stiffness and strength values were normalised by calculated V_{fF}.

3.3.4 Fibre analysis & Fractography

Fibre surfaces were qualitatively evaluated using a scanning electron microscope (SEM) to determine surface defects or surface deposition of matrix on fibres in the dried preform state. Differences in fibre surface can affect fibre-matrix adhesion, represented by the interfacial shear strength (IFSS), τ_i, which in turn has a significant effect on mechanical performance.

Fibre length distribution (FLD) analysis was carried out to determine the effects on the fibre length after each loop. A portion of each preform was cut, dispersed in water and slowly gravity filtered until an even distribution of fibres remained on the filter paper. A portion of this distribution was scanned using an Epson 11000XL. Each fibre, within a consistent sample region of the high-resolution image, was measured and collated using ImageJ software.

A fibre below the critical fibre length (L_c) is not bearing its maximum load and therefore not functioning effectively [190]. Beyond L_c, a fibre will carry an increasing proportion of the applied force, possibly fracturing before the matrix, this is especially so for more ductile matrices such as thermoplastics [190]. Therefore, the critical fibre length distinguishes between fibre failure and fibre pull-out failure modes; these are observable through SEM of fracture surfaces. L_c can be determined using the following equation:

$$L_c = \frac{\sigma_F^* d}{2\,.\,\min\{\tau_M, \tau_i\}} \qquad 3.3$$

Where σ_F^* is the ultimate tensile strength of the fibre, d is the fibre diameter, τ_M is the shear strength of the matrix, and τ_i is the interfacial shear strength.

SEM was used to analyse the fracture surfaces of the composite materials post-testing. Evaluation of the surfaces provides additional qualification of possible failure mechanisms that may be directly influenced by the recycling process, including qualification of length dependant failure modes.

3.4 CLRP: Finalised experimental method

This section details how the experimental method from section 3.2 and the experimental analysis methods from section 3.3 were combined to produce the final CLRP evaluation method. The final experimental method and the step at which the experimental analysis was taken are shown in Fig. 3.15.

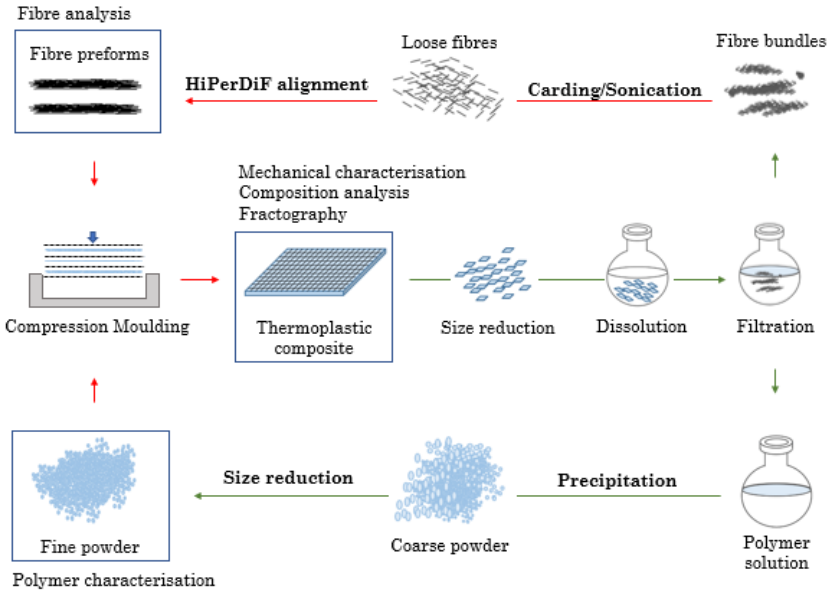

Fig. 3.15. A schematic of the final experimental method annotated with the locations where the experimental analysis was taken. The reclamation and remanufacturing steps are denoted by green arrows and red arrows, respectively.

The method starts at the manufacture of the virgin composite material and is repeated two times, producing two iterations of recycled material. All proceeding experimental chapters use this recycling method. The process and its evaluation, in terms of output material properties and resource yields, can be described as follows:

1. A virgin composite was manufactured from aligned, virgin fibre preforms and virgin matrix powder, and composite composition was

determined. The composite was mechanically tested, and the fracture surfaces analysed using SEM.

2. The fractured specimens were reclaimed (r_1), leaving dry reclaimed carbon fibres and dry, comminuted reclaimed polymer. The masses of each were collected and yields calculated.

3. Polymer characterisation was carried out on the reclaimed polymer. The dry fibres were aligned and the preforms were analysed using SEM.

4. The reclaimed constituents were remanufactured into a composite and steps 1-4 were repeated, *i.e.* a second recycling loop was conducted (r_2).

5. Step 1 was carried out on the final recycling loop (r_2) then the evaluation was terminated.

4 A closed-loop recycling process: proof-of-concept

The closed-loop process was evaluated initially using pure thermoplastic to determine the effects without the added complexity afforded by the fibres. Section 4.2 describes the fibre and matrix material used in this study, Section 4.3 details the experimental method used in the pure polymer analysis and the relative results and discussion, followed by the conclusions presented in Section 4.3.3.

Section 4.4 describes the experimental method used in the composite analysis and the relative results and discussion, followed by the conclusions presented in 4.4.3.

The overall conclusions of the proof-of-concept evaluation are presented in Section 4.5

4.1 Introduction

This chapter details the proof-of-concept experimental evaluation of the recycling process outlined in Chapter 3. This was achieved by analysing the polymer properties and mechanical performance of a recyclable composite after two recycling loops. The aims of the studies reported in this Chapter are to:

- Evaluate the closed-loop recycling process by producing a CF reinforced polypropylene composite (CFPP), over two recycling loops.

- Investigate any effects the closed-loop recycling process may be having on the constituent and composite mechanical performance.

For both material cases the process was repeated two times on the same batch of material. Additional material was recycled alongside tested specimens to ensure enough material was available. Repeatability of each stage of the process was tested by producing two panels from the same batch of material at each recycling loop, however, repeatability of the entire process was not tested.

4.2 Materials

PP was used as the thermoplastic in this study due to the following advantages:

- It is a semi-crystalline thermoplastic that is soluble in low hazard solvents.

- It requires lower melt processing temperatures compared with other commodity and engineering thermoplastics.

- It is readily available and comparative data is available as it has been widely used in the literature [191–204].

PP was sourced in pellet form from Sigma Aldrich, the material properties of PP can be found in Table 4.1.

Table 4.1. Properties of the PP used in this study.

	Density	T_m	T_g	Crystallinity	M_W	M_n	PDI
	g/cm^3	°C	°C	%	g/mol	g/mol	-
PP	0.91	166	-10	45	3.4 x 10^5	9.7 x 10^4	3.5

Data collected experimentally, see subsequent analysis for conditions. * Data from manufacturer.

Discontinuous CFs used in this study were supplied by TohoTenax (standard type C124). The TohoTenax fibres were 3 mm in length and came with a proprietary water-soluble sizing (3.8 wt.%) used to aid dispersion in the alignment carrier liquid. Material properties of the CFs used can be found in Table 4.2.

Table 4.2. Properties of the carbon fibres used in this study.

	Length	Density	Diameter	E_T	X_T	e
	mm	g/cm^3	µm	GPa	MPa	%
CF	3	1.82	7	225	4344	1.93

Material properties sourced from literature [205].

Solvents used during reclamation were certified American Chemical Society (ACS) reagent grade xylene (xylenes mixture) and acetone, sourced from Fisher Scientific.

4.3 CLRM: Polypropylene

4.3.1 Closed-loop recycling process

This section details the experimental evaluation of the CLRP with pure polypropylene specimens. The closed-loop recycling process coupled with the experimental analysis used in the un-reinforced polymer analysis is presented in Fig. 4.1.

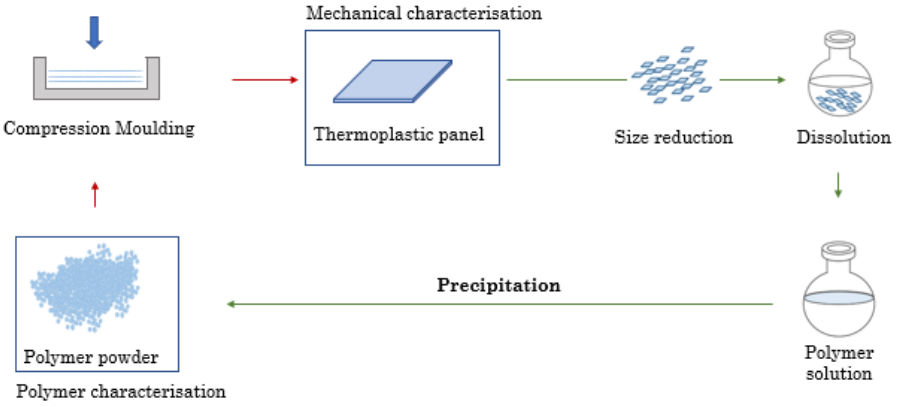

Fig. 4.1. Schematic of the closed-loop recycling method used in the pure thermoplastic study, with material characterisation annotation. The green and red arrows represent the reclamation and remanufacturing procedures, respectively.

Two panels of PP were manufactured in an aluminium tool directly from pellets. Two panels of each iteration were produced to increase sample set sizes and to evaluate process repeatability. Pellets were housed in the tool cavity and the closed tool was placed in a vacuum bag and into the oven. Tool cavity was of dimensions 1 mm x 100 mm x 170 mm. The tool was subjected to heat and vacuum pressure until a homogenous melt had formed. At melt, the tool was cooled under vacuum pressure. The compression moulding cycle parameters are displayed in Fig. 4.2.

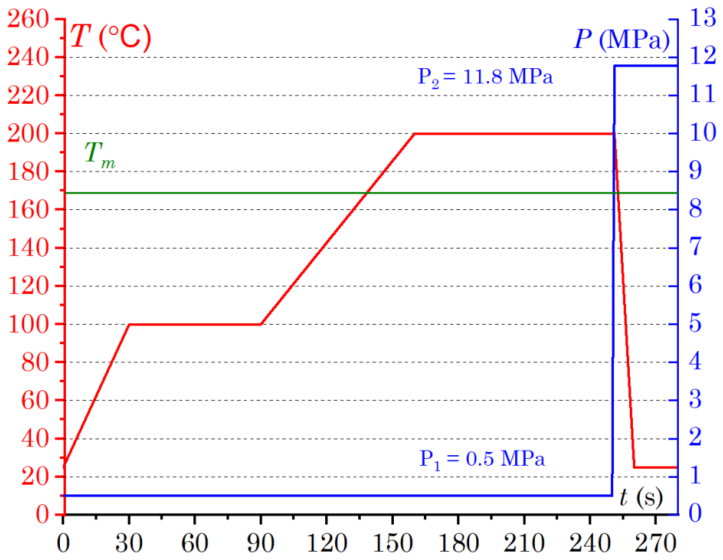

Fig. 4.2. Compression moulding cycle used to mould PP panels. Specimens were held at 0.5 MPa (P_1) for 4 hours until transfer from oven to hot press for consolidation at 11.8 MPa (P_2). T_m denotes the melting temperature of PP.

4.3.1.1 Reclamation

After mechanical testing and polymer characterisation, the bulk panel and tested specimens were washed, and comminuted. Defected specimen regions from mechanical testing, *i.e.* necking, were rejected. The reclamation method used was as described in Chapter 3, using the parameters defined in Table 4.3.

Table 4.3. Reclamation parameters used for PP recycling.

	Shred Size	Solvent	Temp.	Time	Non-solvent	Conc.	Solvent Ratio
	mm^3	-	°C	mins	-	% w/v	S:NS
PP	100	xylene	135	180	acetone	15	1:3

Temp. = Temperature, Conc. = Concentration, S = Solvent, NS = Non-solvent.

Full dissolution was observable as a homogenous polymer solution of increased viscosity. PP precipitated on cooling to room temperature, forming a solvated powder with gelatinous properties, in xylene solvent. Acetone was added to encourage the precipitation of any polymer still in solution and to minimise

residual xylene in the precipitate. Non-solvent was only added after cooling the solution to below 50 °C (acetone boiling point = 56 °C). The precipitate suspension was vacuum filtered using Buchner filtration apparatus. Liberal washings of non-solvent were used to minimise residual solvent. Filtered precipitate was dried in a vacuum oven (~ - 29 inHg) at 80 °C for 14 hours. The rCF bundles were separated by the dry carding method, as described in Section 3.2.1. This method was not 100 % effective in its ability to completely separate fibre agglomerations as some were still visible in the preforms after alignment, these were then transferred to the preform. There was also broken fibre residue remaining on the carding surface.

Solvent traps were used to reclaim the solvent removed during drying. Solvents were collected and separated using fractional distillation. Acetone and xylene recovery yields were 87 % and 91 % respectively; xylene contained some residual acetone (~ 3 %). The reclamation yield for PP was 90 % as determined by comparing the panel and dried precipitate masses.

The yields obtained were not from reclamation conditions optimised for maximum yield therefore higher yields may be expected. For the solvents this may be closer to those obtained in the literature, see Section 3.1.1.

4.3.1.2 Remanufacture

Dried, precipitated PP from the first reclamation process, *i.e.* r_1PP, was remanufactured into a r_1PP panel, following the same method used to form the virgin panel, vPP. The CLRP was repeated once more so that polymer characterisation data was performed on vPP and two successive recycled panels, r_1PP and r_2PP. Images of the pure polypropylene panels are provided in Fig. 4.3. There were no discernible qualitative variations in panel quality between the two panels of each recycling loop, therefore a representative panel from each loop is shown.

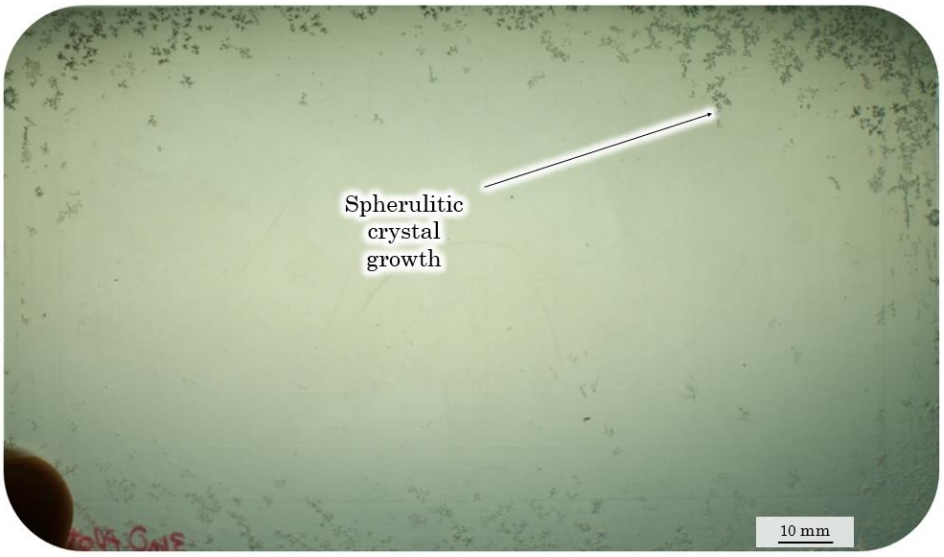

a) vPP panel

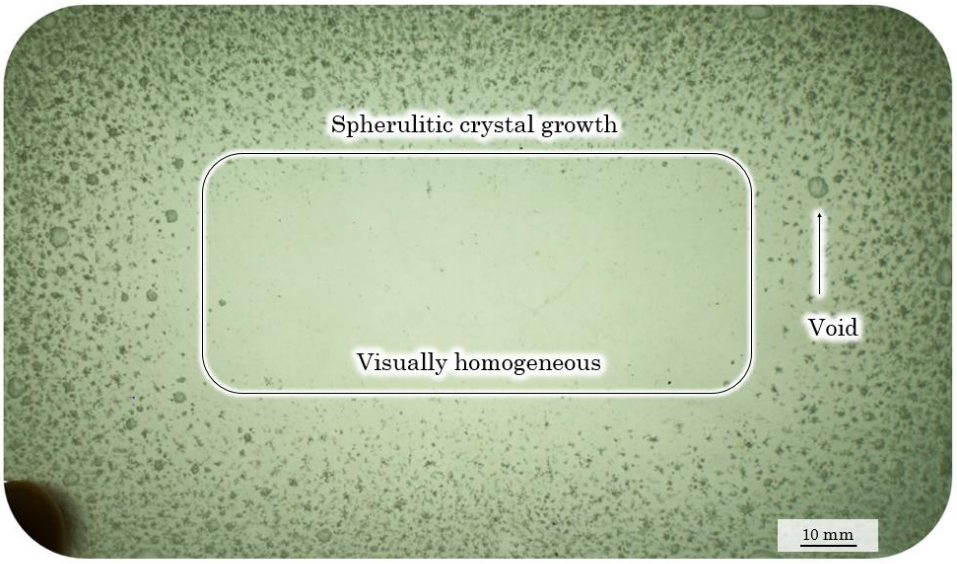

b) r_1PP panel

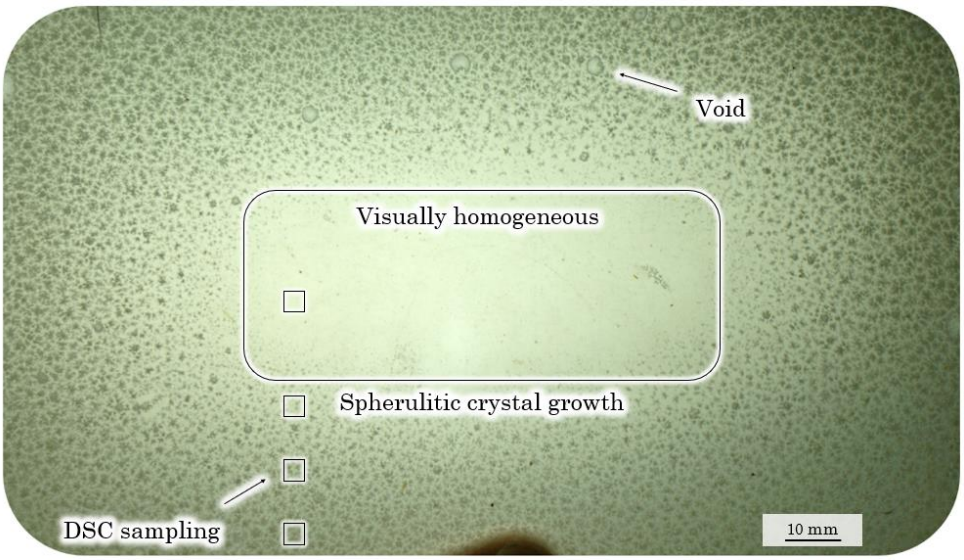

c) r_2PP panel

Fig. 4.3. *a-c)* Images of representative panels from each recycling batch: vPP, r_1PP and r_2PP. An increase in panel voidage and spherulitic crystal growth as a function of recycling can be seen. Growth increases radially towards the panel edge.

The images are annotated showing; the gradual increase of spherulitic crystal growth, the voidage observed and the location where DSC sample were taken from each panel (Fig. 4.3c). There is a gradual increase in spherulitic crystal growth as a function of recycling, with r_1PP and r_2PP panels exhibiting approximately 50 % and 75 % spherulitic content respectively. Voidage was apparent after the first recycling loop however there is no increase in the voidage after the second recycling loop, observed qualitatively. As explored below, their prevalence may be due to: the extraction of additive molecules which may have affected crystal formation, or, differences in crystal formation due to the variation in feedstock material, *i.e.* pellet and powder. Differences in feedstock may also explain the increase in voidage. In powder form, air trapped during powder compression may not have been removed by the vacuum during the melt, as effectively as they would for pellets, due to a reduction in gas flow channels. The prevalence of spherulites had no effect on the mechanical properties and were therefore deemed superficial and not investigated further. However, from a

product development perspective, the reintroduction of additive molecules and the material format should be considered to guarantee consistency.

4.3.2 Results and discussion

4.3.2.1 Polymer characterisation

DSC was used to examine the effect of recycling on the T_m and X of the polymer. All thermal ramp experiments were carried out using a TA Auto Q2000 DSC in pierced, hermetically sealed aluminium pans on samples cut from panels (10 ± 3 mg), under flowing N_2 (50 cm^3/min) at a heating rate of 10 °C/min. Four samples were taken across the width of both panels, totalling eight samples per recycling loop.

DSC thermograms collected for vPP, r_1PP and r_2PP are overlaid in Fig. 4.4. Crystallinity was determined using the values displayed in Table 4.4. A comparison of thermograms from each recycling loop indicates that both the X and T_m of the polymer were unaffected by reclamation. There was a slight shift in T_m for r_1PP, however this was within measurement variance.

Degradation causes changes in the MWD which affects the degree of crystallinity within a semi-crystalline polymer and the quality of the crystal structure formed. This would be observable as variation in the X and T_m, respectively. This suggests that the crystalline regions, and the polymer chains they consist of, were unaffected by the recycling process. The small variance in results between sample sets suggests that there is little variation between panels and that the process has good repeatability.

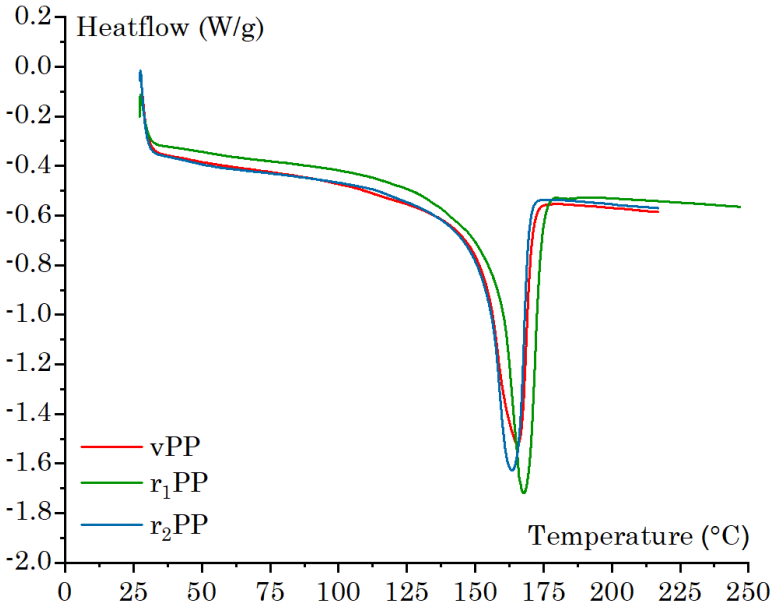

Fig. 4.4. DSC thermograms for polypropylene panels as a function of recycling loop.

Table 4.4. DSC results from recycled polypropylene used for percentage crystallinity calculations.

	T_m	ΔH_m	$\Delta H_m{}^0$	X
	℃	J/g	J/g	%
vPP	166 (0.3)*	97.9	207	47.3 (4.2)
r1PP	167 (0.3)	92.9		44.9 (4.9)
r2PP	165 (1.7)	104.3		50.4 (2.3)

* Coefficient of variance determined from eight samples, four from each of two panels for each recycling loop.

A TA Q500 TGA was used to quantify PP mass loss under the conditions of remanufacture. Isothermal analysis at 200 °C were carried out for 160 min in both air and N_2 atmospheres (60 cm^3/min). Pellets were used for vPP and precipitate powder was used for r_1PP and r_2PP.

TGA thermograms from isothermal analysis (200 ℃) of vPP and r_2PP in air and N_2 atmospheres can be found in Fig. 4.5. Isothermal analysis in flowing N_2 showed no degradation after 160 minutes of either vPP or r_2PP. Thermograms taken in air atmosphere showed no degradation of vPP for the first 75 minutes,

then gradually dropped to 85 % after 140 minutes. The r_2PP thermogram showed degradation starting after 25 minutes and gradually decreasing in weight until a plateau at 50 % weight after 150 minutes. The mass loss observed was characteristic of thermo-oxidative degradation typical of polymers exposed to air at elevated temperatures. The increase in degradation seen in the r_2PP specimen was likely due to significantly increased surface area of the r_2PP powder, compared to vPP pellet for the same experimental conditions.

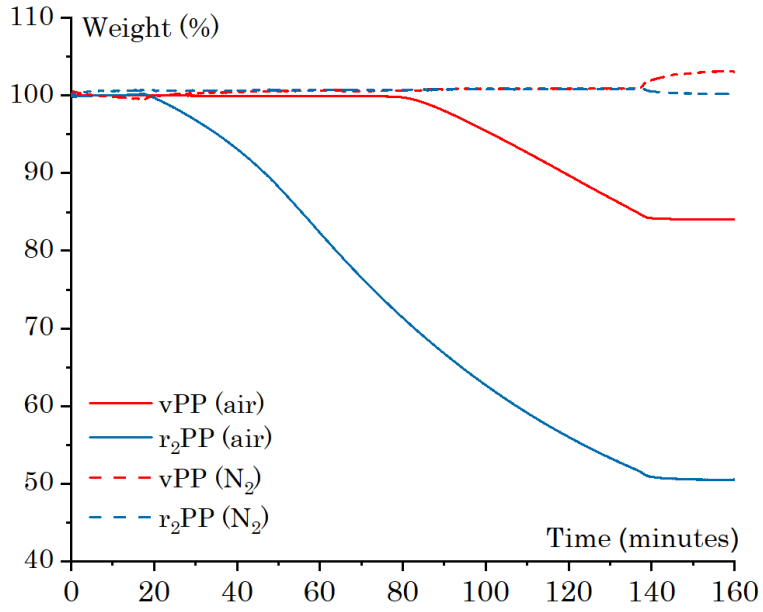

Fig. 4.5. Isothermal TGA thermograms of vPP and r_2PP in both air and N_2 atmospheres at 200 ℃.

A Perkins Elmer Spectrum 100 Fourier Transform Infrared Spectrometer was used to compare polymer functionalities between virgin and recycled polymers. vPP pellet and r_2PP precipitate were used as samples.

The FTIR spectra collected for vPP and r_2PP are overlaid in Fig. 4.6. The FTIR spectrum of vPP showed all the vibrational peaks for specific functional groups expected for PP; these are presented in Table 4.5. A peak at 1734 cm^{-1} was present in vPP but not in r_2PP, which indicated the removal of a substance. This peak was very close to the v_s (carbonyl group -C=O) – 1735 cm^{-1} (*i*) vibration of Irganox 1010, a hindered phenol antioxidant additive typically used in

commercial PP [206]. The other peaks associated with this functional group vibration are not found in vPP however, which could be due to: *a) signal swamping by the signals of other additives that were not removed by reclamation* or *b) the signal source is from a carbonyl group of an unidentified additive*. As the vibrational frequencies of the main chain methylene and aliphatic regions remain constant it can be concluded that the polymer chains are not chemically altered during recycling.

Table 4.5. Vibrational peaks for polypropylene observed in the FTIR spectra.

Wavenumber	Vibrational peaks
cm^{-1}	
1370	$-CH_3$ symmetric bending
1460	$-CH_2$ asymmetric bending
2840	$-CH_2$ symmetric stretching
2870	$-CH_2$ asymmetric stretching
2910	$-CH_3$ symmetric stretching
2970	$-CH_3$ asymmetric stretching

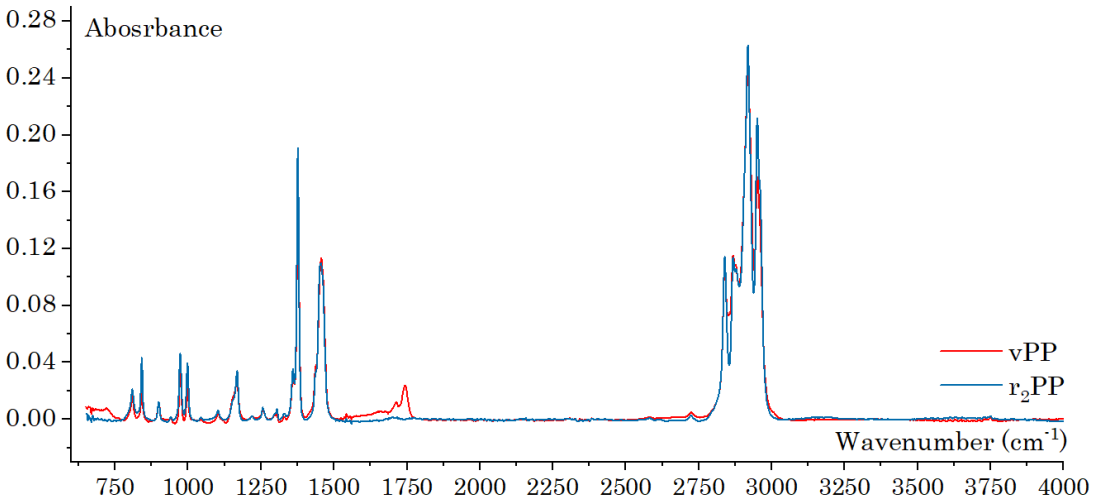

Fig. 4.6. FTIR spectra for recycled polypropylene specimens vPP and r_2PP.

The M_w, M_n, PDI, and MWD of each recyclate was determined using GPC/SEC. Samples were analysed using an Agilent PL220 high temperature GPC system with two Agilent PLgel Mixed D columns (300 x 7.5 mm) and a PLgel 5 µm guard column, in a TCB mobile phase (with 250 ppm BHT) at 160 °C at a rate of 1 ml/min. Samples were prepared by solubilising panel cuttings in 140 °C TCB overnight, in an Agilent PL-SP 260VS. Two samples were analysed for each recycling loop, the coefficient of variance of each loop is reported in Table 4.6.

The MWD curves obtained from GPC/SEC of vPP, r_1PP an r_2PP are shown in Fig. 4.7 and the M_n, M_w and PDI values are tabulated in Table 4.6. The MWDs are representative of polydisperse, mono-modal semi-crystalline polymers, as expected from the PP used. From left to right the plots ran from low to high molecular weights.

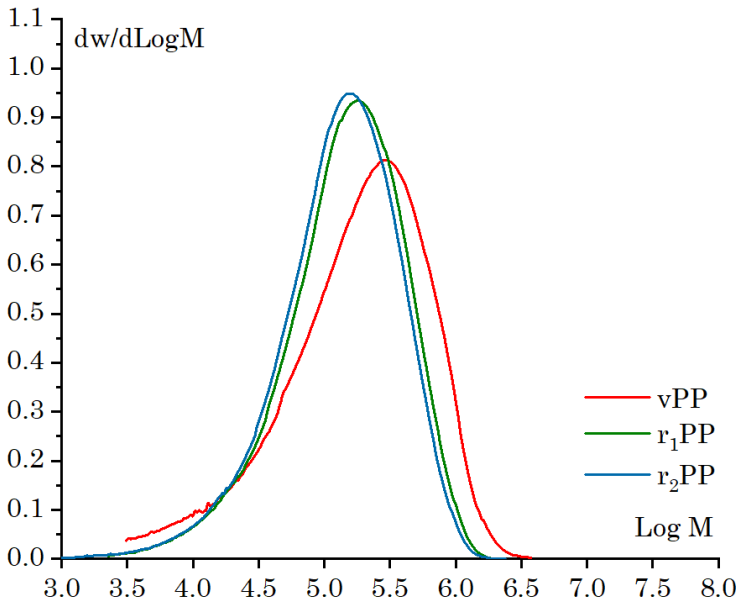

Fig. 4.7. MWD from GPC/SEC analysis of recycled polypropylene after each recycling loop.

Table 4.6. The GPC/SEC analysis of polypropylene after each recycling loop.

	M_n	M_w	PDI
	x10^4 g/mol	x10^5 g/mol	
vPP	6.58 (1.0)*	3.28 (2.0)	4.87
r_1PP	6.30 (14)	2.21 (0.1)	3.59
r_2PP	6.00 (5.1)	1.95 (2.4)	3.25

* Coefficient of variance determined from two samples of the same batch.

M_n, M_w and PDI all decreased after each iteration, represented as a negative shift on the x-axis. The drop in M_w after the first recycling loop was greater (-32.6 %) than that between r_1PP and r_2PP (-11.8 %). The drop in M_n was effectively even between the recycling loops (-4.3 % and -4.8 %, respectively); this was represented by an overall, successive decrease in PDI and observed as a narrowing of the distribution curves. The observed reductions in M_w for the first and second loops are less than that reported in the literature for repeated extrusions of PP. After the first and second extrusion cycles of a melt recycling process, Hinsken *et al.* reported a 30 % and 23 % reduction in M_w, and a 29 % and 11 % reduction in M_n, respectively [134]. This suggests that for both processes, the large polymer chains undergo scission in relatively similar proportions, although this process performs favourably. It also indicates that the product of scission is less extensive, producing a higher proportion of medium length chains than small length chains.

The MWD narrowing after vPP suggested a reduction of the low molecular weight region and the loss of a slight shoulder in the high molecular weight region. This indicated that initial dissolution of the polymer is extracting small molecules into the organic solvent. These small molecules may be a combination of: *a) small PP chain fragments produced by degradation or as polymerisation by-products, b) polymerisation additives i.e. catalysts, or c) soluble stabiliser molecules.* The larger chains were fragmented into medium length chains, removing the larger weight value skew on the distribution peak.

There was a successive drop in M_n between r_1PP and r_2PP, a subtle increase in peak height, *i.e.* an increase in number of molecules with median length, and

a subtle negative curve shift. This suggests that scission of larger chains is occurring during processing, however the extent is minimal.

4.3.2.2 Mechanical Testing

The in-plane tensile properties of the pure thermoplastic materials were measured in accordance with the ASTM D638 standard, see Section 3.3.2.1. Tensile tests were performed on Type IV dumbbell specimens using a Shimadzu AGS-X servo-electric tensile test machine with a 10 kN load cell and a constant cross-head displacement of 1 mm/min. Six specimens were cut from a panel, sprayed black and speckled with white dots to measure the strain using an Imetrum video-gauge system, an image of a prepared specimen is presented in Fig. 3.12.

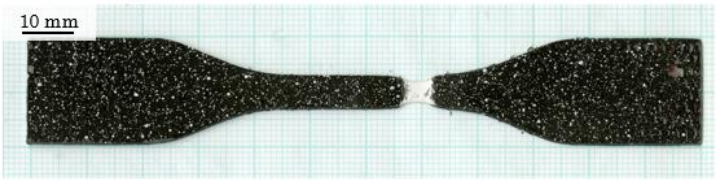

Fig. 4.8. Type IV dumbell used in tensile testing. Specimen shows speckle pattern used for strain mapping.

Representative stress-strain curves obtained from tensile tests of PP, as a function of recycling loop, are shown in Fig. 4.9. Tensile specimens showed a linear-elastic region and subsequent plastic yielding, typical for semi-crystalline polymers. Yielding continued until ductile failure by necking (> 100 % ε), which continued until termination of the test. A typical example of the necking observed can be seen in Fig. 4.8. Stress-strain curves do not show the full extent of necking and the data is only presented to a strain proceeding the ultimate tensile strength (σ_{ult}).

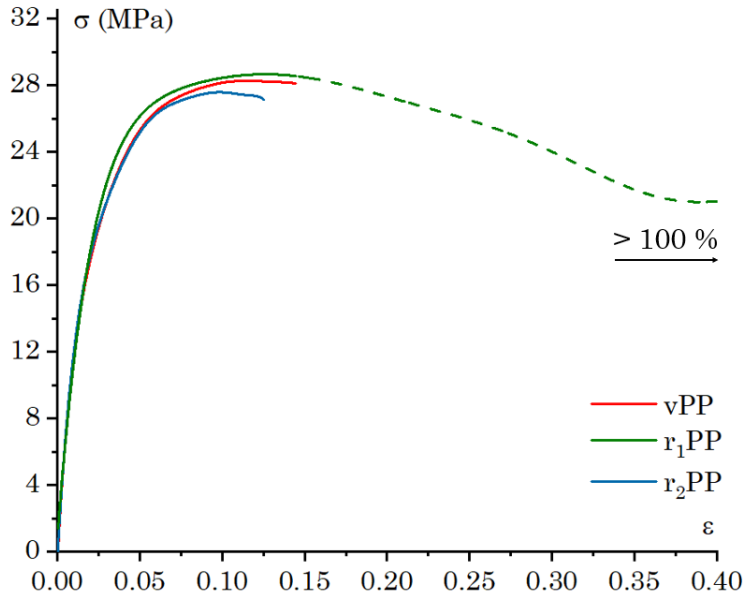

Fig. 4.9. Stress-strain curves for tensile tests of polypropylene as a function of recycling loop.

σ_{ult} was taken as the curve maxima as tests were not continued until ductile fracture; tests were terminated at 20 % strain as it was not possible to track large displacements with the selected video gauge parameters. The tensile stiffness (E_T) was determined by taking the gradient of the linear-elastic region section, of bounds $0.01 < \varepsilon < 0.03$. The ultimate tensile strain (ε_{ult}) was determined as the σ_{ult} corresponding ε. The results of the tensile tests are recorded in Table 4.7, and presented in the bar charts in Fig. 4.10.

Table 4.7. Mechanical performance data collected from tensile and shear test of polypropylene after each recycling loop.

	E_T	σ_{ult}	ε_{ult}	τ
	GPa	MPa		MPa
vPP	1.38 (1.8)*	27.8 (1.5)	0.11 (4.9)	59.7 (3.8)
r_1PP	1.44 (6.9)	27.1 (4.7)	0.12 (9.0)	58.2 (5.4)
r_2PP	1.39 (6.7)	27.3 (5.8)	0.90 (16.5)	50.4 (6.4)

* Coefficient of variance calculated from six specimens of the same batch.

Overall the curves showed no significant deviation in shape through recycling and had almost negligible variance in E_T. Degradation-induced chain length variation would affect the crystalline and amorphous regions of the polymer and thus affect the tensile performance as crystallinity contributes significantly to polymer E_T. The invariable tensile results, as a function of recycling loop, suggested that if degradation was present it had negligible effect on the tensile performance.

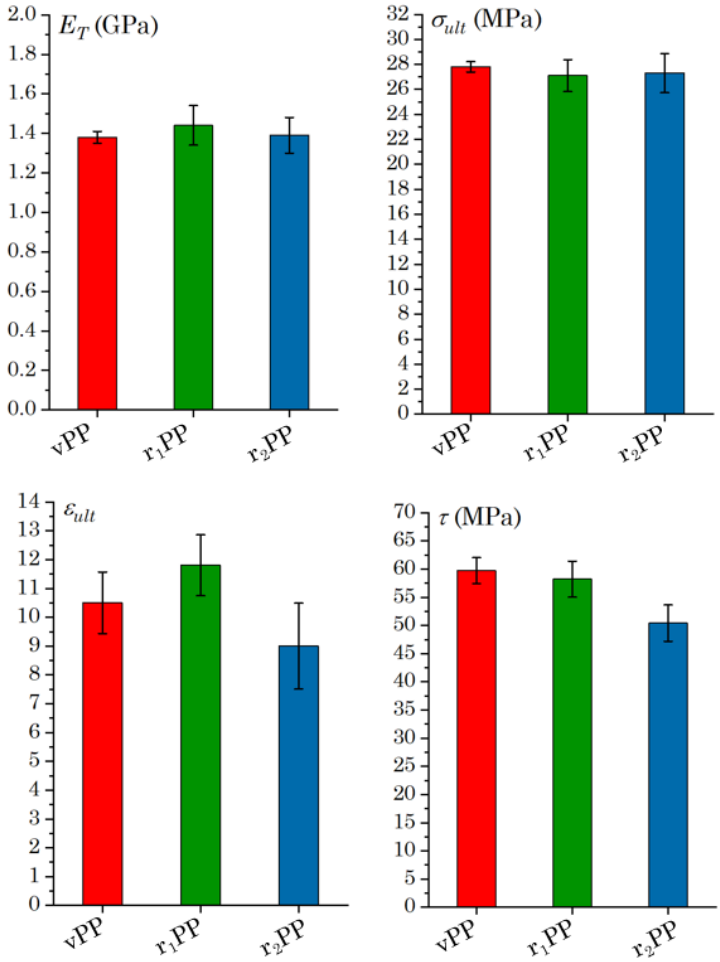

Fig. 4.10. Bar charts showing the tensile stiffness, ultimate tensile strength, corresponding strain and shear strength of pure polypropylene. Error bars represent standard deviation of six specimen batch.

Referring to ASTM D732, the shear strength tests were performed using a shear punch tool. A servo-electric tensile test machine was used in compression

mode using a constant crosshead displacement speed of 1.25 mm/min; load was recorded using a 10 kN load cell.

Stress-displacement curves for shear testing are plotted in Fig. 4.11. They showed typical ductile response to shear stress for semi-crystalline thermoplastics. Under shear stress the polymer exhibited three distinct phenomena: *1) an initial linear-elastic response, followed by 2) a yielding and subsequent visco-elastic response i.e. reduction in stiffness and 3) a final strain hardening before mode I shear failure*. Specimens exhibited analogous failure with no significantly premature failures. The initial linear-elastic region represented elastic deformation of the polymer chains. The second, visco-elastic stage represented a combination of plastic deformations and molecular translation as chains start to uncoil and slide past each other. The final stage suggested a stiffening of the polymer which represents the temporary alignment of uncoiled and stretched polymer chains, causing the apparent increase in pseudo-shear modulus. As the graph plots shear stress as a function of deformation, and not strain, it is not the shear modulus.

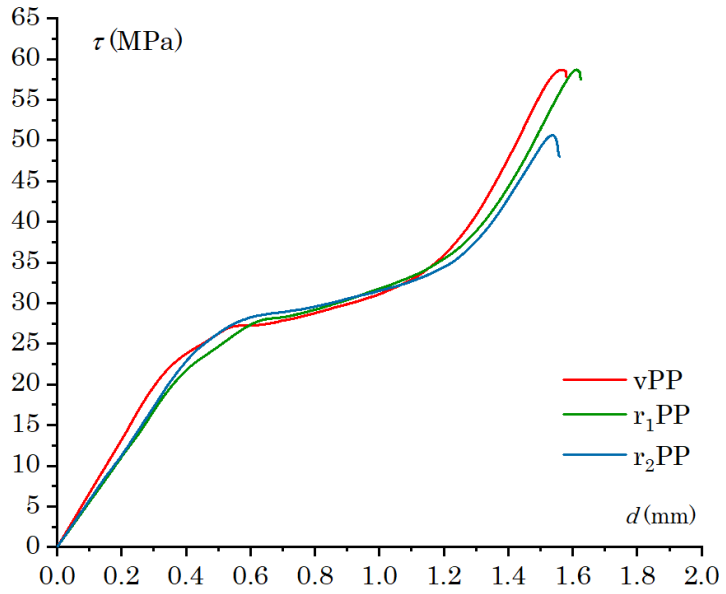

Fig. 4.11. Shear stress-displacement curves for polypropylene after each recycling loop.

Specimen response to shear stress varied minimally between iterations, until the strain hardening stage where there was a slight deviation in strain hardening and a decrease in shear strength (14 % ± 5.2 %) between r_1PP and r_2PP. This could be attributed to a combination of the drop in M_w, Table 4.6, and the increased micro voids observed in the outer edges of the recycled panels, Fig. 4.3 and Fig. 4.12.

Shear specimens were punched from the outer sections of the panel where there was an increased prevalence of micro voids, both as a function of distance from the panel centre, and, as a function of recycling loop. A micro void located at a shear surface decreased the total shear area and thus reduced the shear strength. Micro voids were clearly visible in the r_2PP shear surface micrograph displayed in Fig. 4.12c. Micro voids are likely a consequence of a remanufacturing error and not a phenomenon resulting from an intrinsic polymer change due to recycling.

A M_w decrease reflects the breaking of long polymer chains into smaller, medium length chains. During loading the polymer is straining, a shorter chain has less intermolecular bonds between neighbouring chains, requiring less shear force for failure, resulting in a drop in the shear strength. However, the most significant drop in M_w was between vPP and r_1PP where the shear strength remains unchanged. This suggests that the contribution from M_w is less significant. It is therefore reasonable to conclude that recycling had little effect on the shear properties of PP.

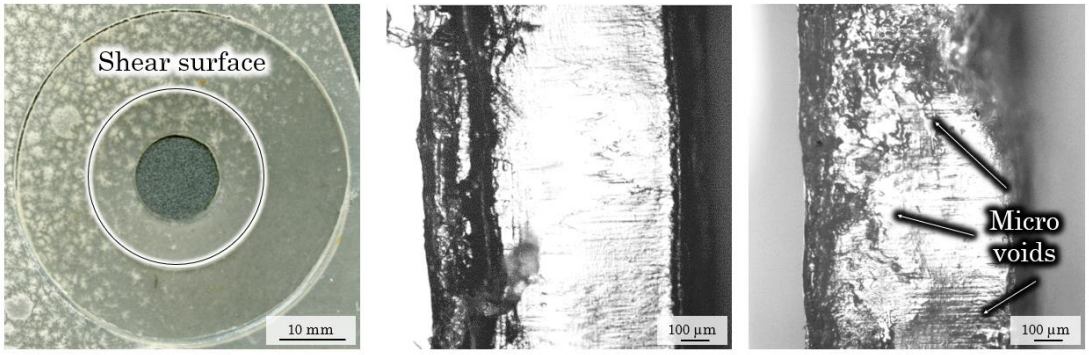

a) Shear specimen cutting from r_2PP panel

b) vPP shear surface

c) r_2PP shear surface

Fig. 4.12. *a)* Shear specimen cutting from r_2PP panel edge highlighting the shear surface. *b)* A micrograph of a portion of a vPP shear specimen with a homogeneous shear surface. *c)* A micrograph of a portion of a r_2PP shear specimen with an inhomogeneous shear surface due to micro voids.

4.3.3 Conclusions

The polymer characterisation results suggest that recycling has the following effects on polypropylene:

1. The reclamation process may have extracted stabilisers from the polymer mixture. This was supported by the loss of peaks in the FTIR spectra of r_2PP, and isothermal stability in air, however further analysis is required.

2. DSC analysis showed no observable changes in the crystallinity of recycled panels and FTIR spectra indicated no significant changes in the polymer structure over two recycling loops.

3. GPC/SEC analysis reported an initial reduction of small molecular weight groups which further indicated the extraction of stabilisers during the first reclamation. Successive decrease of M_w and PDI pointed to the degradation of high molecular weight chains.

The mechanical testing results built on the polymer characterisation findings by indicating that:

1. The tensile properties of recycled polypropylene were unaffected by recycling after two loops. The extent of the degradation suggested from the polymer characterisation is not a significantly contributing factor to the tensile performance.

2. There was a slight decrease in the shear strength after the second recycling loop, however this may have been due to micro voids. These are likely a result of remanufacturing and not intrinsic to the polymer.

Overall, the closed-loop recycling process was able to produce pure thermoplastic material over two recycling loops with invariable mechanical performance, and thus had the potential to recycle composite material without a significant drop in value.

4.4 CLRM: Carbon fibre reinforced polypropylene

4.4.1 Closed-loop recycling process

This section details the experimental parameters used in the recycling of a CFPP composite following the methodology outlined in Section 3.2.1. A schematic of the closed-loop recycling method and the experimental analysis method is presented in Fig. 4.13. The reclamation methodology was analogous to the previous one except it involved an additional filtration step for fibre separation. Remanufacture included the alignment of rCFs and an adapted compression moulding cycle to incorporate fibre impregnation and consolidation.

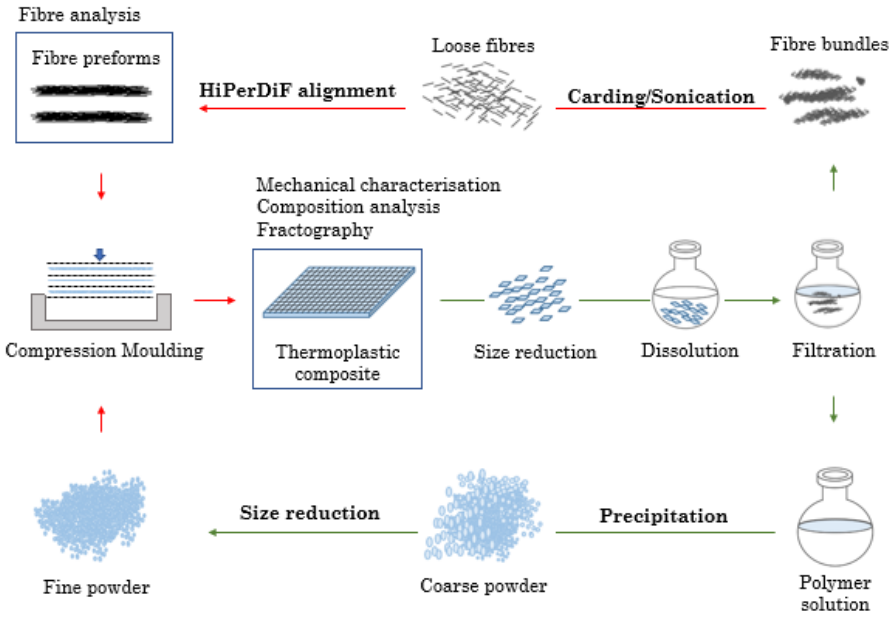

Fig. 4.13. The closed-loop recycling method used, with material characterisation annotation. The green and red arrows represent the reclamation and remanufacturing procedures, respectively.

vCFPP specimens were manufactured following the methodology outlined in Section 3.2.2. vCFPP material was recycled over two loops so that mechanical testing and fibre analysis was conducted on virgin, primary recycled and secondary recycled CFPP, denoted vCFPP, r_1CFPP, and r_2CFPP, respectively.

4.4.1.1 Reclamation

The reclamation of fibre and matrix from CFPP specimens involved an additional filtration step and required a lower solution concentration (1 % w/v) than matrix reclamation from panels (15 % w/v). Experimental parameters used in this reclamation can be found in Table 4.8. A reduction of the polymer solution concentration was required to decrease solution viscosity, to optimise fibre filtration and washing. A positive consequence of this was increased dissolution rates over the comparatively concentrated pure PP solution.

The key stage of the composite reclamation process was the separation of fibres from the polymer solution. rCFs were dried in a vacuum oven (~ - 29 inHg) at 80 °C for 14 hours. The rCF bundles were separated by the dry fibre carding method.

Table 4.8. Reclamation parameters used for CFPP recycling.

	Shred Size	Solvent	Temp.	Time	Non-solvent	Conc.	Solvent Ratio
	mm^3	-	°C	mins	-	% w/v	S:NS
CFPP	125	xylene	135	60	acetone	1	1:3

Temp. = Temperature, Conc. = Concentration, S = Solvent, NS = Non-solvent

PP was precipitated by cooling to room temperature and the addition of non-solvent. Precipitation did not occur upon cooling due to the low solution concentration. The precipitate was vacuum filtered using Buchner apparatus, washed and dried in a vacuum oven (~ - 29 inHg) at 80 °C for 14 hours.

Solvent traps were used to reclaim the solvent removed during drying. Solvents were collected and separated using fractional distillation. Acetone and xylene recovery yields were unchanged from those achieved in the un-reinforced PP study. The reclamation yield for PP was 87 % as determined by comparing the total vPP powder mass with the subsequent reclaimed precipitate masses. The decreased yield compared with the un-reinforced PP study was a consequence of solution concentration effects on precipitation, *i.e.* some polymer remained in the supernatant.

The fibre yield achieved was 94 %, this was determined by comparing total preform and subsequent dried rCF masses. The remaining 6 % of fibres were not salvageable from processing; *e.g.* fractured fibres passing through filter papers, fibres lost during handling, and fibres trapped on the filter paper. The yields obtained were not from reclamation conditions optimised for maximum yield therefore higher yields may be expected. For the solvents, this may be closer to those obtained in the literature, see Section 3.1.1

All specimens were recycled, including the fracture surfaces, as the combination of pull-out dominated failure and the negligible amount of failed

fibres involved, in comparison to the total amount in the specimen, made any influence from fractured fibres insignificant. Any fractured fibres, from failure or otherwise, are accounted for in the fibre length distribution analysis.

4.4.1.2 Remanufacture

The remanufacturing method used was as described in Section 3.2.2 Dried rCF were aligned into dry preforms using the HiPerDiF alignment method. The rCF preforms, and polymer precipitate, were combined in an alternate stacking sequence so that each composite stack was made up of four preform layers and three matrix layers. Remanufacturing parameters used are reported in Table 4.9. Stacks were compression moulded in a steel tool and under vacuum conditions. The compression moulding cycle used is plotted in Fig. 4.14.

Table 4.9. Remanufacturing parameters used for CFPP recycling.

	CF mass	PP mass	Predicted Vf_F	Temp.	Pressure	Actual Vf_F	Flash
	mg	mg	%	℃	MPa	%	wt%
CFPP	123[a]	200[a]	25	200	11.8	26	16

[a] Per specimen. Temp. = Temperature

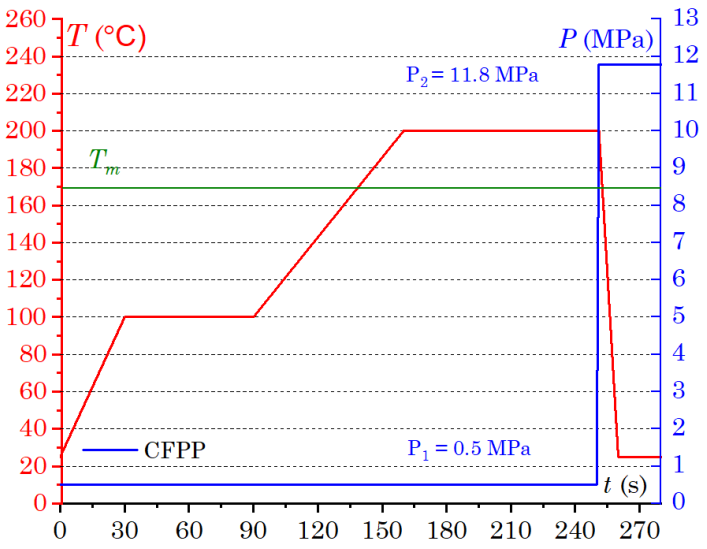

Fig. 4.14. Compression moulding cycle used to manufacture CFPP specimens. Specimens were held at 0.5 MPa (P_1) for 4 hours until transfer from oven to hot press for consolidation at 11.8 MPa (P_2).

4.4.2 Results and discussion

4.4.2.1 Mechanical testing

CFPP specimens were tested for their tensile properties in accordance with ASTM D3039. Axial force was provided by a Shimadzu AGS-X servo-electric tensile test machine with a 10 kN load cell and a constant crosshead displacement of 1 mm/min. Strain was measured using the Imetrum video gauge software, over a gauge length of 50 mm. specimens were sprayed back and speckled with white dots to aid with strain mapping; an example of this is shown in Fig. 4.15.

Fig. 4.15. Image of a composite specimen prepped for tensile test showing the speckle pattern used for strain mapping.

Representative stress-strain curves obtained from tensile tests of CFPP, as a function of recycling loop, are shown in Fig. 4.16. The results of the tensile tests are recorded in Table 4.10, and are presented as bar charts in Fig. 4.17. σ_{ult} was determined as the maximum stress and ε_{ult} refers to the corresponding strain. E_T was determined by taking the gradient of the linear-elastic region section of bounds $0.001 < \varepsilon < 0.003$. $E_{T(0.26)}$ denotes the tensile stiffness normalised to a 26 % Vf_F, following the rules of mixture.

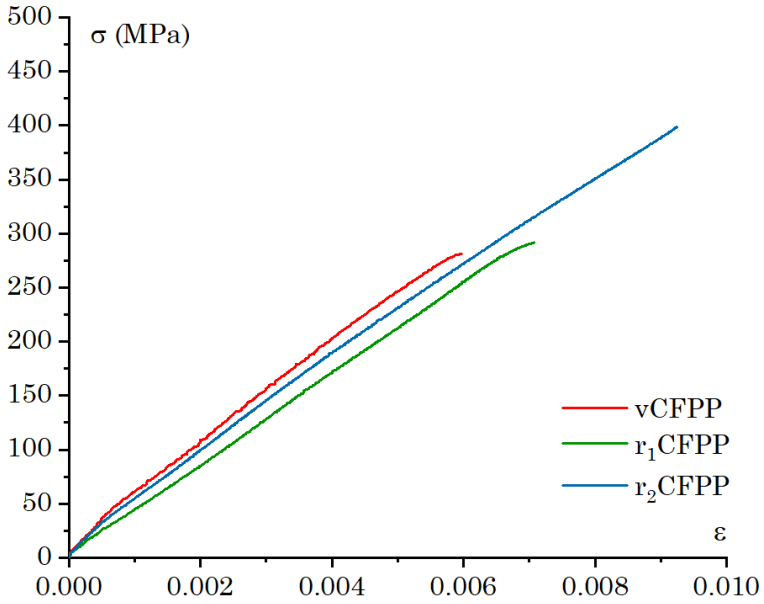

Fig. 4.16. Representative stress-strain curves obtained from tensile test of CFPP as a function of recycling loop.

Table 4.10. Mechanical performance data collected from tensile tests of CFPP after each recycling loop.

	$E_{T(0.26)}$	σ_{ult}	ε_{ult}	ρ	Vf_F
	GPa	MPa		MPa	%
vCFPP	43.9 (5.1)*	285 (9.7)	0.69 (12)	1.00 (2.6)	26.2 (8.4)
r1CFPP	39.0 (5.5)	281 (13)	0.70 (8.8)	1.00 (2.5)	26.2 (4.6)
r2CFPP	42.3 (5.1)	396 (5.4)	0.99 (4.4)	1.00 (4.3)	26.3 (3.6)

* Coefficient of variance calculated from six specimens of the same batch.

Tensile specimens exhibited a typical linear-elastic response followed by rapid failure. vCFPP and r1CFPP showed a region of increased compliance just before failure. This was representative of pull-out dominated failure where less force is required for the same displacement. Fibre pull-out occurs if full stress transfer from matrix to fibres is not possible, therefore the composite failure is not caused by fibres reaching their failure strain (1.93 %) but by the formation of a fracture surface at the interface. This is a result of poor interfacial shear strength (IFSS) and thus a high critical fibre length, see Equation 3.3. The IFSS

between CF and PP is typically low, less than 10 MPa, as reported in the literature [207]. Using Equation 3.2, this results in a fibre critical length of approximately L_c = 1.5 mm. For vCF (3 mm CF), this would mean that all the fibres were above L_c and could be maximally loaded, however, the extensive pull-out failure suggests that the IFSS was lower than 10 MPa.

For vCFPP and r$_1$CFPP, the IFSS must have been significantly less than the tensile strength of the composite to explain the fibre pull-out dominated failure observed. The failure of r$_2$CFPP was of a brittle nature suggesting that there was an increase in the IFSS, which increased composite strain and resulted in increased fibre fracture.

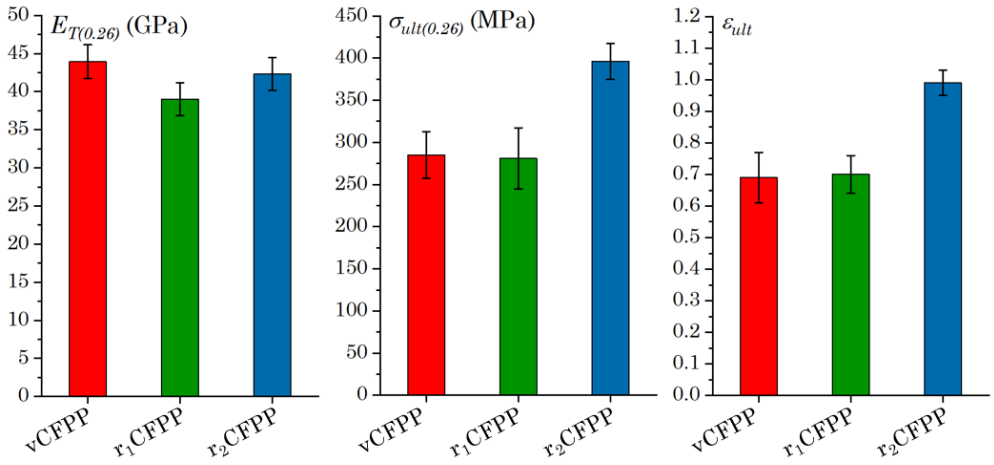

Fig. 4.17. Bar charts showing the normalised tensile stiffness, normalised ultimate tensile strength and ultimate tensile strian. Error bars represent standard deviation of six specimen batch.

Overall, the plots showed no significant reduction in $E_{T(0.26)}$ between recycling loops. The decrease after the first recycling loop was within the coefficient of variance and there was an increase after the second recycling loop. This suggests that both the degree of alignment and the intrinsic stiffness of the fibres are both unaffected by recycling, the latter being difficult to achieve under the recycling conditions used. Kruskall-Wallis analysis reported that statistically there was no change in the σ_{ult} and ε_{ult} between vCFPP and r$_1$CFPP.

A 30 % increase in σ_{ult} and ε_{ult} was recorded after the second recycling loop whilst $E_{T(0.26)}$ remained statistically unchanged. As the σ_{ult} increased after the second recycling loop there must have been an increase either, in matrix tensile strength, IFSS or Vf_F. The results of Section 4.3 suggested that the matrix tensile strength is unaffected by recycling and quantitative analysis showed that the Vf_F remained constant therefore the increased σ_{ult} is most likely due to an increase in IFSS.

IFSS analysis was not carried out due to the experimental complexity of testing 3 mm carbon fibres and, conversely, the HiPerDiF alignment consistency drops with rCF longer than 12 mm due to fibre agglomerations in the tanks and piping. Quantitative IFSS would be advantageous however overall conclusions could still be accurately drawn.

4.4.2.2 Fibre analysis

Fibre length distribution analysis was used to determine the effect of recycling on the average fibre length. The FLD of preforms after each recycling loop are presented in Fig. 4.18.

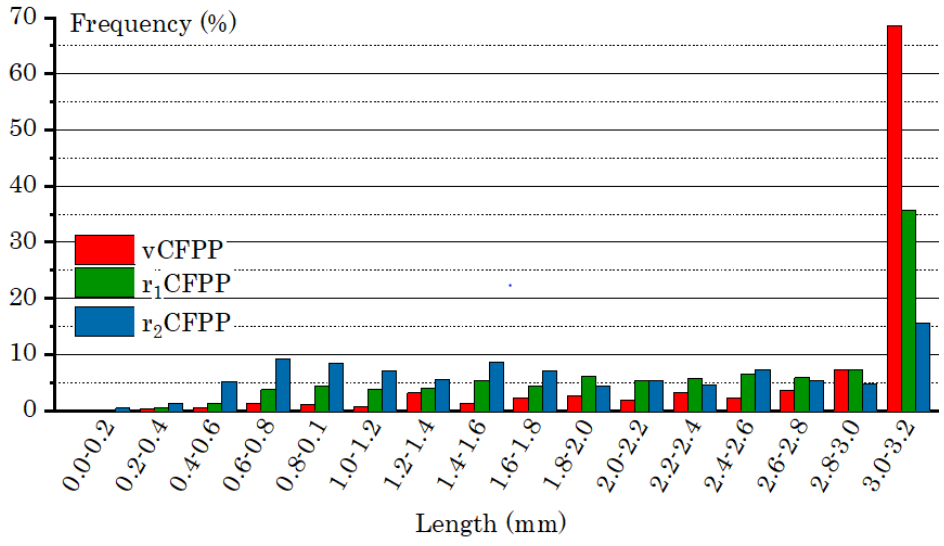

Fig. 4.18. Fibre length distributions of fibre preforms used in vCFPP, r_1CFPP and r_2CFPP.

An error of ± 0.2 mm was applied for the by-eye length measurement of fibres. In the vCFPP preform sample 74 % of fibres are in the range of 2.8 - 3.2 mm; a similar value to that obtained in other studies involving 3 mm carbon fibres and the HiPerDiF alignment method [63]. After the first recycling loop, 42 % of fibres are in the range 2.8 - 3.2 mm. For r_2CFPP the FLD was more evenly distributed with 0.8 - 0.1 mm and 1.4 - 1.6 mm having 9 % of the distribution and 3.0 – 3.2 mm containing 15 %. A combination of the high compaction pressure, fibre carding and the alignment process could be causing fibre breakages and the evening out of the FLD; It is assumed that the high compaction pressure is the largest contributing factor [150].

The alignment head consisted of numerous parallel plates spaced at a distance, d, much less than the length of the fibre. If d is close to the average fibre length then the fibres have more space to misalign in the xy plane, resulting in poor alignment [207]. Therefore, minimising d increases the alignment potential not only for fibres of the maximum length, in this case 3.0-3.2 mm, but also for any fibres of length > d. The experimental d used was approximately 0.3 mm, which was about the same size as the smallest fibres reported in the FLD, which in each loop only represented 2 % of the fibres used. This explains why the tensile stiffness remained constant despite significant spreading of the FLD.

A flattening of the FLD should cause a decrease in σ_{ult}, if the IFSS remains constant, as less fibres will have $l > L_c$. σ_{ult} was unaffected after the first recycling loop despite a flattening of the FLD, therefore it can be concluded that the IFSS must have increased in parallel with the decrease in FLD. Yet as strength did not increase, and pull-out still occurred, the increased IFSS served to counterbalance the loss of strength accrued through fibre fracture.

A Hitachi TM3000 SEM was used (5000 V accelerating voltage) to investigate the surface quality of fibre preforms collected from each recycling iteration.

SEM micrographs of fibres were taken from aligned preforms before impregnation of vCFPP, r_1CFPP and r_2CFPP, see Fig. 4.19a-c. Fig. 4.19a shows the vCFPP preforms with clean surfaces in both magnifications. Fig. 4.19b similarly shows relatively clean fibre surfaces for the r_1CFPP preform, however

there was a marginal increase in a residual substance. It can be clearly seen in the magnified preform micrographs of r_2CFPP, Fig. 4.19c that fibres have been coated with a substance; this was assumed to be PP residue left after reclamation.

It was possible that the PP residue acted as a form of sizing that increased the IFSS. This corroborates the increase in σ_{ult} and ε_{ult} observed from tensile testing. L_c is inversely proportional to IFSS, which means that a decrease in average fibre length will not reduce overall composite strength if the IFSS is increasing in parallel. This supports the results of the FLD. This also results in increased specimen extension under loading, ε_{ult}, as the fibre strain limit is reached before the fibre pull-out strength, *i.e.* the IFSS.

The pull-out dominated failure of vCFPP and r_1CFPP can therefore be attributed to the poor adhesion between the inorganic surface of carbon fibre and the organic, non-polar polypropylene chains. The deposition of PP on fibres act as a sizing providing a region of increased adhesion at the interface, improving overall fibre-matrix adhesion.

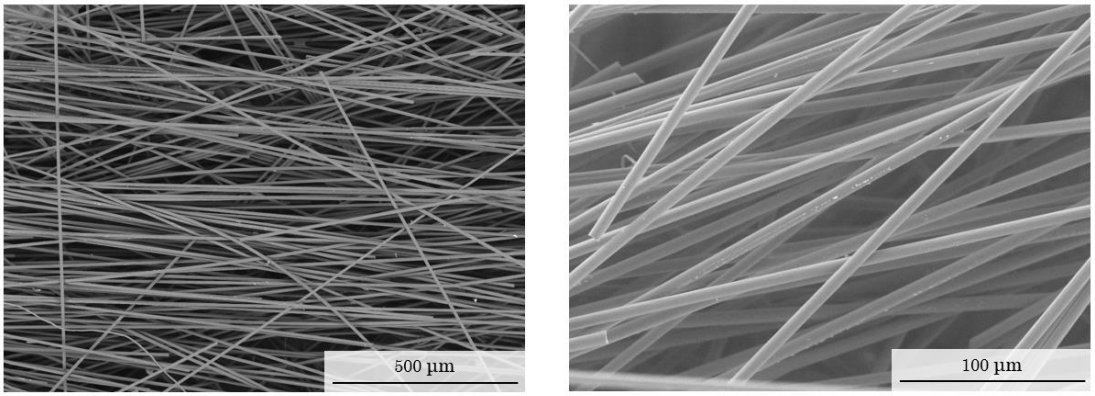

a) SEM micrograph of preform cutting from vCFPP

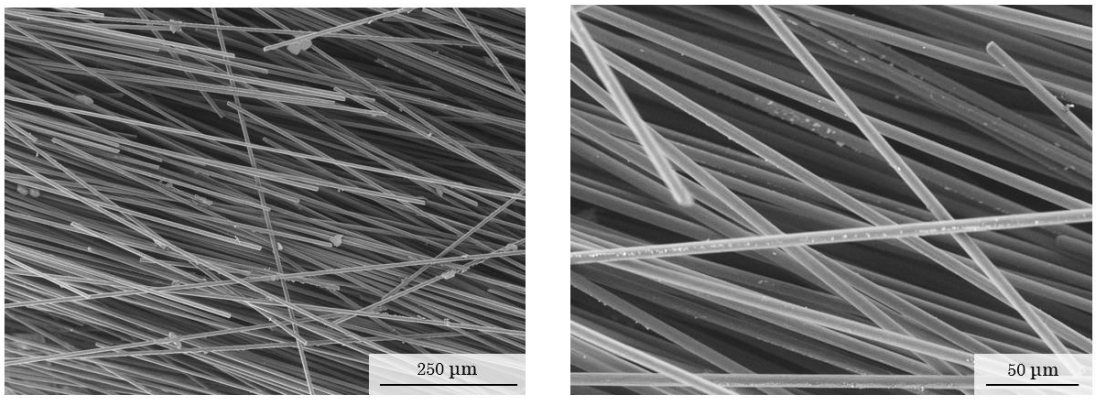

b) SEM micrograph of preform cutting from r_1CFPP

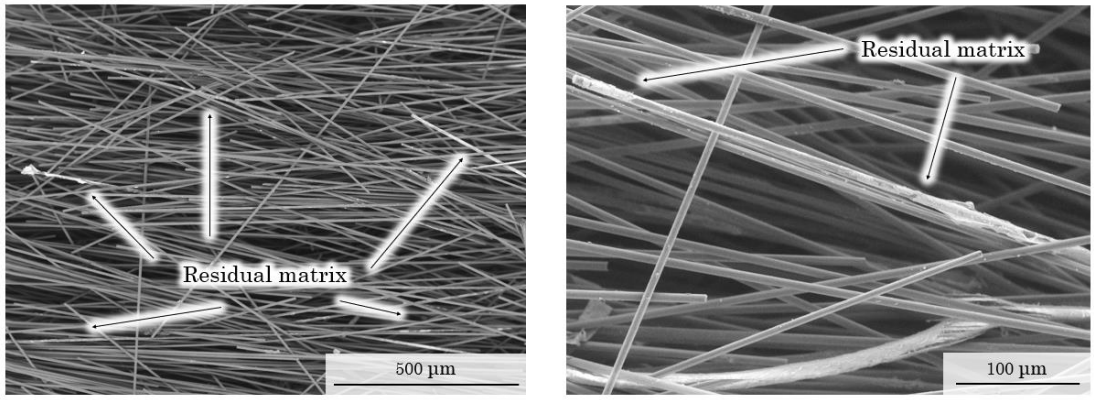

c) SEM micrograph of preform cutting from r_2CFPP

Fig. 4.19. *a-c)* SEM micrographs of preform cuttings taken from aligned preforms, of each recycling loop, before impregnation. r_2CFPP shows deposition of residue on fibre surface which is deemed to be unwashed matrix.

4.4.2.1 Fractography

Fracture surfaces were inspected using a Hitachi TM3000 SEM (5000 V accelerating voltage). SEM micrographs of vCFPP and r_2CFPP fracture surfaces are shown in Fig. 4.20a-b. Fig. 4.20a shows extensive fibre pull-out for vCFPP which explains the increased compliance observed in the tensile stress-strain curve. Less fibre pull-out and an increase in matrix coated fibres is observed in the r_2CFPP fracture surface, Fig. 4.20b. This indicates an increase in fibre-matrix adhesion, which explains the brittle fracture observed in the tensile stress-strain

curve and supports the ongoing conclusion that the IFSS has increased due to residual matrix deposition on the fibre surface of r_2CFPP.

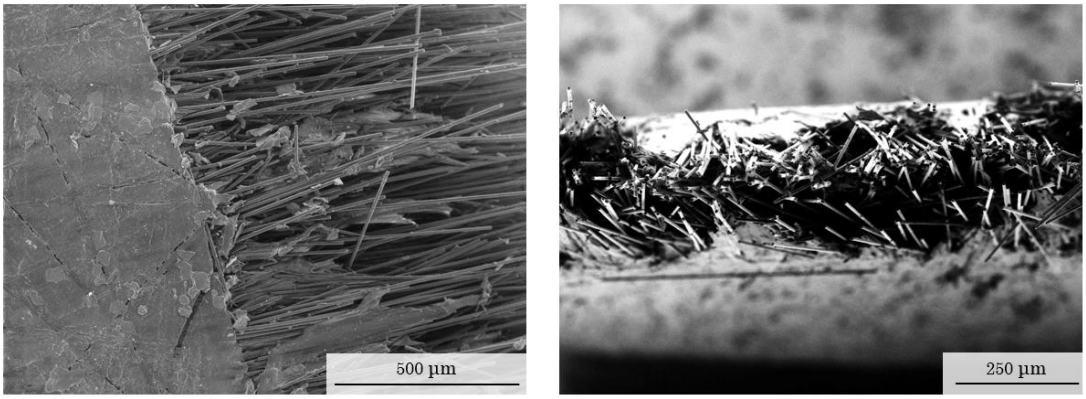

a) SEM micrograph of vCFPP fracture surface

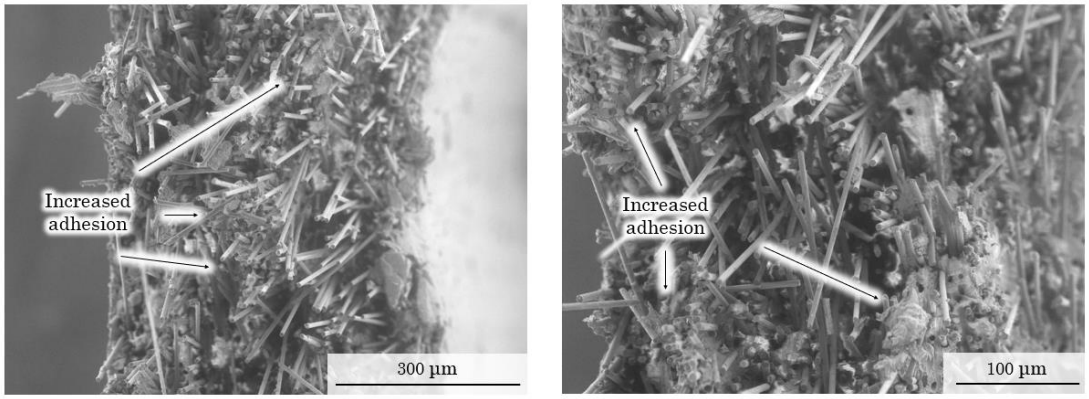

b) SEM micrograph of r_2CFPP fracture surface

Fig. 4.20. *a)* vCFPP fracture surface showing extensive fibre pull-out. *b)* r_2CFPP fracture surface where a decrease in fibre pull-out is clearly visible.

4.4.3 Conclusions

The mechanical performance and fibre properties of recycled CFPP material were examined experimentally. The analysis linked macroscopic performance with microscopic fibre surface phenomena, fibre length and polymer behaviour.

Overall, there was no reduction in the mechanical performance of the composite material as a function of recycling. The secondary recycled specimen exhibited a 30 % increase in σ_{ult} and ε_{ult}. This was deemed the result of an increase in IFSS which was supported by residual matrix found on the surface of r_2CFPP fibres. There was a successive broadening of the fibre length distribution which was most likely caused by the high compaction pressure but may also be due to damage from handling during the process, or as a result of carding. Lower compaction pressures resulted in specimens with incomplete wet-out of the fibres, therefore the lowest practical pressure was selected. It should be noted that optimisation of the manufacturing process was not carried out as it was deemed outside the scope of this study.

Fibre alignment was not significantly affected by recycling as tensile stiffness remained statistically constant throughout. Recycling does gradually reduce fibre length as observed in the FLD. This could have the potential to reduce fibre alignment and composite strength. The former caused by increased mis-alignment of fibre in the *xy* plane during deposition on the conveyor belt and the latter caused by a reduction in fibres with length greater than the critical fibre length. However, these consequences did not occur as the alignment plate spacing was sufficiently less than the smallest fibre lengths and the increased IFSS lowered the critical fibre length below that of the average fibre length.

IFSS plays a crucial role in the mechanical performance of the recycled composite and would be useful to quantify, however it is experimentally complex to test fibres as short as 3 mm and alignment is difficult for rCF fibre lengths > 12 mm due to agglomeration.

For the development of a proof-of-concept material, the absolute mechanical performances were of secondary importance, therefore the Vf_F of 26 % was been selected to guarantee maximum fibre impregnation for consistent results.

4.5 Overall conclusions

The aim of this proof-of-concept investigation was to determine if it was possible to reclaim and remanufacture a carbon fibre thermoplastic composite over two recycling loops, *i.e.* using a closed-loop recycling process. This aim was achieved as CFPP material was manufactured, reclaimed and remanufactured over two loops using a closed-loop recyclable process.

To the author's knowledge, the closed-loop process is the only recycling procedure available, for any matrix system, that can retain performance from both fibre and matrix and retain mechanical performance of the rCFRP after the first and subsequent recycling loops. The mechanical performance of the r_2CFPP is, to the author's best knowledge, the highest performance recycled CFPP composite available in the literature. Fig. 4.21 presents a comparison of the closed loop material with the highest performance discontinuous CFPP materials in the literature; these are also presented in Table 4.11.

Table 4.11. Properties of CFPP material sourced from the literature.

Author	Architecture	Vf_F	E_T	σ_{ult}
		%	GPa	MPa
Hashimoto *et al.* [208]	Aligned DCF	20.0	24.6	432
Harper *et al.* [204]	Aligned DCF	45.0	21.6	60.1
Akonda *et al.* [106]	Aligned rDCF	27.7	33.0	160
CFPP	Aligned rDCF	26.0	42.3	396

DCF = discontinuous carbon fibre. (r-) denotes recycled fibre

The mechanical performances in Fig. 4.21 are normalised to 26 % Vf_F to aid comparison. The author acknowledges that this normalisation for discontinuous CF composites, based on rule of mixtures, is not strictly appropriate as the level of alignment and interfacial shear strengths differ between materials. The bar charts indicate that the tensile stiffness achieved is greater than any reported in the literature and the strength is almost comparable to a vCFPP material made by Hashimoto *et al.* [194].

The process can be deemed closed loop as fibres (94 % yield), matrix (90 % yield) and recycling solvents (acetone = 87 %, xylene 91 % yield) were all reclaimed after each loop. Although there is evidence to suggest the removal of polymer additives during reclamation this had no significant effect on the mechanical performance. If additives are removed during reclamation, they must remain in the supernatant, which can be evaporated down to the solutes. These can be collected and remixed with the precipitate powder before impregnation therefore closing the loop.

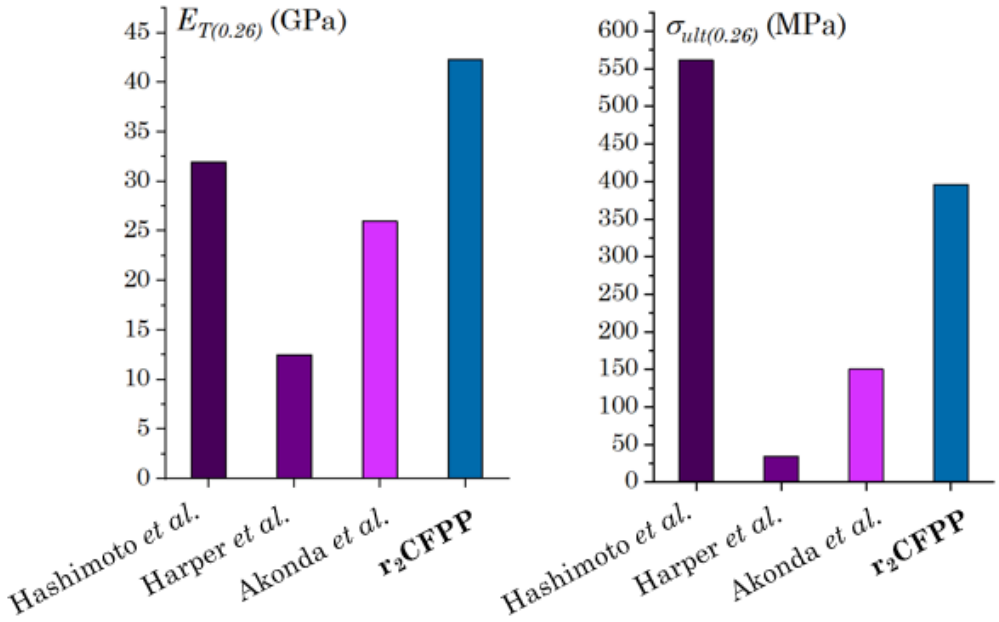

Fig. 4.21. Bar charts comparing the tensile stiffness and strength of r_2CFPP material with discontinuous carbon fibre PP composites from the literature. Performance is normalised to 26 % fibre volume fraction.

The main objective of the process was to recycle a carbon fibre thermoplastic composite material over two recycling loops without reducing the mechanical properties of the composite and thus retaining the value of the recyclate so that a rCFRP of equivalent value could be produced. This objective was successfully met, as the mechanical performance did not decrease as a function of recycling.

5 A closed-loop recycling process

Section 5.2 describes the fibre and matrix material used in this study and Section 5.3 thoroughly details the closed-loop recycling process, results and discussion of each batch of specimens. This section is split into five separate Sections; Section 5.3.1 outlines the closed-loop recycling process used and how it differs between solvent systems. Sections 5.3.2, 5.3.3, and 5.3.4 consist of the results and discussion for the three main studies; the two solvent systems and a constituent exclusion study; these are described below. Each section includes concluding remarks, the overall conclusions are drawn in Section 5.4.

5.1 Introduction

Chapter 4 demonstrated that the closed-loop recycling process can be used to produce a CFRP over two recycling loops, without degradation of the mechanical properties. The whole process was not

This Chapter builds on the previous work, upgrading the CFRP to incorporate a high-performance thermoplastic matrix, *i.e.* polyamide 6 (PA6), with the aim of:

- Producing a high-performance CF reinforced PA6 composite (CFPA6), able to retain properties comparable to those of

currently available materials, over two recycling loops, to be used in industrial applications, *e.g.* semi-structural automotive components.

- Investigating any effect the closed-loop recycling process may have on the constituent and composite mechanical performance. A comparison of two solvent systems is provided to understand their effect on properties.

5.2 Materials

PA6 was used as the thermoplastic in this study due to the following advantages:

- It is a semi-crystalline thermoplastic that is soluble in low hazard solvents.

- It can provide higher composite mechanical performance than polypropylene, due to increased matrix tensile stiffness, strength, and interfacial shear strength with CF.

- It has the best compromise of mechanical properties and processing temperature out of the other polyamide variants, *i.e.* higher mechanical performance than polyamide 12 and lower processing temperatures than polyamide 6,6.

- PA6 is commercially available and comparative composite data is available as CFPA6 have been widely evaluated in the literature [209–225].

- The industrial applicability is demonstrated by its commercial availability [226].

vPA6 was sourced in powder form from Goodfellow distributors. The material properties of vPA6, as determined through in-house polymer characterisation, can be found in Table 5.1.

Table 5.1. Properties of the PA6 used in this study.

	Density	T_m	T_g	Crystallinity	M_W	M_n	PDI
	g/cm^3	°C	°C	%	g/mol	g/mol	-
PA6	1.13*	217	45.0	34.9	5.53 x 10^4	7.83 x 10^3	7.70

Data collected experimentally, see subsequent analysis for conditions. * Data from manufacturer.

DCFs used in this study were the same as used in Chapter 4, the material properties of these fibres are available in Table 4.2

Two solvent system are compared in this study:

1. Formic acid solvent and water non-solvent. This system can provide full dissolution at room temperature, which reduces the recycling process energy demand; this may become substantial at scaled volumes. However, this may be in compromise with dissolution rate. The boiling points of the two solvents are very similar which may cause solvent reclamation issues; this will be explored in Section 5.3.1.1.

2. Benzyl alcohol solvent with acetone non-solvent. This system requires dissolution at elevated temperatures, which increases the energy demand of recycling. However, elevated temperatures may result in a comparatively faster dissolution rate to other systems. The boiling point disparity between solvents enables reclamation through fractional distillation; this will be explored in Section 5.3.1.1.

Solvents used during reclamation for the first solvent system were certified ACS reagent grade formic acid, sourced from Fisher Scientific, and tap water. For the second solvent system, the reagent grade benzyl alcohol and acetone were sourced from Alfa Aesar and Fisher Scientific, respectively.

5.3 CLRM: Carbon fibre reinforced polyamide 6

5.3.1 Closed-loop recycling process

This section details the experimental parameters used in the recycling of CFPA6 composite following the reclamation, remanufacture and experimental analysis methodologies outlined in Fig. 5.1. vCFPA6 material was recycled over two loops so that mechanical testing and fibre analysis was conducted on virgin, primary recycled and secondary recycled CFPA6.

The matrix degradation observed in Chapter 4 did not have a significant effect on composite mechanical performance. This indicated that the contribution of matrix mechanical performance is less impactful than that of the fibres and the fibre-matrix interface. Therefore, this chapter does not include an initial evaluation of the pure thermoplastic mechanical properties. Instead, to account for this, the study performs polymer characterisation on the reclaimed precipitate and compares the composite mechanical performance of specimens made from virgin and recycled fibres with both virgin and recycled matrix. This will provide enough information about matrix degradation and demonstrate the relative magnitude of matrix and fibre contributions to composite performance.

The composite specific closed-loop process is identical to that used previously, except for adaptations made for the PA6 such as, solvent systems, reclamation parameters, and remanufacturing parameters. The study also compares the effects of using two different solvent systems for reclamation, benzyl alcohol with acetone non-solvent and formic acid with water non-solvent.

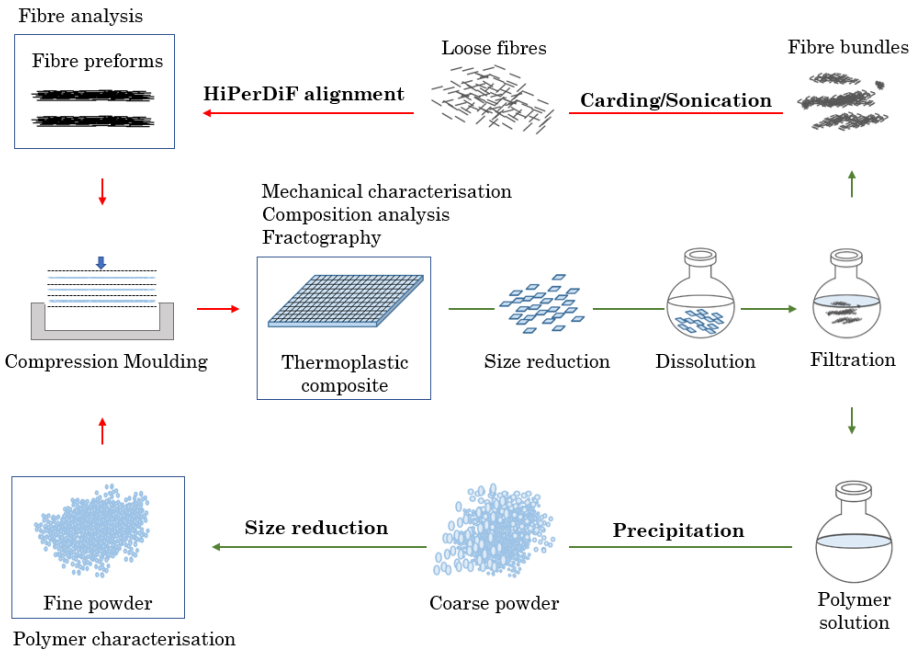

Fig. 5.1. The closed-loop recycling method used with material characterisation annotation. The green and red arrows represent the reclamation and remanufacturing procedures, respectively.

Benzyl alcohol reclamation requires higher temperatures whereas PA6 is soluble in formic acid at room temperature. There are obvious advantages to avoiding additional heating costs in an industrial process however acidic solvents are more hazardous and less favourable at commercial scales.

The reclamation, remanufacturing and experimental analysis methodologies of CFPA6-FA (*i.e.* recycled with the formic acid system) and CFPA6-BA (*i.e.* recycled with the benzyl alcohol system) will be presented in the same section. However, the results collected from each specimen set will be reported separately. The only difference between the two systems is the reclamation process; the remanufacturing procedures and the experimental analysis methods are identical.

5.3.1.1 Reclamation

Experimental parameters used in both reclamation processes, *i.e.* the two solvent systems, can be found in Table 5.2. Full dissolution of PA6 occurred in benzyl alcohol at 160 ℃ after 1 hour and in formic acid at 25 ℃ after 3 hours.

Table 5.2. Reclamation parameters used for CFPP recycling.

	Solvent	Temp.	Time	Non-solvent	Conc.	Solvent Ratio	Fibre Yield
	-	°C	mins	-	% w/v	S:NS	%
CFPA6-BA	benzyl alcohol	160	60	acetone	1	1:1	96
CFPA6-FA	formic acid	25	180	water	1	1:1	95

Temp. = Temperature, Conc. = Concentration, S:NS = solvent : non-solvent

The key stage of the composite reclamation process was the separation of fibres from the polymer solution. rCFs were filtered at 25 ℃ and rCFs were dried in a vacuum oven (~ - 29 inHg) at 80 °C for 14 hours.

The rCF bundles were separated by the wet sonication method. Approximately 100 mg of carbon fibres were suspended in a 1 L beaker of water placed in an ultrasonic bath. Stirring separated most fibres however some agglomerations required additional manual separation. This was changed from the dry carding method, used in Chapter 4 and described in Section 3.2.1, as the harsh brushing was thought to be causing fibre fracture resulting in the evening-out of the fibre length distribution. There was also a loss of fibres on the carding surface that could potentially have been avoided using the wet sonication method.

Both separation methods were not 100 % effective in their ability to completely separate fibre agglomerations, as some were still visible in the preforms after alignment; these were then transferred to the preform.

For benzyl alcohol, PA6 was precipitated by cooling to room temperature and the addition of acetone at a 1:1 volume ration. For formic acid, PA6 was precipitated by the addition of water at a 1:1 volume ratio. It was important to add the acid solution to water, and not *vice versa*, to avoid the reaction of water with the high, relative concentration of acid and any potential effects on precipitation this may have had. The precipitate was vacuum filtered using

Buchner apparatus, washed and dried in a vacuum oven (~ - 29 inHg) at 80 °C for 14 hours.

Benzyl alcohol and acetone were easily separated and reclaimed by fractional distillation, in yields of 92 % and 85 %, respectively. This is due to the disparity in boiling point of the two solvents, 205 ℃ and 56 ℃, respectively. However, formic acid and water could not be reclaimed using the fractional distillation method as their boiling points, 100.8 ℃ and 100 ℃, respectively, were too similar, forming an azeotropic mixture. Azeotropic mixtures cannot be separated directly by boiling point, but can be separated by more complex separation methods, such as continuous reactive distillation or salt distillation, where the boiling point/vapour pressure of one component is modified to enable distillation [227]. These require additional materials and additional processes to provide solvent reclamation, which will likely increase the energy demand, duration, and cost of reclamation.

The average fibre yield achieved over both solvent system studies was 96 %, this was determined by comparing total preform and subsequent dried rCF masses.

5.3.1.2 Remanufacture

The remanufacturing method used was as described in Section 3.2.2. Dried rCF were aligned into dry preforms using the HiPerDiF alignment method. The rCF preforms, and polymer precipitate, were combined in an alternate stacking sequence so that each composite stack was made up of four preform layers and three matrix layers. Stacks were compression moulded in a steel tool and under vacuum conditions. Remanufacturing parameters used are reported in Table 4.9.

Table 5.3. Remanufacturing parameters used for CFPA6 recycling.

	CF mass	PA6 mass	Temp.	Pressure	Actual Vf_F	Flash
	mg	mg	℃	MPa	%	wt.%
CFPA6	105[a]	180[a]	250	11.8	28	11

[a] Per specimen. Temp. = Temperature

The preform areal weight varied due to intrinsic, experimental variations of the HiPerDiF alignment method, however, the average total preform mass for each specimen was approximately 105 mg.

There were no differences in the remanufacturing procedures used for the two reclamation variants. The compression moulding cycle used is plotted in Fig. 4.14.

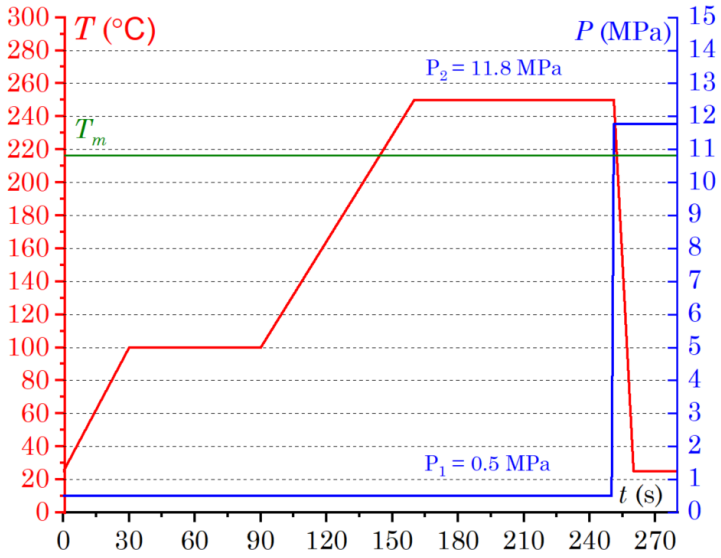

Fig. 5.2. Compression moulding cycle used to manufacture CFPA6 specimens. Specimens were held at 0.5 MPa (P_1) for 4 hours until transfer from oven to hot press for consolidation at 11.8 MPa (P_2). T_m denotes the melting temperature of PA6.

5.3.2 Results and discussion: CFPA6-FA

5.3.2.1 Polymer characterisation

Polymer characterisation is carried out on the virgin PA6 (vPA6) powder and the reclaimed powders after each recycling loop, r_1PA6-FA and r_2PA6-FA.

DSC was used to examine the effect of recycling on the T_m and $\%X$ of the polymer. DSC routines included two thermal ramps; the first ramp heated from 30 °C to 250 °C and cooled to 30 °C, the second ramp heated from 30 °C to 250 °C

again, then cooled to room temperature. Analysis was carried out using a TA Auto Q2000 DSC in pierced, hermetically sealed aluminium pans on powdered samples (10 ± 3 mg), under flowing N_2 (50 cm^3/min), at a heating rate of 10 °C/min and cooling rate of 20 °C/min.

The DSC thermograms are overlaid in Fig. 5.3. Melt and crystallisation temperatures are reported alongside crystallinities in Table 5.4. Following the x-axis from left to right, the first endothermic peak, first exothermic peak and second endothermic peak represent the initial melting (T_{m_1}), the crystallisation (T_c), and the second melting (T_{m_2}) phase transitions of the polymers. One sample of the homogenised precipitate was run for each recycling loop.

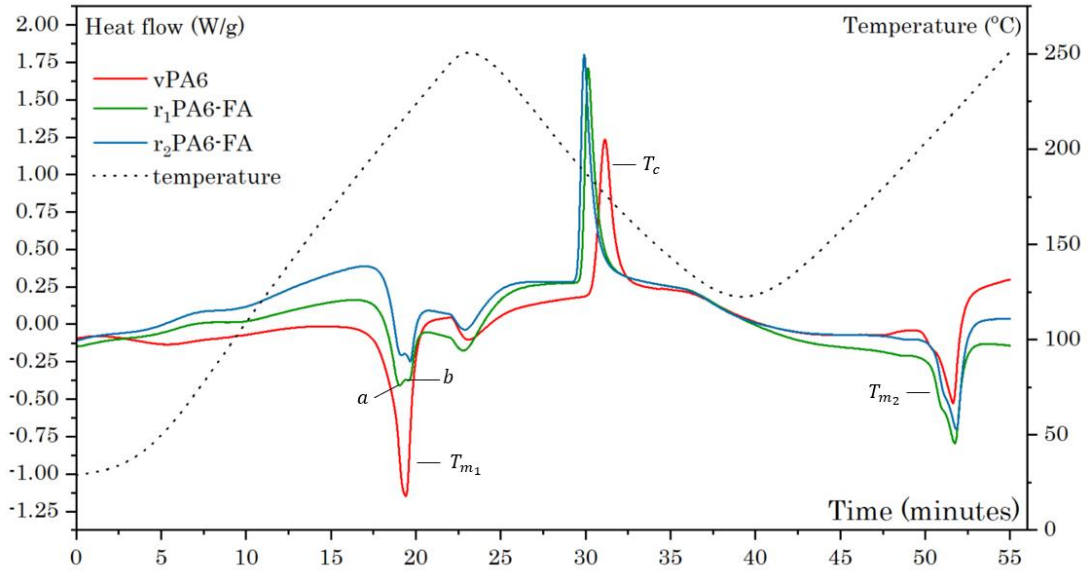

Fig. 5.3. Multi-ramp DSC thermograms for PA6 as a function of recycling loop.

vPA6 exhibited a sharp initial melting peak at 217 °C with a crystallinity of 34.9 %. Both r_1PA6-FA and r_2PA6-FA showed a broader T_{m_1} peak split into two distinct peaks, *a* and *b*, at 213 °C and 219 °C for r_1PA6-FA, and 215 °C and 220 °C for r_2PA6-FA, respectively. This peak also exhibited a crystallinity of 18.1 % and 18.8 % for the first and second recyclate, respectively; a 53 % average decrease compared with vPA6.

Table 5.4. DSC results from virgin and recycled PA6 as a function of recycling loop.

	T_{m_1}	T_c	T_{m_2}	X_{m_1}	X_c	X_{m_2}
	℃	℃	℃	%	%	%
vPA6	217	177	218	34.9	24.7	20.0
r_1PA6-FA	213[a]	187	220	18.1	28.8	20.2
	219[b]					
r2PA6-FA	215[a]	188	221	18.8	31.1	21.5
	220[b]					

[a, b] 1st and 2nd T_{m_1} split peak melting temperatures.

This reflected the kinetic dependency of polymer crystal formation. In solution, polymers form coils that curl back themselves in a spherical morphology called the hydrodynamic volume. Upon precipitation, the coil is immediately forced into the solid phase giving little time for polymer chains to align and form crystal structures. This results in a substantially different combination of the three possible PA6 crystal morphologies, $\alpha, \beta, and\ \gamma$, compared with vPA6. The split peaks at T_{m_1} represent the different melting points of two different crystal morphologies, of relatively equal quantities, that were present in the precipitates. The sharp vPA6 T_{m_1} peak is the result of the existence of just one crystal morphology, or, the presence of multiple morphologies with one in significant excess. The split peaks were not present in the final melting peak suggesting that this was a consequence of different crystal formation conditions and not a change in the molecular weight distribution.

The crystallisation transition, at T_c, shifted from 177 ℃ for vPA6, to 187 ℃ and 188 ℃ for r_1PA6-FA, and r_2PA6-FA, respectively. There was a gradual increase in the crystallinity of 14 % after the first recycling loop and 7.4 % after the second recycling loop. As the vPA6 and precipitate production processes were not equivalent it can be assumed that the spatial distribution of long polymer chains, *i.e.* not the numerical distribution of weights reported from GPC/SEC analysis, was also different; observable as a variance in crystallisation behaviour. If, however, the polymer was homogenously melted prior to crystallisation, this must have represented a change in the molecular weight distribution of the

polymer. The difference between r_1PA6-FA and r_2PA6-FA was subtle, suggesting no significant change.

The final melt transition occurred at roughly the same temperature for each sample with roughly the same crystallinity, suggesting no substantial variation in the polymer chains associated with crystallinity, *i.e.* long chains, as a function of recycling loop.

A Perkins Elmer Spectrum 100 Fourier Transform Infrared Spectrometer was used to compare the vibrational frequencies of polymer functionalities as a function of recycling loop.

The FTIR spectra collected for vPA6, r_1PA6-FA and r_2PA6-FA are overlaid in Fig. 5.4. The characteristic vibrational peaks for polyamide 6 were present in all specimens, these are presented in Table 5.5. The vPA6 peak at 3060 cm^{-1} represents a the stretching vibration of crystalline hydrogen bonded -N-H [228].

Table 5.5. Vibrational peaks for polyamide 6 observed in the FTIR spectra [217,228].

Wavenumber	Vibrational peaks
cm^{-1}	
684	-NH symmetric bending
1372	-NH symmetric bending, -CN symmetric stretching, -CH_2 symmetric bending
1419	-CH_3 symmetric bending
1458	-CH_3 symmetric bending
1541	-NH symmetric bending -CN symmetric stretching
1637	-C=O symmetric stretching
2860	-CH_2 symmetric stretching
2933	-CH_2 asymmetric stretching
3060	-NH symmetric stretching (secondary hydrogen bonding)
3291	-NH symmetric stretching

After the first recycling loop there are several shifted and additional peaks in the spectrum. Additional Peaks at 630 cm^{-1}, 1250 cm^{-1}, 1300 cm^{-1}, and 1720 cm^{-1} appear in the r_1PA6-FA and r_2PA6-FA spectra. These correspond with the vibrational frequencies of caprolactam, the monomeric unit used to polymerise PA6 and the depolymerisation product: δ_s (-N-C=O) – 630 cm^{-1} (*i*); ν_s (amide III - C-N) – 1250 cm^{-1} and 1300 cm^{-1} (*i*); ν_s (amide I C=O) – 1720 cm^{-1}. As the peaks appeared only after reclamation it suggested that depolymerisation was occurring. Depolymerisation into caprolactam is a well reported thermal degradation mechanism of PA6 in the absence of oxygen [229].

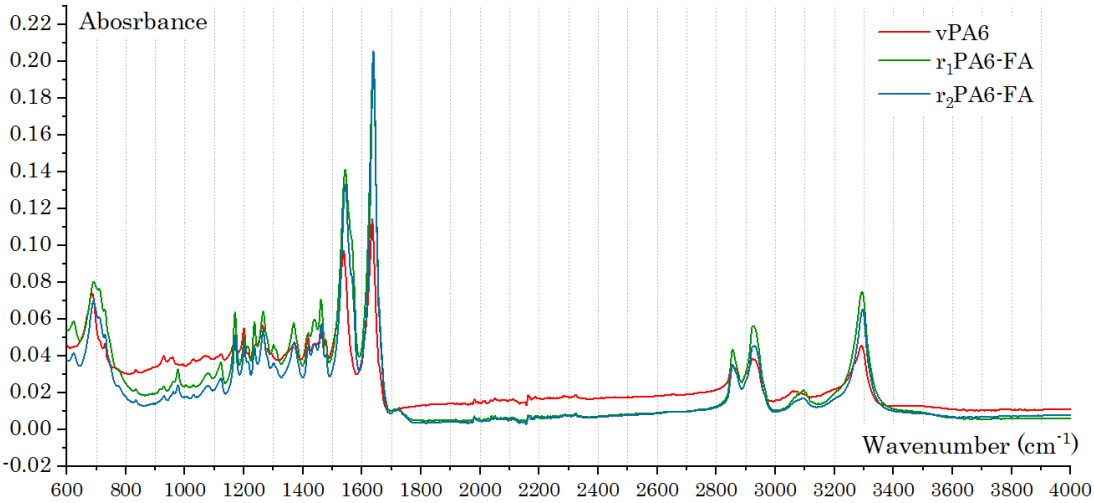

Fig. 5.4. FTIR spectra of PA6 as a function of recycling loop.

The vPA6 peak at 1412 cm^{-1} has shifted, to 1450 cm^{-1} after the first recycling loop. This peak lies in the aliphatic region of the spectrum and indicates a change in the methylene -CH_2 deformation from open chain to constrained ring. This reinforces the presence of caprolactam; a seven-membered ring.

The vPA6 peak at 3060 cm^{-1} has shifted, to 3100 cm^{-1} and subtle grown in intensity after the first recycling loop. There is no observable shift after the second recycling loop. As this peak refers to the crystalline, hydrogen bonded -N-H amine it suggests that there is a variation in the crystallinity of the polymer.

This corroborates the shift in crystallinity observed in the DSC thermograms for the reclamation precipitates.

The M_w, M_n, PDI and MWD of each recyclate was determined using GPC/SEC. Samples were analysed using a Malvern/Viscotek TDA 301 GPC system with associated pump and autosampler, with two PL HFIPgel 300 x 7.5 mm², 9 µm columns and an Agilent PL HFIPgel guard column. The mobile phase used was 1,1,1,3,3,3-hexafluoropropan-2-ol (with 25 mM NaTFAc) at 40 °C at a rate of 0.8 ml/min. A refractive index detector (with differential pressure/viscosity and right-angle light scattering) was used. Samples were prepared by adding the mobile phase (10 ml) to the sample (20 mg) to dissolve overnight. Solutions were then thoroughly mixed and filtered through a 0.45 µm PTFE membrane, directly onto autosampler vials. The vials were placed in an autosampler where injection of a vial aliquot was carried out automatically. Two samples were analysed for each recycling loop, the coefficient of variance of each loop is reported in Table 5.6

The MWD curves obtained from GPC/SEC of vPA6, r_1PA6-FA an r_2PA6-FA are shown in Fig. 5.5 and the M_n, M_w and PDI values are tabulated in Table 5.6. From left to right the plots ran from low to high molecular weights.

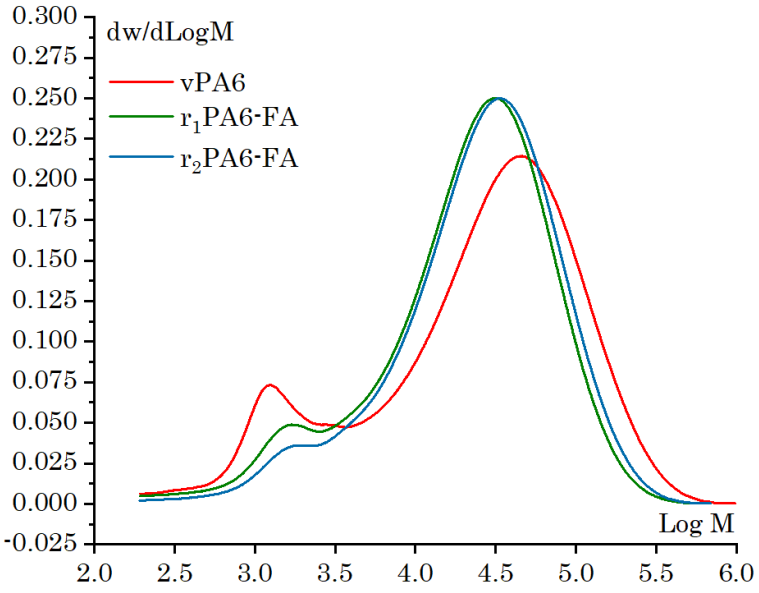

Fig. 5.5. MWD from GPC/SEC analysis of recycled PA6 as a function of recycling loop.

Table 5.6. The M_n, M_w and PDI values obtained from GPC/SEC analysis of PA6 as a function of recycling loop.

	M_n	M_w	PDI
	x10^3 g/mol	x10^4 g/mol	
vPA6	7.83 (0.1)*	5.53 (0.1)	7.70
r_1PA6-FA	8.74 (0.1)	3.88 (0.1)	4.44
r_2PA6-FA	11.1 (0.1)	4.41 (0.1)	3.96

* Coefficient of variance calculated from two sample runs.

The MWDs are representative of polydisperse semi-crystalline polymers, as expected from the PA6 used. The MWD is bi-modal, showing a primary and secondary peak. The secondary peak indicates the substantial presence of smaller molecular weight chains. This could represent the presence of shorter PA6 chains in the MWD either intentional or unremoved by-products of the step-growth of polymerisation typical of PA6.

After the first recycling loop there is a 30 % drop in M_w and an 11.2 % increase in M_n, where the primary peak maximum increases. There is a successive drop in the secondary peak maximum, which indicates the degradation or extraction, *i.e.* into the reclamation supernatant, of the secondary peak chains. The drop in M_w corresponds to the combination of scission of large molecular weight chains into medium lengths and the loss of skew from the secondary peak reduction.

After the second recycling loop there is no observable change in the primary peak maximum however the secondary peak maximum decreases. This explains the final increase in the M_w and M_n values as the secondary peak skew is diminished. This suggests that there was unsubstantial degradation and that the secondary peak reduction was primarily caused by extraction.

The solids extracted into the supernatant after the first recycling loop were separated using HPLC and analysed using MS. The base peak chromatogram obtained is presented in Fig. 5.6 and the corresponding molecular mass values from MS are tabulated in Table 5.7. The chromatogram indicates the presence of a varied mixture of compounds in a range of different quantities. These peaks represent any molecules soluble in formic acid that were not precipitated from

the solution thus remaining in the supernatant. The corresponding molecular mass values of the main chromatogram peaks are all small, < 700 g/mol, and are unlikely to be polymer chains which have larger masses by several orders of magnitude; suggesting the presence of additive molecules.

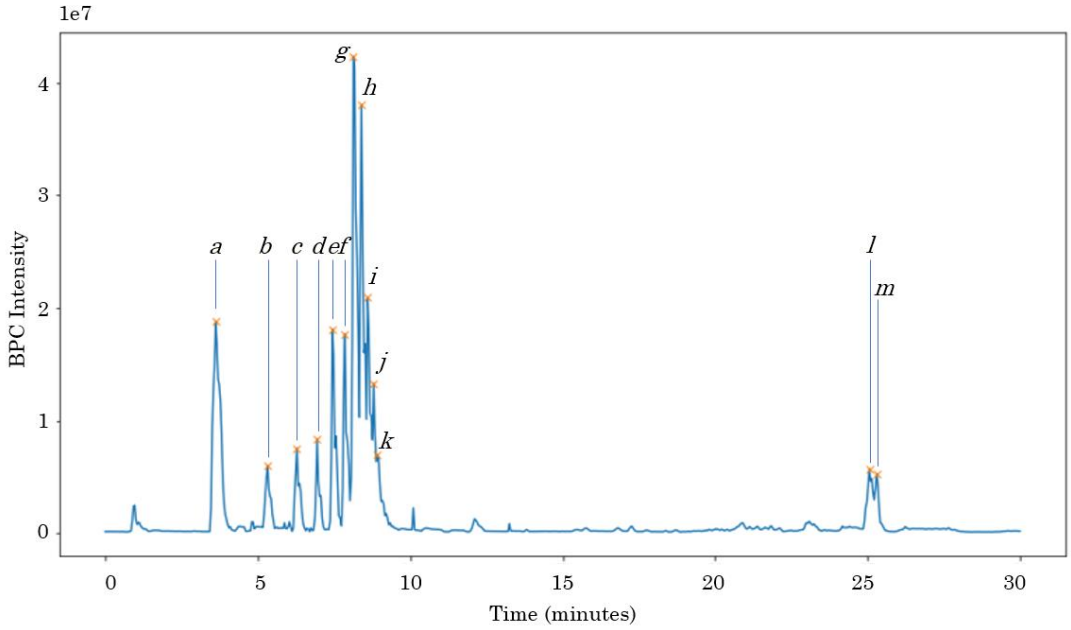

Fig. 5.6. The base peak chromatogram (BPC) obtained from the HPLC separation of the r_1PA6-FA supernatant.

Table 5.7. HLPC-MS data showing base peak chromatogram peaks from the r_1PA6-FA supernatant with corresponding mass values from mass spectrometry.

Peak	Molecular mass	Peak	Molecular mass
	g/mol		g/mol
a	227.2	*h*	509.9
b	340.3	*i*	566.4
c	453.3	*j*	623.0
d	566.4	*k*	623.0
e	679.5	*l*	338.3
f	396.8	*m*	338.3
g	453.3		

The additive mixtures used in polymers a generally guarded, proprietary information, however there exist a variety of known antioxidants with molecular masses ranging from 220 g/mol – 1178 g/mol [230,231]. Peak *b* had the highest intensity on the mass spectrum suggesting it is the molecular ion peak. With a mass of 340.3 it is similar in mass to the known additive Antioxidant 2246 [231]. The other peaks, especially those of larger masses, must correspond to the molecular ion peaks or fragment ions of other additives used. In any case it is apparent that a mixture of small molecules is extracted in the reclamation supernatant.

5.3.2.2 Mechanical testing

CFPA6-FA specimens were tested for their tensile properties in accordance with ASTM D3039. Axial force was provided by a Shimadzu AGS-X servo-electric tensile test machine with a 10 kN load cell and a constant cross-head displacement of 1 mm/min. Strain was measured using the Imetrum video gauge software, over a gauge length of 50 mm. specimens were sprayed back and speckled with white dots to aid with strain mapping; an example of this is shown in Fig. 4.15.

Representative stress-strain curves obtained from tensile tests of CFPA6-FA as a function of recycling loop are shown in Fig. 5.7. The results of the tensile tests are recorded in Table 5.8, and represented graphically in the Fig. 5.8 bar charts. σ_{ult} was determined as the maximum stress and ε_{ult} refers to the corresponding strain. E_T was determined by taking the gradient of the linear-elastic region section of bounds $0.001 < \varepsilon < 0.003$. $E_{T(0.28)}$ and $\sigma_{ult(0.28)}$ denote the tensile stiffness and ultimate tensile strength normalised to a 28 % Vf_F, following the rules of mixture.

Tensile specimens exhibited a typical linear-elastic response followed by rapid, brittle failure. Statistical variance between data sets was determined using a Kruskall-Wallis test. vCFPA6-FA6 has a significantly higher tensile stiffness, ultimate tensile strength and ultimate tensile strain than the subsequent specimens.

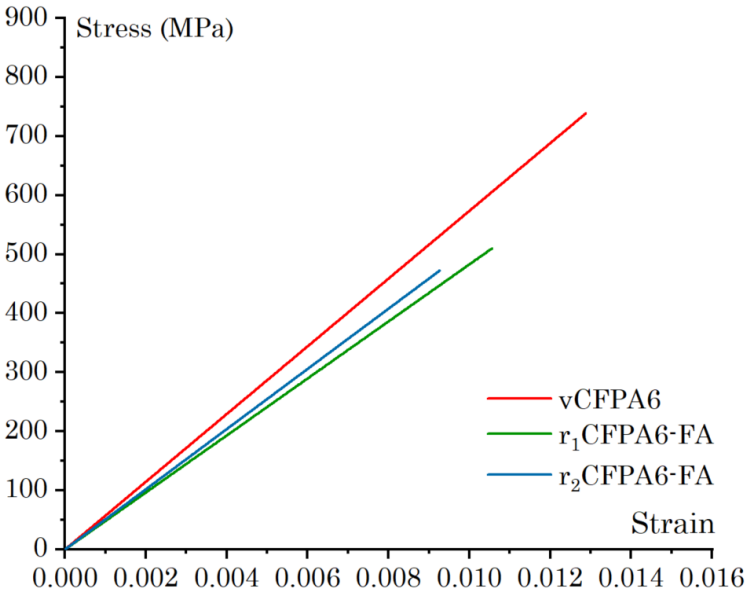

Fig. 5.7. Representative stress-strain curves obtained from tensile test of CFPA6-FA as a function of recycling loop (formic acid).

Table 5.8. Average mechanical performance data collected from tensile tests of CFPA6-FA after each recycling loop.

	$E_{T(0.28)}$	$\sigma_{ult(0.28)}$	ε_{ult}	ρ	Vf_F
	GPa	MPa		MPa	%
vCFPA6	56.5 (1.28)*	768 (5.32)	1.36 (4.91)	1.18 (4.02)	28.2 (4.61)
r1CFPA6-FA	45.3 (9.65)	475 (14.3)	1.05 (11.3)	1.16 (9.04)	27.5 (11.1)
r2CFPA6-FA	50.0 (1.49)	454 (13.06)	0.91 (12.2)	1.08 (2.35)	27.1 (0.91)

* Coefficient of variance calculated from six specimens of the same batch.

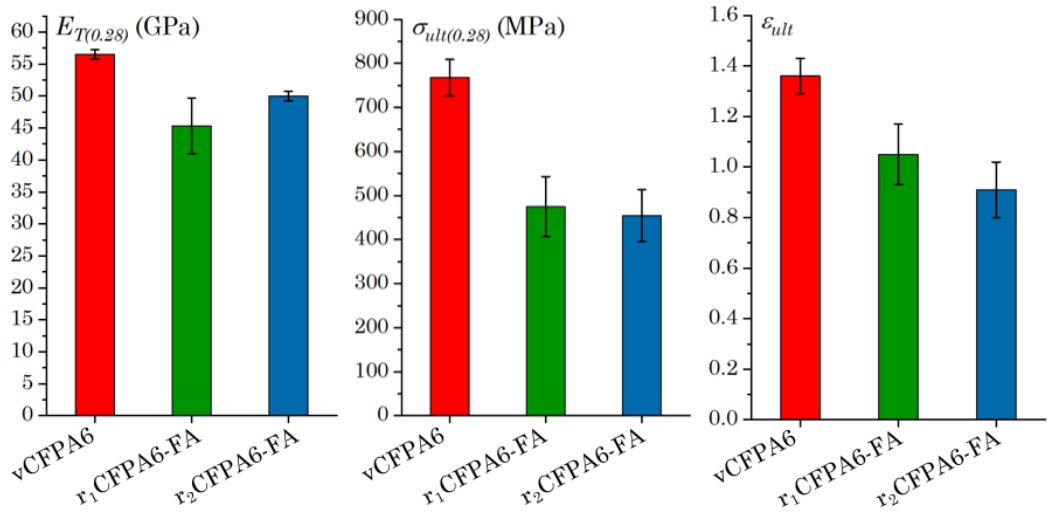

Fig. 5.8. Bar charts showing the normalised tensile stiffness, ultimate tensile strength and ultimate tensile strain of vCFPA6 as a function of recycling loop (formic acid). Error bars represent standard deviation of specimen batch.

After the first recycling loop the tensile stiffness, ultimate tensile strength and ultimate strain drop by 20 %, 38 % and 23 %, respectively. After the second recycling loop these values remain within statistical variance.

The brittle failure exhibited by all specimens suggested that the IFSS between the CF and PA6 effective load transfer between fibres and matrix resulting in significant fibre fracture. The IFSS between CF and PA6 is typically around 40 – 50 MPa, as reported in the literature [224]. Using Equation 3.2, this resulted in a fibre critical length of approximately L_c = 0.3 mm. For vCF, this meant that all the fibres were above L_c and could be maximally loaded. Despite this being an approximation, as the exact IFSS of the fibre and matrix used was unknown, the value can be assumed accurate and therefore for vCF all fibres were above the L_c.

5.3.2.3 Fibre analysis

Fibre length distribution analysis was used to determine the effect of recycling on the average fibre length. The fibre length distribution of preforms

made from vCF, and rCF after each recycling loop, are presented in Fig. 5.9. An error of ± 0.2 mm was applied for the by-eye length measurement of fibres.

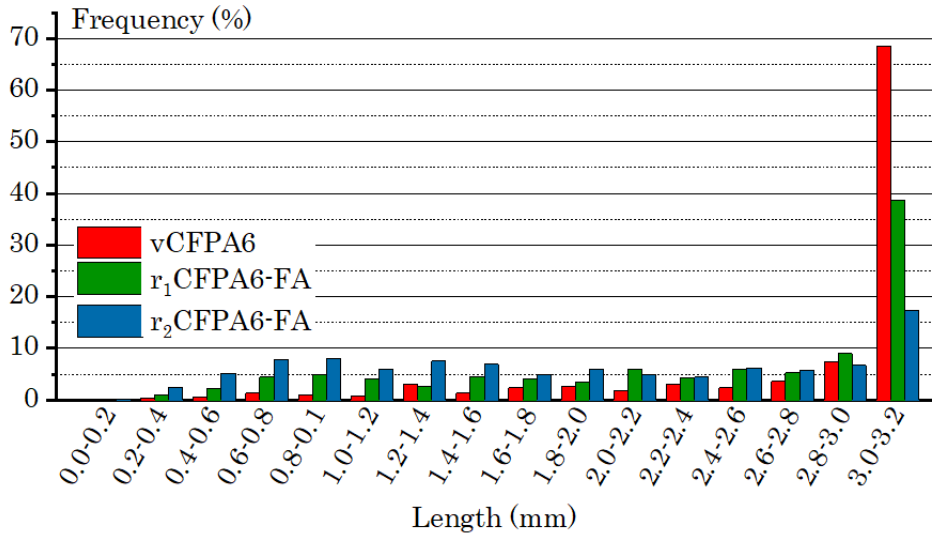

Fig. 5.9. Fibre length distributions of fibre preforms used in vCFPA6, r_1CFPA6-FA and r_2CFPA6-FA.

In the vCFPA6 preform sample 68.6 % of fibres are in the range of 2.8 - 3.2 mm. After the first recycling loop 38.7 % of fibres are in the range 2.8 - 3.2 mm. r_2CFPA6-FA fibre length was more evenly distributed with 0.6 - 0.8 mm, 0.8 – 0.1 mm and 1.2 - 1.4 mm a having 7.5 % of the distribution and 3.0 – 3.2 mm representing 17.3 %. This distribution variation is like that obtained in Chapter 4 therefore it can be assumed that the main contributor is a part of the remanufacturing process and not reclamation.

The 0.3 mm alignment plate spacing was equal to only the shortest fibre length so the alignment, and therefore the composite stiffness should not be significantly affected by the evening out of the distribution.

A Hitachi TM3000 SEM was used (5000 V accelerating voltage) to investigate the surface quality of fibre preforms collected from each recycling iteration.

SEM micrographs were taken of aligned preforms before impregnation of vCFPA6, r_1CFPA6-FA and r_2CFA6-FA, see Fig. 5.10a-c. Fig. 5.10a shows the

vCFPA6 preform with clean surfaces in both magnifications. Fig. 5.10b shows the r_1CFPA6-FA preform with a coating of a residual substance, most likely unwashed matrix adhered to the fibre surface. The micrographs of r_2CFPA6-FA, Fig. 5.10c, show the same residual matrix but in qualitatively unchanged quantities to r_1CFPA6.

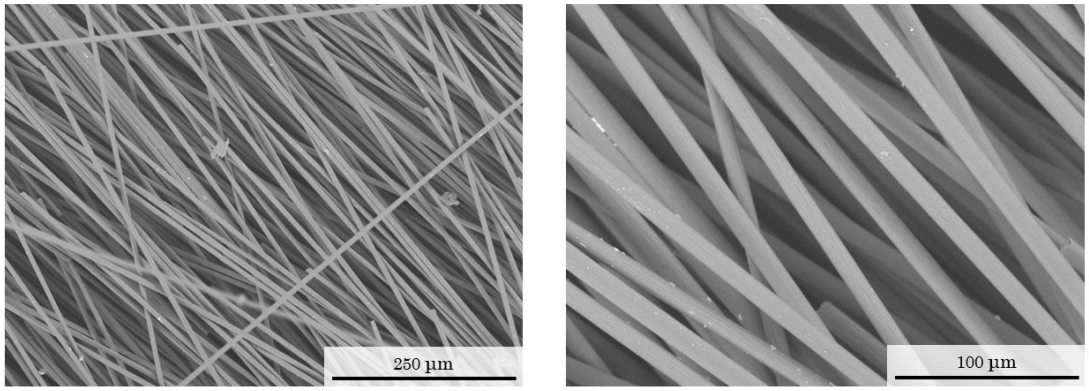

a) SEM micrographs of a preform used in vCFPA6

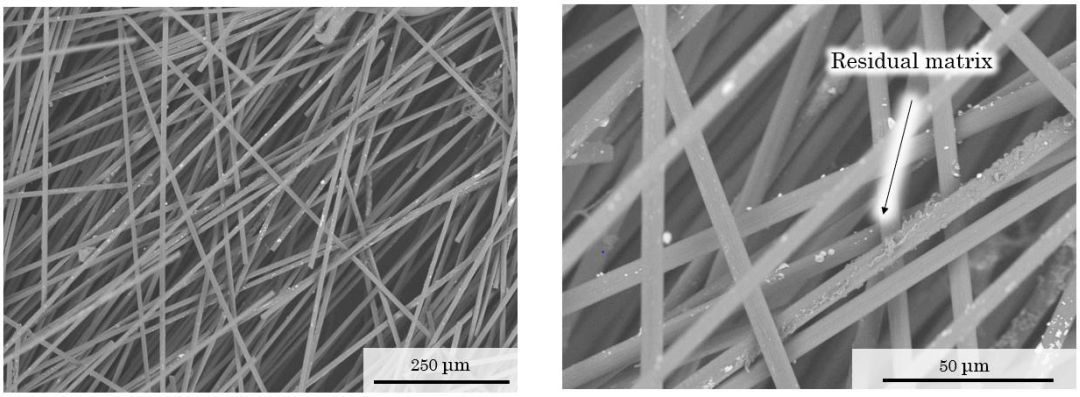

b) SEM micrographs of a preform used in r_1CFPA6-FA

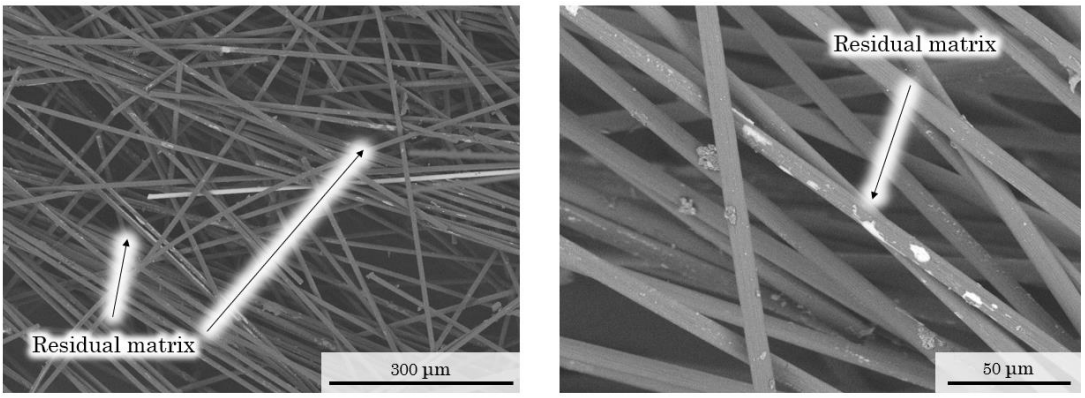

c) SEM micrographs of a preform used in r_2CFPA6-FA

Fig. 5.10. *a-c)* Preform cuttings taken from aligned preforms, of each recycling loop, before impregnation. r_1CFPA6 and r_2CFPA6 show deposition of residue on fibre surface which is deemed to be unwashed matrix.

5.3.2.1 Fractography

Fracture surfaces were inspected using a Hitachi TM3000 SEM (5000 V accelerating voltage). One fracture surface was examined per six specimen batch to maximise the amount of material being recycled.

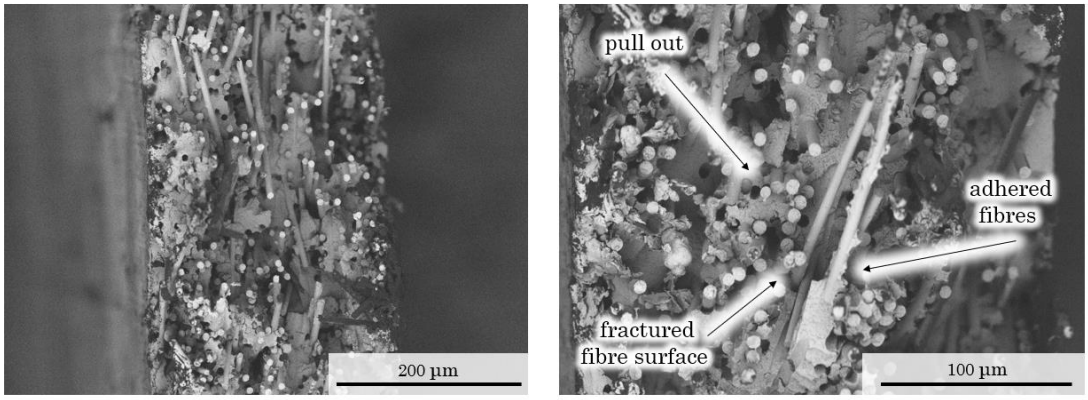

a) SEM micrographs of a vCFPA6 fracture surface

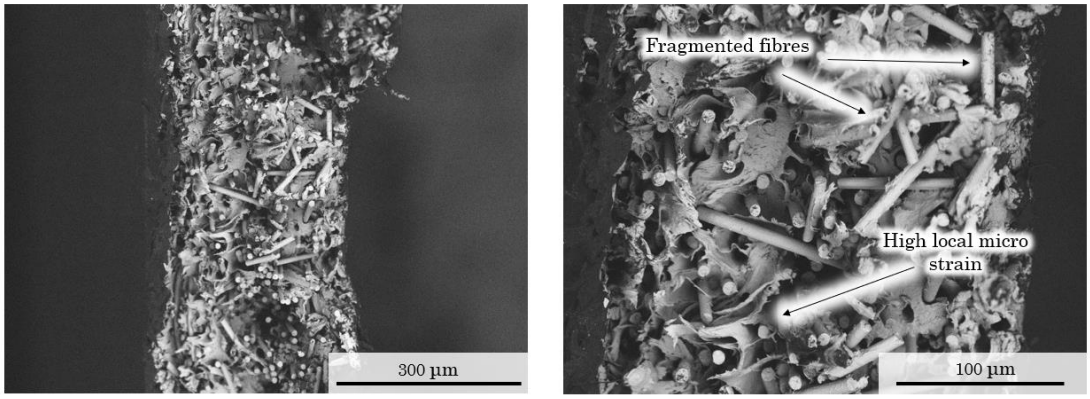

b) SEM micrographs of a r_1CFPA6-FA fracture surface

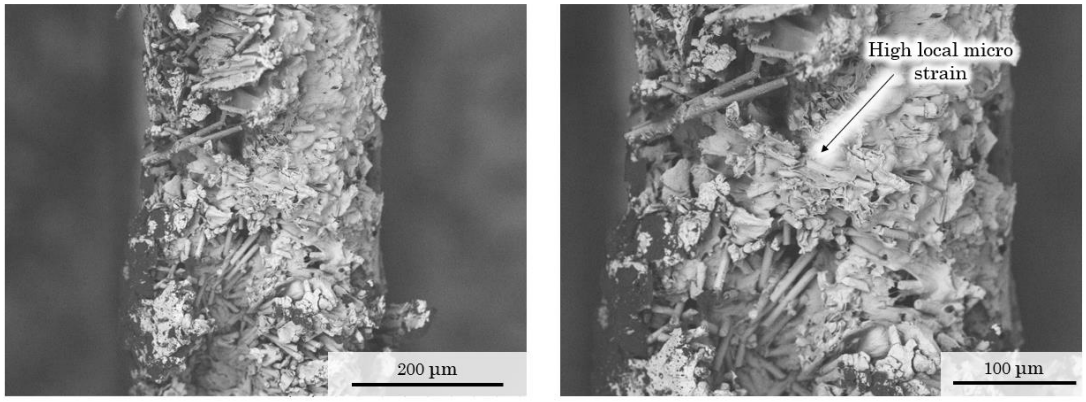

c) SEM micrographs of a r_2CFPA6-FA fracture surface

Fig. 5.11. *a)* A vCFPA6 fracture surface showing pull-out, well coated fibre surfaces and fracture fibre ends. *b)* A r_1CFPA6-FA fracture surface where an increase in local micro strian is visible. *c)* A r_2CFPA6-FA fracture surface showing enhance local micro strain.

SEM micrographs of vCFPA6, r_1CFPA6-FA and r_2CFPA6-FA fracture surfaces are shown in Fig. 5.11a-b. Fig. 5.11a shows a typical vCFPA6 fracture surface where pull-out, fractured fibre ends and well coated fibres are clearly visible. This reflects the linear elastic strain response and brittle failure as the fibres are well adhered to the matrix enabling effective stress transfer. High local micro strain can be observed in Fig. 5.11b which suggests the matrix failure strain has reduced after the first recycling loop; reflecting the reduction in global composite strain observed. The high local strain is also visible in the r_2CFP6-FA fracture surface in Fig. 5.11c.

5.3.2.2 Conclusions

The mechanical performance, polymer properties and fibre properties of virgin and recycled CFPA6 was examined experimentally. The analysis linked macroscopic performance with microscopic fibre surface phenomena, fibre length and polymer behaviour.

Considering the DSC thermograms obtained from rPA6 of both solvent systems, precipitation resulted in random crystal formation due to rapid precipitation rate and the kinetic dependency of crystallisation. The random precipitation resulted in an inhomogeneous spatial distribution of polymer lengths in the melt. This was observed as different crystallisation behaviour observed between vPA6 and the precipitates. The final melting peak ensured similar thermal history for all crystallites and therefore indicated insubstantial change in the polymer crystallinity and the long polymer chains associated with it. FTIR spectra showed signs of degradation after the first reclamation and there was evidence to support the variance in crystallinity of the precipitates.

The MWD was bi-modal with a primary contribution of large molecular weights and a secondary contribution of smaller molecular weights. The large chains exhibited degradation after the first but remained similar after the second. There was a secondary major chain length in the polymer, which is either gradually degraded or gradually extracted during reclamation. This was the likely cause of the increased local micro strain observed in the specimen fracture surfaces after the first and second recycling loops. It also explained the strain

knockdown observed in the tensile test results. The secondary polymer distribution may have provided a toughening mechanism influencing matrix failure strain; possibly through enhancing the molecular sliding interactions of the amorphous regions. This indicated that either: *a) the matrix degradation was initially effectual but plateaued after the first loop,* or, *b) the fibre reclamation process produced a change in the fibre properties, or distribution in the preform, i.e. fibre agglomerations, that are transferred after the second loop*.

High local micro-strain is observed on the fracture surfaces of r_1CFPA6-FA and on r_2CFPA6-FA surfaces. This correlates with the gradual reduction of the MWD secondary peak therefore it may be possible that the secondary peak chains influenced polymer toughness. Lower molecular weight chains would reside in the amorphous regions of the polymer which, during loading, would enhance molecular slipping interactions and increase the energy absorbed during failure, *i.e.* toughness. PA6 is typically manufactured using step- growth polymerisation which, depending on the process parameters used, is susceptible to the production of mixed chain lengths [232]. It may be that the secondary peak corresponds to lower molecular weight PA6 formed by prematurely terminated polymerisation because of unselective polymerisation control.

HPLC-MS indicated the extraction of small molecules into the supernatant; these masses are substantially less than even small polymer chains. Polymers would have been insoluble in the HLPC carrier solvent and removed before analysis and are therefore not visible in the chromatogram. Small molecules had similar masses to known PA6 additives and their fragment ions.

After the first recycling loop there was a 20 %, 38 % and 23 % decrease in tensile stiffness, ultimate tensile strength, and ultimate tensile strain, respectively. After the second loop there was no statistical variance in the mechanical performance, suggesting that the composite performance did not cumulatively degrade as a function of recycling.

Overall, the mechanical performance achieved by the vCFPA6 specimens was considerable, to the authors knowledge these were the highest mechanical performances achieved by any discontinuous CFPA6 composite in the literature. There was a knockdown in performance after the first recycling loop, however,

the mechanical performance of r_1CFPA6-FA and r_2CFPA6-FA were the highest observed for any recycled thermoplastic composite and for any recycled discontinuous CF composite with either thermosetting or thermoplastic matrices.

5.3.3 Results and discussion: CFPA6-BA

Benzyl alcohol and acetone were used as an alternative solvent system to provide an option with simple solvent reclamation and a faster dissolution rate. A comparison of solvent systems may also aid in understanding the contribution of the solvent system on the composite properties.

5.3.3.1 Polymer characterisation

Polymer characterisation is carried out on the virgin PA6 (vPA6) powder and the reclaimed powders after each recycling loop, r_1PA6-BA and r_2PA6-BA.

DSC was used to examine the effect of recycling on the T_m and $\%X$ of the polymer; the experimental conditions used previously were replicated. The DSC thermograms are overlaid in Fig. 5.12. Melt and crystallisation temperatures are reported alongside crystallinities in Table 5.9. Following the x-axis from left to right, the first endothermic peak, first exothermic peak and second endothermic peak represent the initial melting (T_{m_1}), the crystallisation (T_c), and the second melting (T_{m_2}) phase transitions of the polymers.

vPA6 exhibited a sharp initial melting peak at 217 ℃ with a crystallinity of 34.9%. Both r_1PA6-BA and r_2PA6-BA showed a sharp T_{m_1} peak at 219 ℃ and 220 ℃, with a crystallinity of 19.8 % and 31.1 % for the first and second recyclate, respectively.

Again, this reflected the kinetic dependency of polymer crystal formation. However, the variation in the precipitate crystallinity is greater than that observed for the formic acid precipitates. As the hydrodynamic volume of a polymer chain is solvent dependant a variation in crystallinity between solvent systems is not surprising.

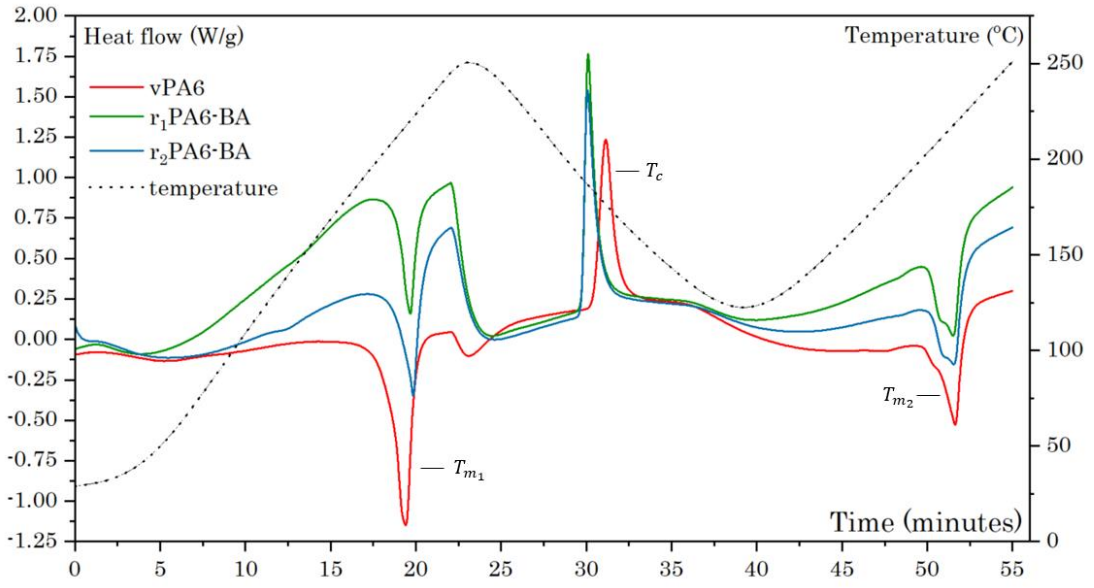

Fig. 5.12. Multi-ramp DSC thermograms for PA6 as a function of recycling loop.

There is a second, broad melting peak after T_{m_1} which is not present in the subsequent reclaimed precipitates. This suggests the extraction of a substance during the first reclamation.

The crystallisation transition, at T_c, shifted from 177 ℃ for vPA6, to 186 ℃ and 187 ℃ for r_1PA6-BA, and r_2PA6-BA, respectively. With an initial increase in the crystallinity by 23 % after the first recycling loop and a 6.3 % decrease after the second recycling loop. The second decrease in crystallinity is small and assumed to be within the machine measurement variance. The difference between r_1PA6-BA and r_2PA6-BA was subtle, suggesting no significant change in the polymer structure. However, there is a significant change in the crystallisation behaviour after the first recycling loop. This shift is analogous to that observed in the formic acid study; suggesting that this is either *a) a consequence of the remanufacturing process, i.e. a change in the molecular weight distribution of the polymer. b) both solvent systems cause similar effects on the crystallisation behaviour of the polymer after both the first and second recycling loops, i.e. the polymer chains that form crystalline regions are not proximal, and thus will exhibit different crystallisation behaviour.*

The final melt transition occurred at the same temperature with the same crystallinity for each sample, however, the peak splits into two broad peaks. This represents the presence of two distinct crystalline phases in the polymer that were not in vPA6. The peak splitting was not observed in the formic acid study suggesting the benzyl alcohol reclamation has a different effect on the polymer.

Table 5.9. DSC results from virgin and recycled PA6 as a function of recycling loop.

	T_{m_1}	T_c	T_{m_2}	X_{m_1}	X_c	X_{m_2}
	℃	℃	℃	%	%	%
vPA6	217	177	218	34.9	24.7	20.0
r_1PA6-BA	219	186	218	19.8	30.4	20.3
r_2PA6-BA	220	187	218	31.1	28.5	18.2

A Perkins Elmer Spectrum 100 Fourier Transform Infrared Spectrometer was used to compare the vibrational frequencies of polymer functionalities as a function of recycling loop; the experimental conditions used previously were replicated.

The FTIR spectra collected for vPA6, r_1PA6-BA and r_2PA6-BA are overlaid in Fig. 5.13. The FTIR spectrum of vPA6 showed all the vibrational peaks for specific functional groups expected for PA6, see Section 5.3.2.1. The spectra are almost indistinguishable, apart from the shifted vPA6 peak at 3060 cm^{-1}. As this peak refers to the crystalline, hydrogen bonded -N-H amine it reflects the variation in polymer crystallinity observed in the DSC thermograms. This peak shift is also present in the formic acid spectra suggesting both solvent systems cause similar variance in the crystal structure of the precipitate.

There are no observable peaks associated with the depolymerisation product caprolactam which suggests that either any degradation that had occurred was unsubstantial, or, that the caprolactam produced was extracted into the supernatant and did not precipitate out with the bulk polymer.

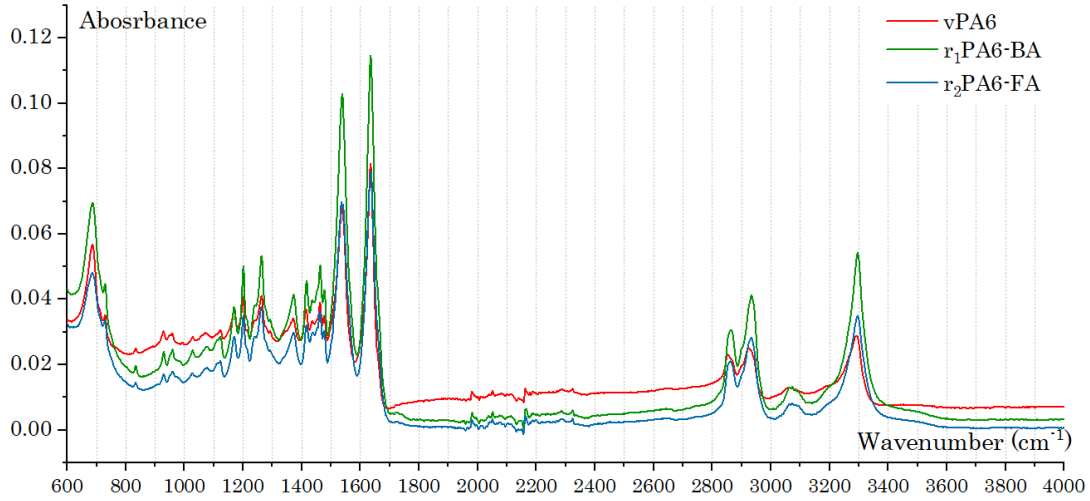

Fig. 5.13. FTIR spectra of PA6 as a function of recycling loop.

The M_w, M_n, PDI and MWD of each recyclate was determined using GPC/SE; the experimental condition used previously were replicated. The MWD curves obtained from GPC/SEC of vPA6, r_1PA6-BA an r_2PA6-BA are shown in Fig. 5.14, and the M_n, M_w and PDI values are tabulated in Table 5.10. From left to right the plots ran from low to high molecular weights.

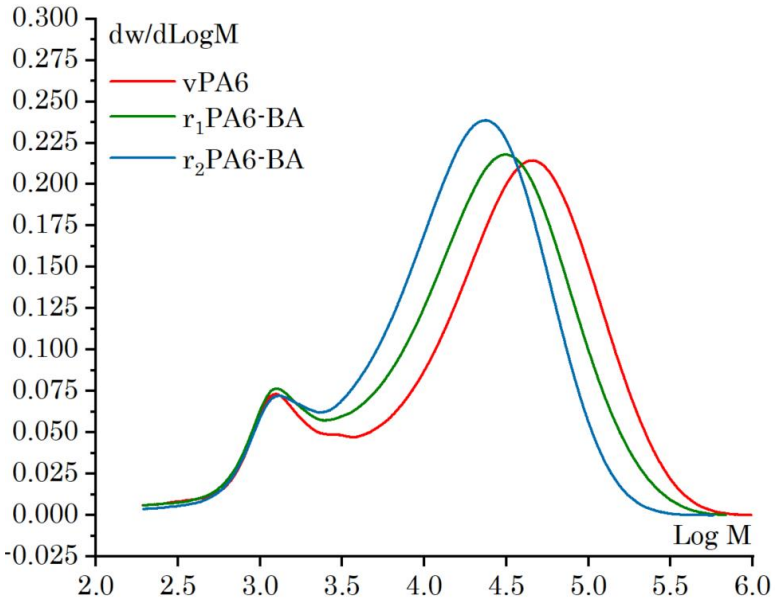

Fig. 5.14. MWD from GPC/SEC analysis of recycled PA6 as a function of recycling loop.

Table 5.10. The M_n, M_w and PDI values obtained from GPC/SEC analysis of PA6 as a function of recycling loop.

	M_n	M_w	PDI
	x10^3 g/mol	x10^4 g/mol	
vPA6	7.19 (0.1)*	5.53 (0.1)	7.69
r_1PA6-BA	6.35 (0.1)	4.01 (0.1)	6.31
r_2PA6-BA	6.38 (0.1)	2.83 (0.1)	4.43

* Coefficient of variance determined from two sample runs form each batch.

The MWDs are representative of polydisperse semi-crystalline polymers, as expected from the PA6 used. The MWD is bi-modal, showing a primary and secondary peak.

After the first recycling loop there is a 27 % and 12 % decrease in M_w and M_n, respectively. The primary peak maximum remains the same height but shifts to a lower molecular weight. This corresponds to the scission of large molecular weight chains into short lengths. The secondary peak remains unchanged suggesting that the corresponding chains are unaffected by reclamation.

After the second recycling loop the primary peak maximum increases in height and shifts to lower molecular weights. This represents the scission of larger chains into medium lengths and an increase in shorter chain lengths. Again, the secondary peak is unaffected.

Overall, the GPC/SEC analysis shows successive degradation of the primary peak but no change in the secondary peak. This shows that benzyl alcohol reclamation has a different effect on the polymer to formic acid reclamation. It is most likely that the secondary peak is not extracted into benzyl alcohol as is observed with formic acid.

The solids extracted into the supernatant after the first recycling loop were separated using HPLC and analysed using MS. The base peak chromatogram obtained is presented in Fig. 5.15 and the corresponding molecular mass values from MS are tabulated in Table 5.11.

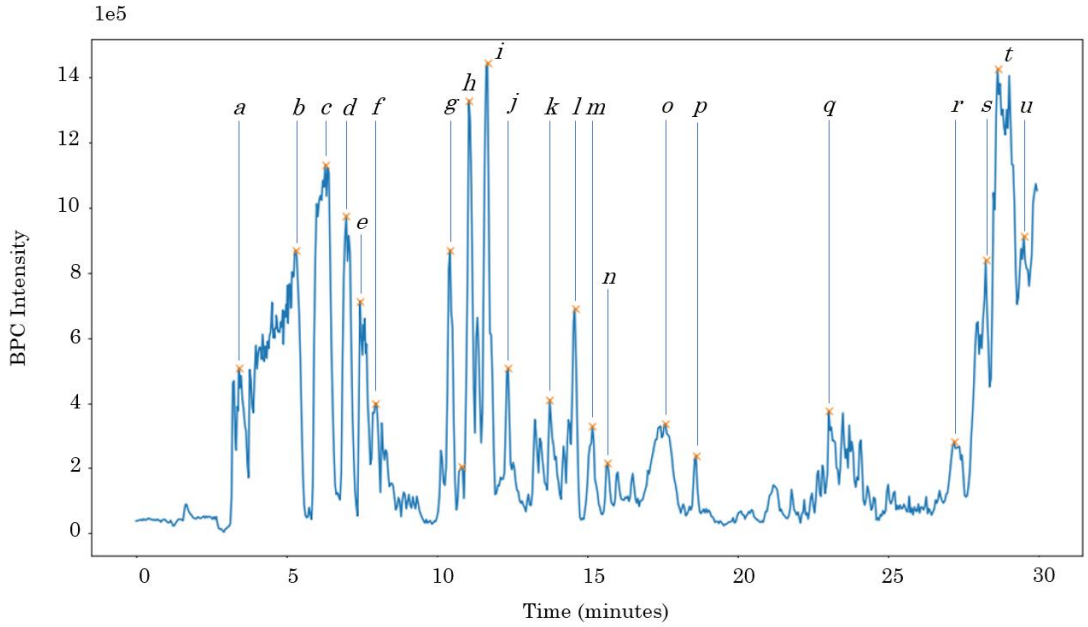

Fig. 5.15. The base peak chromatogram (BPC) obtained from the HPLC separation of the r1PA6-BA supernatant.

Table 5.11. HLPC-MS data showing base peak chromatogram peaks from the r1PA6-BA supernatant with corresponding mass values from mass spectrometry.

Peak	Molecular mass	Peak	Molecular mass
	g/mol		g/mol
a	475.3	*k*	461.2
b	362.2	*l*	389.2
c	475.3	*m*	403.2
d	588.4	*n*	403.2
e	701.5	*o*	360.4
f	814.6	*p*	304.3
g	299.2	*q*	743.6
h	304.2	*r*	806.6
i	317.2	*s*	806.6
j	430.3	*t*	782.6
k	313.2	*u*	758.6

The chromatogram indicates the presence of a varied mixture of compounds in a range of different quantities. These peaks represent any molecules soluble in benzyl alcohol that were not precipitated from the solution. The corresponding molecular mass values of the main chromatogram peaks are all small, < 900 g/mol, and are unlikely to be polymer chains which have larger masses by several orders of magnitude; suggesting the presence of additive molecules.

The additive mixtures used in polymers are generally guarded, proprietary information, however a range of known antioxidants with molecular masses ranging from 220 g/mol – 1178 g/mol is known [230,231]. Peak *h* had a mass of 340.2 it is the mass of the known additive Antioxidant 2246 [231]. The other peaks, especially those of larger masses, must correspond to the molecular ion peaks or fragment ions of other additives used. In any case, it is apparent that a mixture of small molecules is extracted in the reclamation supernatant.

5.3.3.2 Mechanical testing

CFPA6-BA specimens were tested for their tensile properties in accordance with ASTM D3039. Axial force was provided by a Shimadzu AGS-X servo-electric tensile test machine with a 10 kN load cell and a constant cross-head displacement of 1 mm/min. Strain was measured using the Imetrum video gauge software, over a gauge length of 50 mm. specimens were sprayed back and speckled with white dots to aid with strain mapping; an example of this is shown in Fig. 4.15.

Representative stress-strain curves obtained from tensile tests of CFPA6-BA as a function of recycling loop are shown in Fig. 5.16. These may not exactly match the tabulated averaged results. The results of the tensile tests are recorded in Table 5.12, and represented graphically in the Fig. 5.17 bar charts.

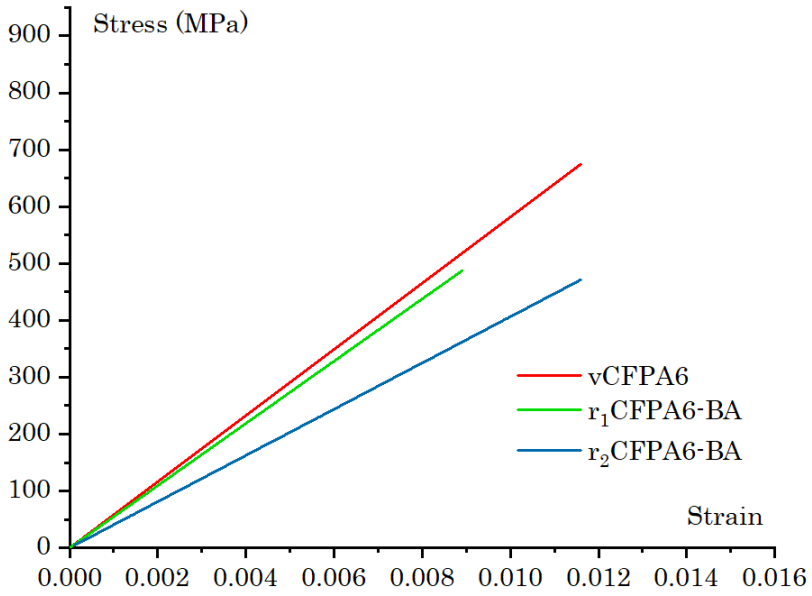

Fig. 5.16. Representative stress-strain curves obtained from tensile test of CFPA6-BA as a function of recycling loop.

σ_{ult} was determined as the maximum stress and ε_{ult} refers to the corresponding strain. E_T was determined by taking the gradient of the linear-elastic region section of bounds $0.001 < \varepsilon < 0.003$. $E_{T(0.28)}$ and $\sigma_{ult(0.28)}$ denote the tensile stiffness and ultimate tensile strength normalised to a 28 % Vf_F, following the rules of mixture.

Tensile specimens exhibited a typical linear-elastic response followed by rapid, brittle failure. Statistical variance between data sets was determined using a Kruskall-Wallis test. vCFPA6-BA has a significantly higher tensile stiffness, ultimate tensile strength and ultimate tensile strain than the subsequent specimens. After the first recycling loop the tensile stiffness and ultimate tensile strength decreased by 25 % and 39 %, respectively. After the second recycling loop the ultimate tensile strength and the ultimate tensile strain remained statistically unchanged, however, the tensile stiffness dropped by a further 20 %. Composite stiffness is fibre dominated which suggested a successive decrease in fibre alignment, as a function of recycling. The second recycling loop did not reduce the ultimate tensile strength, similarly to the formic acid study.

The brittle failure exhibited by all specimens suggested that the IFSS between the CF and PA6 provided effective load transfer between fibres and matrix resulting in significant fibre fracture, see Section 3.3.4.

Table 5.12. Average mechanical performance data collected from tensile tests of CFPA6-BA after each recycling loop.

	$E_{T(0.28)}$	$\sigma_{ult(0.28)}$	ε_{ult}	ρ	Vf_F
	GPa	MPa		MPa	%
vCFPA6	60.2 (3.18)*	695 (7.75)	1.16 (7.24)	1.09 (8.38)	27.7 (4.61)
r_1CFPA6-BA	45.4 (8.02)	425 (4.67)	1.10 (8.61)	1.13 (6.93)	30.3 (11.1)
r_2CFPA6-BA	36.3 (2.78)	414 (2.66)	1.12 (5.10)	1.16 (2.87)	29.2 (0.91)

* Coefficient of variance

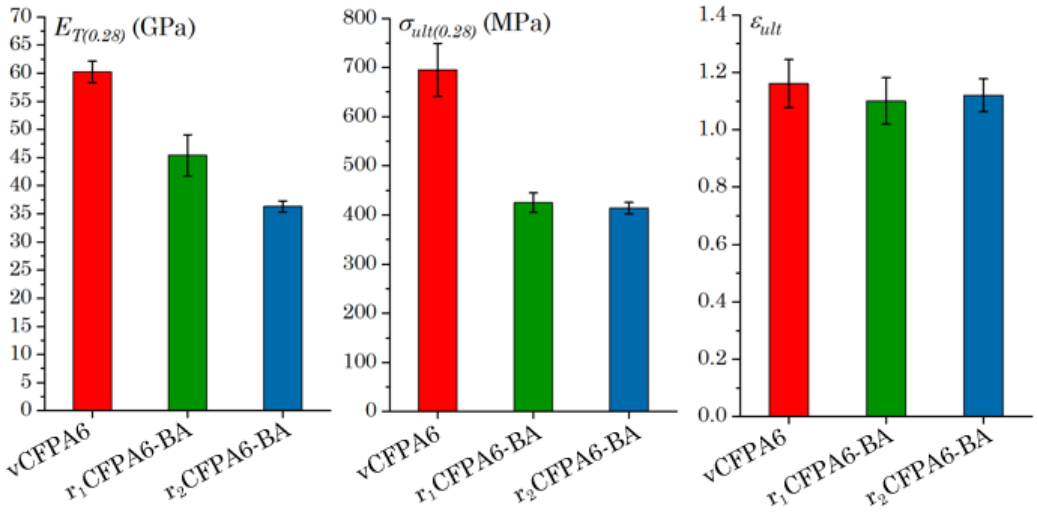

Fig. 5.17. Bar charts showing the normalised tensile stiffness, ultimate tensile strength and ultimate tensile strain of vCFPA6 as a function of recycling loop (benzyl alcohol). Error bars represent standard deviation of six specimen batch.

5.3.3.3 Fibre analysis

Fibre length distribution analysis was used to determine the effect of recycling on the average fibre length. The fibre length distribution of preforms made from vCF, and rCF after each recycling loop, are presented in Fig. 5.18. An error of ± 0.2 mm was applied for the by-eye length measurement of fibres.

In the vCFPA6 preform sample 63.9 % of fibres are in the range of 2.8 - 3.2 mm. After the first recycling loop 38.6 % of fibres are in the range 2.8 - 3.2 mm. r_2CFPA6-BA fibre length was more evenly distributed with 0.4 – 0.6 mm, 0.6 - 0.8 mm, and 0.8 – 0.1 mm having 7.5 %, 9.1 % and 9.8 % of the distribution and 3.0 – 3.2 mm representing 15.9 %. This distribution variation is like that obtained in Chapter 4 and in the formic acid study therefore it can be assumed that the main contributor to fibre breakage is within the remanufacturing process, either the compaction pressure or the alignment procedure, and not reclamation, *i.e.* the solvent system or carding process employed.

The 0.3 mm alignment plate spacing was equal to only the shortest fibre length so the alignment, and therefore the composite stiffness should not be significantly affected by the evening out of the distribution.

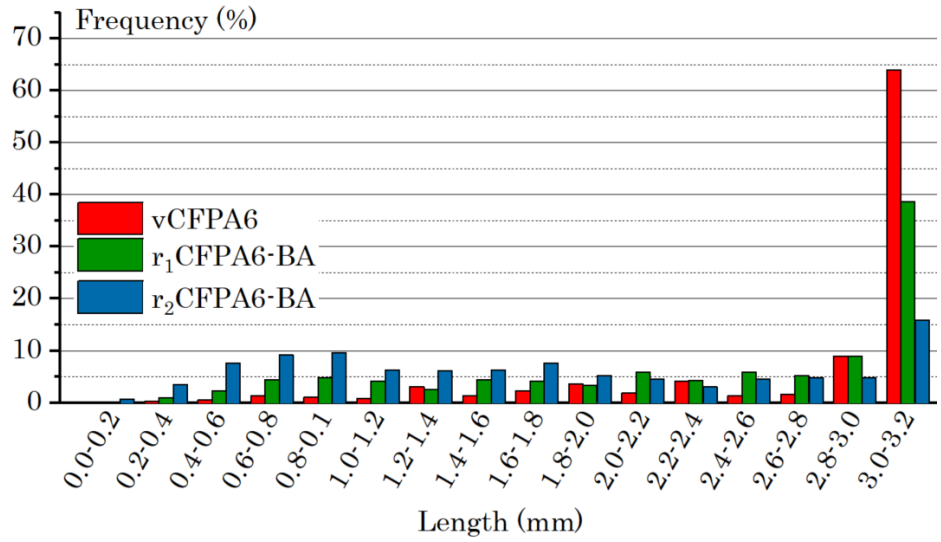

Fig. 5.18. Fibre length distributions of fibre preforms used in vCFPA6, r_1CFPA6-BA and r_2CFPA6-BA.

A Hitachi TM3000 SEM was used (5000 V accelerating voltage) to investigate the surface quality of fibre preforms collected from each recycling iteration.

SEM micrograph were taken of aligned preforms before impregnation of vCFPA6, r_1CFPA6-BA and r_2CFA6B-BA, see Fig. 5.19a-c. Fig. 5.19a shows the

vCFPA6 preform with clean surfaces in both magnifications. Fig. 5.19b shows the r_1CFPA6-BA preform with a coating in residual matrix adhered to the fibre surface. The micrographs of r_2CFPA6-BA, Fig. 5.19c, show the same residual matrix but in qualitatively unchanged quantities to r_1CFPA6-BA.

It is possible that the PA6 residue acted as a form of sizing that increased the IFSS. However, this did not significantly affect the ultimate tensile strength, as seen in Chapter 4, which decreased after the first recycling loop.

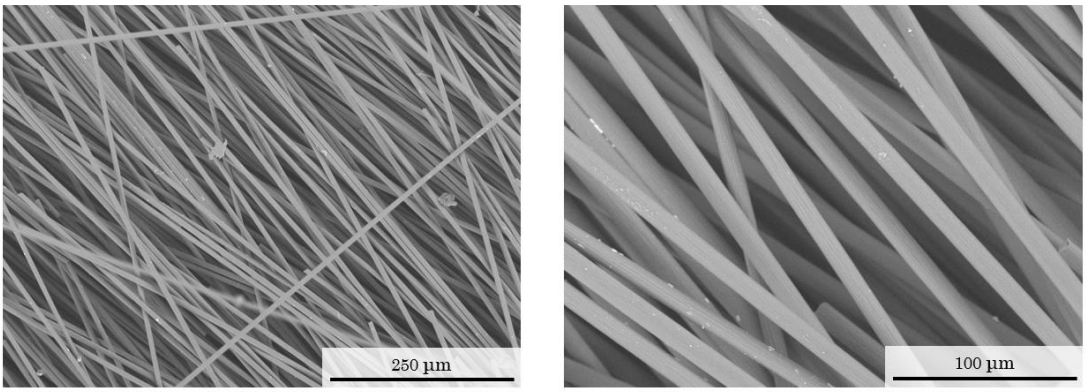

a) SEM micrographs of a preform used in vCFPA6

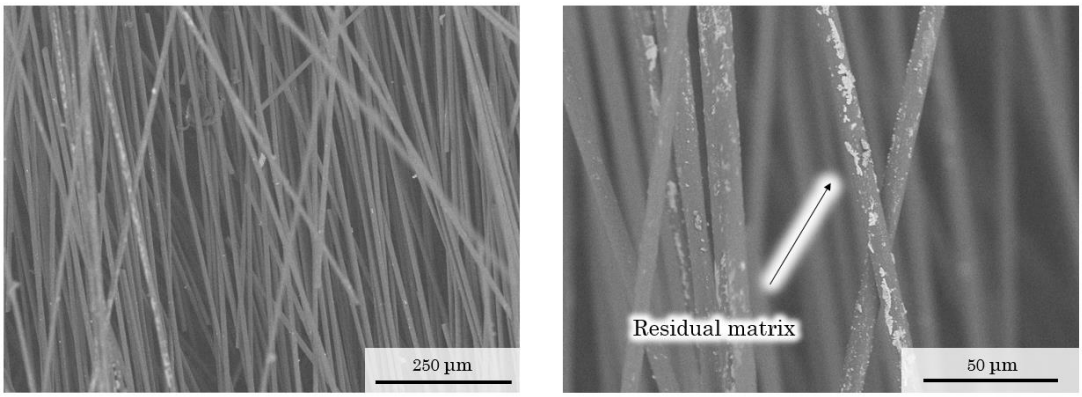

b) SEM micrographs of a preform used in r_1CFPA6-BA

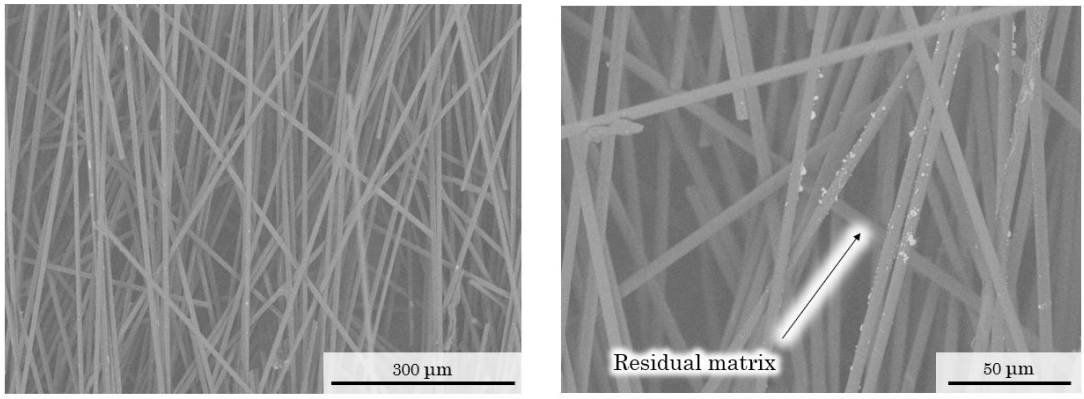

c) SEM micrographs of a preform used in r_2CFPA6-BA

Fig. 5.19. *a-c)* Preform cuttings taken from aligned preforms, of each recycling loop, before impregnation. r_1CFPA6-BA and r_2CFPA6 -BA show slight deposition of residue on fibre surface which is deemed to be unwashed matrix.

5.3.3.4 Fractography

Fracture surfaces were inspected using a Hitachi TM3000 SEM (5000 V accelerating voltage). One fracture surface was examined per six specimen batch to maximise the amount of material being recycled.

SEM micrographs of vCFPA6, r_1CFPA6-BA and r_2CFPA6-BA fracture surfaces are shown in Fig. 5.20a-b. Fig. 5.20a shows a typical vCFPA6 fracture surface where pull-out, fractured fibre ends and well coated fibres are clearly visible. This reflects the linear elastic strain response and brittle failure as the fibres are well adhered to the matrix enabling effective stress transfer. Fig. 5.20b showed similarly clean matrix crack surfaces however there were large 'valleys; along the cross-section where large sections of composite had cracked off. The large 'valleys' were also visible in the r_2CFP6-BA fracture surface in Fig. 5.20c.

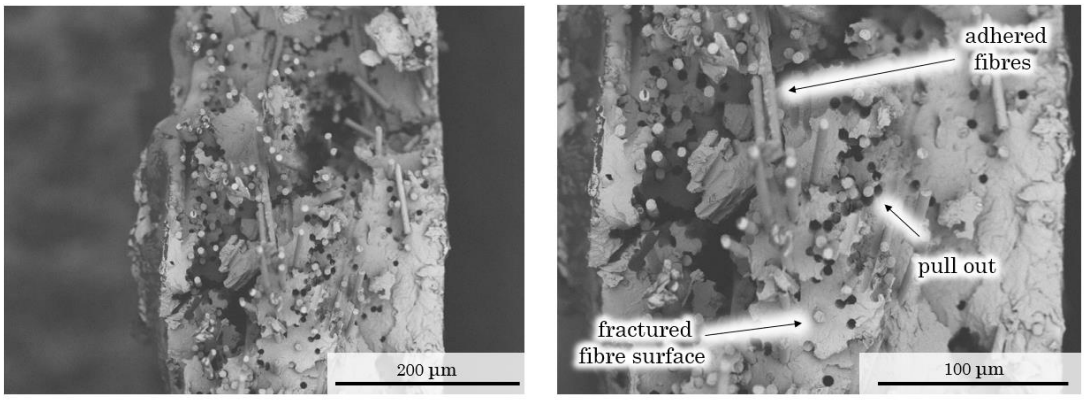

a) SEM micrographs of a vCFPA6 fracture surface

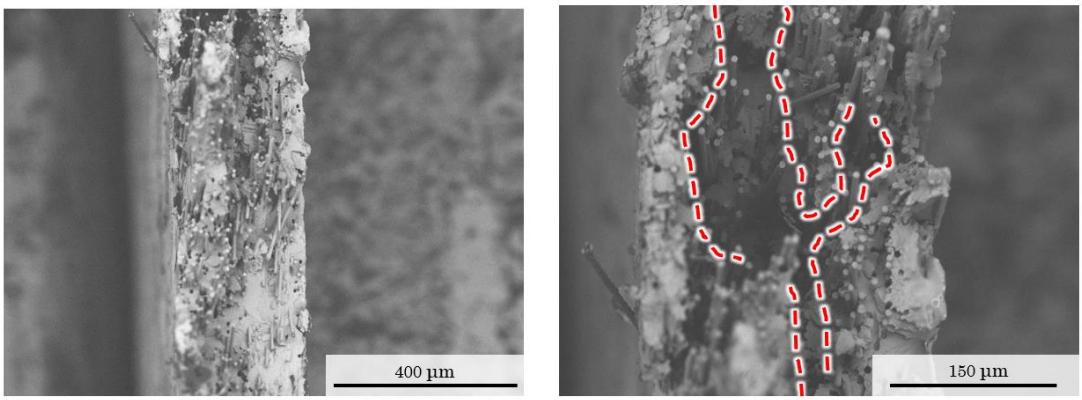

b) SEM micrographs of a r_1CFPA6-BA fracture surface

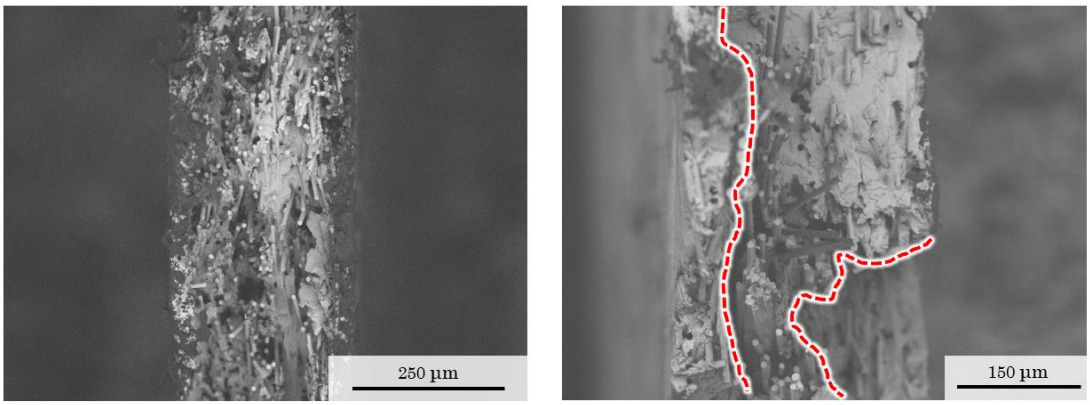

c) SEM micrographs of a r_2CFPA6-BA fracture surface

Fig. 5.20. *a)* A vCFPA6 fracture surface showing pull-out, well coated fibre surfaces and fracture fibre ends. *b)* A r_1CFPA6-BA fracture surface where large 'valleys' can be seen. *c)* A r_2CFPA6-BA fracture surface showing more 'valleys'.

The fracture surface 'valleys' suggest that large sections of composite have broken off from the opposite face. This is a consequence of crack propagation past a fibre-dense region, through the matrix-rich regions that typically surround them. The stiffness variation between the two regions initiates and rapidly propagates cracks through the matrix, resulting in reduced tensile strength.

The fibre-dense regions are likely to be caused fibre agglomerations that were not separated by the wet-sonication method. This provides a plausible explanation for the reduction in strength observed in the recycled composite specimens. It also explains the reduction in stiffness as the fibre agglomerations will likely cause misalignment of the surrounding fibres.

5.3.3.5 Conclusions

The mechanical performance, polymer properties and fibre properties of virgin and recycled CFPA6 was examined experimentally. The analysis linked macroscopic performance with microscopic fibre surface phenomena, fibre length and polymer behaviour.

The precipitate crystallinity variance observed was similar to the results of the formic acid study. However, the final melting peak split into two broad peaks after the first recycling loop. As the thermal history of the crystal formation was similar it suggested a change in the long polymer chains. FTIR spectra showed no signs of degradation however caprolactam may have been extracted in the supernatant.

GPC/SEC analysis reported successive degradation of the large polymer chains, however, the secondary peak chains were unchanged. HPLC-MS indicated the extraction of small molecules into the supernatant; these masses are substantially less than even small polymer chains. Polymers would have been insoluble in the HLPC carrier solvent and removed before analysis and are therefore not visible in the chromatogram. Small molecules had similar masses to known PA6 additives and their fragment ions.

The ultimate tensile strain obtained for the benzyl alcohol system was statistically invariable as a function of recycling. Considering this with the

unchanged secondary MWD peak and comparing them with the ultimate tensile strain and secondary MWD peak reduction from the formic acid study, it is reasonable to conclude that the secondary peak may have provided additional toughness to the polymer.

The tensile stiffness decreased by 25 % and 20 % after the first and second recycling loops, respectively. This was caused by the presence of fibre agglomerations in the preforms, which formed fibre-dense stress-raisers in the composite resulting in early failure. Evidence of the fibre agglomerations was observed in the fracture surfaces of the recycled composites.

The fracture surfaces of r_1CFPA6-BA and r_2CFPA6-BA showed relatively deep 'valleys', which suggested that large sections were cleaved during fracture. This indicated the presence of fibre-rich regions surrounded by matrix-dense regions through which cracks easily propagate. Fibre agglomerations were the likely cause of the early failure observed in the recycled specimens. Agglomerations occur during reclamation and are difficult to separate; some are passed through the alignment process without enough prior separation and end up in the preforms. They were not observed in the Chapter 4 study, this is likely a consequence of the different separation methods used, suggesting that dry carding is the most effective rCF separation method with regards to minimising agglomerations. The effect of the fibre agglomerations on the mechanical performance indicated that the fibre contribution to composite stiffness and strength was significantly greater than that of the matrix.

The mechanical performance achieved by the vCFPA6 specimens was considerable, to the authors knowledge these were the highest mechanical performances achieved by any discontinuous CFPA6 composite in the literature. There was a knockdown in performance after the first recycling loop, however, the mechanical performance of r_1CFPA6-BA and r_2CFPA6-BA were, to the authors knowledge, the highest observed for any recycled thermoplastic composite, and, for any recycled discontinuous CF composite with either thermosetting or thermoplastic matrices.

5.3.4 Results and discussion: Constituent exclusion

This study was used to qualitatively determine the significance of the fibre and matrix contributions to composite mechanical performance, as a disparity was suggested from the results of the formic acid and benzyl alcohol studies. The typical closed-loop recycling process, seen in Chapter 4 and above, used the same batch of constituent materials throughout. An example of this is presented in Fig. 5.21, emphasising the recycling status of the constituents.

This study used a variation of the typical closed-loop process formats, manufacturing composite specimens using: vPA6 with second iteration recycled fibres (r_2CF) and first iteration recycled PA6 (r_1PA6) with vCF. The composites produced from these conditions were denoted r_2CF.vPA6 and vCF.r_1PA6, respectively. A schematic of the variation in constituent combination is presented in Fig. 5.21. All recycled constituents used were reclaimed using benzyl alcohol to remove the strain knockdown observed with formic acid.

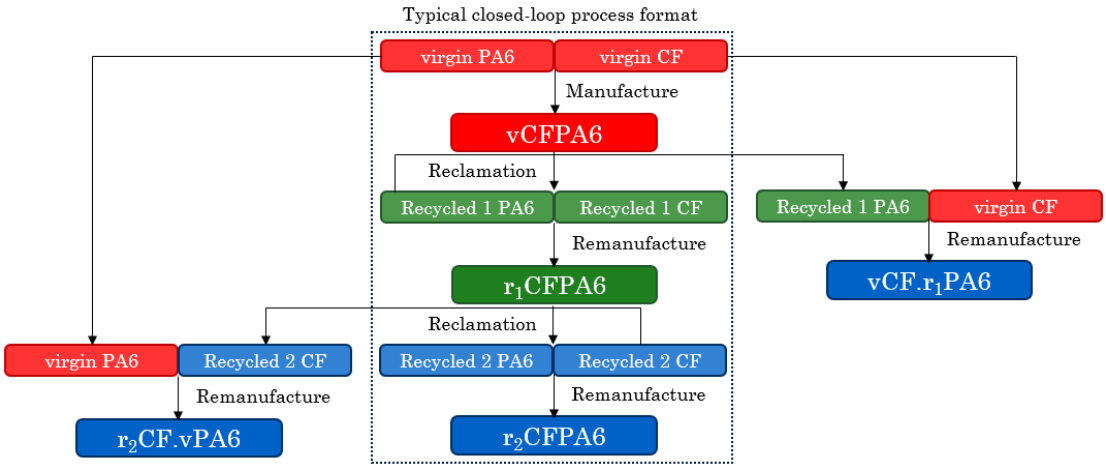

Fig. 5.21. Schematic showing the variation in constituent combination used in the constituent exclusion study.

5.3.4.1 Mechanical testing

r_2CF.vPA6 and vCF.r_1PA6 specimens were tested for their tensile properties in accordance with ASTM D3039. Axial force was provided by a Shimadzu AGS-

X servo-electric tensile test machine with a 10 kN load cell and a constant cross-head displacement of 1 mm/min. Strain was measured using the Imetrum video gauge software, over a gauge length of 50 mm. Specimens were sprayed back and speckled with white dots to aid with strain mapping; an example of this is shown in Fig. 4.15.

Representative stress-strain curves obtained from tensile tests of r_2CF.vPA6 and vCF.r_1PA6 are shown in Fig. 5.22. These may not exactly match the tabulated averaged results. The results of the tensile tests are recorded in Table 5.13, and represented graphically in the Fig. 5.23 bar charts.

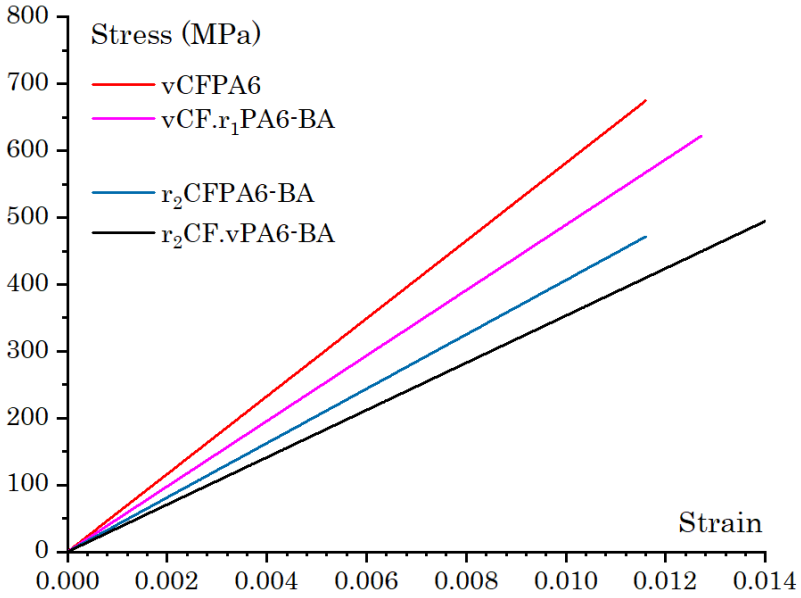

Fig. 5.22. Representative stress-strain curves obtained from tensile test of r_2CF.vPA6 and vCF.r_1PA6. Representative curves from vCFPA6 and r_2CFPA6-BA are plotted for reference.

σ_{ult} was determined as the maximum stress and ε_{ult} refers to the corresponding strain. E_T was determined by taking the gradient of the linear-elastic region section of bounds $0.001 < \varepsilon < 0.003$. $E_{T(0.28)}$ and $\sigma_{ult(0.28)}$ denote the tensile stiffness and ultimate tensile strength normalised to a 28 % Vf_F, following the rules of mixture.

Tensile specimens exhibited a typical linear-elastic response followed by rapid, brittle failure. vCF.r$_1$PA6 exhibited a 27 % and 20 % lower stiffness and strength than vCFPA6, respectively, but achieved a similar strain. The assumption was made that, because both specimens contained vCF preforms, any differences must be caused primarily by the matrix. However, there was a variance in the areal weights produced by the alignment process. This meant that the property reduction was a consequence of either *a) an influential matrix contribution to composite performance,* or, *b) There is a significant variance in the preform properties produced by the alignment process.*

r$_2$CF.vPA6 exhibited a 40 % and 34 % reduction in stiffness and strength compared with vCFPA6. The ultimate tensile strain remained within variance. The mechanical performance was analogous to r$_2$CFPA6-BA despite the presence of vPA6, which indicated that the influence of the fibre contribution was substantial and greater than the matrix contribution.

Table 5.13. Average mechanical performance data collected from tensile tests of r$_2$CF.vPA6 and vCF.r$_1$PA6.

	$E_{T(0.28)}$	$\sigma_{ult(0.28)}$	ε_{ult}	ρ	Vf_F
	GPa	MPa		MPa	%
vCF.r$_1$PA6-BA	44.1 (3.67)[a]	559 (7.80)	1.10 (8.61)	1.14 (6.65)	30.1 (1.64)
r$_2$CF.vPA6-BA	36.0 (10.2)	460 (13.1)	1.30 (10.1)	1.20 (6.9)	29.7 (15.7)

[a] Coefficient of variance determined from six specimen batch.

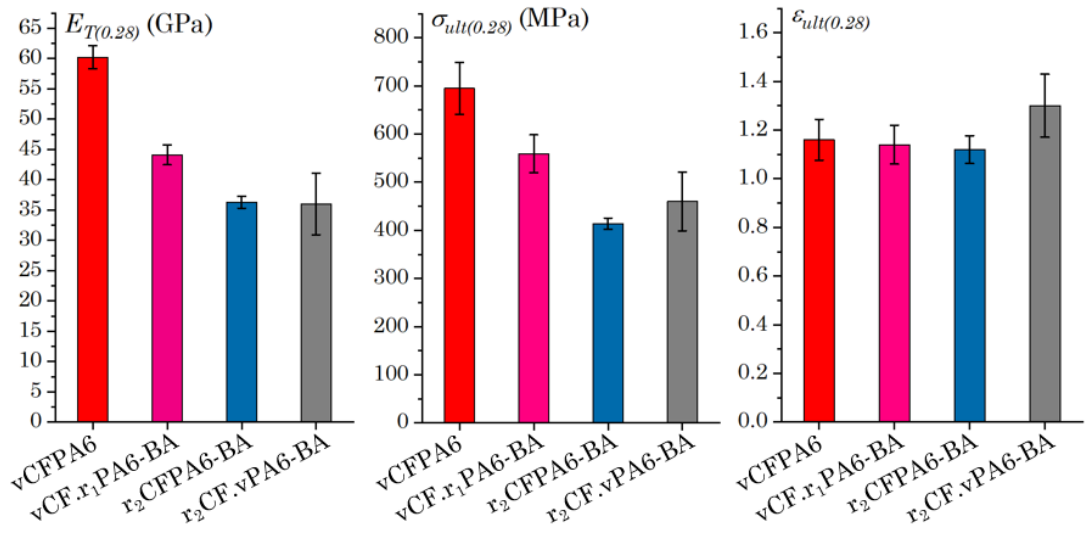

Fig. 5.23. Bar charts showing the normalised tensile stiffness, ultimate tensile strength and ultimate tensile strain of r_2CF.vPA6 and vCF.r_1PA6 with data from vCFPA6 and r_2CFPA6-BA for reference. Error bars show standard deviation of six specimen batch.

5.3.4.2 Fractography

Fracture surfaces were inspected using a Hitachi TM3000 SEM (5000 V accelerating voltage). One fracture surface was examined per six specimen batch to maximise the amount of material being recycled.

SEM micrographs of vCF.r_1PA6-BA and r_2CF.vPA6-BA fracture surfaces are shown in Fig. 5.24a-b. Fig. 5.24a showed the presence of well-adhered fibres, fibre pull-out, and fractured fibre ends. This reflected the linear elastic strain response and brittle failure as strong fibre-matrix adhesion enables effective stress transfer.

Fig. 5.24b showed a fibre-dense region in the fracture surface of r_2CF.vPA6 indicating the presence of fibre agglomerations in the recycled preforms. The fibre agglomeration is composed of misaligned, mechanically entangled fibre fragments with poor impregnation. Regions like this were the likely cause of the strength knockdowns observed as the variation in properties between

agglomerations and the surrounding composite can initiate cracks, resulting in early failure.

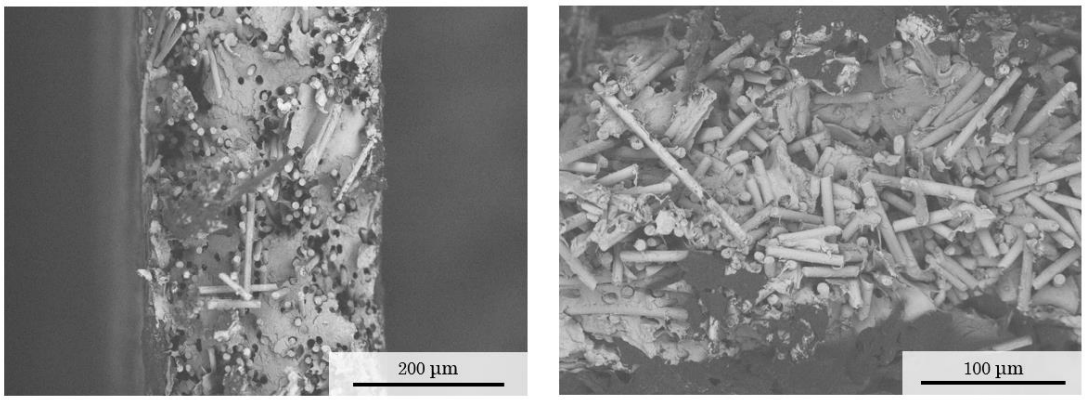

a) SEM micrograph of a vCF.r$_1$PA6-BA fracture surface

b) SEM micrograph of a r$_2$CF.vPA6-BA fracture surface

Fig. 5.24. *a)* vCF.r$_1$PA6-BA fracture surface. *b)* r$_2$CF.vPA6-BA fracture surface where a fibre-dense region is clearly visible.

5.4 Overall conclusions

The aim of this investigation was to determine if it was possible to reclaim and remanufacture a high-performance carbon fibre thermoplastic composite over two recycling loops, *i.e.* using a closed-loop recycling process. The primary goal of the composite was that its performance after recycling was high enough for it be used in high-value applications, *i.e.* as semi-structural automotive components.

A performance reduction was observed after the first recycling loop suggesting a reduction in fibre or matrix properties. A constituent exclusion study suggested that the fibre contribution to this reduction was substantially greater than the matrix. Fractography indicated that reclamation increases the prevalence of preform fibre agglomerations. These were the likely cause of the strength reductions, due to crack initiation and propagation resulting from variations in composite properties around the agglomeration. Agglomerations also cause misalignment of fibres resulting in stiffness reduction. There was a variation in the composite mechanical properties within each batch, which was

due to the variations in the alignment process output caused by fibre agglomerations.

Two solvent systems were used for reclamation and the resulting composite properties were compared. The two solvent systems were selected as they offered different process benefits. Stiffness and strength reductions were similar between solvent systems indicating that these properties are independent of the solvents used. A strain reduction was observed in the formic acid study, which matched the reduction in a secondary polymer distribution in the MWD. It was assumed that these secondary chains were extracted during reclamation. The results of this study corroborate the notion that the fibre contribution to mechanical performance is predominant. Due to the complex solvent reclamation for formic acid and water, in addition to the lower dissolution rate and enhanced hazards associated with formic acid, benzyl alcohol provided the most benefits in terms of reclamation yield and process energy intensity.

As the mechanical performance reductions were based primarily on the fibre agglomerations accrued through reclamation, and not a reduction in the intrinsic fibre properties, there is potential, after optimisation of the fibre separation/carding process, for the closed-loop process to produce no property reduction.

The highest performance CFPA6 found in the literature is compared with the highest performance virgin and recycled CFPA6 produced in this study, Fig. 5.25. Material properties of each are provided in Table 5.14. The mechanical performances in Fig. 5.25. are normalised to 28 % Vf_F to aid comparison. The author acknowledges that this normalisation for discontinuous CF composites, based on rule of mixtures, is not strictly appropriate as the level of alignment and interfacial shear strengths differ between materials.

Table 5.14. Properties of CFPA6 material sourced from the literature.

Author	Architecture	Vf_F	E_T	σ_{ult}
		%	GPa	MPa
Wu *et al.* [214]	Random DCF	30	6.38	111
Do *et al.* [225]	Random DCF	20	13.1	174
Botelho *et al.* [216]	Woven	40	28.3	296
Feng *et al.* [220]	Random rDCF	20	13.0	120
Pelin *et al.* [218]	Woven	30	56.3	505
vCFPA6	Aligned DCF	28	56.5	768
r_1CFPA6-FA	Aligned rDCF	28	45.3	475

DCF = discontinuous carbon fibre. (r-) denotes recycled fibre

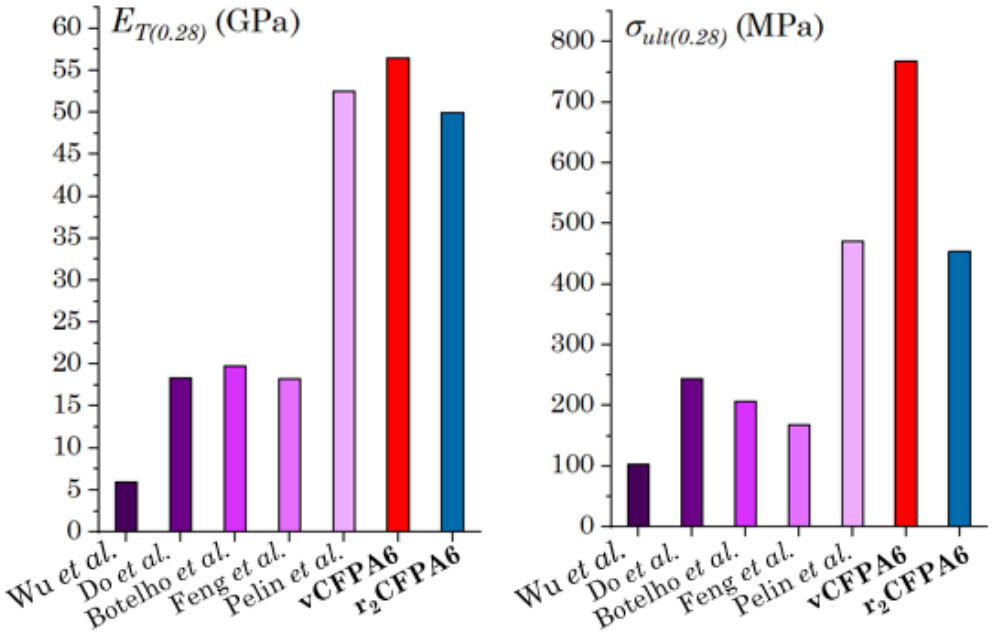

Fig. 5.25. Bar charts comparing the tensile stiffness and strength of vCFPA6 and r2CFPA6-FA material with vCFPA6 and rCFPA6 composites from the literature. Mechanical performances are normalised to 28 % fibre volume fraction.

When compared with Table 2.1, rCFPA6 after each recycling loop has a mechanical performance high enough to match current virgin materials used in semi-structural vehicle locations.

To the author's knowledge vCFPA6 specimens achieved the highest stiffness and strength of any discontinuous fibre CFPA6 available in the literature. The recycled specimens also achieved the highest mechanical performance of any discontinuous CF recycled composites, either thermoplastic or thermosetting, reported in the literature.

Although there is evidence to suggest the removal of polymer additives during reclamation this had no significant effect on the mechanical performance. If additives are removed during reclamation, they remain in the supernatant, which can be evaporated down to the solutes. These can be collected and remixed with the precipitate powder before impregnation therefore closing the loop.

It is possible that the PA6 residue observed in the preform micrographs acted as a form of sizing that increased the IFSS. However, this did not significantly affect the ultimate tensile strength, which decreased after the first recycling loop. This is contrary to the effect of the residual matrix observed in Chapter 4, The residue had a diminished affect, due to the IFSS of virgin CF-PA6 being of enough strength to enable effective load transfer. The IFSS of virgin CF-PP was low enough that any IFSS enhancement would cause a marked increase in the IFSS and the composite tensile strength.

The main objective of the process was to recycle a carbon fibre thermoplastic composite material over two recycling loops without reducing the mechanical properties of the composite and thus retaining the value of the recyclate. Despite the property reductions observed, the mechanical performance of the recycled composites was still suitable for use in semi-structural automotive applications.

6 Life cycle assessment of the developed process and materials

6.1 Introduction

Chapters 4 and 5 have shown that the mechanical performance of closed-loop recyclable materials can be retained, and are suitable for high-value applications, over two recycling loops. For the closed-loop materials to be desired by industry they must also be competitive in terms of environmental impact and cost. This Chapter uses the LCA framework to qualitatively determine the environmental impact of the closed-loop recycling process and the material produced.

Section 6.2 contains a thorough review of how LCA has been used to evaluate the recycling of CFRP. It determines the advantages and disadvantages of the current available methodologies and highlights stages where the benefits of rCFRP can be magnified. It is split into five sub-sections which detail the relevant LCA background (Section 6.2.1), the general methodology of an LCA (Section 6.2.2), the boundaries in which a typical LCA operates (Section 6.2.3) followed by the interpretation and discussion of the findings (Section 6.2.4).

The findings of the review section are applied in the LCA evaluation of the closed-loop recycling process, and materials, in Section 6.3. Section 6.3.1 defines

the goal and scope of the LCA, Section 6.3.2 details the life cycle inventory, from material production to end of life, the results and discussion are presented in Section 6.3.3, followed by the concluding remarks in Section 6.3.4

6.2 Life cycle assessment for CFRP: A review

6.2.1 Background

A life cycle assessment is an internationally standardised methodological framework for analysing the cradle-to-grave environmental impacts of products, processes or activities. For a product, this is accomplished through [233]:

1. The summation of the relevant inputs and outputs of a collection of processes;

2. The evaluation of potential impacts of this list;

3. The final interpretation of results in the context of the goal and scope, as defined at the beginning of the assessment.

LCA is a valuable tool for decision-making and for generating insight into environmental 'pinch-points', savings opportunities, and process trade-offs. These benefits, along with a shift in public opinion towards environmental protection, have led to LCA becoming a recognised industrial tool for the evaluation and selection of novel materials and processes. Its presence is gradually increasing in the construction [234–236], aerospace [237,238], wind [239,240] and automotive [241,242] sectors. Current requirements for the automotive industry are to reduce vehicle life cycle emissions [243] and increase recycling at the end of life [27]; assessment criteria from LCA can provide the valuable process modelling and quantitative analysis required to make informed improvements to meet these goals. In contrast, the composites industry uses the LCA approach to highlight the benefits of lightweight materials as alternatives to conventional materials [244]. Typically,

lightweighting materials such as aluminium, magnesium, carbon fibre reinforced polymer composites, and glass fibre reinforced composites are compared with conventional steels, over a product's lifetime [15,242,245].

CFRP can provide weight savings of up to 65 % when compared to steel automotive parts [15] and up to 20% when replacing aluminium in aviation [246]. However, the suitability of CFRP for a given application is not solely driven by weight, there are many other considerations such as part complexity, production volume, manufacturing lead time, environmental impact, and costs [26]. The production and manufacturing burden (PMB) of CFRP, *i.e.* the total environmental impact, cumulative energy demand (CED), and financial cost of raw material production and component manufacture, rules them out as an alternative material for many industries as they do not meet industrial, legislative or commercial requirements [5]. One method of reducing this burden is through recycling, as the energy required for recycling is typically far less than that of primary production [242]. However, these benefits have so far not been widely quantified or, in most cases, developed into a practically feasible technology.

This review explores the relevant theory behind LCA evaluation for CFRP recycling to aid material selection by reviewing the available literature. It establishes the pitfalls and advantages of the traditional LCA framework, and its contemporary equivalents, and illustrates how they can be adapted for the assessment of rCFRP. From these findings, the available strategies for defining and evaluating the benefits of a closed-loop recycling process, or a closed-loop recyclable material are analysed. This is achieved through various EOL allocation approaches and the application of multiple use-phases.

6.2.2 Life cycle assessment methodology

As stipulated by the International Organisation of Standardisation (ISO) standards (ISO 14040 2006; ISO 14044 2006), an LCA consists of four categories [247,248]:

1. goal and scope definition,

2. life cycle inventory analysis,

3. impact assessment,

4. interpretation of results.

The goal and scope outline the system to be studied, describe the environmental impact categories and identify any limitations or assumptions made during the assessment. It is important to first establish the decision that will be informed by the result of the assessment, for material selection this is a comparison of alternative systems for a reference unit, *i.e.* a *functional unit*, this can be a specific amount of material [80], or a specific component *e.g.* an aircraft undercarriage stay beam [249].

The life cycle inventory (LCI) comprises the identification, and summation, of all relevant unit process flows associated with the product system. Product systems for CFRP encompass all the interconnected *unit processes* of a product's life cycle, from raw material extraction to EOL processing. The LCI is composed of the key phases of the functional unit life cycle as limited by the system boundaries. An example of a typical LCI is presented in Fig. 6.1. For most product-focussed LCA this spans the cradle-to-grave life cycle of a product, which in turn comprises the following phases; *a) raw material production, b) manufacturing, c) use, and d) EOL* [29].

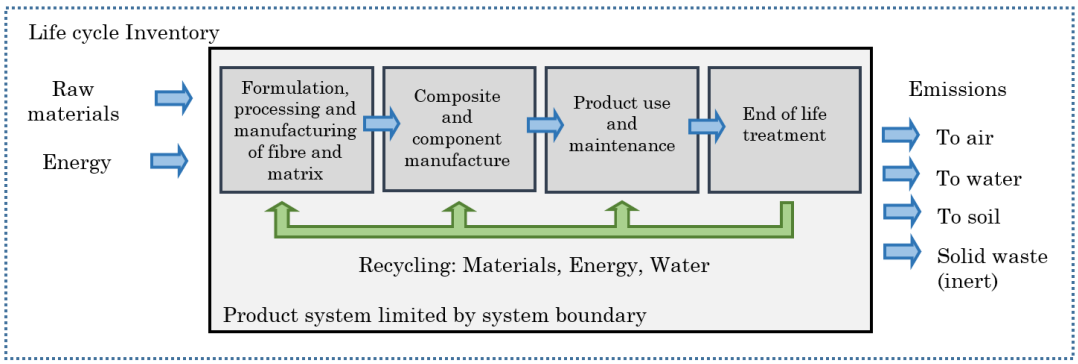

Fig. 6.1. Schematic of a typical LCI.

For an automotive CFRP component, this would include every unit process from the extraction of raw materials, through fibre sizing, matrix polymerisation, resin transfer moulding of the panel, panel lifetime in vehicle, disassembly, and EOL. Each of these unit processes is joined by its input and output flows where each flow could be materials, resources or emissions. One of the most common inputs of a unit process is the CED (units MJ/kg), *i.e.* required energy for all processing operations.

The databases available for LCA include Ecoinvent [250], GaBi [251], ELCD [252] and, specifically for composites, EuCIA [253], although direct data from experimentation, or industry, have been used in previous studies, despite being in limited supply [238,254]. EuCIA developed an Eco Impact calculator tool for evaluating the environmental impact of composite products without the user requiring specialised knowledge on LCAs, this is especially valuable to the small composite manufacturing companies that are prevalent in the industry [255]. One of the main drawbacks to this tool, and similarly with other databases, is that the data are typically acquired from the product manufacturers themselves and are rarely audited. There is also the limitation of misrepresentation as databases are seldom updated from their initial inception providing outdated and potentially unreliable data points [253].

It is useful to create limitations in the amount of unit processes considered in the analysis *i.e.* create a *system boundary*, however this is a trade-off between the accuracy of the evaluation and the time required to complete it [256]. Ignoring all common operations between two alternatives for a functional unit is a typical example of this. The necessity of setting a system boundary will undoubtedly lead to the omission of external effects that could result in a significant underestimated result [254]. Therefore, LCA is very much a user specific evaluation based upon subjective interpretation of the importance of the many facets of the assessment and its conclusions. This can make comparison of LCAs on the same topic complex and regularly impractical.

The suitability of an LCI process is determined by its contribution to the *impact categories* selected in the life cycle impact assessment (LCIA). The LCIA applies a variety of impact categories to the LCI which best contrast their

quantified impacts in the context of the assessment scope [257]. These typically cover: Global Warming Potential (GWP), *i.e.* Greenhouse Gas (GHG) emissions, Fossil Fuel Depletion, and Ozone Depletion, *etc.* [247,248]. GHG (unit $kgCO_{2eg}/kg$) is the most common form of emissions impact for comparative studies.

The selection of the most appropriate inputs/outputs in the LCI is an important factor when determining the validity of the LCA, especially when considering the system boundaries. For example, the number of Carcinogens emitted during production may be insignificant in comparison to the product mass, however the indirect environmental impacts may be considerable, and therefore of consideration. This is especially pertinent when most of the impact from a process is in a category that lies outside the system boundaries, or conversely, the most impactful process, within a given boundary, has not been included in the LCI.

Despite the real advantages of LCA there are drawbacks associated with its key stages that can result in widely varying results. As an LCA is user constructed, there are elements which require personal judgement, *i.e.* the system boundary breadth, and the detail employed in the mapping of production phases [242]. There is also the issue of *allocation*, this describes the need to ensure the assignment of an impact to only one process in the system; some impacts appear in other supply chains within a shared system boundary and therefore should not be accounted for twice [258].

It is important to combine economic as well as environmental assessments, especially when considering the comparison of composite materials with conventional materials as the production of CFRP is an expensive process [259]. Life Cycle Costing (LCC) is an integrated LCA approach with the additional metric of economic cost. LCC considers all of the relevant projected costs associated with a product in its life cycle, split into the same four key stages as an LCA [260]. It has been used by many companies, driven primarily by cost sensitivity, especially during the R&D and design stages. Witik *et al.* performed an integrated LCA/LCC evaluation of: a glass fibre sheet moulding compound, glass matt thermoplastic (GMT), reaction injection moulded carbon fibre composite (RIMCF), reaction injection moulded glass fibre composite (RIMGF), and die-cast magnesium part

to replace a conventional steel vehicle bulkhead [241]. The study showed that GF SMC provided the lowest environmental impact and economic cost for the entire cradle-to-grave life cycle, despite offering the lowest weight savings [241].

When considering material selection from a wide range of material types, *e.g.* choosing between composite, metal and wood in recreational aviation and boating applications, it is also important to include a technical dimension to the evaluation as the resulting component will have a design envelope with mechanical property limits and varying manufacturing requirements. The Life Cycle Engineering (LCE) framework has seen recent development due its ability to capture environmental, economic and technical aspects of the material selection process [261,262]. Materials are scored based on the three aspects and can be compared by either the *CLUBE* or *ternary* mapping methods depending on the importance placed in the technical performance [261].

Integrated LCE methods are also useful for highlighting areas where cost is unnecessarily high or areas in which it may be possible to reclaim some of the expenditure and help reduce the overall economic burden of a material. It is possible in some recycling procedures to reclaim some of the costs by down-cycling recyclate or energy harvesting [237,242]. In some cases, the environmental savings achieved over the life cycle of a functional unit may be offset by the costs incurred during material manufacture or use phases; therefore, a fully comprehensive account of economic and environmental impacts over a material life cycle is paramount.

6.2.3 Composite material life cycle inventory (LCI) phases

6.2.3.1 Material

The initial phase of the material life cycle is represented by the production of the constituent materials. For fibre and matrix manufacture, the conversion of raw material into a feedstock material can vary significantly in CED, due to the variation in CED of the unit processes involved. The production CED, GHG

emissions and cost of common reinforcements and matrices for FRPs are collated in Table 6.1.

Both the literature and LCA databases report different values for environmental impact, cost and CED for the same constituents. Selection of the best representative value should therefore be approached with caution. Individual countries usually rely on different energy source ratios, *i.e.* fossil fuels, natural gas, renewables and nuclear, for electrical power. For example, a significant portion of global CF production comes from Japan, which has high average GHG emissions (484 gCO_{2e}/kWh) associated with energy demand contribution from grid electricity. Alternatively, Sweden has lower emissions per MJ of electricity produced as its electricity production is predominantly provided by renewable sources [263].

Resource use, *i.e.* energy, water and cost, vary depending on the infrastructure, technology and methodology used; this range is broader in more common, widely available, materials as the variety of production technologies increases. For composite matrices the choice between thermoplastic and thermoset is typically application and cost driven; pure thermoplastics tend to be cheaper (1-3 £/kg) than pure thermosets (2-15 £/kg). Resource depletion for raw material production can also vary as a result of economies of scale between companies of small and large scale production [254]. Multinational corporations typically have processes with optimised consumptions, *i.e.* iron and steel suppliers, which result in substantial energy savings over smaller competitors.

The PMB of CF is significantly greater than that of conventional materials; it is widely considered as the main deterrent to the adoption of CFRP [285]. Reduction has been investigated using renewable fibre precursors, more efficient production techniques and renewable energy sources [29]. Natural fibres and bio-derived precursors have been investigated extensively as potential replacements for CF [249,286]. Joshi *et al.* stated that NF production is of lower environmental impact across all categories [275]. Wötzel *et al* also reported a 45 % decrease in energy requirements for NF production over CF. However, this is in combination with an increase in water emissions due to the fertilizer use during cultivation [287]. Water emissions are not the only trade-off when considering NF alternatives

as they have reduced mechanical performance in comparison with CFRP and are only recently competitive with GFRP [288].

Table 6.1. Table summarising EI and GHG and costs of common CFRP constituents found in the literature.

Material	CED	GHG	Cost
	MJ/kg	kg CO2eq/kg	£/kg
Steel	13-56 [242]		
	25.0-44.6 [31]	2.26-2.49 [31]	0.48-0.58 [264]
Recycled Steel	9.0-52 [242]		
Aluminium	197-298 [265]	5.92-41.1 [266]	
Fibre			
Virgin Carbon	171 [267]		
	183-286 [245,268]	-	-
	353 [269]	-	-
	478 [245,268,270]		
	198-595 [271]	-	-
	286-704 [30]	24.4-31.0 [264]	
	-	-	21.2-47.0 [89,272]
Glass	13.0-54.3 [254,273]	-	-
	45.6 [274]	2.50 [274]	
	48.3 [275]	2.04 [275]	-
			1.59-3.54 [264,272]
Aramid	222-245 [264]	16.4-18.2 [264]	21.2 [9]
Flax	6.50-11.6 [89]	0.45 [89]	1.57-3.14 [264]
Matrix			
Thermoset			
Epoxy	140-144 [275,276]		3.00-15.0 [277]
	76-80 [245,274]		
	76-137 [30]	4.7-8.10 [30]	
Polyester	63-78 [245,278]	2.8-3.10 [245,278]	1.00-2.00 [277]
Thermoplastic			
ABS	95 [275,279]	3.10	1.22
PVC	53-80 [21–23]	2.20 [13]	1.36 [13]
Polypropylene	22.4-112 [245,275,276]	1.85-2.60 [245,275,276]	1.23 [264,279]
Nylon	139-145 [276,280]	6.50-8.33 [276,280]	1.66-2.55 [264,279]
PC	80-112 [254,281]	6.00-7.50 [254,281]	1.82 [264,279]
LDPE	65-92 [254,282]	1.80 [283]	1.22 [284]

A comparative LCA by Summerscales *et al.* contrasted flax fibre as a GF alternative. The study established that flax fibre has a total energy requirement of 54.2 – 146 MJ/kg, depending on the reinforcement format and the agricultural processes involved, compared to a glass mat reinforcement embodied energy of 54.7 MJ/kg. This leads to the conclusion that due to the significant PMB, which will be similar to most natural fibres with agricultural cultivation being the largest contributing factor, flax fibres may only become a realistic alternative to GF when sourced as a by-product from other processes and not grown specifically for this purpose [289].

6.2.3.2 Manufacture

A variety of manufacturing procedures exist for CFRP manufacture therefore selection is driven by the design requirements of the application. Manufacture typically refers to the conversion of constituent feedstock into a component, this includes the production of manufacturing intermediates like prepregs. CED, cost and emissions data for the most common CFRP manufacturing processes can be found in Table 6.2; these data are typically quoted for the manufacturing process only and therefore do not include those required to produce constituent materials.

Generally, the largest proportion of manufacturing energy is spent by the application of heat and pressure needed for matrix curing and/or fibre impregnation. Parameters such as manufacturing rate and component complexity are not considered in the calculations, yet they have consequences in processes down-stream that can lead to significant increases in environmental impact, *e.g.* transportation. For example, pultrusion is considered a low energy process however it is limited to non-complex parts with simple cross-sections and has more intensive transport energy requirements that scale with component size [254]. Transportation requirements can have significant environmental impacts ranging from fuel emissions to societal congestion *i.e.* impacts associated with inner city congestion and motorway usage [254]. LCE may provide a solution to this issue as a part complexity and manufacturability parameter can be factored into the technical dimension of the assessment.

Table 6.2. Table summarising E, GHG emissions and typical productivity of common CFRP manufacturing processes. For production volumes Low < 5k ppa, Medium = 5k – 15k ppa and High = 15k – 100k.

Process	CED[(a)]	GHG	Production volume [42]
	MJ/kg	Kg CO2eq/kg	
Autoclave	21.9-29 [254,290]	-	Low
Spray up	14.9 [245]	-	
RTM (CF)	6.39-12.8 [245,291]	0.33 [291]	Medium
RTM (GF)	6.39-11.6 [291,292]	0.33 [291]	Medium
LRI/VARI	10.2-18.4 [245,291]	1.25	Medium
Cold press	11.8 [245]	-	High
Preform matched die	10.1 [245]	-	
SMC	3.5-3.8 [245]	-	High
Thermoplastic moulding	-	-	High
ATL	-	-	
Filament winding	2.70 [245]	-	Medium
Pultrusion	3.10 [245]	0.57 [291]	High
Injection moulding	19-29.9 [254,291]	0.5-1.33 [291,293]	High
Prepreg	40 [245]	17.9-19.7 [294]	Low
Casting (metal)	2.35 [265]	0.48-0.62 [266]	
Comp. mould.	7.2-26.5 [245,290,291]	1.59 [291]	

[(a)] Process CED is equivalent to onsite energy. RTM = Resin transfer moulding. LRI = liquid reactive injection. VARI = vacuum assisted reactive injection. ATP = Automated tape laying. Comp. mould. = Compression moulding.

Production volumes and cycle times can also alter the suitability of a material for a given application. Simões *et al.* reported a win-win scenario for the replacement of a single, stainless steel storage tank with a GFRP counterpart [295]. The LCA/LCC evaluation showed the composite part to have a lower environmental impact and part cost over the life cycle. However, the more advanced production infrastructure for stainless steel enables the production of far greater quantities in less time than the current manufacturing processes for composite materials can permit [15]. If the system boundary in the study undertaken by Simões *et al.* was expanded to include the production of a greater number of storage tanks in a given time, the impacts of the LCA and LCC may not be so disparate.

6.2.3.3 Use

The use phase refers to the period of a component life cycle in which it is functioning in its predetermined application. For any application the associated CED, environmental impacts and costs of the use phase can be split into those incurred through general usage and those from maintenance activities. For example, the major metrics for evaluating the CED and emissions of vehicles are lifetime travel distance and fuel economy. Any maintenance/repair contributions are insignificant compared to fuel consumption [242]. This phase dominates the life cycle energy consumption of vehicles; contributing anywhere between 60 - 84 % of the total life cycle energy consumed, primarily due to impacts of vehicle weight, *i.e.* fuel economy [245,296]. Comparatively, the manufacturing phase contributes only 4 - 7 % of the total lifetime energy demand of a passenger vehicle [297]. 75 % of fuel consumption is directly dependent on vehicle weight, mostly due to reduced powertrain demands, *e.g.* rolling resistance and acceleration and a 6 – 8 % increase in fuel economy can be realised with every 10 % weight reduction [298]. Therefore, the lightweighting benefits of CFRP are greater realised in the transport sector where use phases are the longest; the PMB may potentially be offset by the fuel consumption savings made during the use phase, providing it is of suitable length.

For components in passenger vehicles the use phase covers the lifetime of the vehicle, typically 10-20 years covering a range of distances, anywhere between 57,000 - 350,000 km, depending on geography and culture [242,297]. The United States Environmental Protection Agency (US EPA) and Canadian Standards Association (CSA) stipulated a 'useful lifetime distance' value of 240,000 km and 250,000 km for the average American and Canadian vehicle, respectively [297,299]. However, many studies have used an average of 150,000 km [237,241,269].

The total net change in the use phase energy demand, ΔE_{Use_i}, of a lightweighting material, i, over a conventional baseline material, b, can be determined following Equation 6.1 [299,300].

$$\Delta E_{Use_i} = C_i \times E_{FP} \times R_{WTW} \times \rho_F \qquad 6.1$$

where, E_{FP} is the energy required to produce 1 kg of petrol (MJ/kg), R_{WTW} is the conversion factor used to determine the energy demand of petrol from well-to-wheel (WTW). ρ_F is the density of petrol (kg/L) and C_i is the total mass-induced fuel savings which was calculated according to 6.2 [299,300].

$$C_i = (m_i - m_b) \times F_{CP} \times LTDD_v \quad 6.2$$

where, m_i and m_b are the lightweight and baseline masses respectively. F_{CP} is the mass-induced fuel consumption change potential value, *i.e.* fuel (L) required to move 100 kg by 100km. $LTDD_v$ is the chosen lifetime driving distance (km). As $m_i < m_b$, negative fuel consumptions are returned from Equation 6.1 which represents a fuel saving compared to the baseline material with a fuel saving value of zero.

A useful tool in use phase comparisons is the determination of the breakeven distance, which describes the minimum distance required for the energy savings accrued through use to offset the energy demand amassed during production. Recent literature shows that the breakeven point for vCFRP *versus* steel can be between 132,000-250,000 km, however this is entirely dependent on a number of factors including vehicle location, vehicle type, energy demand of fuel production, CFRP production CED and the primary energy source used during processing [241,290,301]. Timmis *et al*. reported a lifetime breakeven distance of 190,000 km and 75,000 km for CFRP and Al alternatives for a steel airframe [246]. Despite the 20 % reduction in CO_2 emissions afforded by the CFRP component, one lifetime was not enough to reach the 50 % reduction target for 2020. This was a direct consequence of the significant PMB of CFRP [246]. Kelly *et al*. compared the GWP of CFRP and steel components at different substitution ratios for components throughout a vehicle where breakeven distance for GWP increased proportionally with the ratio of CFRP to steel [302]. The mass-induced fuel consumption change potential value had a significant effect on the breakeven distances, for a 50 % substitution of steel to CFRP a change of 0.5 to 0.15 L/(100 km, 100kg) resulted in a 70 % increase in breakeven distance to 250,000 km [302]. Finally, Witik *et al.* reported similar findings when comparing rCFRP and vGFRP against a vCFRP component; the rCFRP component, reclaimed from pyrolysis,

was able to break even at 41,000 km compared to vCFRP which did not break even in the vehicle lifetime (200,000 km) [241].

Durability of a material can dramatically reduce its operational lifetime; therefore, durability is an important consideration when performing material selection. Some constituents can provide peak performance for longer durations than others, resulting in materials with shorter use-phases and higher maintenance/replacement costs for the same functional unit, this is especially true for NF. In some studies, NF composites have exhibited lower cost, weight and environmental impact for functionally equivalent cases [202,303,304]. However, Corbiere-Nicollier *et al.* indicated that a NF composite pallet only remained environmentally superior to a GFRP counterpart if the expected lifetime remained above 3 years, after this the GFRP equivalent would perform better, unless its expected lifetime dropped below 5 years [249]. This is important as there are insufficient data for the fatigue and longevity of NF composites therefore there are no guarantees that the NF composite can provide the purported environmental benefits even over GFRP.

Mechanical performance inequalities can also drastically alter the environmental impacts and costs of composites in an LCA. Dufluo *et al.* conducted a comparative study between flax fibre and GF reinforced polypropylene. The inferior mechanical performance of the flax composite limited its potential as a replacement material, despite flax offering lower global warming potential [305]. Equal strength equivalent material required a higher flax fibre volume fraction, which reduced the environmental savings to below what was required for it to be a feasible alternative [305].

6.2.3.4 End of Life (EOL)

The final stage of an LCA evaluates how a material is processed when it reaches the end of the use phase. For steel and aluminium this involves the melt reprocessing of EOL scrap which varies in yield but is commonly around 95 % [15,299]. The predominant EOL treatments for CFRP are landfill, incineration and, more recently, recycling processes. These are typically mechanical grinding or fibre reclamation techniques followed by a manufacturing stage.

The availability of commercial scale remanufacturing techniques is currently limited, resulting in a negligible market for rCF. The vast majority of CFRP recycling LCA are only covering fibre reclamation and do not incorporate a realistic remanufacturing step.

Landfill has been the most common disposal route for CFRP material as it can easily handle large waste quantities alongside being the most economical [25]. Incineration has been an alternative to landfilling in many LCA studies, as there is the potential for energy harvesting. Simões *et al.* showed that the LCA performance of a GFRP storage tank could be improved by selecting incineration with energy recovery as its EOL treatment over landfilling [295]. This can reduce the overall CED, despite the higher process emissions compared with landfill, as the energy recovered is deducted from the total CED [29,241,265,269]. However, the significance of the impact is determined by the scope of study, *i.e.* cost or emissions driven application, therefore the benefits are subjective. Witik *et al.* reported that the CO_2 emissions avoided by the reuse of recovered energy were not sufficient to offset those produced during incineration, making landfilling the most appropriate from an emissions perspective [108]. The problem with landfill and incineration is that most or even all the embodied energy of the CFRP is lost. Recycling is an EOL alternative that has the potential to provide recyclate of value typically through down-cycling into separate product systems; this could be as filler, or as a low-performance reinforcement. Mechanical grinding is a popular alternative to landfilling as it has a lower energy demand and can provide some recyclate value as a filler material, however this is minimal and is rarely economically viable [306,307].

Pyrolysis is reported as having a much lower energy demand than vCF production [15,37,241,290]. Pyrolysis is viewed as a superior alternative to landfill and incineration because rCF can be reused, reducing the total life cycle CED despite pyrolysis having far greater process CED and emissions. The environmental impacts of landfilling, incineration and reclamation processes have previously been contrasted in the literature and the conclusions of each vary depending on energy source [29,80,307]. A summary of the CED, emissions and costs of state-of-the-art fibre reclamation processes for CFRP can be found in Table 6.3.

Table 6.3. Energy intensity, environmental impact and recyclate value estimates for CFRP recycling technologies.

Process	Process CED	GHG
	MJ/kg	kg CO2eq/kg
Landfilling	0.11-0.4 [293,308]	0.09-4.61 [108,256]
Incineration	32-34 [(a) 108,269]	2.17-3.05 [308]
Incineration (energy harvesting)	(-)31.7 to (-)34 [(b) 293]	2.01-3.4 [293,308]
Mechanical grinding	0.14-51 [59,309]	-36 [310]
FB Pyrolysis	7.7-30 [290]	5.4-11 [108,310]
Microwave Pyrolysis	-	-
Pyrolysis	2.8-30 [29,293]	-
High voltage fragmentation	4 [311]	-
Solvolysis	15-64 [102,312]	-
Steel recycling	11.7-19.2 [293]	0.5-1.2 [293]
Aluminium	2.4-5.0 [293]	0.3-0.6 [293]

[(a)] Based on CFRP epoxy component bond energies, [(b)] Lit value based on CFRP epoxy calorific content with unknown harvesting efficiency. FB = Fluidised bed.

6.2.3.4.1 EOL recycling allocation

In LCA the EOL stage CED, emissions, and costs are typically a summation of the EOL operations required to dispose of, or, to convert the component into a reusable material; such as disassembly, size reduction, transport, recycling and landfill. The reuse of material results in a reduction in the amount of production energy required, how this reduction is accounted for, or *allocated*, can produce substantial variation in results. Recycling credits can be assigned based upon 'recycled content' or through 'EOL' approaches, in which there are subtle differences categorised as 'Cut-Off', 'Closed-loop' and 'Substitution' [313]. There are subtle differences in the EOL subcategories; Nicholson *et al.* compared the impact of each EOL method on the validity of two materials in a comparative LCA. It concluded that the differences in EOL approach are insignificant until the PMB of a material is far greater than an alternative [314]. The recycled content approach assigns credits for any secondary material in the total virgin production energy value [313]. For example, the reuse of manufacturing waste in the same process will be accounted for by a reduction in the total virgin production energy equal to that of the reused material. It lends itself well to the traditional linear production

processes in that it doesn't account for material that may be used in other product streams, *i.e.* down-cycling.

For closed-loop product systems where there are no changes in the inherent properties of the recycled material, such as steel and aluminium production, the EOL approach is best suited. The EOL approach assumes that there is a material 'pool' available where any unrecycled material is compensated by primary material; recycling therefore offsets primary production by the given recycling factor for the material. The recycling factor is determined by balancing the scrap output with scrap input to avoid double counting. The total production CED for a metal is therefore the primary production CED multiplied by the recycling factor, generally 0.16 for steel and 0.72 for aluminium, which accounts for the proportion sourced from recycled scrap [285,299,300]. This results in a reduced production stage CED and an EOL stage contribution from the recycling process CED. Closed-loop recycling of metals has been practiced for decades so the LCA framework to evaluate the EOL allocation is well defined [265]. Closed-loop CFRP recycling research is in its infancy, therefore detailed LCA frameworks are limited [80]. The standard Closed-Loop approach is not applicable as the recycled material is not directly reusable and has reduced mechanical performance. LCA evaluations that include CFRP approach this in different ways depending on the goal and scope of the study.

If the study compares the environmental impacts of an EOL operation, vCFRP has an EOL stage contribution for landfilling, incineration or pyrolysis and solvolysis [108,110,302,308,315,316]. The energy harvesting credits from incineration are counted as a negative burden and cause a reduction in life cycle CED. The CED of pyrolysis and solvolysis methods result in an increased life cycle CED however the GWP benefits, and economic cost reductions due to recyclate resale, can provide overall life cycle improvements. If the study is comparing the total life cycle environmental profile of a rCFRP over vCFRP, and other lightweighting materials, this is approached in a similar manner to the EOL approach. In the literature, it is usually presented in two distinct ways:

1. The rCFRP, made from reclaimed rCF, is treated as a separate material option and compared with alternatives. The production CED

does not include the raw material energy required for vCF but accounts for the pyrolysis CED in the EOL stage [282,290,300].

2. The vCFRP is evaluated over multiple life cycles, where the EOL stage of the first life cycle accounts for the CED required for recycling. The production stage of the second life cycle includes a reduction for the CF sourced from the previous recycling operation [245,317]. This is closer to the Cut-Off subcategory of the EOL approach found in the literature [318].

For CFRP, the recycled content approach may provide scenarios that better reflect the current recycling market for rCFRP which has no large-scale market of the rCF produced. An EOL approach will be the best suited for future scenarios where an appropriate recycling infrastructure is in place for large-scale production and recycling of CFRP [297]. Suzuki and Takahashi followed the Cut-Off EOL approach and suggested a 3R (reduce, recycle and reuse) system for LCA evaluation of recycled CFRP [245]. The 3R system enabled three use phases for an automotive component, which provided the lifetime savings required to make CFRP a superior lightweighting alternative to steel. However, this study only provides a model for a 3R product system and does not offer any real industrially applicable technologies for how the CFRTS/TP material will be reclaimed and remanufactured. The central problem that the industry faces for rCF remanufacture is that the current rCFs are produced in a filamentised, randomly oriented, and low bulk-density form [5]. As well as being fragmented into shorter lengths due to waste size reduction [60]. Without significant alignment, high fibre volume fractions are difficult to achieve and remanufacture typically results in rCFRP with significant mechanical performance reductions [70].

Until recently, LCA has not accounted for the economic influences or technical feasibility of the real world recycling market which play a vital role in passenger vehicle production [47]. Without a high value application for the rCF recyclate, the purported financial and environmental savings cannot be achieved [5]. A recent LCA by Meng *et al.* evaluated the environmental impacts of rCFRP material and compared them with steel and aluminium using the recycled content

approach [290]. The rCFRP materials were made by a range of remanufacturing techniques, notably the compression moulding of aligned rCF fibre mats and virgin epoxy matrix. The highly aligned rCFRP component (60 % Vf_F) offered the lowest life cycle energy demand and GHG of all materials, with a 94 % reduction compared with steel alone. It stated that vCFRP becomes favourable to steel at a lifetime driving distance > 250,000 km, but that rCFRP can offset production CED at distances of < 50,000 km [290].

6.2.4 Interpretation and discussion

The current PMB of virgin CFRP material remains significantly high despite the reduction efforts of recent years. There are a variety of different data sources available when selecting the production process for a CFRP product system and care should be taken when choosing the most appropriate representation. In addition to the environmental burdens the financial cost of fibre production is in constant flux, reduction in CF cost is a heavily researched area that is slowly making improvements; however, it remains far from competitive.

From an LCA perspective the recuperation of energy can help to reduce total energy demand and environmental impact, however this may only be a fraction of the PMB and does not reclaim any of the value of the constituent materials. As environmental impact is rarely as influential as cost for a material selection metric in the design phase, the reclamation of high value fibre and matrix is equally as important as reclaiming energy for many industries. The variation in source data for both CED values and others used in calculations, *i.e.* lifetime travel distance, fuel-consumption change potential, can result in significant variance in the final life cycle values. Most studies have applied a sensitivity analysis on the LCA results to account for the substantial variation in input data, reporting the variation in the final results obtained [15,47,108,241,282,290,319].

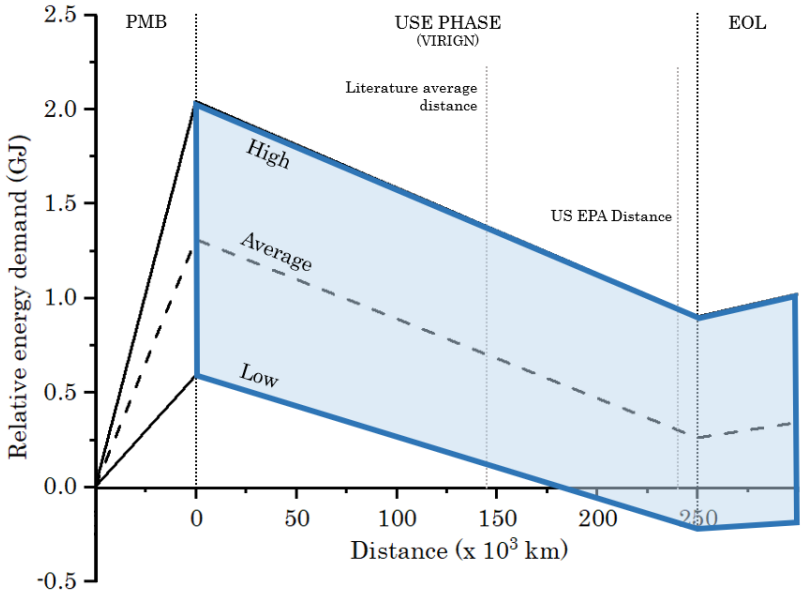

Fig. 6.2. Breakeven envelope plot showing sensitivity analysis of life cycle energy demand.

The variations in the literature PMB, EOL and total lifetime distance values can cause substantially different results in LCA. The significance of these is explored in the Fig. 6.2 sensitivity analysis. It shows the range of potential life cycle CED values for a component from using the range of input data available in the literature. The functional unit is a 10 kg CFRP component made from woven epoxy prepregs (60 % Vf_F). It offers a 60 % weight saving over a steel baseline for a vehicle lifetime, *i.e.* PMB through Use to EOL. The weight saving was calculated using the mass ratio expression in Equation 6.3 [320]:

$$R_{mass} = (\rho_C/\rho_S) \times (E_S/E_C)^{1/\lambda} \qquad 6.3$$

where, ρ is the density, E is the stiffness and the subscripts C and S refer to CFRP and steel, respectively. λ is a structural index which can be used to predict weight savings from material substitution when the part stiffness is assumed constant [320]. Precise determination of weight saving requires complex finite element models; however, this index can be used to provide useful approximations [320]. It expresses the response of the design to a change in thickness afforded using lightweighting materials and is effectively a measure of thickness-dependent non-

linearities in stress distribution in a thin-walled structure [320]. λ can be anything between 1 and 3, where 1 denotes components under tension, 2 represents beams under bending and compression in one plane, *i.e.* a vertical pillar, and 3 which describes a flat panel under bending and buckling in two planes, *i.e.* a car bonnet. Most automotive components are between 1 and 2 therefore an average value of 1.5 was selected [320]. A CFRP stiffness and density of 69 GPa and 1.5 g/cm^3 and a steel stiffness and density of 210 GPa and 7.85 g/cm^3 were applied to produce a mass ratio of 0.4 and thus a 60 % weight saving.

The envelope is constructed using the maximum, minimum, and average PMB and EOL values found in the literature, these are displayed in Table 6.1, Table 6.2, and Table 6.3. PMB and EOL values include a reduction for the replaced steel burden. Maximum, average and minimum values for steel production were used with a reduction factor of 0.16 applied following the Closed-Loop EOL allocation approach assuming virgin steel had an 84 % recycled steel content. Maximum values are combined for the upper envelope boundary and the minimum values are combined for the lower boundary to create the life cycle CED envelope. The CSA lifetime driving distance of 250,000 km was selected however the US EPA (240,000 km) and average literature value (150,000 km) were provided for sensitivity analysis. Equations 6.1 and 6.2 were used to determine the mass-induced fuel savings, where, E_{FP}, ρ_F and F_{CP} were 43.5 MJ/kg, 0.74 kg/L and 0.16 L/(100km, 100kg) respectively. R_{WTW} can vary depending on geography therefore a maximum (1.47 MJ/MJ), minimum (1.05 MJ/MJ) and average (1.36 MJ/MJ) value was applied to the relative boundary combination using the values obtained from Sweden, Europe, and other international sources [321], respectively.

EOL allocation for CFRP followed the recycled content approach and assumes that the fibre weight fraction (0.67) are reclaimed by pyrolysis and the epoxy weight fraction (0.33) is unreclaimed. As the rCF is downcycled into other product streams no recycling credits are applied in the CFRP PMB. The maximum EOL burden is used in combination with the maximum PMB for the envelope, however in reality the EOL burden magnitude is independent from that chosen for PMB. The plot highlights the large range of possibilities for lifetime energy demand of a vehicle based on the significant variation in literature values.

The maximum and average PMB do not breakeven within any lifetime distance. The minimum PMB results in a breakeven distance within the US EPA and CSA vehicle lifetime distances providing net energy savings after 180,000 km. Net fuel savings are also ensured after application of the minimum EOL burden which does not intercept again.

Both scenarios are likely widely misrepresentative of a real CFRP lifetime energy summation. The central dashed line represents the average burden determined using the literature range and may be considered a more accurate depiction of the burdens observed in a real CFRP part. The use phase savings are almost enough to breakeven on the PMB and, when combined with the EOL burden, a second use phase is required to breakeven. No matter the data source or LCI employed the energy demand of CFRP production and manufacture is significant (165-595 MJ/kg). The use phase offers the greatest potential for CFRP emissions savings therefore providing multiple use phases will enable enhanced reductions that could breakeven or possibly provide net environmental savings gains over vCFRP.

It is increasingly apparent that the best-case scenario for rCFRP is that it can be remanufactured into high-value applications to provide additional use phase savings. The tandem breakeven plot in Fig. 6.3 illustrates how an additional use phase can provide net energy savings in the life cycle of a CFRP material.

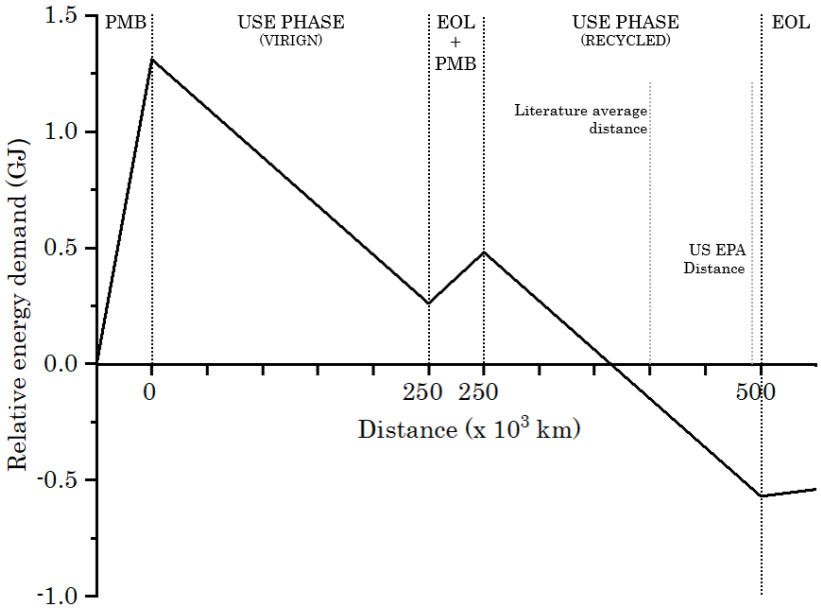

Fig. 6.3. Tandem breakeven plot showing the lifecycle energy demand of a CFRP material with two use phases i.e. virgin and recycled. Use phase fuel savings are compared against a steel baseline.

The plot is based upon the same functional unit and use phase calculations as Fig. 6.2, however only the average PMB values are used. The CFRP part has two use phases, virgin and recycled, after the second use phase the component is disposed of *via* landfill. The initial PMB CED includes primary production and manufacture with a deduction for the steel PMB. The EOL burden applied is the same used in Fig. 6.2. The second PMB CED does not include a CF contribution, following the Closed-Loop allocation approach; only the CED for the weight fraction of epoxy and the part manufacturing CED is applied.

The PMB is not offset within any of the lifetime driving distances in the first use phase. The part breakeven distance is within the second use phase, at 115,000 km even after paying for the pyrolysis of the fibres, landfill of the epoxy, steel production and CFRP remanufacture.

The tandem plot is a useful method for displaying the potential benefit of CFRP closed-loop recycling from an LCA perspective. Despite the use of averaged PMB, EOL, lifetime distances and other constants the conclusions drawn from

the plot are valid for a realistic component. However, the suggested benefits are only attainable with the application of a recycling process that can reclaim and remanufacture the virgin constituents into a recycled component of equivalent performance.

The closed-loop recyclable materials developed in Chapters 4 and 5 should have a lower CED than the material production CED of the constituents and should therefore have a favourable impact when compared with alternative lightweighting materials. The benefits of the second use phase can be realised as the closed-loop recycling process can maintain enough mechanical performance for reuse in the same application as the virgin material. The actual CED of the closed-loop recycling process, and the cumulative environmental savings accrued through use of the closed-loop recycling materials are determined in the following section.

6.3 Life cycle assessment of the closed-loop recycling process

6.3.1 Goal and scope definition

The aim of this LCA assessment is to evaluate the life cycle environmental impacts and costs of the closed-loop recycling process and the closed-loop recyclable material produced. The structure was analogous to comparative lightweighting materials LCAs and followed the standards ISO 14040:2006 and 14044:2006 [247,248].

The closed-loop recyclable materials evaluated in Chapters 4 and 5, *i.e.* CFPP and CFPA6 will be assessed, however, they will be normalised to a 50 % Vf_F and a quasi-isotropic lay-up to aid in comparison with conventional materials. This was achieved by rule of mixtures and halving the tensile stiffness and strength properties. Although this Vf_F is greater than that achieved experimentally in this thesis, it has been achieved by the HiPerDiF in previous studies and may therefore be attainable through optimisation [178].

The full life cycle of the closed-loop recyclable materials is presented in Fig. 6.4, where activities start at material production and progress through component manufacture, the use phase, *i.e.* automotive lifetime, and, end of life processing. For the closed-loop materials the manufacturing and EOL processing were as defined by the relative closed-loop recycling processes from Chapters 4 and 5.

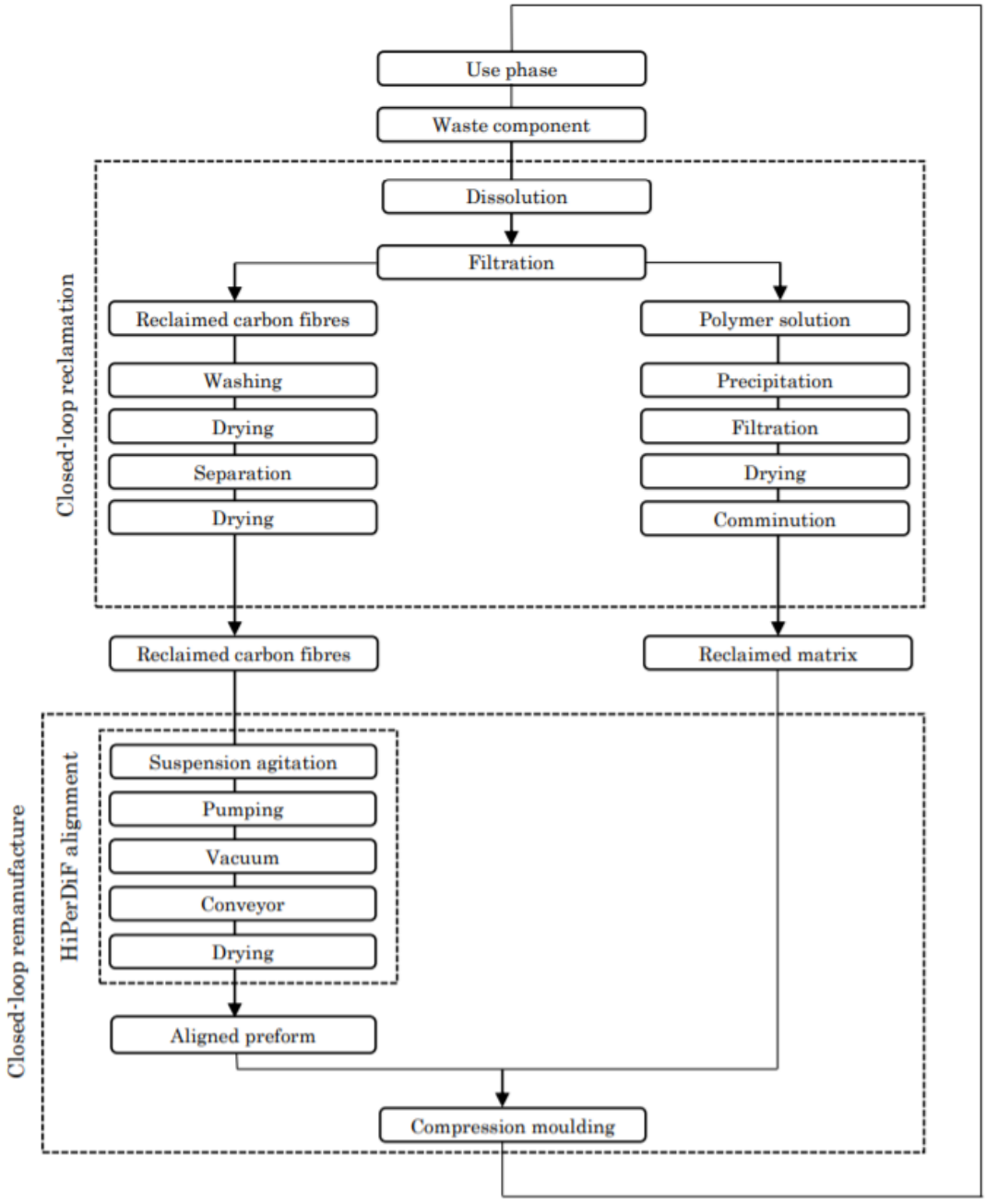

Fig. 6.4. Life cycle inventory of processes involved in the closed-loop recycling process for rCFPP and rCFPA6. vCFPP and vCFPA6 follow similar pathways except using virgin constituents.

Table 6.4. Properties of the materials used in this life cycle assessment.

Material	Matrix	Manufacture	Density	Stiffness*	Strength*
Vf_F (%)			g/cm^3	GPa	MPa
rCFPP (QI aligned rDCF 50 %)[(b)]	PP	CLR	1.27*	35*	330*
rCFPA6-FA (QI aligned rDCF 50 %)[(b)]	PA6	CLR	1.30*	41.7*	378*
rCFPA6-BA (QI aligned rDCF 50 %)[(b)]	PA6	CLR	1.30*	37.5*	353*
vCFRP [60] (woven vCF prepreg 50 %)[(c)]	Epoxy	Autoclave	1.59*	59.7*	803*
rCFRP [60] (woven rCF 50 %)[(d)]	Epoxy	Comp. mould.	1.48	55.9	634
vGFRP (woven QI 60 %)	Epoxy	RTM	1.61	21	260
Aluminium (Al 2014)		Casting	2.80	75.0	270
Steel (AISI 1010)		Casting	7.85	210	244

[(a)] 3 mm fibre length. [(b)] 1 – 3 mm fibre distribution. [(c)] continuous fibre. [(d)] continuous fibres reclaimed from pyrolysis. CLR = closed-loop remanufacture. DCF = discontinuous carbon fibre. Comp. mould. = compression moulding. QI = Quasi-isotropic. RTM = Resin transfer moulding. * indicates normalised values.

The structural index λ, representative of the thickness-dependent non-linearities in the stress distribution of thin-walled structures, can be anywhere between 1 and 3, however, most automotive components are between 1 and 2, therefore an average value of 1.5 was selected [320].

6.3.2 Life cycle inventory

6.3.2.1 Material

The closed-loop recyclable materials were compared with alternative automotive lightweighting materials, such as aluminium, vGFRP, vCFRP, and conventional automotive materials, *i.e.* steel. Materials were selected based on their potential to be replaced by the closed-loop materials, *i.e.* their properties

permit use in semi-structural automotive applications; details of the selected materials are presented in Table 6.4.

vCFRP was represented by two separate material options, one with a pyrolysis recycling credit, rCFRP, and one with conventional landfilling as the waste treatment method, vCFRP. The rCFRP represented the highest performance rCFRP material available, as discerned from Chapter 2, and therefore provides useful comparison for the closed-loop recyclable material. It should be noted that the remanufacturing method relies on the reclamation of a fully intact woven architecture after pyrolysis. Although this is possible, and will naturally provide superior properties to nonwoven mats, it is unlikely to be a product of commercial pyrolysis. This would rely on large sections of unused waste prepreg/dry fibre offcuts which will undoubtedly be inferior in volume to the rCFRP demand.

vGFRP represents the highest mechanical performance achievable for GF epoxy material. As the properties afforded by GF are inferior to the other materials it was important to reduce the disparity for fair analysis. It should be noted that QI vGFRP will not likely be used in semi-structural automotive applications, due to the inferior mechanical performance, however, the closed-loop materials may be used to replace vGFRP in less demanding applications and therefore the comparison is still prudent.

PMB data used in the study were averaged from literature values; these are displayed in Table 6.1, Table 6.2, and Table 6.3. Steel and aluminium production included a reduction factor of 0.16 and 0.72, respectively, following the Closed-Loop EOL allocation approach, assuming virgin steel and aluminium had a 84 % and 28 % recycled content, respectively [285,299,300]. rCFPP and both rCFPA6 materials are entirely reclaimed therefore the applied reduction factor was 0; The CED of closed-loop remanufacture was determined and applied, see Section 6.3.2.2. rCFRP was composed of pyrolysed CF, therefore the CF burden was not included in the PMB.

6.3.2.2 Manufacture

The CED values used for the closed-loop reclamation and remanufacturing processes were calculated using a Watt meter. Kilowatt hours were then converted into CED by using the British Energy Mix data set in the SimaPro LCA software [322] and the Ecoinvent database [250]. The measured values and the calculated CED are presented in Table 6.5.

The literature vGFRP, vCFRP and rCFRP were manufactured by resin transfer moulding, autoclave curing of prepregs and compression moulding of woven fibre and epoxy resin films, respectively. These techniques represent a large proportion of common industrial manufacturing processes. The CED values were obtained from the literature [60]. The metals were manufactured by stamping, the CED for this was obtained from the literature [80,285].

Table 6.5. Measured power requirements of the closed loop remanufacturing process and the relative cumulative energy demand.

		CED
Process		MJ/kg
Fibre alignment	Suspension agitation	5.52×10^{-2}
	Pumping	7.88
	Vacuum	2.17
	Conveyor	5.9×10^{-3}
	Heater	0.49
Compression moulding		15.9
	Total	26.5
Greenhouse gas emissions	kg CO_2 eq/ kg	5.83

6.3.2.3 Use

The use phase was determined following the same process outlined in Section 6.2.4. The average lifetime driving distance of a mass-manufactured passenger vehicle. The CSA lifetime driving distance of 250,000 km was selected.

Equations 6.1 and 6.2 were used to determine the mass-induced fuel savings, where, E_{FP}, ρ_F and F_{CP} were 43.5 MJ/kg, 0.74 kg/L and 0.16 L/(100km, 100kg) respectively. R_{WTW} can vary depending on geography therefore an average (1.36 MJ/MJ) value was applied as sourced from the literature [321].

Table 6.6. Lifetime mass-induced fuel savings accrued from the automotive use phase.

Material	Weight saving	Lifetime fuel demand	Lifetime mass-induced fuel savings
Vf_F (%)	%	MJ	L
rCFPP (QI aligned rDCF 50 %)[(b)]	46.6	90.9	1.87
rCFPA6-FA (QI aligned rDCF 50 %)[(b)]	51.2	72.9	2.30
rCFPA6-BA (QI aligned rDCF 50 %)[(b)]	47.6	72.9	2.30
vCFRP [60] (woven vCF prepreg 50 %)[(c)]	53.2	79.7	2.14
rCFRP [60] (woven rCF 50 %)[(d)]	54.4	77.6	2.19
vGFRP (woven QI 60 %)	5.00	161	0.20
Aluminium (Al 2014)	29.1	120	1.20
Steel (AISI 1010)		170	

[(a)] 3 mm fibre length. [(b)] 1 – 3 mm fibre distribution. [(c)] continuous fibre. [(d)] continuous fibres reclaimed from pyrolysis. CLR = closed-loop remanufacture. DCF = discontinuous carbon fibre. Comp. mould. = compression moulding. QI = Quasi-isotropic. RTM = Resin transfer moulding.

6.3.2.4 End of life (EOL)

EOL allocation for the metals follows the Closed-Loop allocation method with applied reduction factors sourced from the literature; the CED of the recycling process is applied. vCFRP was assumed to be landfilled and therefore pays the relative energy burden, whereas rCFRP followed the recycled content approach and assumed that the fibre weight fraction (0.67) are reclaimed by pyrolysis; the CED of pyrolysis is applied. It should be noted that the energy demand of distillation is not included as although the closed-loop reclamation of

solvents is an additional benefit it is not paramount for the reprocessing of the recyclate.

Table 6.7. Measured power requirements of the closed loop reclamation process and the relative cumulative energy demand.

		CFPP	CFPA6-FA	CFPA6-BA
		CED	CED	CED
Process		MJ/kg	MJ/kg	MJ/kg
Constituent reclamation	Dissolution heating	27.0	-	11.7
	Vacuum filtration	0.12	0.12	0.12
	Drying	26.1	26.1	26.1
	Wet separation	8.69	8.69	8.69
	Comminution	0.04	0.04	0.04
	Total	62.0	34.9	46.7
Greenhouse gas emissions	kg CO_2 eq/ kg	4.24	2.39	3.19

The closed-loop materials are reclaimed using the closed-loop recycling process, therefore the CED for reclamation was determined, in the same manner as remanufacture, and the measured CED was applied. The measured values and the calculated CED are presented in Table 6.7. The reclamation process is at the lab scale and therefore not benefiting from the economies of scale contributing to aluminium and steel recycling. [285,299,300].

6.3.3 Results and discussion

The LCA results are reported using two metrics for environmental impact: CED and GHG emissions. The lifetime CED and GHG emissions plots, for the functional unit made using the suite of materials, are presented in Fig. 6.5. They display the lifetime CED and GHG split into the four main lifetime categories: material production, manufacture, use phase, and end of life.

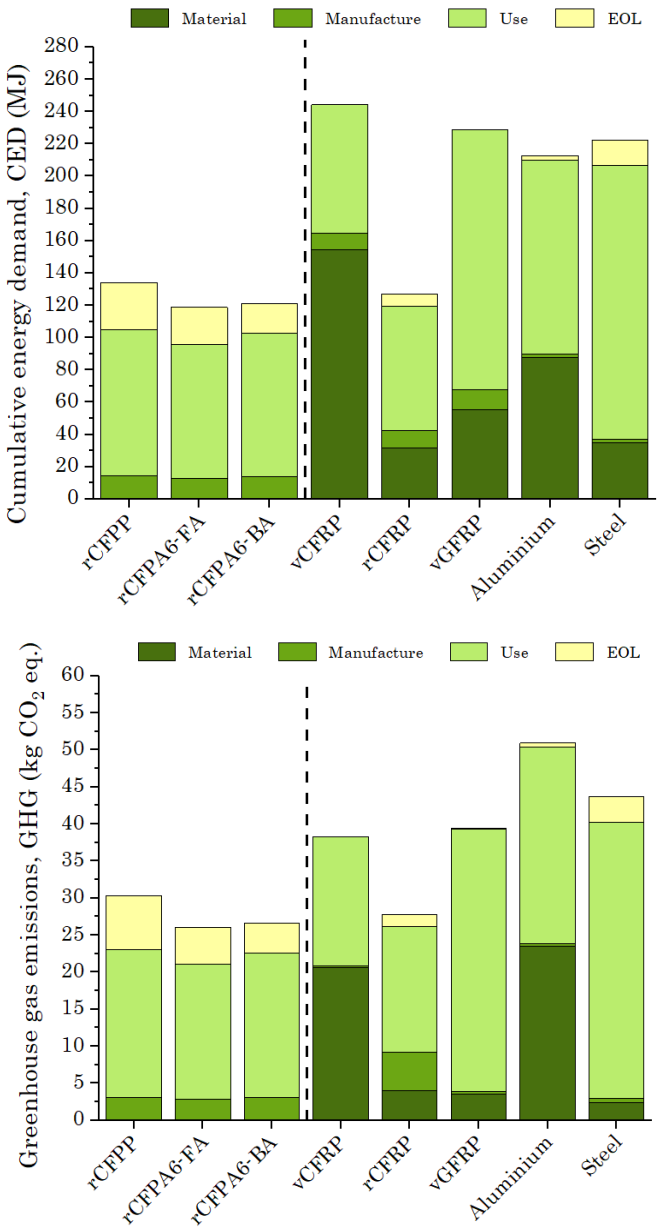

Fig. 6.5. *Top* - The lifetime cumulative energy demand values of the various material solutions. *bottom* – The lifetime greenhouse gas emissions of the various material solutions. Dashed line separates the materials of this study.

The largest CED values were achieved by vCFRP (244 MJ) and vGFRP (229 MJ). For vCFRP this is due to the substantial energy required to produce the CF and epoxy constituents, despite providing a 53 % saving on use phase energy demand over steel. The inferior mechanical performance of vGFRP means that a

greater thickness is required to meet the same performance requirements. This results in only a 5 % weight saving over steel, which significantly affected the use phase savings and is the primary reason for the high CED value. Steel had the third largest CED (222 MJ) followed closely by aluminium (213 MJ). For aluminium, versus steel, the 30 % energy saving during the use phase was offset by the 150 % greater energy required for material production.

The four recycled composite materials: rCFPP (134 MJ), rCFRP (127 MJ), rCFPA6-BA (121 MJ), and, rCFRPA6-FA (129 MJ) had the lowest life cycle CED values. Despite incurring no energy contribution from material production, rCFPP had a slightly higher energy demand than rCFRP. This is due to the greater energy demand of the closed-loop reclamation compared with pyrolysis. This is to be expected for a novel process as the equipment used has not been optimised for scale. It is therefore somewhat impractical to compare with a process that has been optimised as such, *i.e.* pyrolysis. Nevertheless, the energy savings from other stages of the life cycle are favourable and thus the comparison has utility. The rCFs used to remanufacture the rCFRP were woven mats reclaimed from the pyrolysis of unused prepregs. The high mechanical performance of the rCFRP is a direct consequence of this, which ultimately results in the largest weight saving and thus the largest use phase fuel savings (54 %). It should be noted that this is an isolated case used for comparative purposes and does not reflect the possibilities of a commercial scale rCFRP recycling process. As the woven rCF has a highly aligned architecture, the mechanical performance would be far greater than that achieved through commercial reclamation and remanufacturing processes and thus these use phase savings are not currently achievable at any substantial volumes.

The metals have the highest GHG emissions, followed by vGFRP and vCFRP. This is primarily a consequence of material production emissions. The closed-loop recycled materials have a substantially reduced emissions profile compared with the virgin composites. This is due to the lack of material contribution as the constituents are fully reclaimed and therefore production has zero material contribution. The impact of the matrix reclamation was marked,

observable in the material production contribution to rCFRP which only includes the matrix.

From both plots, the environmental impact profiles of the closed-loop recycled materials are noticeably favourable to commercially available lightweighting materials and steel. rCFPP offers a slightly superior mass-induced fuel saving to rCFPA6 due to a lower density and similar mechanical performance; vCFPA6 provides the best mass-induced fuel saving of the closed-loop materials due to the superior mechanical performance. The advantage of reclaiming the matrix in addition to the fibres; for rCFPP and rCFPA6 a decrease of 19.4 MJ and 0.65 kg CO_2 eq, and, 44 MJ and 2.9 kg CO_2 eq was achieved for the CED and GHG, respectively.

The benefits from the combination of low PMB and high lifetime mass-induced fuel savings over two use phases are best represented in a breakeven tandem plot, Fig. 6.6.

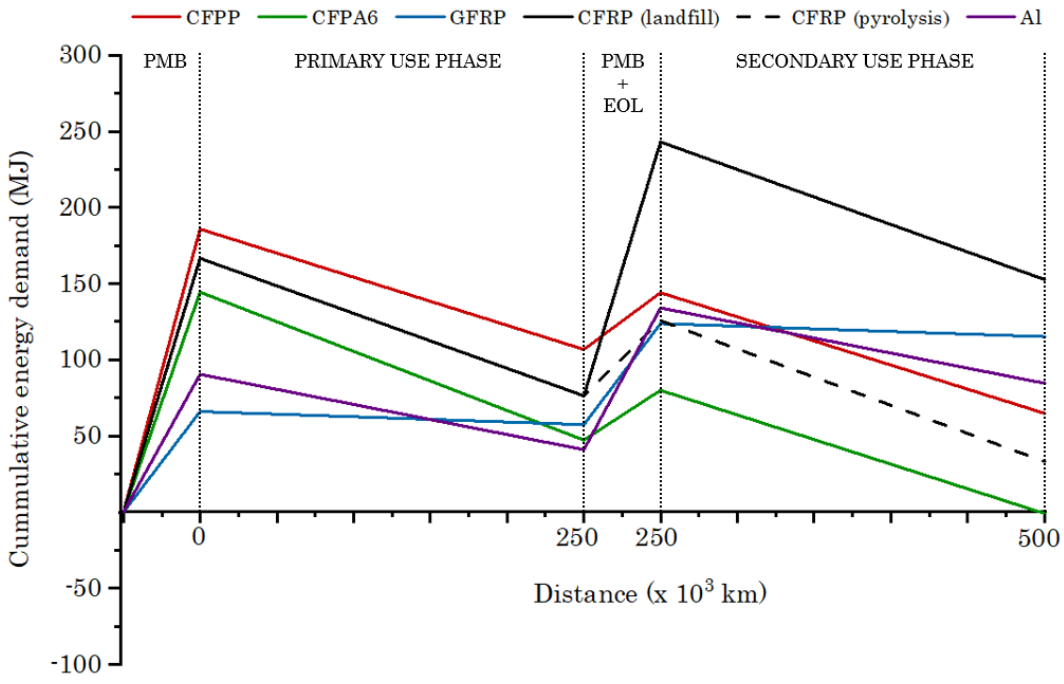

Fig. 6.6. A breakeven tandem plot showing the total CED for the range of materials over two vehicle lifetimes.

The plot compares the CFPP and CFPA6 (BA) materials produced in this body of work with; GFRP, CFRP, and Al. CFPA6 BA was selected as the CFP6 comparison material as it had the inferior environmental performance of the two and therefore provides a more conservative evaluation. The CFRP component is represented by two outcomes determined by EOL processing after the primary use phase, landfill or reclamation by pyrolysis, before which the component impacts are identical. GFRP is landfilled after the primary use phase therefore the GFRP component used in the secondary use phase is virgin. This is due to the inferior mechanical performance of rGFRP and thus unsuitability for the application. The Al PMB for the secondary use phase is a combination of the material production, manufacture and EOL burdens. Al is recycled after the primary use phase, the production CED has the same recycled content used previously (see Section 6.2.3.4) and the EOL burden includes a CED for the recycling process. The CFPP and CFPA6 materials are initially virgin and include standard PMB associated with virgin production. The secondary use phase PMB is a combination of remanufacturing and reclamation burdens. As they are completely closed-loop, the material production is not included.

The plot shows that the use of virgin materials makes it difficult to provide net environmental gains, over two use phases, for lightweighting materials, despite the fuel savings accrued during both use phases. For CFRP, this is primarily due to the CED of material production and manufacture however, for GFRP and Al this is also due to comparatively low mass-induced fuel savings. For Al, GFRP and landfilled CFRP the combination of either a substantial PMB or a minimal mass-induced fuel saving results in a tandem plot that increases proportionally with the number of use phases and will therefore never breakeven.

All the reclaimed composite materials have the potential of breaking even however, for reclaimed CFRP and CFPP, this is only in the third use phase. For CFRP, a third use phase is reliant on the retention of mechanical performance after a second pyrolysis treatment. However, conclusive data on the possibility of this is lacking. It may be possible for a third CFPP use phase as the closed-loop experimentation in Chapter 4 does not suggest a decrease in properties after additional recycling loops. The initial PMB of CFPP is the highest out of all the

lightweighting materials. This is due to PP having the lowest matrix density, which means it has the highest mass fraction of CF for equivalent Vf_F. The higher density of PA6 results in a lower PMB than CFPP and enables break even at the very end of the secondary use phase. CFPA6 is the only lightweighting material that breaks even within the two vehicle lifetimes, although this is marginal.

6.3.4 Conclusions

A life cycle assessment of the novel closed-loop recycling process was carried out in this Chapter. The virgin and recycled materials made using this process were compared with alternative lightweighting materials and conventional steel. The metrics used were cumulative energy demand and greenhouse gas emissions.

LCA evaluation of the closed-loop recycling process showed that reclamation of composites reduces the environmental impact through reducing energy demand and greenhouse gas emissions. It was also apparent that reclaiming both fibre and matrix, *i.e.* through closed-loop recycling, provides marked additional reductions in impact to alternative recycled materials. The superior environmental performance compared with alternative lightweight materials may prove to be a deciding factor for the adoption of composite materials in weight-sensitive mass-manufactured applications. This study reinforces the importance of LCA evaluation for CFRP and how the results can help inform positive change in materials selection.

7 Conclusions

The concluding remarks will be presented in this Chapter, split into three sections; An overall discussion of how the results of the experimental chapters are relevant to the industrial context explored in Chapter 2 is detailed in Section 7.1, The overall conclusions drawn from the thesis are presented in Section 7.2, and the considerations for future development of the research are described in 7.3.

7.1 Overall discussion

The literature review in Chapter 2 indicated several issues faced by the composites industry with regards to CFRP adoption into emerging markets that rely on mass-manufacturing, *i.e.* the automotive industry. The automotive industry faces stringent fuel economy standards which can be met using composite materials, but there exist several obstacles to the adoption. CFRP are currently too expensive to incorporate into vehicles on a mass-manufacturing scale. They are also unrecyclable which goes against vehicle and material recyclability legislation driven by increased social awareness and government action. A lack of adherence to these standards will result in heavy penalties, both as financial penalties and growing landfilling costs.

Solutions to these drawbacks have been approached over the last decade with the emergence and development of composite recycling technologies. Some processes are currently operating at the industrial scale however the supply of

recycled fibres and the future demand of recycled composites remain disparate. This is a direct consequence of the limited market opportunities for recycled composites due to the low mechanical performance achieved through current methods.

Performance reductions observed in recycled composites are due to the reclaimed fibre property reductions observed with pyrolytic and solvolytic methods, and, primarily, due to their low bulk-density. Current methods rely on the complete degradation of the matrix material for the reclamation of fibres, a consequence of the thermosetting material properties. The potential for high-performance rCFRP is achievable with the development of alignment technologies, which can provide composite performance to match virgin, however these are currently in the early stages of development and industrial feasibility is still unevaluated.

Overall, it was deemed that the main drawbacks for composite adoption are the high costs and environmental impacts of virgin material, and, the low mechanical performance of rCFRP. The aim of this work was therefore to develop a closed-loop recyclable material, and the relative closed-loop recycling process, that can retain mechanical performance after two recycling loops. The objective being that the mechanical performance retention will be enough that the rCFRP is capable of functioning in a high-value application after recycling and will therefore be of high-value. The material produced may then have the potential for use in mass-manufacture applications due to sufficient mechanical performance, low environmental impact and low cost as a result of constituent reuse.

From these insights, a closed-loop recycling process was developed in Chapter 3, which aimed to resolve these issues. The key principles of the process, reclamation and remanufacture, relied upon fibre alignment and full fibre-matrix separation, which, in turn, required the use of discontinuous carbon fibres and thermoplastic matrix. Unless a thermoplastic matrix is used, full separation of fibre and matrix is difficult to achieve without experiencing matrix degradation. The closed-loop recycling process was developed with an experimental evaluation method to analyse its performance.

Chapter 4 detailed the proof-of-concept evaluation of the closed-loop process. It was determined that a discontinuous carbon fibre thermoplastic composite could be recycled over two recycling loops without substantial deterioration of mechanical performance. To the best of the author's knowledge, the properties of the recycled composite were the highest reported for a recycled discontinuous thermoplastic composite.

The closed-loop process was developed, in Chapter 5, to incorporate a matrix of higher mechanical performance, *i.e.* polyamide 6, to assess if a high-performance composite could be recycled without substantial loss of value. It was found that the process can be used to make thermoplastic composites of high-mechanical performance. To the best of the author's knowledge, the virgin composite produced had the highest reported mechanical performance for a discontinuous thermoplastic material. There was a decrease in properties after the first recycling loop, however the properties remained higher than, to the authors best knowledge, any recycled discontinuous carbon fibre composite produced. The properties were analogous to materials currently used in semi-structural automotive applications.

Chapters 4 and 5 concluded that a closed-loop recycling process can produce a recycled composite material of high-value after two recycling loops. The mechanical performance of the CFPP materials was driven by the fibre-matrix adhesion as the virgin adhesion was initially poor. The mechanical performance of the CFPA6 materials was driven primarily by the fibre alignment and preform homogeneity. Prevalence of fibre agglomerations resulted in performance reductions irrespective of recycling solvent or recycling loop, indicating that this effect was due to reclaimed fibre processing and therefore may potentially be eradicated through process optimisation. Overall, the results of the experimental chapters met the primary aim of developing a recyclable composite of high enough mechanical performance for high-value applications.

Chapter 6 determined the environmental impact of the closed-loop recycling process and the closed-loop material over two life cycles. The two metrics for this evaluation were the total cumulative energy demand and the greenhouse gas emissions. The study showed that both closed-loop materials provided the lowest

cumulative energy demand and greenhouse gas emissions compared with alternative lightweighting materials, the highest mechanical performance recycled composite material reported, and conventional steel. This proved that in addition to being of suitable mechanical performance, the closed-loop material was also of superior environmental impacts.

The most comprehensive assessment framework for composites material selection is LCE, which is a combination of LCA, LCC, and component mechanical performance. The component mechanical performance assessment requires a detailed finite element analysis and is beyond the scope of this work. To determine the cost of the closed-loop material there exist several activities available, each with a varying level of comprehension and labour intensity assigned. LCC thoroughly evaluates the total cost of manufacture for a component at a range of production capacities. This is the most detailed determination of costing available, however, it requires complex analysis with the incorporation of multiple variables and is beyond the scope of the current study. The most appropriate method, given the scope of the current research, was the application of relevant data from the literature to provide reasonable predictions for material cost. The literature suggests that recycled carbon fibre is commercially available at a substantially lower cost than virgin. This is due to lower recycling process costs in comparison with virgin fibre production. It is reasonable to assume that the same reduction can be applied to reuse of the matrix, and, that the overall recycled composite can be supplied at a significantly reduced cost compared with virgin. There are very few cost analyses for rCFRP material in the literature, however, a comprehensive LCC conducted by Meng *et al.* showed that an aligned rCFRP component can provide cost savings over alternative lightweighting materials over a vehicle lifetime; more than 35 % providing technology development targets are met [282]. The closed-loop recycling process is currently at the lab scale; however, it is on a similar scale to the aforementioned study therefore a positive correlation in cost reduction is reasonable to assume.

Overall, the mechanical performance evaluation from the experimental chapters confirms that the closed-loop process can produce high-value composite

material over two recycling loops. The LCA evaluation proves that the closed-loop materials have a desirably low environmental impact compared to alternative materials. From consideration of literature insight into the low cost of rCF and rCFRP it can be assumed that the closed-loop materials may also perform favourably in terms of cost.

7.2 Overall conclusions

The main aims of the thesis were to develop a novel, closed-loop recycling process for CFRP that can produce material of value after each recycling loop, primarily *via* the retention of mechanical performance. The conclusions drawn throughout this work are presented in the proceeding text.

The emerging markets require CFRP recycling processes to limit the environmental burden of composites and reduce component costs whilst providing appropriate mechanical performance for an economically sustainable rCF market. Current recycling processes rely on the complete degradation of the matrix to retrieve fibres, due to the use of thermosetting matrices, reducing potential cost and environmental savings. They are also unable to achieve high-performance from the reclaimed fibres. Recycling processes therefore need to provide high-quality recyclate so that it can be re-used as feedstock for a new production loop, *i.e.* closed-loop recycling. A closed-loop recycling process for high-performance CFRP can only be achieved through using fibre alignment and full matrix-fibre separation which, in turn, is facilitated only by discontinuous carbon fibres and thermoplastic matrices.

A closed-loop recycling process has been developed which can recycle discontinuous carbon fibre thermoplastics composites. It can be defined as closed-loop as all materials, solvents and constituents, are reclaimed above 85 % yield. Performances achieved were the highest reported for virgin and recycled discontinuous carbon fibre thermoplastic composites. The environmental performance of closed-loop recyclable materials is superior to that of alternative lightweighting materials, alternative rCFRP and conventional steel. With the consideration of literature insights into low rCF and rCFRP cost, it is reasonable

to assume that the high-value closed loop materials are a high-performance, low-cost and environmentally superior alternative to current lightweighting materials.

7.3 Future work

A novel closed-loop recycling process was developed which produced material with competitive mechanical performance, cost reductions and a superior environmental impact compared with alternative materials. Despite this, there are several areas for development which became apparent during the thesis; these are presented in the subsequent text.

Additive loss analysis was suggested in both experimental chapters. The effects of this varied depending on polymer type and solvent system. A detailed analysis of how additives are removed during reclamation is a complex undertaking and beyond the scope of this work. However, understanding it may provide opportunities to optimise properties and is therefore advantageous. Any additives removed can potentially be retrieved from the supernatant and added back to the precipitate. This can be provided by a suite of qualitative and quantitative chemical analysis, i.e. ^{1}H NMR, ^{13}C NMR etc., along with data from the matrix manufacturer would be useful.

Volume fraction optimisation would increase the mechanical performance of the CLRM. This can be achieved through optimising remanufacture; increasing alignment or increasing fibre wet-out during consolidation, i.e. through increasing temperature, pressure, precipitate application and reducing precipitate grain size. Anything that can improve the fibre packing or reduce the time it takes for the polymer to reach the fibre.

Scaling-up production volume is required to increase the technology readiness level of the technology and close the gap between the research and industry. This will help validate its applicability to industry and may also provide more accurate environmental impact and life cycle costing data. The closed-loop

process was designed with scalability in mind, i.e. to scale without dramatic changes in process.

Demonstrator production is a logical next step for process development. Specimen dimensions were limited to tensile test production. If carried out using scaled production an industrially applicable component could be manufactured. Closed-loop material will be produced in a format analogous to industrial manufacturing feedstock and manufactured into a simple part. Performance and cost analysis of this component could form the basis of the LCE evaluation.

Comprehensive LCE analysis of the process will provide a more accurate evaluation of the closed-loop process/material, improving any comparative assessments. This requires detailed component mechanical performance and LCC assessment. If carried out on the scaled process it would avoid any of the inaccuracies associated with the evaluation of lab scale processes. It would be pertinent to compare the multiple use phase performance of this material in a conventional combustion powered vehicle with that of an electric vehicle.

8 Bibliography

(1) Carvalho, A.; Silva, T.; Loja, M.; Carvalho, A.; Silva, T. A. N.; Loja, M. A. R. Assessing Static and Dynamic Response Variability Due to Parametric Uncertainty on Fibre-Reinforced Composites. *J. Compos. Sci.* **2018**, *2* (1), 6. https://doi.org/10.3390/jcs2010006.

(2) Mallick, P. K. *Fiber-Reinforced Composites: Materials, Manufacturing, and Design*, 3rd ed.; Taylor & Francis Group, L.L.C: London, 2008.

(3) Drown, E. K.; Moussawi, H. Al; Drzal, L. T. Glass Fiber "sizings" and Their Role in Fiber-Matrix Adhesion. **2012**. https://doi.org/10.1163/156856191X00260.

(4) Dušek, K.; Apicella, A. *Epoxy Resins and Composites I*, 1st ed.; Springer Berlin Heidelberg: Berlin, Heidelberg, 1985.

(5) Pimenta, S.; Pinho, S. T. Recycling Carbon Fibre Reinforced Polymers for Structural Applications: Technology Review and Market Outlook. *Waste Manag.* **2011**, *31* (2), 378–392. https://doi.org/10.1016/j.wasman.2010.09.019.

(6) Acmite. *Global Carbon Fiber Composite Market Report*; Acmite Market Intelligence, 2016.

(7) Azapagic, A.; Emsley, A.; Hamerton, I. Polymers in Everyday Use: Principles, Properties and Environment. In *Polymers: The Environment and Sustainable Development*; Wiley, 2003.

(8) Billingham, N. Fundamentals of Degradation and Stabilisation of Polymers. In *Handbook of Plastics Recycling*; La Mantia, F., Ed.; Rapra,

2002; pp 23–64.

(9) Ege, S. N. *Organic Chemistry: Structure and Reactivity*, 5th ed.; Houghton Mifflin Harcourt: Independence, Kentucky, 2003.

(10) Ishikawa, T.; Amaoka, K.; Masubuchi, Y.; Yamamoto, T.; Yamanaka, A.; Arai, M.; Takahashi, J. Overview of Automotive Structural Composites Technology Developments in Japan. *Compos. Sci. Technol.* **2018**, *155*, 221–246. https://doi.org/10.1016/j.compscitech.2017.09.015.

(11) Yousefpour, A.; Immarigeon, J.-P. Fusion Bonding/Welding of Thermoplastic Composites. *J. Thermoplast. Compos. Mater.* **2004**, *17* (July), 303–342. https://doi.org/10.1177/0892705704045187.

(12) Witten, E.; Thomas, M.; Michael, K. *Composites Market Report 2017*; 2017.

(13) The promise of composites in automotive https://www.compositesworld.com/articles/the-promise-of-composites-in-automotive (accessed Aug 29, 2018).

(14) Mazumdar, S. Opportunity and Challenges in Automotive Composites Industry. Lucintel 2013, p 23.

(15) Das, S. *The Cost of Automotive Polymer Composites: A Review and Assessment of DOE's Lightweight Materials Composite Research*; 2001.

(16) Red, C. Automotive CFRP: The Shape of Things to Come. *Composites World*. 2013.

(17) Visser, C. M. To Adopt or Not to Adopt: The Case of Advanced Thermoplastic Composites in the Automotive Industry, University of Twente, 2017.

(18) Job, S.; Leeke, G.; Mativenga, P. T.; Oliveux, G.; Pickering, S.; Shuaib, N. A. *Composites Recycling: Where Are We Now?*; 2016.

(19) UK Department for Business Innovation and Skills. The UK Composites Strategy. *Innovation* **2009**, 1–36.

(20) Composites Leadership Forum. *The 2016 UK Composites Strategy*; 2016.

(21) Ellen MacArthur Foundation. Circular Economy https://www.ellenmacarthurfoundation.org/circular-economy (accessed Apr 24, 2018).

(22) Webster, K. Introduction. In *The Circular Economy: A Wealth of Flows*; Ellen MacArthur Foundation Publishing, 2015; pp 6–26.

(23) Panesar, S. Converting Composite Waste into High Quality Reusable Carbon Fibre. In *JEC Composties*; Paris, France, 2009.

(24) Shuaib, N. A.; Mativenga, P. T.; Kazie, J.; Job, S. Resource Efficiency and Composite Waste in UK Supply Chain. *Procedia CIRP* **2015**, *29*, 662–667. https://doi.org/10.1016/j.procir.2015.02.042.

(25) Job, S. Composite Recycling: Summary of Recent Research and Development. Kowledge Transfer Network 2010.

(26) Halliwell, S. End of Life Options for Composite Waste Recycle , Reuse or Dispose ? National Composites Network Best Practice Guide. *Natl. Compos. Netw.* **2006**, 1–41.

(27) Composites UK. End-of-Life Solutions for FRP Composites. 2015.

(28) HM Revenue & Customs. Excise Notice LFT1: A general guide to Landfill Tax - GOV.UK https://www.gov.uk/government/publications/excise-notice-lft1-a-general-guide-to-landfill-tax/excise-notice-lft1-a-general-guide-to-landfill-tax (accessed May 25, 2018).

(29) Witik, R. A.; Teuscher, R.; Michaud, V.; Ludwig, C.; Månson, J.-A. E. Carbon Fibre Reinforced Composite Waste: An Environmental Assessment of Recycling, Energy Recovery and Landfilling. *Compos. Part A Appl. Sci. Manuf.* **2013**, *49*, 89–99. https://doi.org/10.1016/j.compositesa.2013.02.009.

(30) Deng, Y.; Duflou Karel Van Acker, J.; Dewulf Bart Muys Ignace Verpoest Martin Kumar Patel, W. Life Cycle Assessment of Biobased Fibre-Reinforced Polymer Composites, 2014.

(31) Jones, C. I.; Hammond, G. P.; Jones, C. I. Embodied Energy and Carbon in Construction Materials. *Proc. Inst. Civ. Eng.* **2008**, *Energy 161* (EN2), 87–98. https://doi.org/10.1680/ener.2008.161.2.87.

(32) Oliveux, G.; Dandy, L. O.; Leeke, G. a. Current Status of Recycling of Fibre Reinforced Polymers: Review of Technologies, Reuse and Resulting Properties. *Prog. Mater. Sci.* **2015**, *72*, 61–99. https://doi.org/10.1016/j.pmatsci.2015.01.004.

(33) La Mantia, F.; Gaztelumendi, M.; Eguiazabal, J.; Nazabal, J. Properties - Reprocessing Behaviour of Recycled Plastics. In *Handbook of Plastics Recycling*; Rapra, 2002; pp 127–194.

(34) Pickering, S. J. Recycling Technologies for Thermoset Composite Materials—current Status. *Compos. Part A Appl. Sci. Manuf.* **2006**, *37* (8), 1206–1215. https://doi.org/10.1016/j.compositesa.2005.05.030.

(35) Morin, C.; Loppinet-Serani, A.; Cansell, F.; Aymonier, C. Near- and Supercritical Solvolysis of Carbon Fibre Reinforced Polymers (CFRPs) for Recycling Carbon Fibers as a Valuable Resource: State of the Art. *J. Supercrit. Fluids* **2012**, *66*, 232–240. https://doi.org/10.1016/j.supflu.2012.02.001.

(36) Flake, M.; Fleissner, T.; Hansen, A. Ecological Assessment of Natural Fibre Reinforced Components and Thermoplastics for Automotive Parts. *Plast. Recycl. Technol.* **2002**, *18* (4).

(37) Rybicka, J.; Tiwari, A.; Leeke, G. A. Technology Readiness Level Assessment of Composites Recycling Technologies. *J. Clean. Prod.* **2016**, *112*, 1001–1012. https://doi.org/10.1016/J.JCLEPRO.2015.08.104.

(38) Worrell, E.; Reuter, M. A. *Handbook of Recycling: State-of-the-Art for Practitioners, Analysts, and Scientists*; 2014. https://doi.org/10.1016/C2011-0-07046-1.

(39) Stewart, R. Automotive Composites Offer Lighter Solutions. *Reinf. Plast.* **2010**, *54* (2), 22–28. https://doi.org/10.1016/S0034-3617(10)70061-8.

(40) Stewart, R. Lightweighting the Automotive Market. *Reinf. Plast.* **2009**.

https://doi.org/10.1016/S0034-3617(09)70109-2.

(41) Kodjak, D. Policies to Reduce Fuel Consumption, Air Pollution and Carbon Emissions from Vehicles in G20 Nations. The International Council on Clean Transportation 2015.

(42) Bax, L.; Vasiliadis, H.; Magallon, I.; Ong, K. Polymer Composites for Automotive Sustainability, 2017, 29.

(43) Grünig, M.; Witte, M.; Marcellino, D.; Selig, J.; van Essen, H. Impacts of Electric Vehicles: An Overview of Electric Vehicles on the Market and in Development. ICF International: Delft 2011, p 87.

(44) Vaidya, U. *Composites for Automotive, Truck and Mass Transit*, 1st ed.; DEStech Publications, Inc.: Birmingham, Alabama, 2011.

(45) Crow, R. Carbon Fibre in Mass Automotive Applications: Challenges and Drivers for Composites. In *Franco-British Symposium on Composite Materials*; London, 2015.

(46) Barnes, F. Commercial Aspects of Carbon Fibre Recycling. In *GoCarbon Fibre Recycling 2015*; Manchester, 2015.

(47) Mayyas, A.; Qattawi, A.; Omar, M.; Shan, D. Design for Sustainability in Automotive Industry: A Comprehensive Review. *Renew. Sustain. Energy Rev.* **2012**, *16* (4), 1845–1862. https://doi.org/10.1016/j.rser.2012.01.012.

(48) Meng, F. Environmental and Cost Analysis of Carbon Fibre Composites Recycling, University of Nottingham, 2017.

(49) ELG Carbon Fibre Ltd. LCA Benefits of RCF. In *Composite Recycling & LCA*; Stuttgart, 2017.

(50) Sloan, J. Molding i3 body panels.

(51) Bledzki, A.; Sperber, V.; Wolff, S. Methods of Pretreatment. In *Handbook of Plastics Recycling*; La Mantia, F., Ed.; Rapra, 2002; pp 89–127.

(52) Huang, Z.; Ge, H.; Zhao, Y.; Liu, F.; Yin, J. Reuse FRP Waste as Filler Replacement for Sisal Fiber Reinforced Sheet Molding Compound. *Polym.*

Compos. **2018**, *39* (6), 1896–1904. https://doi.org/10.1002/pc.24146.

(53) Uhlmann, E.; Meier, P. Carbon Fibre Recycling from Milling Dust for the Application in Short Fibre Reinforced Thermoplastics. In *Procedia CIRP*; 2017; Vol. 66, pp 277–282. https://doi.org/10.1016/j.procir.2017.03.277.

(54) Marsh, G. Facing up to the Recycling Challenge. *Reinf. Plast.* **2001**, *45* (6), 22–26. https://doi.org/10.1016/S0034-3617(01)80204-6.

(55) Palmer, J.; Savage, L.; Ghita, O. R.; Evans, K. E. Sheet Moulding Compound (SMC) from Carbon Fibre Recyclate. *Compos. Part A Appl. Sci. Manuf.* **2010**, *41* (9), 1232–1237. https://doi.org/10.1016/J.COMPOSITESA.2010.05.005.

(56) Kouparitsas, C. E.; Kartalis, C. N.; Varelidis, P. C.; Tsenoglou, C. J.; Papaspyrides, C. D. Recycling of the Fibrous Fraction of Reinforced Thermoset Composites. *Polym. Compos.* **2002**, *23* (4), 682–689. https://doi.org/10.1002/pc.10468.

(57) Ogi, K.; Nishikawa, T.; Okano, Y.; Taketa, I. Mechanical Properties of ABS Resin Reinforced with Recycled CFRP. *Adv. Compos. Mater.* **2007**, *16* (2), 181–194. https://doi.org/10.1163/156855107780918982.

(58) Nishikawa, T.; Ogi, K.; Tanaka, T.; Okano, Y.; Taketa, I. Electrical Properties of ABS Resin Reinforced with Recycled CFRP. *Adv. Compos. Mater* **2007**, *16* (1), 1–10. https://doi.org/10.1163/156855107779755282doi.org/10.1163/15685510777 9755282.

(59) Howarth, J.; Mareddy, S. S. R.; Mativenga, P. T. Energy Intensity and Environmental Analysis of Mechanical Recycling of Carbon Fibre Composite. *J. Clean. Prod.* **2014**, *81*, 46–50. https://doi.org/10.1016/J.JCLEPRO.2014.06.023.

(60) Pimenta, S.; Pinho, S. T. The Effect of Recycling on the Mechanical Response of Carbon Fibres and Their Composites. *Compos. Struct.* **2012**, *94* (12), 3669–3684. https://doi.org/10.1016/j.compstruct.2012.05.024.

(61) Meyer, L. O.; Schulte, K.; Grove-Nielsen, E. CFRP-Recycling Following a

Pyrolysis Route: Process Optimization and Potentials. *J. Compos. Mater.* **2009**, *43* (9), 1121–1132. https://doi.org/10.1177/0021998308097737.

(62) López, F. A.; Rodríguez, O.; Alguacil, F. J.; García-Díaz, I.; Centeno, T. A.; García-Fierro, J. L.; González, C. Recovery of Carbon Fibres by the Thermolysis and Gasification of Waste Prepreg. *J. Anal. Appl. Pyrolysis* **2013**, *104*, 675–683. https://doi.org/10.1016/J.JAAP.2013.04.012.

(63) Longana, M. L. Multiple Closed Loop Recycling of Carbon Fibre Composites with the HiPerDiF (High Performance Discontinuous Fibre) Method. *Compos. Struct.* **2016**, *153*, 271–277. https://doi.org/10.1016/j.compstruct.2016.06.018.

(64) Barrales-Rienda, J. Energy Recvoery Form Plastic Materials. In *Handbook of Plastics Recycling*; La Mantia, F., Ed.; Rapra, 2002; pp 337–410.

(65) ELG. ELG Carbon Fibre Ltd. http://www.elgcf.com/home (accessed Jun 6, 2018).

(66) Sara Black. Composites recycling: Gaining traction https://www.compositesworld.com/articles/composites-recycling-gaining-traction (accessed May 30, 2018).

(67) CFK Valley Stade Recycling GmbH & Co. KG https://www.cfk-recycling.de/index.php?id=5 (accessed Jun 6, 2018).

(68) Black, S. Composites recycling is gaining traction: CompositesWorld https://www.compositesworld.com/blog/post/composites-recycling-is-gaining-traction (accessed Jun 6, 2018).

(69) The Japan Carbon Fibre Manufacturers Association (JCMA) http://www.carbonfiber.gr.jp/english/ (accessed Jun 6, 2018).

(70) Wood, K. Carbon fiber reclamation: Going commercial : CompositesWorld https://www.compositesworld.com/articles/carbon-fiber-reclamation-going-commercial (accessed May 29, 2018).

(71) Carbon Conversions. Carbon Fiber Recycling

https://carbonconversions.com/ (accessed Jun 6, 2018).

(72) Janney, M.; Jr., E. G.; Baitcher, N. Fabrication of Chopped Fiber Preforms by the 3-DEP Process. In *Composites and Polycon 2007*; American Composites Manufacturers Association: Tampa, Florida, USA, 2007.

(73) Company | Karborek Recycling Carbon Fibres http://www.karborekrcf.it/home/en/azienda/ (accessed Sep 5, 2018).

(74) Vo Dong, P. A.; Azzaro-Pantel, C.; Cadene, A.-L. Economic and Environmental Assessment of Recovery and Disposal Pathways for CFRP Waste Management. *Resour. Conserv. Recycl.* **2018**, *133*, 63–75. https://doi.org/10.1016/j.resconrec.2018.01.024.

(75) Lester, E.; Kingman, S.; Wong, K. H.; Rudd, C.; Pickering, S.; Hilal, N. Microwave Heating as a Means for Carbon Fibre Recovery from Polymer Composites: A Technical Feasibility Study. *Mater. Res. Bull.* **2004**, *39* (10), 1549–1556. https://doi.org/10.1016/J.MATERRESBULL.2004.04.031.

(76) Akesson, D.; Foltynowicz, Z.; Christeen, J.; SkrifvarsS, M. Products Obtained from Decomposition of Glass Fibre-Reinforced Composites Using Microwave Pyrolysis. *Polimery* **2013**, *58* (7/8), 582–586. https://doi.org/10.14314/polimery.2013.582.

(77) Jiang, G.; Pickering, S. J.; Walker, G. S.; Wong, K. H.; Rudd, C. D. Surface Characterisation of Carbon Fibre Recycled Using Fluidised Bed. *Appl. Surf. Sci.* **2008**, *254* (9), 2588–2593. https://doi.org/10.1016/j.apsusc.2007.09.105.

(78) Wong, K. H.; Pickering, S. J.; Turner, T. A.; Warrior, N. A. Preliminary Feasibility Study of Reinforcing Potential of Recycled Carbon Fibre for Flame-Retardant Grade Epoxy Composite. In *Composites Innovation 2007, NetComposites*; 2007.

(79) Pickering, S. J.; Turner, T. A.; Meng, F.; Morris, C. N.; Heil, J. P.; Wong, K. H.; Melendi-Espina, S. Developments in the Fluidised Bed Process for Fibre Recovery from Thermoset Composites. In *2nd Annual Composites*

and Advanced Materials Expo, CAMX; Dallas USA, 2015.

(80) Meng, F.; McKechnie, J.; Turner, T. A.; Pickering, S. J. Energy and Environmental Assessment and Reuse of Fluidised Bed Recycled Carbon Fibres. *Compos. Part A Appl. Sci. Manuf.* **2017**, *100*, 206–214. https://doi.org/10.1016/J.COMPOSITESA.2017.05.008.

(81) Pickering, S. J.; Kelly, R. M.; Kennerley, J. R.; Rudd, C. D.; Fenwick, N. J. A Fluidised-Bed Process for the Recovery of Glass Fibres from Scrap Thermoset Composites. *Compos. Sci. Technol.* **2000**, *60* (4), 509–523. https://doi.org/10.1016/S0266-3538(99)00154-2.

(82) Liu, Y.; Meng, L.; Huang, Y.; Du, J. Recycling of Carbon/Epoxy Composites. *J Appl Polym Sci* **2004**, *95*, 1912–1916. https://doi.org/10.1002/app.20990.

(83) Lee, S.-H.; Choi, H.-O.; Kim, J.-S.; Lee, C.-K.; Kim, Y.-K.; Ju, C.-S. Circulating Flow Reactor for Recycling of Carbon Fiber from Carbon Fiber Reinforced Epoxy Composite. *Korean J. Chem. Eng* **2011**, *28* (1), 449–454. https://doi.org/10.1007/s11814-010-0394-1.

(84) Feraboli, P.; Kawakami, H.; Wade, B.; Gasco, F.; DeOto, L.; Masini, A. Recyclability and Reutilization of Carbon Fiber Fabric/Epoxy Composites. *J. Compos. Mater.* **2012**, *46* (12), 1459–1473. https://doi.org/10.1177/0021998311420604.

(85) Das, M.; Chacko, R.; Varughese, S. An Efficient Method of Recycling of CFRP Waste Using Peracetic Acid. *ACS Sustain. Chem. Eng.* **2018**, *6* (2), 1564–1571. https://doi.org/10.1021/acssuschemeng.7b01456.

(86) Li, J.; Xu, P.-L.; Zhu, Y.-K.; Ding, J.-P.; Xue, L.-X.; Wang, Y.-Z. A Promising Strategy for Chemical Recycling of Carbon Fiber/Thermoset Composites: Self-Accelerating Decomposition in a Mild Oxidative System. *Green Chem.* **2012**, *14* (12), 3260. https://doi.org/10.1039/c2gc36294e.

(87) Ma, Y.; Kim, D.; Williams, T. J.; Nutt, S. R. Recycling of Carbon Fiber Composites Using Chemical Treatment: Reaction Characterization and Optimizaiton. In *SAMPE 2017*; Seattle, 2017.

(88) Piñero-Hernanz, R.; Dodds, C.; Hyde, J.; García-Serna, J.; Poliakoff, M.; Lester, E.; Cocero, M. J.; Kingman, S.; Pickering, S.; Wong, K. H. Chemical Recycling of Carbon Fibre Reinforced Composites in Nearcritical and Supercritical Water. *Compos. Part A Appl. Sci. Manuf.* **2008**, *39* (3), 454–461. https://doi.org/10.1016/J.COMPOSITESA.2008.01.001.

(89) Oliveux, G.; Dandy, L. O.; Leeke, G. A. Degradation of a Model Epoxy Resin by Solvolysis Routes. *Polym. Degrad. Stab.* **2015**, *118*, 96–103. https://doi.org/10.1016/j.polymdegradstab.2015.04.016.

(90) Bai, Y.; Wang, Z.; Feng, L. Chemical Recycling of Carbon Fibers Reinforced Epoxy Resin Composites in Oxygen in Supercritical Water. *Mater. Des.* **2010**, *31* (2), 999–1002. https://doi.org/10.1016/j.matdes.2009.07.057.

(91) Hyde, J. R.; Lester, E.; Kingman, S.; Pickering, S.; Wong, K. H. Supercritical Propanol, a Possible Route to Composite Carbon Fibre Recovery: A Viability Study. *Compos. Part A Appl. Sci. Manuf.* **2006**, *37* (11), 2171–2175. https://doi.org/10.1016/j.compositesa.2005.12.006.

(92) Oliveux, G.; Bailleul, J.-L.; Gillet, A.; Mantaux, O.; Leeke, G. A. Recovery and Reuse of Discontinuous Carbon Fibres by Solvolysis: Realignment and Properties of Remanufactured Materials. *Compos. Sci. Technol.* **2017**, *139*, 99–108. https://doi.org/10.1016/j.compscitech.2016.11.001.

(93) Bai, Y.; Wang, Z.; Feng, L. Chemical Recycling of Carbon Fibers Reinforced Epoxy Resin Composites in Oxygen in Supercritical Water. *Mater. Des.* **2010**, *31* (2), 999–1002. https://doi.org/10.1016/J.MATDES.2009.07.057.

(94) Okajima, I.; Watanabe, K.; Haramiishi, S.; Nakamura, M.; Shimamura, Y.; Sako, T. Recycling of Carbon Fiber Reinforced Plastic Containing Amine-Cured Epoxy Resin Using Supercritical and Subcritical Fluids. *J. Supercrit. Fluids* **2017**, *119*, 44–51. https://doi.org/10.1016/J.SUPFLU.2016.08.015.

(95) Idzumi OKAJIMA, et al. Chemical Recycling of Carbon Fibre Reinforced Plastic with Supercritical Alcohol. *J. Adv. Res. Phys.* **2012**, *3* (2).

(96) Recycling Technologies - Adherent Technologies https://www.adherent-tech.com/recycling_technologies (accessed Jun 7, 2018).

(97) Allred, R. E.; Busselle, L. D.; Shoemaker, J. M. Catalytic Process for the Reclamation of Carbon Fibers from Carbon/Epoxy Composites. In *Society of Plastics Engineering Annual Recycling Conference (ARC)*; Detroit, Michigan, 1999.

(98) Gosau, J. M.; Wesley, T. F.; Allred, R. E. Integrated Composite Recycling Process. In *38th SAMPE Technology Conference*; 2006.

(99) Allred, R. E.; Busselle, L. D. Tertiary Recycling of Automotive Plastics and Composites. *J. Thermoplast. Compos. Mater.* **2000**, *13* (2), 92–101. https://doi.org/10.1177/089270570001300201.

(100) Gosau, J. M.; Wesley, T. F.; Allred, R. E. Carbon Fiber Reclamation from State-of-the-Art 2nd Generation Aircraft Composites. In *International SAMPE Symposium and Exhibition*; 2009.

(101) Knight, C. C.; Zeng, C.; Zhang, C.; Wang, B. Recycling of Woven Carbon-Fibre-Reinforced Polymer Composites Using Supercritical Water. *Environ. Technol.* **2012**, *33* (6), 639–644. https://doi.org/10.1080/09593330.2011.586732.

(102) Leeke, G. A. Recycling Processes of Carbon Fibre and Directions for the Future. In *GoCarbon Fibre Recycling 2015*; Manchester, 2015.

(103) Vallee, M.; Tersac, G.; Destais-Orvoen, N.; Durand, G. Chemical Recycling of Class A Surface Quality Sheet-Molding Composites. **2004**. https://doi.org/10.1021/IE049871Y.

(104) Palmer, J.; Ghita, O. R.; Savage, L.; Evans, K. E. Successful Closed-Loop Recycling of Thermoset Composites. *Compos. Part A Appl. Sci. Manuf.* **2009**, *40* (4), 490–498. https://doi.org/10.1016/j.compositesa.2009.02.002.

(105) Yazdanbakhsh, A.; Bank, L. A Critical Review of Research on Reuse of

Mechanically Recycled FRP Production and End-of-Life Waste for Construction. *Polymers (Basel).* **2014**, *6* (6), 1810–1826. https://doi.org/10.3390/polym6061810.

(106) Akonda, M. H.; Lawrence, C. A.; Weager, B. M. Recycled Carbon Fibre-Reinforced Polypropylene Thermoplastic Composites. **2012**. https://doi.org/10.1016/j.compositesa.2011.09.014.

(107) Achilias, D. S.; Roupakias, C.; Megalokonomos, P.; Lappas, A. A.; Antonakou, V. Chemical Recycling of Plastic Wastes Made from Polyethylene (LDPE and HDPE) and Polypropylene (PP). *J. Hazard. Mater.* **2007**, *149* (3), 536–542. https://doi.org/10.1016/j.jhazmat.2007.06.076.

(108) Witik, R. A.; Teuscher, R.; Michaud, V.; Ludwig, C.; Månson, J.-A. E. Carbon Fibre Reinforced Composite Waste: An Environmental Assessment of Recycling, Energy Recovery and Landfilling. *Compos. Part A Appl. Sci. Manuf.* **2013**, *49*, 89–99. https://doi.org/10.1016/j.compositesa.2013.02.009.

(109) Pickering, S.; Liu, Z.; Turner, T.; Wong, K. Applications for Carbon Fibre Recovered from Composites. *IOP Conf. Ser. Mater. Sci. Eng.* **2016**, *139* (1), 012005. https://doi.org/10.1088/1757-899X/139/1/012005.

(110) Prinçaud, M.; Aymonier, C.; Loppinet-Serani, A.; Perry, N.; Sonnemann, G. Environmental Feasibility of the Recycling of Carbon Fibers from CFRPs by Solvolysis Using Supercritical Water. *ACS Sustain. Chem. Eng.* **2014**, *2* (6), 1498–1502. https://doi.org/10.1021/sc500174m.

(111) Arturi, K. R.; Sokoli, H. U.; Søgaard, E. G.; Vogel, F.; Bjelić, S. Recovery of Value-Added Chemicals by Solvolysis of Unsaturated Polyester Resin. *J. Clean. Prod.* **2018**, *170*, 131–136. https://doi.org/10.1016/j.jclepro.2017.08.237.

(112) Hamad, K.; Kaseem, M.; Deri, F. Recycling of Waste from Polymer Materials: An Overview of the Recent Works. *Polym. Degrad. Stab.* **2013**, *98* (12), 2801–2812.

https://doi.org/10.1016/j.polymdegradstab.2013.09.025.

(113) Al-Salem, S. M.; Lettieri, P.; Baeyens, J. Recycling and Recovery Routes of Plastic Solid Waste (PSW): A Review. *Waste Manag.* **2009**, *29* (10), 2625–2643. https://doi.org/10.1016/j.wasman.2009.06.004.

(114) Younke, J.; Laino, T. Does Size Really Matter? http://www.recyclingtoday.com/article/sdb1011-electronic-media-destruction-computers/ (accessed Jun 13, 2018).

(115) Roux, M.; Egué Mann, N.; Dransfeld, C.; Dé, F.; Thié Baud, R.; Perreux, D. Thermoplastic Carbon Fibre-Reinforced Polymer Recycling with Electrodynamical Fragmentation: From Cradle to Cradle. *J. Thermoplast. Compos. Mater.* **2017**, *30* (3), 381–403. https://doi.org/10.1177/0892705715599431.

(116) Yin, S.; Tuladhar, R.; Shi, F.; Shanks, R. A.; Combe, M.; Collister, T. Mechanical Reprocessing of Polyolefin Waste: A Review. *Polym. Eng. Sci.* **2015**, *55* (12), 2899–2909. https://doi.org/10.1002/pen.24182.

(117) Li, H.; Englund, K. Recycling of Carbon Fiber-Reinforced Thermoplastic Composite Wastes from the Aerospace Industry. *J. Compos. Mater.* **2017**, *51* (9), 1265–1273. https://doi.org/10.1177/0021998316671796.

(118) Moritzer, E.; Heiderich, G. Mechanical Recycling of Continuous Fiber-Reinforced Thermoplastic Sheets. *AIP Conf. Proc.* **2016**, *1200131* (10), 20001–140002. https://doi.org/10.1063/1.4965582.

(119) Guo, G.; Chen, J. C.; Gong, G. Injection Molding of Polypropylene Hybrid Composites Reinforced with Carbon Fiber and Wood Fiber. *Polym. Compos.* **2017**.

(120) Nakao, R.; Inoya, H.; Hamada, H. Mechanical Properties of Injection Molded Products Fabricated by Direct Fiber Feeding Injection Molding. *Energy Procedia* **2016**. https://doi.org/10.1016/j.egypro.2016.05.039.

(121) Lafranche, E.; Krawczak, P.; Ciolczyk, J.-P.; Maugey, J. Injection Moulding of Long Glass Fiber Reinforced Polyamide 66: Processing Conditions/Microstructure/Flexural Properties Relationship. *Adv. Polym.*

Technol. **2005**, *24* (2), 114–131. https://doi.org/10.1002/adv.20035.

(122) Zhang, Z.; Breidt, C.; Chang, L.; Friedrich, K. Wear of PEEK Composites Related to Their Mechanical Performances. *Tribol. Int.* **2004**, *37* (3), 271–277. https://doi.org/10.1016/J.TRIBOINT.2003.09.005.

(123) Papathanasiou, T. D. Flow-Induced Alignment in Injection Molding of Fiber-Reinforced Polymer Composites. In *Flow-Induced Alignment in Composite Materials*; Elsevier, 1997; pp 112–165. https://doi.org/10.1201/9781439822739.ch4.

(124) Hausnerova, B.; Honkova, N.; Lengalova, A.; Kitano, T.; Saha, P. Rheology and Fiber Degradation during Shear Flow of Carbon-Fiber-Reinforced Polypropylenes. *Polym. Sci. Ser. A* **2006**, *48* (9), 951–960. https://doi.org/10.1134/S0965545X06090100.

(125) Eriksson, P.-A.; Albertsson, A.-C.; Boydell, P.; Eriksson, K.; Månson, J.-A. E. Reprocessing of Fiberglass Reinforced Polyamide 66: Influence on Short Term Properties. *Polym. Compos.* **1996**, *17* (6), 823–829. https://doi.org/10.1002/pc.10675.

(126) Eriksson, P.-A.; Albertsson, A.-C.; Boydell, P.; Prautzsch, G.; Månson, J.-A. E. Prediction of Mechanical Properties of Recycled Fiberglass Reinforced Polyamide 66. *Polym. Compos.* **1996**, *17* (6), 830–839. https://doi.org/10.1002/pc.10676.

(127) Da Costa, H. M.; Ramos, V. D.; Rocha, M. C. G. Rheological Properties of Polypropylene during Multiple Extrusion. *Polym. Test.* **2005**, *24* (1), 86–93. https://doi.org/10.1016/j.polymertesting.2004.06.006.

(128) Bernardo, C. A.; Cunha, A. M.; Oliveira, M. J. The Recycling of Thermoplastics: Prediction of the Properties of Mixtures of Virgin and Reprocessed Polyolefins. *Polym. Eng. Sci.* **1996**, *36* (4), 511–519. https://doi.org/10.1002/pen.10437.

(129) Sarasua, J. R.; Pouyet, J. Recycling Effects on Microstructure and Mechanical Behaviour of PEEK Short Carbon-Fibre Composites. *J. Mater. Sci.* **1997**, *32* (2), 533–536. https://doi.org/10.1023/A:1018598610260.

(130) TenCate Advanced Composites https://www.tencatecomposites.com/company/about-us (accessed Jun 13, 2018).

(131) TenCate Advanced Composites. Recycling Thermoplastic Composites: Beyond Grinding the Materials. 2018.

(132) Howell, D. D.; Fukumoto, S. *Compression Moulding of Long Chopped Fibre Thermoplastic Composites*; 2015.

(133) Burn, D. T.; Harper, L. T.; Johnson, M.; Warrior, N. A.; Nagel, U.; Yang, L.; Thomason, J. The Usability of Recycled Carbon Fibres in Short Fibre Thermoplastics: Interfacial Properties. *J. Mater. Sci.* **2016**, *51*. https://doi.org/10.1007/s10853-016-0053-y.

(134) Hinsken, H.; Moss, S.; Pauquet, J. R.; Zweifel, H. Degradation of Polyolefins during Melt Processing. *Polym. Degrad. Stab.* **1991**, *34* (1–3), 279–293. https://doi.org/10.1016/0141-3910(91)90123-9.

(135) Incarnato, L.; Scarfato, P.; Acierno, D.; Ponte, V. Rheological and Mechanical Properties of Recycled Polypropylene. *Polym. Eng. Sci.* **1999**, *39* (4), 749–755.

(136) La Mantia, F.; Scaffaro, R. Reprocessing of Polyethyleneterephthalate and Characterisation of Monopolymer Blends of Virgin and Recycled Polymers. *Polym. Recycl.* **1997**, *3* (3), 209–215.

(137) Valenza, A.; La Mantia, F. P. Recycling of Polymer Waste: Part II-Stress Degraded Polypropylene. *Polym. Degrad. Stab.* **1988**, *20* (1), 63–73. https://doi.org/10.1016/0141-3910(88)90094-8.

(138) Scaffaro, R.; La Mantia, F. P. Virgin/Recycling Homopolymer Blends. In *Handbook of Plastics Recycling*; La Mantia, F. P., Ed.; Rapra, 2002; pp 195–220.

(139) Bifa Environmental Institute. CFC recycling in the Augsburg region of expertise http://www.bifa.de/en/projects/project-details/news/cfc-recycling-in-the-augsburg-region-of-expertise (accessed Jun 6, 2018).

(140) Such, M.; Ward, C.; Potter, K. Aligned Discontinuous Fibre Composites: A Short History. *J. Multifunct. Compos.* **2014**, *2* (3), 155–168. https://doi.org/10.12783/issn.2168-4286/2/3/4.

(141) Boylan, S.; Castro, J. M. Effect of Reinforcement Type and Length on Physical Properties, Surface Quality, and Cycle Time for Sheet Molding Compound (SMC) Compression Molded Parts. *J. Appl. Polym. Sci.* **2003**, *90* (9), 2557–2571. https://doi.org/10.1002/app.12726.

(142) Piñero-Hernanz, R.; García-Serna, J.; Dodds, C.; Hyde, J.; Poliakoff, M.; Cocero, M. J.; Kingman, S.; Pickering, S.; Lester, E. Chemical Recycling of Carbon Fibre Composites Using Alcohols under Subcritical and Supercritical Conditions. *J. Supercrit. Fluids* **2008**, *46* (1), 83–92. https://doi.org/10.1016/j.supflu.2008.02.008.

(143) Turner, T. A.; Warrior, N. A.; Pickering, S. J. Re-Use of Carbon Fibres in High-Value Moulding Compounds & Pre-Pregs. In *ICCM17*; Edinburgh, 2009.

(144) Turner, T. A.; Warrior, N. A.; Pickering, S. J. Development of High Value Moulding Compounds from Recycled Carbon Fibres. **2013**. https://doi.org/10.1179/174328910X12647080902295.

(145) Shah, D. U.; Schubel, P. J. On Recycled Carbon Fibre Composites Manufactured through a Liquid Composite Moulding Process. *J. Reinf. Plast. Compos.* **2016**, *35* (7), 533–540. https://doi.org/10.1177/0731684415623652.

(146) Technical Fibre Products (TFP). Carbon Veils & Mats http://www.tfpglobal.com/materials/carbon/ (accessed Jun 4, 2018).

(147) Wong, K. H.; Pickering, S. J.; Rudd, C. D. Recycled Carbon Fibre Reinforced Polymer Composite for Electromagnetic Interference Shielding. *Compos. Part A Appl. Sci. Manuf.* **2010**, *41* (6), 693–702. https://doi.org/10.1016/J.COMPOSITESA.2010.01.012.

(148) Edwards, K. L. An Overview of the Technology of Fibre-Reinforced Plastics for Design Purposes. *Mater. Des.* **1998**, *19* (1–2), 1–10.

https://doi.org/10.1016/S0261-3069(98)00007-7.

(149) Nakagawa, M.; Kuriya, H.; Shibata, K. Characterization of CFRP Using Recovered Carbon Fibers from Waste CFRP. In *Fifth International Symposium on Fiber Recycling*; Chengdu China, 2009.

(150) Wei, H.; Nagatsuka, W.; Lee, H.; Ohsawa, I.; Sumimoto, K.; Wan, Y.; Takahashi, J. Mechanical Properties of Carbon Fiber Paper Reinforced Thermoplastics Using Mixed Discontinuous Recycled Carbon Fibers Mechanical Properties of Carbon Fiber Paper Reinforced Thermoplastics Using Mixed Discontinuous Recycled Carbon Fibers. *Adv. Compos. Mater.* **2017**. https://doi.org/10.1080/09243046.2017.1334274.

(151) ELG Carbon Fibre Ltd. New nonwoven line manufactures market's first 2.7m wide recycled carbon mats http://www.elgcf.com/news/elg-carbon-fibre-new-nonwoven-line (accessed Jun 12, 2018).

(152) Warrior, N. A.; Turner, T. A.; Pickering, S. J. AFRECAR and HIRECAR Project Results. In *Carbon Fibre Recycling and Reuse Conference*; Hamburg, Germany, 2009.

(153) TFP: New Range of Recycled Carbon Nonwovens http://www.tfpglobal.com/news-events/news/2014/06/new-range-of-recycled-carbon-nonwovens/ (accessed Jun 12, 2018).

(154) Sigmatex. Carbon fibre for composite material applications http://www.sigmatex.com/ (accessed Jul 10, 2018).

(155) Sigmatex. SigmaRF Product Information Sheet http://www.sigmatex.com/wp-content/uploads/2016/11/sigmaRF-Product-Information-Sheet.pdf (accessed Jul 10, 2018).

(156) Wong, K. H.; Pickering, S. J.; Turner, T. A.; Warrior, N. A. Compression Moulding of a Recycled Carbon Fibre Reinforced Epoxy Composite. In *SAMPE 2009*; 2009.

(157) Wong, K. H.; Turner, T. A.; Pickering, S. J.; Warrior, N. A. The Potential for Fibre Alignment in the Manufacture of Polymer Composites from Recycled Carbon Fibre. *SAE Int. J. Aerosp.* **2009**, *2*, 225–231.

(158) Yu, H.; Potter, K. D.; Wisnom, M. R. A Novel Manufacturing Method for Aligned Discontinuous Fibre Composites (High Performance-Discontinuous Fibre Method). *Compos. Part A Appl. Sci. Manuf.* **2014**, *65*, 175–185. https://doi.org/10.1016/j.compositesa.2014.06.005.

(159) Takahashi, J.; Matsutsuka, N.; Okazumi, T.; Uzawa, K.; Ohsawa, I.; Yamaguchi, K.; Kitano, A. Mechanical Properties of Recycled CFRP By Injection Molding Method. *16th Int. Conf. Compos. Mater.* **2007**, No. July, 1–6.

(160) Szpieg, M. Development and Characteristics of a Fully Recycled CF/PP Composite. **2011**.

(161) Pimenta, S.; Pinho, S. T.; Robinson, P.; Wong, K. H.; Pickering, S. J. Mechanical Analysis and Toughening Mechanisms of a Multiphase Recycled CFRP. *Compos. Sci. Technol.* **2010**, *70* (12), 1713–1725. https://doi.org/10.1016/j.compscitech.2010.06.017.

(162) S.J., P. Recycling Technologies for Thermoset Composite Materials—current Status. *2nd Int. Conf. Adv. Polym. Compos. Struct. Appl. Constr.* **2006**, *37* (8), 1206–1215. https://doi.org/10.1016/j.compositesa.2005.05.030.

(163) George, P. An opportunistic time for composites www.futurematerialsgroup.com (accessed Jul 16, 2018).

(164) Hillier, G.; Hill, J. New Materials and the Circular Economy. *Inst. Environ. Sci.* **2015**, *24* (1).

(165) Hazell, J. Developing a Circular Economy for Novel Materials. Green Alliance: London 2017.

(166) Goodship, V. Plastic Recycling. *Sci. Prog.* **2007**, *90* (4), 245–268. https://doi.org/10.3184/003685007X228748.

(167) Halliwell, S. FRPs — The Environmental Agenda. *Adv. Struct. Eng.* **2010**, *13* (5), 783–791. https://doi.org/10.1260/1369-4332.13.5.783.

(168) Carberry, W. Airplane Recycling Efforts Benefit Boeing Operators. *Aero*

Quarterly. 2011.

(169) Shuaib, N. A.; Mativenga, P. T. Energy Intensity and Quality of Recyclate in Composite Recycling. **2015**, 1–11. https://doi.org/10.1115/MSEC20159387.

(170) Job, S. Recycling Composites Commercially. *Reinf. Plast.* **2014**, *58* (5), 32–38. https://doi.org/10.1016/S0034-3617(14)70213-9.

(171) Gutiérrez, C.; García, M. T.; Gracia, I.; De Lucas, A.; Rodríguez, J. F. The Selective Dissolution Technique as Initial Step for Polystyrene Recycling. *Waste and Biomass Valorization* **2013**, *4* (1), 29–36. https://doi.org/10.1007/s12649-012-9131-9.

(172) Hopewell, J.; Dvorak, R.; Kosior, E. Plastics Recycling: Challenges and Opportunities. *Philos. Trans. R. Soc. Lond. B. Biol. Sci.* **2009**, *364* (1526), 2115–2126. https://doi.org/10.1098/rstb.2008.0311.

(173) Kartalis, C. N.; Poulakis, J. G.; Tsenoglou, C. J.; Papaspyrides, C. D. Pure Component Recovery from Polyamide 6/6 6 Mixtures by Selective Dissolution and Reprecipitation. *J. Appl. Polym. Sci.* **2002**, *86* (8), 1924–1930. https://doi.org/10.1002/app.11147.

(174) Papaspyrides, C.; CN, K. A Model Study for the Recovery of Polyamides Using the Dissolution/Reprecipitation Technique. *Polym. Eng. Sci.* **2000**, *40* (4), 979–984.

(175) Gouli, S.; Poulakis, J. G.; Papaspyrides, C. D. Solvent Recycling of Poly(Methyl Methacrylate) Decorative Sheets. *Adv. Polym. Technol.* **1994**, *13* (3), 207–211. https://doi.org/10.1002/adv.1994.060130303.

(176) Poulakis, J. G.; Papaspyrides, C. D. Recycling of Polypropylene by the Dissolution/Reprecipitation Technique: I. A Model Study. *Resour. Conserv. Recycl.* **1997**, *20* (1), 31–41. https://doi.org/10.1016/S0921-3449(97)01196-8.

(177) Hadi, J.; Najmuldeen, F.; Ahmed, I. Quality Restoration of Waste Polyolefin Plastic Material through the Dissolution-Reprecipitation Technique. *Chem. Ind. Chem. Eng. Q.* **2014**, *20* (2), 163–170.

https://doi.org/10.2298/CICEQ120526119H.

(178) Yu, H.; Potter, K. D. Discontinuous Fibre Alignment Method, High Performance-Discontinuous Fibre (HiPerDiF) Method. 1306762.4, 2014.

(179) Longana, M. L.; Yu, H.; Jalavand, M.; Wisnom, M. R.; Potter, K. D. Aligned Discontinuous Intermingled Reclaimed/Virgin Carbon Fibre Composites for High Performance and Pseudo-Ductile Behaviour in Interlaminated Carbon-Glass Hybrids. *Compos. Sci. Technol.* **2017**, *143*, 13–21. https://doi.org/10.1016/J.COMPSCITECH.2017.02.028.

(180) Longana, M.; Ondra, V.; Yu, H.; Potter, K.; Hamerton, I.; Longana, M. L.; Ondra, V.; Yu, H.; Potter, K. D.; Hamerton, I. Reclaimed Carbon and Flax Fibre Composites: Manufacturing and Mechanical Properties. *Recycling* **2018**, *3* (4), 52. https://doi.org/10.3390/recycling3040052.

(181) Höhne, G. W. H.; Hemminger, W. F.; Flammersheim, H.-J. *Differential Scanning Calorimetry*; Springer Berlin Heidelberg: Berlin, Heidelberg, 2003. https://doi.org/10.1007/978-3-662-06710-9.

(182) Blaine, R. L. Polymer Heats of Fusion. *Thermal Applications Note*. TA Instruments 2011, pp 1–2.

(183) Solvay, L.-A. F.; Lame, O.; Seguela, R.; Millot, C.; Fillot, L.-A.; Lame, ・ Olivier; Sotta, ・ Paul; Seguela, ・ Roland. Assessment of Polyamide-6 Crystallinity by DSC: Temperature Dependence of the Melting Enthalpy. *J. Therm. Anal. Calorim.* **2015**. https://doi.org/10.1007/s10973-015-4670-5.

(184) Vyazovkin, S. Thermogravimetric Analysis. In *Characterization of Materials*; John Wiley & Sons, Inc.: Hoboken, NJ, USA, 2012; pp 1–12. https://doi.org/10.1002/0471266965.com029.pub2.

(185) Gaffney, J. S.; Marley, N. A.; Jones, D. E. Fourier Transform Infrared (FTIR) Spectroscopy. In *Characterization of Materials*; John Wiley & Sons, Inc.: Hoboken, NJ, USA, 2012; pp 1–33. https://doi.org/10.1002/0471266965.com107.pub2.

(186) Held, D.; Kilz, P. GPC/SEC as a Key Tool for Assessment of Polymer Quality and Determination of Macromolecular Properties. In *Monitoring*

Polymerization Reactions; John Wiley & Sons: Hoboken, NJ, 2014; pp 171–199. https://doi.org/10.1002/9781118733813.ch9.

(187) Yergey, A. L.; Edmonds, C. G.; Lewis, I. A. S.; Vestal, M. L. *Liquid Chromatography/Mass Spectrometry*; Springer US: Boston, MA, 1990. https://doi.org/10.1007/978-1-4899-3605-9.

(188) American Society for Testing and Materials. D638 Standard Test Method for Tensile Properties of Plastics. *ASTM International*. 2013, pp 1–16. https://doi.org/10.1520/D0638-10.1.

(189) American Society for Testing and Materials. D732 Standard Test Method for Shear Strength of Plastics by Punch Tool 1. *ASTM International*. 2015, pp 10–13. https://doi.org/10.1520/D0732-10.2.

(190) Bader, M. G.; Bowyer, W. H. The Mechanical Properties of Thermoplastics Strengthened by Short Discontinuous Fibres? *J. Phys. D Appl. Phys* **1972**, *5* (0).

(191) Meredith, J.; Bilson, E.; Powe, R.; Collings, E.; Kirwan, K. A Performance versus Cost Analysis of Prepreg Carbon Fibre Epoxy Energy Absorption Structures. *Compos. Struct.* **2015**, *124*, 206–213. https://doi.org/10.1016/j.compstruct.2015.01.022.

(192) Duflou, J. R.; Yelin, D.; Van Acker, K.; Dewulf, W. Comparative Impact Assessment for Flax Fibre versus Conventional Glass Fibre Reinforced Composites: Are Bio-Based Reinforcement Materials the Way to Go? *CIRP Ann.* **2014**, *63* (1), 45–48. https://doi.org/10.1016/J.CIRP.2014.03.061.

(193) Kuriger, R. J.; Alam, M. K.; Anderson, D. P. Strength Prediction of Partially Aligned Discontinuous Fiber-Reinforced Composites. **2017**. https://doi.org/10.1557/JMR.2001.0035.

(194) Hashimoto, M.; Okabe, T.; Sasayama, T.; Matsutani, H.; Nishikawa, M. Prediction of Tensile Strength of Discontinuous Carbon Fiber/Polypropylene Composite with Fiber Orientation Distribution. **2012**. https://doi.org/10.1016/j.compositesa.2012.05.006.

(195) Fu, S.-Y.; Lauke, B.; Mäder, E.; Yue, C.-Y.; Hu, X. Tensile Properties of Short-Glass-Fiber-and Short-Carbon-Fiber-Reinforced Polypropylene Composites. *Compos. - Part A* **2000**, *31*, 1117–1125.

(196) Li, M.; Wen, X.; Liu, J.; Tang, T. Synergetic Effect of Epoxy Resin and Maleic Anhydride Grafted Polypropylene on Improving Mechanical Properties of Polypropylene/ Short Carbon Fiber Composites. **2014**. https://doi.org/10.1016/j.compositesa.2014.09.001.

(197) Sims, G.; Bishop, G. Foresight Study and Competitive Analysis. National Physical Laboratory: Middlesex 2001.

(198) Das, S. Evaluating LCA for Virgin vs . Recycled Carbon Fibre Composites - Focus Areas and Development Opportunities. *GoCarbon 2015* **2015**, 23.

(199) Guerrica-Echevarria, G.; Eguiazaibal, J. I.; Nazaibal, J. Effects of Reprocessing Conditions on the Properties of Unfilled and Talc-Filled Polypropylene. *Polym. Degrad. Stab. 53*.

(200) Akonda, M. H.; Lawrence, C. A.; Weager, B. M. Recycled Carbon Fibre-Reinforced Polypropylene Thermoplastic Composites. *Compos. Part A Appl. Sci. Manuf.* **2012**, *43* (1), 79–86. https://doi.org/10.1016/j.compositesa.2011.09.014.

(201) Wong, K. H.; Mohammed, D. S.; Pickering, S. J.; Brooks, R. Effect of Coupling Agents on Reinforcing Potential of Recycled Carbon Fibre for Polypropylene Composite. **2012**. https://doi.org/10.1016/j.compscitech.2012.02.013.

(202) Deng, Y.; Tian, Y. Assessing the Environmental Impact of Flax Fibre Reinforced Polymer Composite from a Consequential Life Cycle Assessment Perspective. *Sustainability* **2015**, *7* (9), 11462–11483. https://doi.org/10.3390/su70911462.

(203) Liu, Y.; Zhang, X.; Song, C.; Zhang, Y.; Fang, Y.; Yang, B.; Wang, X. An Effective Surface Modification of Carbon Fiber for Improving the Interfacial Adhesion of Polypropylene Composites. *JMADE* **2015**, *88*, 810–819. https://doi.org/10.1016/j.matdes.2015.09.100.

(204) Harper, L.; Burn, D.; Johnson, M.; Warrior, N. Long Discontinuous Carbon Fibre/Polypropylene Composites for High Volume Structural Applications. *J. Compos. Mater.* **2018**, *52* (9), 1155–1170. https://doi.org/10.1177/0021998317722204.

(205) Yu, H.; Longana, M. L.; Swolfs, Y.; Wisnom, M. R.; Potter, K. D. Hybrid Effect of Carbon/Glass Composites as a Function of the Strength Distribution of Aligned Short Carbon Fibres. *17th Eur. Conf. Compos. Mater.* **2016**, No. June, 26–30.

(206) Barbeş, L.; Rădulescu, C.; Stihi, C. ATR-FTIR Spectrometry Characteristics of Polymeric Materials. *Rom. Reports Phys.* **2014**, *66* (3), 765–777.

(207) Yu, H.; Longana, M. L.; Grail, G.; Pimenta, S.; Robinson, P.; Wisnom, M. R.; Potter, K. D. Aligned Short Fibre Composites With Nonlinear Behaviour. In *ICCM 20*; 2015; pp 19–24.

(208) Hashimoto, M.; Okabe, T.; Sasayama, T.; Matsutani, H.; Nishikawa, M. Prediction of Tensile Strength of Discontinuous Carbon Fiber/Polypropylene Composite with Fiber Orientation Distribution. *Compos. Part A* **2012**, *43*, 1791–1799. https://doi.org/10.1016/j.compositesa.2012.05.006.

(209) Ma, Y.; Yang, Y.; Sugahara, T.; Hamada, H. A Study on the Failure Behavior and Mechanical Properties of Unidirectional Fiber Reinforced Thermosetting and Thermoplastic Composites. *Compos. Part B Eng.* **2016**, *99*, 162–172. https://doi.org/10.1016/j.compositesb.2016.06.005.

(210) Li, J.; Xia, Y. C. The Reinforcement Effect of Carbon Fiber on the Friction and Wear Properties of Carbon Fiber Reinforced PA6 Composites. *Fibers Polym.* **2009**, *10* (4), 519–525. https://doi.org/10.1007/s12221-009-0519-5.

(211) Experimental Data on Carbon Fibre Reinforced Polyamide-6 Composite (CF60/PA-6) under Longitudinal and Transverse Compression Loading. **2018**, *1*. https://doi.org/10.17632/VPR4TFG27J.1.

(212) Ma, Y.; Jin, S.; Zhang, S. Effect of Trigger on Crashworthiness of

Unidirectional Carbon Fibre Reinforced Polyamide 6 Composites. *Plast. Rubber Compos.* **2018**, *47* (5), 208–220. https://doi.org/10.1080/14658011.2018.1466502.

(213) Ma, Y.; Yan, C.; Xu, H.; Liu, D.; Shi, P.; Zhu, Y.; Liu, J. Enhanced Interfacial Properties of Carbon Fiber Reinforced Polyamide 6 Composites by Grafting Graphene Oxide onto Fiber Surface. *Appl. Surf. Sci.* **2018**, *452*, 286–298. https://doi.org/10.1016/j.apsusc.2018.04.274.

(214) Wu, S.-H.; Wang, F.-Y.; Ma, C.-C. M.; Chang, W.-C.; Kuo, C.-T.; Kuan, H.-C.; Chen, W. Mechanical, Thermal and Morphological Properties of Glass Fiber and Carbon Fiber Reinforced Polyamide-6 and Polyamide-6rclay Nanocomposites. *Mater. Lett.* **2001**, *49*, 327–333.

(215) Ude, A. U.; Ratnam, C. T.; Azhari, C. H. The Effect of Composition of Carbon Fibre on the Mechanical and Morhpological Properties of Carbon Fibre Reinforced Polyamide 6 (PA6/CF). 2007, pp 31–40.

(216) Botelho, E. .; Figiel, L.; Rezende, M. C.; Lauke, B. Mechanical Behavior of Carbon Fiber Reinforced Polyamide Composites. *Compos. Sci. Technol.* **2003**, *63* (13), 1843–1855. https://doi.org/10.1016/S0266-3538(03)00119-2.

(217) Iwamoto, R.; Murase, H. Infrared Spectroscopic Study of the Interactions of Nylon-6 with Water. *J. Polym. Sci. Part B Polym. Phys.* **2003**, *41*, 1722–1729.

(218) Pelin, C. E.; Pelin, G.; Ştefan, A.; Andronescu, E.; Dincă, I.; Ficai, A.; Truşcă, R. Mechanical Properties of Polyamide/Carbon-Fiber-Fabric Composites. *Mater. Tehnol.* **2016**, *50* (5), 723–728. https://doi.org/10.17222/mit.2015.171.

(219) Pillay, S.; Vaidya, U. K.; Janowski, G. M. Liquid Molding of Carbon Fabric-Reinforced Nylon Matrix Composite Laminates. *J. Thermoplast. Compos. Mater.* **2005**, *18* (6), 509–527. https://doi.org/10.1177/0892705705054412.

(220) Feng, N.; Wang, X.; Wu, D. Surface Modification of Recycled Carbon Fiber and Its Reinforcement Effect on Nylon 6 Composites: Mechanical

Properties, Morphology and Crystallization Behaviors. *Curr. Appl. Phys.* **2013**, *13* (9), 2038–2050. https://doi.org/10.1016/j.cap.2013.09.009.

(221) Karsli, N. G.; Aytac, A. Tensile and Thermomechanical Properties of Short Carbon Fiber Reinforced Polyamide 6 Composites. *Compos. Part B Eng.* **2013**, *51*, 270–275. https://doi.org/10.1016/j.compositesb.2013.03.023.

(222) Sang, L.; Wang, C.; Wang, Y.; Wei, Z. Thermo-Oxidative Ageing Effect on Mechanical Properties and Morphology of Short Fibre Reinforced Polyamide Composites-Comparison of Carbon and Glass Fibres. *RSC Adv.* **2017**, *7* (69), 43334–43344. https://doi.org/10.1039/c7ra07884f.

(223) Luo, H.; Xiong, G.; Ma, C.; Li, D.; Wan, Y. Preparation and Performance of Long Carbon Fiber Reinforced Polyamide 6 Composites Injection-Molded from Core/Shell Structured Pellets. *Mater. Des.* **2014**, *64*, 294–300. https://doi.org/10.1016/j.matdes.2014.07.054.

(224) Ma, Y.; Jin, S.; Zhang, S. Plastics, Rubber and Composites Effect of Trigger on Crashworthiness of Unidirectional Carbon Fibre Reinforced Polyamide 6 Composites Effect of Trigger on Crashworthiness of Unidirectional Carbon Fibre Reinforced Polyamide 6 Composites. *Macromol. Eng.* **2018**, *8011*. https://doi.org/10.1080/14658011.2018.1466502.

(225) Do, V. T.; Nguyen-Tran, H. D.; Chun, D. M. Effect of Polypropylene on the Mechanical Properties and Water Absorption of Carbon-Fiber-Reinforced-Polyamide-6/Polypropylene Composite. *Compos. Struct.* **2015**, *150*, 240–245. https://doi.org/10.1016/j.compstruct.2016.05.011.

(226) TenCate Advanced Composites. TenCate Cetex ® TC910 - Product Data Sheet. 2018.

(227) Painer, D.; Lux, S.; Siebenhofer, M. Recovery of Formic Acid and Acetic Acid from Waste Water Using Reactive Distillation. *Sep. Sci. Technol.* **2015**, *50* (18), 2930–2936. https://doi.org/10.1080/01496395.2015.1085407.

(228) Socrates, G. *Infrared and Raman Characteristic Group Frequencies : Tables and Charts.*; John Wiley & Sons, 2007.

(229) Parres, F.; Crespo, J. E.; Nadal-Gisbert, A. Thermal Degradation Analysis of Polyamide 6 Processed at Different Cycles Using Sequential Pyrolysis. *J. Appl. Polym. Sci.* **2009**, *114* (2), 713–719. https://doi.org/10.1002/app.30595.

(230) Klampfl, C. W. Mass Spectrometry as a Useful Tool for the Analysis of Stabilizers in Polymer Materials. *TrAC - Trends Anal. Chem.* **2013**, *50*, 53–64. https://doi.org/10.1016/j.trac.2013.04.012.

(231) Block, C.; Wynants, L.; Kelchtermans, M.; De Boer, R.; Compernolle, F. Identification of Polymer Additives by Liquid Chromatography-Mass Spectrometry. *Polym. Degrad. Stab.* **2006**, *91* (12), 3163–3173. https://doi.org/10.1016/j.polymdegradstab.2006.07.015.

(232) Rogers, M. E.; Long, T. E. *Synthetic Methods in Step-Growth Polymers*; Wiley-Interscience, 2003.

(233) Clift, R.; Doig, A.; Finnveden, G. The Application of Life Cycle Assessment to Integrated Solid Waste Management. *Trans IChemE* **2000**, *78* (4), 279–287. https://doi.org/10.1205/095758200530790.

(234) Hong, T.; Hastak, M. Life-Cycle Cost Assessment Model for Fiber Reinforced Polymer Bridge Deck Panels. *Can. J. Civ. Eng.* **2007**, *34* (8), 976–991. https://doi.org/10.1139/l07-019.

(235) Hunkeler, D.; Rebitzer, G. The Future of Life Cycle Assessment. *Int. J. Life Cycle Assess.* **2005**, *10* (5), 305–308. https://doi.org/10.1065/lca2005.09.001.

(236) Zhang, C. The Environmental Impacts of Fibre-Reinforced Polymer Composites in Construction. *Proc. Inst. Civ. Eng. - Constr. Mater.* **2015**, *168* (6), 276–286. https://doi.org/10.1680/coma.14.00059.

(237) Witik, R. A.; Gaille, F.; Teuscher, R.; Ringwald, H.; Michaud, V.; Månson, J.-A. E. Economic and Environmental Assessment of Alternative Production Methods for Composite Aircraft Components. *J. Clean. Prod.* **2012**, *29–30*, 91–102. https://doi.org/10.1016/j.jclepro.2012.02.028.

(238) Bachmann, J.; Hidalgo, C.; Bricout, S. Environmental Analysis of

Innovative Sustainable Composites with Potential Use in Aviation Sector—A Life Cycle Assessment Review. *Science China Technological Sciences*. 2017, pp 1301–1317. https://doi.org/10.1007/s11431-016-9094-y.

(239) Rankine, R. K.; Chick, J. P.; Harrison, G. P. Energy and Carbon Audit of a Rooftop Wind Turbine. *Proc. Inst. Mech. Eng. Part A J. Power Energy* **2006**, *220* (7), 643–654. https://doi.org/10.1243/09576509JPE306.

(240) Merugula, L.; Khanna, V.; Bakshi, B. R. Comparative Life Cycle Assessment: Reinforcing Wind Turbine Blades with Carbon Nanofibers. *Proc. 2010 IEEE Int. Symp. Sustain. Syst. Technol.* **2010**, 1–6. https://doi.org/10.1109/ISSST.2010.5507724.

(241) Witik, R. A.; Payet, J.; Michaud, V.; Ludwig, C.; Månson, J.-A. E. Assessing the Life Cycle Costs and Environmental Performance of Lightweight Materials in Automobile Applications. *Compos. Part A Appl. Sci. Manuf.* **2011**, *42* (11), 1694–1709. https://doi.org/10.1016/j.compositesa.2011.07.024.

(242) Kim, H. C.; Wallington, T. J. Life-Cycle Energy and Greenhouse Gas Emission Benefits of Lightweighting in Automobiles: Review and Harmonization. *Environ. Sci. Technol.* **2013**, *47* (12), 6089–6097. https://doi.org/10.1021/es3042115.

(243) US Environmental Protection Agency. *EPA and NHTSA Set Standards to Reduce Greenhouse Gases and Improve Fuel Economy for Model Years 2017-2025 Cars and Light Trucks*; 2012.

(244) Das, S. Life Cycle Assessment of Carbon Fiber-Reinforced Polymer Composites. *Int. J. Life Cycle Assess.* **2011**, *16* (3), 268–282. https://doi.org/10.1007/s11367-011-0264-z.

(245) Suzuki, T.; Takahashi, J. Prediction of Energy Intensity of Carbon Fiber Reinforced Plastics for Mass-Produced Passenger Cars. *Ninth Japan Int. SAMPE Symp. JISSE-9* **2005**, 14–19.

(246) Timmis, A. J.; Hodzic, A.; Koh, L.; Bonner, M.; Soutis, C.; Schäfer, A. W.; Dray, L. Environmental Impact Assessment of Aviation Emission

Reduction through the Implementation of Composite Materials. *Int. J. Life Cycle Assess.* **2015**, *20* (2), 233–243. https://doi.org/10.1007/s11367-014-0824-0.

(247) International Organisation for Standardisation. *ISO 14040: 2006— Environmental Management—life Cycle Assessment—principles and Framework.*; Geneva, 2006; Vol. 14040.

(248) International Organisation for Standardisation. *ISO 14044: 2006— environmental Management—life Cycle Assessment— Requirements and Guidelines.*; Geneva, 2006; Vol. 14044.

(249) Corbière-Nicollier, T.; Gfeller Laban, B.; Lundquist, L.; Leterrier, Y.; Månson, J.-A. .; Jolliet, O. Life Cycle Assessment of Biofibres Replacing Glass Fibres as Reinforcement in Plastics. *Resour. Conserv. Recycl.* **2001**, *33* (4), 267–287. https://doi.org/10.1016/S0921-3449(01)00089-1.

(250) Wernet, G.; Bauer, C.; Steubing, B.; Reinhard, J.; Moreno-Ruiz, E.; Weidema, B.; Zah, R.; Wernet wernet, G. The Ecoinvent Database Version 3 (Part I): Overview and Methodology. *Int. J. Life Cycle Assess.* **2016**, *21*, 1218–1230. https://doi.org/10.1007/s11367-016-1087-8.

(251) Thinkstep. GaBi LCA Database Documentation http://www.gabi-software.com/international/support/gabi/ (accessed Dec 8, 2018).

(252) European Commission. European Commissionn > JRC > EPLCA > ELCD http://eplca.jrc.ec.europa.eu/ELCD3/datasetDownload.xhtml (accessed Dec 8, 2018).

(253) Scheepens, A.; van der Flier, A.; van Rosmalen, J.; Veugen, R. EuCIA Eco Impact Calculator: Background Report. 2018.

(254) Song, Y. S.; Youn, J. R.; Gutowski, T. G. Life Cycle Energy Analysis of Fiber-Reinforced Composites. *Compos. Part A Appl. Sci. Manuf.* **2009**, *40* (8), 1257–1265. https://doi.org/10.1016/j.compositesa.2009.05.020.

(255) European Composites Industry Association. EuCIA Eco Impact Calculator http://ecocalculator.eucia.eu/Account/Login?ReturnUrl=%2F (accessed Jun 21, 2018).

(256) Luz, S. M.; Caldeira-Pires, A.; Ferrão, P. M. C. Environmental Benefits of Substituting Talc by Sugarcane Bagasse Fibers as Reinforcement in Polypropylene Composites: Ecodesign and LCA as Strategy for Automotive Components. *Resour. Conserv. Recycl.* **2010**, *54* (12), 1135–1144. https://doi.org/10.1016/J.RESCONREC.2010.03.009.

(257) Azapagic, A. Life Cycle Assessment and Its Application to Process Selection, Design and Optimisation. *Chem. Eng. J.* **1999**, *73*, 1–21.

(258) Finnveden, G. Methodological Aspects of Life Cycle Assessment of Integrated Solid Waste Management Systems. *Resour. Conserv. Recycl.* **1999**, *26* (3–4), 173–187. https://doi.org/10.1016/S0921-3449(99)00005-1.

(259) Oliveux, G.; Bailleul, J.-L.; Salle, E. L. G. La. Chemical Recycling of Glass Fibre Reinforced Composites Using Subcritical Water. *Compos. Part A Appl. Sci. Manuf.* **2012**, *43* (11), 1809–1818. https://doi.org/10.1016/j.compositesa.2012.06.008.

(260) Richard, D.; Hong, T.; Hastak, M.; Mirmiran, A.; Salem, O. Life-Cycle Performance Model for Composites in Construction. **2006**. https://doi.org/10.1016/j.compositesb.2006.04.001.

(261) Peças, P.; Ribeiro, I.; Henriques, E. Life Cycle Engineering for Materials and Technology Selection: Two Models, One Approach. *Procedia CIRP* **2014**, *15*, 543–548. https://doi.org/10.1016/j.procir.2014.06.073.

(262) Carvalho, H.; Raposo, A.; Ribeiro, I.; Kaufmann, J.; Götze, U.; Peças, P.; Henriques, E. Application of Life Cycle Engineering Approach to Assess the Pertinence of Using Natural Fibers in Composites – The Rocker Case Study. *Procedia CIRP* **2016**, *48*, 364–369. https://doi.org/10.1016/j.procir.2016.03.144.

(263) Hann Chua, M.; Smyth, B. M.; Murphy, A.; Butterfield, J. Understanding Aerospace Composite Components' Supply Chain Carbon Emissions. Queen's Univeristy Belfast 2015.

(264) Granta Design. CES EduPack: Materials Universe Database. Michael Ashby 2017.

(265) Tempelman, E. Multi-Parametric Study of the Effect of Materials Substitution on Life Cycle Energy Use and Waste Generation of Passenger Car Structures. *Transp. Res. Part D Transp. Environ.* **2011**, *16* (7), 479–485. https://doi.org/10.1016/j.trd.2011.05.007.

(266) Kaluza, A.; Kleemann, S.; Fröhlich, T.; Herrmann, C.; Vietor, T. Concurrent Design & Life Cycle Engineering in Automotive Lightweight Component Development. *Procedia CIRP* **2017**, *66*, 16–21. https://doi.org/10.1016/j.procir.2017.03.293.

(267) Bell, J.; Pickering, S.; Yip, H.; Rudd, C. *Environmental Aspects of the Use of Carbon Firbe Composites in Vehicles - Recycling and Life Cycle Analylsis*; Warwick, UK, 2002.

(268) Zhang, X.; Yamauchi, M.; Takahashi, J. Life Cycle Assessment of CFRP in Application of Automobile. In *18th International Conference on Composite Materials*; 2011.

(269) Duflou, J. R.; De Moor, J.; Verpoest, I.; Dewulf, W. Environmental Impact Analysis of Composite Use in Car Manufacturing. *CIRP Ann. - Manuf. Technol.* **2009**, *58* (1), 9–12. https://doi.org/10.1016/j.cirp.2009.03.077.

(270) Nagai, H.; Takahashi, J.; Kemmochi, K.; Matsui, J.-I. Inventory Analysis in Production and Recycling Process of Advanced Composite Materials. *J. Adv. Sci.* **2001**, *13*, 125–128.

(271) Carberry, W. *Airplane Recycling Efforts Benefit Boeing Operators*; 2008.

(272) Gutiérrez, E.; Bono, F. *Review of Industrial Manufacturing Capacity for Fibre-Reinforced Polymers as Prospective Structural Components in Shipping Containers*; 2013.

(273) Ashby, M. F. *Materials Selection in Mechanical Design*; Butterworth-Heinemann, 2016.

(274) Michaud, V. Les Matériaux Composites, Moteurs de La Mobilité Propre? Ecole Polytechnique Federale De Lausanne 2016.

(275) Joshi, S. .; Drzal, L. .; Mohanty, A. .; Arora, S. Are Natural Fiber

Composites Environmentally Superior to Glass Fiber Reinforced Composites? *Compos. Part A Appl. Sci. Manuf.* **2004**, *35* (3), 371–376. https://doi.org/10.1016/j.compositesa.2003.09.016.

(276) Andrady, A. L. *Plastics and the Environment*, 1st ed.; John Wiley & Sons, 2003.

(277) Cripps, D. Composite materials guide: Resin Systems - Resin Comparison | NetComposites https://netcomposites.com/guide-tools/guide/resin-systems/resin-comparison/ (accessed Feb 8, 2018).

(278) Vladimirov, V. *Comparison of CO2 Emssions from Trenchless and Open-Cut Installation Methods. Installation of OD 3000 Mm Diameter Pipes for Project Czajka*; Warsaw, Poland, 2011.

(279) Plasticker. Raw Materials & Prices http://plasticker.de/preise/preise_monat_single_en.php (accessed Feb 8, 2018).

(280) Boustead, I. *Eco-Profiles of the European Plastics Industry: Polyamide 66 (Nylon 66)*; 2005.

(281) Boustead, I. *Eco-Profiles of the European Plastics Industry: Polycarbonate*; 2005.

(282) Meng, F.; Mckechnie, J.; Pickering, S. J. An Assessment of Financial Viability of Recycled Carbon Fibre in Automotive Applications. *Compos. Part A* **2018**, *109*, 207–220. https://doi.org/10.1016/j.compositesa.2018.03.011.

(283) Posen, I. D.; Jaramillo, P.; Landis, A. E.; Griffin, W. M. Greenhouse Gas Mitigation for U.S. Plastics Production: Energy First, Feedstocks Later. *Environ. Res. Lett.* **2017**, *12* (3), 034024. https://doi.org/10.1088/1748-9326/aa60a7.

(284) Platt, D. Polymer markets recover from December lull | Plastics News http://www.plasticsnewseurope.com/article/20180202/PNE/180209976/polymer-markets-recover-from-december-lull (accessed Feb 8, 2018).

(285) Das, S. Life Cycle Assessment of Carbon Fiber-Reinforced Polymer Composites. *Int. J. Life Cycle Assess.* **2011**, *16* (3), 268–282. https://doi.org/10.1007/s11367-011-0264-z.

(286) George, M.; Chae, M.; Bressler, D. C. Composite Materials with Bast Fibres: Structural, Technical, and Environmental Properties. *Prog. Mater. Sci.* **2016**, *83*, 1–23. https://doi.org/10.1016/j.pmatsci.2016.04.002.

(287) Wötzel, K.; Wirth, R.; Flake, M. Life Cycle Studies on Hemp Fibre Reinforced Components and ABS for Automotive Parts. *Die Angew. Makromol. Chemie* **1999**, *272* (1), 121–127. https://doi.org/10.1002/(SICI)1522-9505(19991201)272:1<121::AID-APMC121>3.0.CO;2-T.

(288) Pickering, K. L.; Efendy, M. G. A.; Le, T. M. A Review of Recent Developments in Natural Fibre Composites and Their Mechanical Performance. *Compos. Part A Appl. Sci. Manuf.* **2016**, *83*, 98–112. https://doi.org/10.1016/J.COMPOSITESA.2015.08.038.

(289) Summerscales, J.; Dissanayake, N. P. J.; Virk, A. S.; Hall, W. A Review of Bast Fibres and Their Composites. Part 1 – Fibres as Reinforcements. *Compos. Part A Appl. Sci. Manuf.* **2010**, *41* (10), 1329–1335. https://doi.org/10.1016/J.COMPOSITESA.2010.06.001.

(290) Meng, F.; McKechnie, J.; Turner, T.; Wong, K. H.; Pickering, S. J. Environmental Aspects of Use of Recycled Carbon Fiber Composites in Automotive Applications. *Environ. Sci. Technol.* **2017**, *51* (21), 12727–12736. https://doi.org/10.1021/acs.est.7b04069.

(291) Norton, A. A Review of LCA Data for Composite Materials and Products A Review of LCA Data for Composite Materials and Products. Renuables: Anglesey 2018.

(292) Dai, Q.; Kelly, J.; Sullivan, J.; Elgowainy, A. Life-Cycle Analysis Update of Glass and Glass Fiber for the GREET Model. **2015**, No. September, 25.

(293) Duflou, J. R.; Deng, Y.; Van Acker, K.; Dewulf, W. Do Fiber-Reinforced Polymer Composites Provide Environmentally Benign Alternatives? A

Life-Cycle-Assessment-Based Study. *MRS Bull.* **2012**, *37* (04), 374–382. https://doi.org/10.1557/mrs.2012.33.

(294) Granta Design. CES EduPack: Process Universe Database. Michael Ashby 2017.

(295) Simões, C. L.; Costa Pinto, L. M.; Simoes, R.; Bernardo, C. A. Integrating Environmental and Economic Life Cycle Analysis in Product Development: A Material Selection Case Study. *Int. J. Life Cycle Assess.* **2013**, *18* (9), 1734–1746. https://doi.org/10.1007/s11367-013-0561-9.

(296) Wheatley, A.; Warren, D.; Das, S. Development of Low-Cost Carbon Fibre for Automotive Applications. In *Advanced Composite Materials for Automotive Applications: Structural Integrity and Crashworthiness*; John Wiley & Sons, 2013; pp 51–77.

(297) Hottle, T.; Caffrey, C.; McDonald, J.; Dodder, R. Critical Factors Affecting Life Cycle Assessments of Material Choice for Vehicle Mass Reduction. *Transp. Res. Part D Transp. Environ.* **2017**, *56*, 241–257. https://doi.org/10.1016/J.TRD.2017.08.010.

(298) Vaidya, U. K.; Chawla, K. K. Processing of Fibre Reinforced Thermoplastic Composites. *Int. Mater. Rev.* **2008**, *53* (4), 185–218. https://doi.org/10.1179/174328008x325223.

(299) Bushi, L.; Skszek, T.; Reaburn, T. New Ultralight Automotive Door Life Cycle Assessment. *Int. J. Life Cycle Assess.* **2018**. https://doi.org/https://doi.org/10.1007/s11367-018-1515-z.

(300) Koffler, C.; Rohde-Brandenburger, K. On the Calculation of Fuel Savings through Lightweight Design in Automotive Life Cycle Assessments. *Int. J. Life Cycle Assess.* **2010**, *15* (1), 128–135. https://doi.org/10.1007/s11367-009-0127-z.

(301) Sun, X.; Liu, J.; Lu, B.; Zhang, P.; Zhao, M. Life Cycle Assessment-Based Selection of a Sustainable Lightweight Automotive Engine Hood Design. *Int. J. Life Cycle Assess.* **2017**, *22* (9), 1373–1383. https://doi.org/10.1007/s11367-016-1254-y.

(302) Kelly, J. C.; Sullivan, J. L.; Burnham, A.; Elgowainy, A. Impacts of Vehicle Weight Reduction via Material Substitution on Life-Cycle Greenhouse Gas Emissions. *Environ. Sci. Technol.* **2015**, *49* (20), 12535–12542. https://doi.org/10.1021/acs.est.5b03192.

(303) Shah, D. U. Developing Plant Fibre Composites for Structural Applications by Optimising Composite Parameters: A Critical Review. https://doi.org/10.1007/s10853-013-7458-7.

(304) La Rosa, A. D.; Recca, G.; Summerscales, J.; Latteri, A.; Cozzo, G.; Cicala, G. Bio-Based versus Traditional Polymer Composites. A Life Cycle Assessment Perspective. *J. Clean. Prod.* **2014**, *74*, 135–144. https://doi.org/10.1016/J.JCLEPRO.2014.03.017.

(305) Duflou, J. R.; Yelin, D.; Van Acker, K.; Dewulf, W. Comparative Impact Assessment for Flax Fibre versus Conventional Glass Fibre Reinforced Composites: Are Bio-Based Reinforcement Materials the Way to Go? *CIRP Ann.* **2014**, *63* (1), 45–48. https://doi.org/10.1016/j.cirp.2014.03.061.

(306) Palmer, J.; Ghita, O. R.; Savage, L.; Evans, K. E. Successful Closed-Loop Recycling of Thermoset Composites. *Compos. Part A Appl. Sci. Manuf.* **2009**, *40* (4), 490–498. https://doi.org/10.1016/J.COMPOSITESA.2009.02.002.

(307) Shuaib, N. A.; Mativenga, P. T. Carbon Footprint Analysis of Fibre Reinforced Composite Recycling Processes. *Procedia Manuf.* **2017**, *7*, 183–190. https://doi.org/10.1016/j.promfg.2016.12.046.

(308) Li, X.; Bai, R.; McKechnie, J. Environmental and Financial Performance of Mechanical Recycling of Carbon Fibre Reinforced Polymers and Comparison with Conventional Disposal Routes. *J. Clean. Prod.* **2016**, *127*, 451–460. https://doi.org/10.1016/J.JCLEPRO.2016.03.139.

(309) Asmatulu, E.; Twomey, J.; Overcash, M. Recycling of Fiber-Reinforced Composites and Direct Structural Composite Recycling Concept. https://doi.org/10.1177/0021998313476325.

(310) Puri, P.; Compston, P.; Pantano, V. Life Cycle Assessment of Australian

Automotive Door Skins. *Int. J. Life Cycle Assess.* **2009**, *14* (5), 420–428. https://doi.org/10.1007/s11367-009-0103-7.

(311) Shuaib, N. A.; Mativenga, P. T. Carbon Footprint Analysis of Fibre Reinforced Composite Recycling Processes. *Procedia Manuf.* **2017**, *7*, 183–190. https://doi.org/10.1016/J.PROMFG.2016.12.046.

(312) Keith, M. J.; Oliveux, G.; Leeke, G. A. Optimisation of Solvolysis for Recycling Carbon Fibre Reinforced Composites. In *ECCM17- 17th European Conference on Composite Materials*; 2016.

(313) Atherton, J. Declaration by the Metals Industry on Recycling Principles. *Int. J. Life Cycle Assess.* **2007**, *12* (1), 59–60. https://doi.org/10.1065/lca2006.11.283.

(314) Nicholson, A. L.; Olivetti, E. A.; Gregory, J. R.; Field, F. R.; Kirchain, R. E. End-of-Life LCA Allocation Methods: Open Loop Recycling Impacts on Robustness of Material Selection Decisions. In *2009 IEEE International Symposium on Sustainable Systems and Technology, ISSST '09 in Cooperation with 2009 IEEE International Symposium on Technology and Society, ISTAS*; IEEE, 2009; pp 1–6. https://doi.org/10.1109/ISSST.2009.5156769.

(315) Scelsi, L.; Bonner, M.; Hodzic, A.; Soutis, C.; Wilson, C.; Scaife, R.; Ridgway, K. Potential Emissions Savings of Lightweight Composite Aircraft Components Evaluated through Life Cycle Assessment. *Express Polym. Lett.* **2011**, *5* (3), 209–217. https://doi.org/10.3144/expresspolymlett.2011.20.

(316) Kireitseu, M. Environmental Strategies for Sustainable Manufacturing Process of Composites. *IOP Conf. Ser. Mater. Sci. Eng.* **2017**, *229* (1), 012007. https://doi.org/10.1088/1757-899X/229/1/012007.

(317) Nunes, A. O.; Viana, L. R.; Guineheuc, P.-M.; da Silva Moris, V. A.; de Paiva, J. M. F.; Barna, R.; Soudais, Y. Life Cycle Assessment of a Steam Thermolysis Process to Recover Carbon Fibers from Carbon Fiber-Reinforced Polymer Waste. *Int. J. Life Cycle Assess.* **2017**.

https://doi.org/10.1007/s11367-017-1416-6.

(318) Ekvall, T.; Tillman, A.-M. Open-Loop Recycling: Criteria for Allocation Procedures. *Int J LCA* **1997**, *2* (3), 155–162.

(319) Simões, C. L.; Pinto, L. M. C.; Bernardo, C. A. Modelling the Economic and Environmental Performance of Engineering Products: A Materials Selection Case Study. *Int. J. Life Cycle Assess.* **2012**, *17* (6), 678–688. https://doi.org/10.1007/s11367-012-0414-y.

(320) Patton, R.; Li, F.; Edwards, M. Causes of Weight Reduction Effects of Material Substitution on Constant Stiffness Components. *Thin-Walled Struct.* **2004**, *42*, 613–637. https://doi.org/10.1016/j.tws.2003.08.001.

(321) Eriksson, M.; Ahlgren, S. LCAs of Petrol and Diesel a Literature Review. 2013.

(322) Starostka-Patyk, M. New Products Design Decision Making Support by SimaPro Software on the Base of Defective Products Management. *Procedia Comput. Sci.* **2015**, *65*, 1066–1074. https://doi.org/10.1016/J.PROCS.2015.09.051.